INVESTIGATION ON THE PROPERTIES OF FEW THERMOTROPIC LIQUID CRYSTALLINE SYSTEMS

Thesis submitted for the degree of
Doctor of Philosophy (Science) of the
University of North Bengal
July 2003

By
PRANAB KUMAR SARKAR

Department of Physics
Government Champhai College
Champhai 796321
Mizoram -INDIA

To The Fond Memory of My Father

DEPARTMENT OF PHYSICS
UNIVERSITY OF NORTH BENGAL
P.O. NORTH BENGAL UNIVERSITY
SILIGURI. DIST. DARJEELING (WB)
PIN: 734430 INDIA

Railway Station: New Jalpaiguri (NFR)
Airport: Bagdogra
Phone: +91 (0) 353 2582107
Fax: +91 (0) 353 2581 546

(TO WHOM IT MAY CONCERN)

This is to certify that the research work reported in this thesis entitled "Investigation on The Properties of Few Thermotropic Liquid Crystalline Systems" by Mr. Pranab Kumar Sarkar has been carried out by the candidate himself under my supervision and guidance. He has fulfilled all the requirements for the submission of the thesis for Ph.D. degree of the University of North Bengal. A small portion of the research work presented in this dissertation has been performed in collaboration with others. Most of the work has been performed by him and his contribution is very substantial. In character and disposition Mr. Pranab Kumar Sarkar is fit to submit the thesis for Ph.D. degree.

Date: 11.7.2003

(Dr. Pradip Kumar Mandal)
Supervisor and Reader,
Department of Physics
University of North Bengal

'There are more things in heaven and earth, Horatio,
Than are dreamt of in your philosophy.'

William Shakespeare, *Hamlet* (Act I, Scene V)

CONTENTS

Acknowledgements

At the outset I express my deep sense of gratitude to Dr P. K. Mandal, Reader in the Department of Physics, University of North Bengal for his supervision, advice and helpful suggestions throughout the present investigation. His active guidance, constant inspiration and constructive criticism have been of immense help in every stage of the work, particularly in experimentation, data analysis, drawing conclusions from the results and, finally, in compilation of the thesis.

I am very much grateful to Dr (Mrs) S. Paul, Reader in Physics, University of North Bengal (Retired), who stimulates every new researcher in this laboratory with motherly affection to work in the beautiful field of liquid crystals, for her invaluable advice and supports at different stages of this work.

I am deeply indebted to Prof. R. Paul, Department of Physics, University of North Bengal (Retired), for his extremely valuable advice, guidelines and discussions.

I wish to gratefully thank Prof. R. A. Vora, University of Vadodara, India for kindly donating two liquid crystal samples (6OBPAA and 8OBPAA) which have been studied in the present work.

I am indebted to the University Grants Commission for awarding me a Junior Research Fellowship (NET) and subsequently a Teacher Fellowship for undertaking the work. Also, I am grateful to the honorable Principal Mr. V. Suak Buanga, Government Champhai College, Mizoram for allowing me to avail the Teacher Fellowship and for sanctioning leaves of short durations several times, since my joining the college in 1995. Without his help and encouragement this thesis would not have been completed.

I must express my heartfelt thanks to all my colleagues in Government Champhai College, particularly, to Mr. H.K.L.Thanga, Mr. Goutam Bit, Mr. Amarendra Behera, Mr. Lalnunpuia and Mr. Lalthanpuia for their constant co-operation and encouragement that I received from them.

It is my privilege to express my thanks to Mr. Sajal Kumar Sarkar, former senior Technical Assistant, Department of Physics, NBU for his constant help in setting up of the experiments as well in data collection stage.

I certainly owe a lot to the unstinting co-operation that I received during my research works from my friends in the Laboratory: Dr. Parimal. Sarkar, Dr. M. K. Das, Dr. (Mrs) B. Adhikari, Dr. S. K. Giri, Mr B. R. Jaishi, Mr P. D. Roy and Miss S. Biswas. My thanks are also due to Mr. Arindam Mukherjee and Dr. Arunava Bhadra, High Energy and Cosmic Ray Research Centre, NBU for their continuous encouragements. It is a pleasure to express my thanks to all the teaching and non-teaching staffs, research scholars of the of Physics Department, NBU. The staff members of USIC are gratefully

acknowledged for their help in constructing and fabricating the different parts of the experimental set ups.

I would like to thank all the Research Scholars of the University of North Bengal for their co-operations. In this respect I gratefully acknowledge the help and co-operation that I received from Mr. Manna Mukherjee, Research Scholar, Department of Sociology, NBU.

Finally, I acknowledge my indebtedness to my mother and my late father not only for their encouragement and co-operation for this work but also for their affectionate teachings that made me what I am today. Also, I express my heartiest thanks to my beloved son Arkaprava and my wife Chhandita who missed me for long many days, especially for last eight months, but still went on encouraging me. My elder brother and other members of my family are acknowledged with thanks for their constant encouragement and unending co-operation in completion of the work.

Place: North Bengal University
Date: 11.07.2003

Pranab Kumar Sarkar
(PRANAB KUMAR SARKAR)

Chapter I

INTRODUCTION

1.1 LIQUID CRYSTALS

The term **liquid crystal** stands for a state of condensed matter that is intermediate between the crystalline solid and amorphous liquid state. A liquid crystal is strongly anisotropic in some of its properties like ordinary crystals and yet exhibits a certain degree of fluidity, which in some cases, is comparable to that of an ordinary liquid. The molecules in a crystal have both positional and orientational ordering whereas in liquids their arrangement is random. In liquid crystals, however, the molecules are more ordered than in liquids but are less ordered than that observed in a typical crystal.

The liquid crystalline state was first discovered in 1888 by an Austrian botanist Friedrich Reinitzer [1] while studying cholesterols in plants. He observed a cloudy liquid between two melting points in cholesteryl benzoate and cholesteryl acetate. Remarkable iridescent colours were also observed between the two melting points. Otto Lehmann, a German Physicist, reaffirmed the observations [2,3] made by Renitzer and termed such materials as **flowing crystals** in 1889, **crystalline liquids** in 1890 and **liquid crystals** in 1900 [4]. Since the liquid crystal phase is observed between the isotropic liquid and crystalline solid phase it is also called **mesophase** or **mesomorphic phase**, as suggested by Georges Friedel [5,6]. Materials, which undergo transition to liquid crystal phase or mesophase, are known as **liquid crystalline materials** or **mesogens**. The historical perspective of the liquid crystal research is found in the refernces [7-10].

Liquid crystal is currently an important phase of matter both from the viewpoint of basic sciences and technological applications. Thousands of compounds – mainly organic, and some organometallic, inorganic and bio-molecules, are now known to form mesophases [10-18]. Molecules of various shapes and nature form liquid crystalline phases. But the common features among them are that the molecules are geometrically anisotropic in shape and highly anisotropic intermolecular forces hold them together. Depending upon the detailed molecular structure, a compound may exhibit one or more mesophases before it is transformed into the isotropic liquid from the solid phase. Transitions to these

intermediate states may be brought about by thermal processes or by the influence of solvents. Though first observed more than a century ago resurgence in liquid crystal research took place in 1960s and at present, members of the scientific community all over the world are working in this fascinating interdisciplinary field. As a result many excellent books and monographs have appeared on all aspects of the liquid crystals ranging from the fundamentals to the forefront of research. Some of these have been referred [12,14,17-57].

1.2 CLASSIFICATION OF LIQUID CRYSTALS

Liquid crystals may be divided into two main categories viz. **lyotropic** and **thermotropic.** A lyotropic liquid crystalline material forms mesophases in a certain range of concentration of the solution of the substance in some solvent. On the other hand, a thermotropic mesogen exhibits a liquid crystalline phase in a certain temperature range and undergoes phase transitions when temperature changes.

1.2.1 Lyotropic liquid crystals

Lyotropic liquid crystals [33,46,57-73] are made up of two or more components. Generally a lyotropic molecule contains a hydrophilic polar head group and one or more long hydrophobic alkyl chains (Figure 1.1). Such amphiphilic molecules form ordered structure in both polar and non-polar solvents. A typical example of this type of liquid crystal is soap and water system where mesomorphic phases appear as a function of concentration. The water molecules penetrate the space between the layers formed by polar groups of the soap molecules and weaken the attractive forces between them to cause transition from solid phase to lyotropic phase. Mainly three different types lyotropic phases viz. lamellar (or neat), hexagonal (or middle) and cubic (or viscous isotropic) are possible. In Figure 1.2 lamellar lyotropic phase structure is illustrated. Temperature range of a lyotropic phase depends upon the concentration. Lyotropic liquid crystals occur abundantly in nature, being ubiquitous in living systems. For example, the tobacco mosaic virus (TMV), many synthetic polypeptides, cell membranes of all

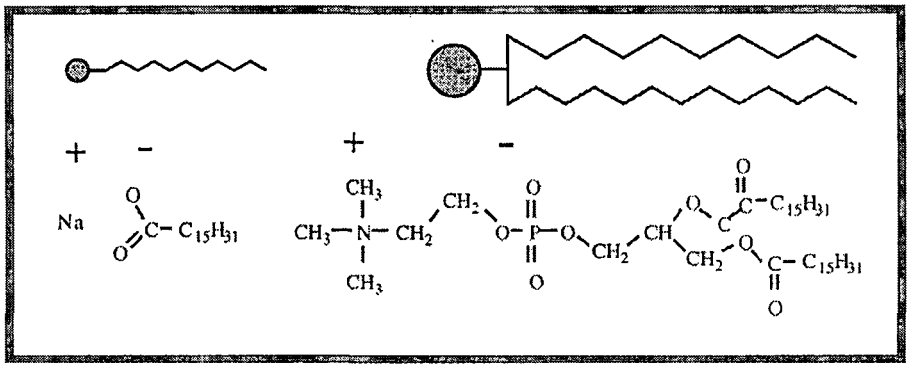

From [39]

Figure 1.1 Lyotropic liquid crystal molecules: Soap (left) and Phospholipid (right)

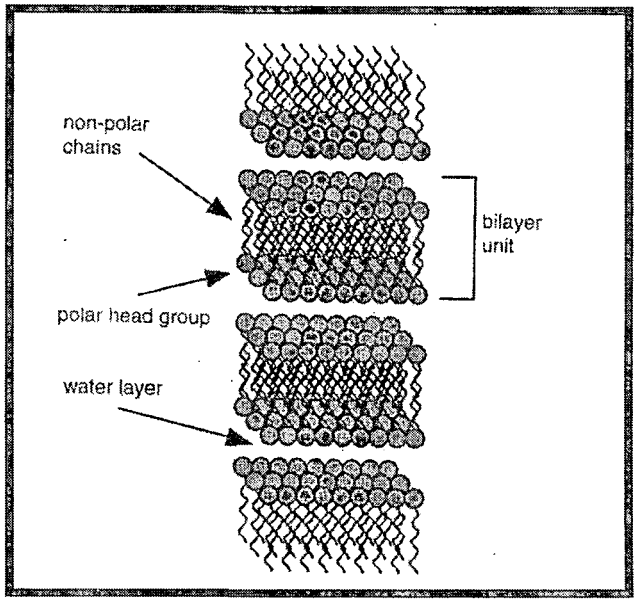

From [39]

Figure 1.2 Structure of the lamellar lyotropic liquid crystal phase.

living organism and some organic fluids like blood, deoxyribonucleic acid (DNA) molecules exhibit lyotropic behaviour when dissolved in an appropriate solvent (usually water) in suitable concentration. Also there is a well-defined family of lyotropic mesogens embracing a range of drugs, dyes, nucleic acids, antibiotics, carcinogens and anti-cancer agents. Since the present thesis contains results of only the thermotropic liquid crystalline systems, no further discussion will be made on lyotropic mesophases.

1.2.2 Thermotropic Liquid crystal

As mentioned earlier, thermotropic liquid crystals are those in which phase transitions occur due to change in temperature. The vast majority of thermotropic liquid crystals are composed of rod-like molecules (one molecular axis is much longer than the other two) and they are known as calamitic liquid crystals. A typical calamitic liquid crystal is shown in Figure 1.3. Following the nomenclature proposed by Friedel [5], they are classified into three main types: **nematic, cholesteric and smectic.**

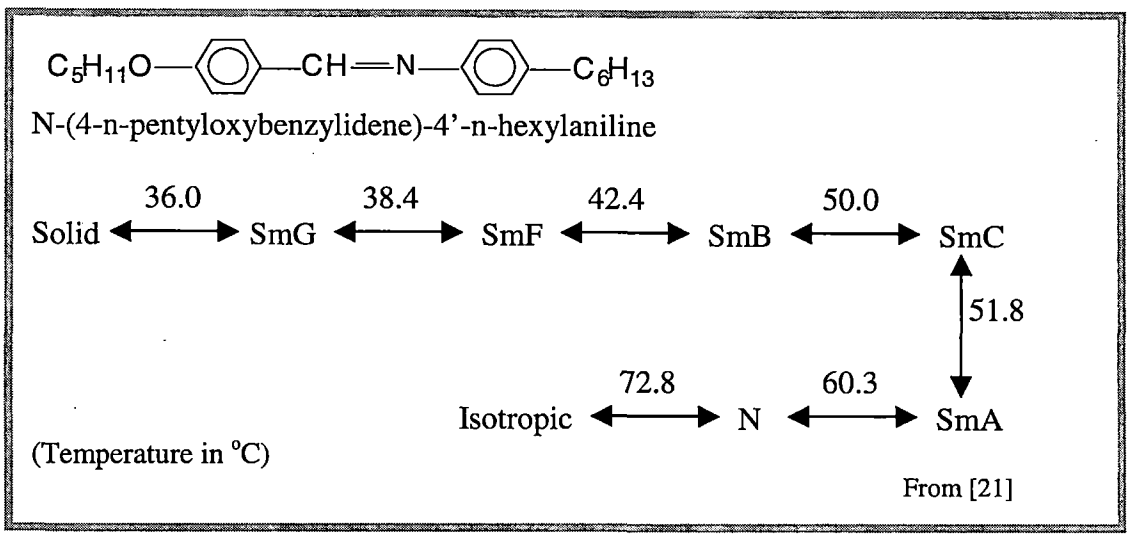

Figure 1.3 A typical calamitic liquid crystal with transition temperatures.

1.2.2.1 *Nematic (N) liquid crystal*

The nematic liquid crystals have a high degree of long-range orientational order of the molecules but no long-range translational order i.e., the long axes of the

molecules tend to be parallel to a particular direction, called the **director** (designated by a unit vector **n**), and their centres are distributed at random. This is shown in Figure 1.4(a). This phase is optically uniaxial but a biaxial modification has also been discovered [74-84]. It is easy to disturb the alignment of the molecules of nematic liquid crystals by external influences. So nematics are able to translate weak external signals (electrical, magnatic, mechanical) into visible optical effects for which they are extremely useful in various display devices.

Adriaan de Vries [85-87] from X-ray studies first proposed the existence of another type of nematic called **cybotactic nematic** where small clusters of molecules are arranged in layers. If the molecules of cybotactic groups are normal to the layers then it is called a **normal cybotactic nematic** (N_{OC}) and if the molecules are titled to the cybotactic layers then it belongs to **skewed cybotactic nematic** (N_{SC}) variety.

1.2.2.2 *Cholesteric (Ch) liquid crystals*

Cholesteric mesophase is also a nematic type of liquid crystal except that the constituent molecules are chiral i.e. optically active. As a result the director is not fixed in space but rotates in helical fashion about an axis perpendicular to the director [23,88-93] as shown in Figure 1.5. The helix may be right handed or left handed depending on the molecular conformation. The pitch of the helix is usually of the order of the wave length of visible range of electromagnatic spectrum and is highly temperature dependent. Optically inactive molecules or racemic mixtures of cholesterics result in a cholesteric of infinite pitch which is nothing but a true nematic. Also, when a small quantity of a cholesteric substance [5], or even a non-mesogenic optically active substance [94], is added to a nematic the mixture adopts a helical configuration like a cholesetric. So, the cholesetric phase may be regarded as a twisted nematic phase [95] or conversely, a nematic phase as a cholesetric phase of infinite pitch. The absence of Ch-N phase transition by variation of temperature [96] and Ch-N transition (rather transformation) by application of strong magnetic field normal to the helical axis [97,98] confirm this fact. The spiral arrangement of the molecules in the cholesteric phase is responsible for the selective

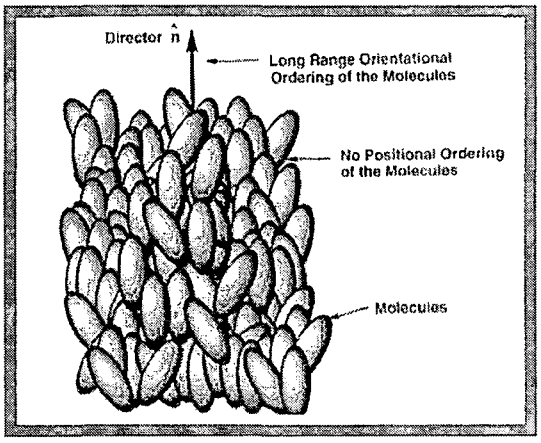

(a)

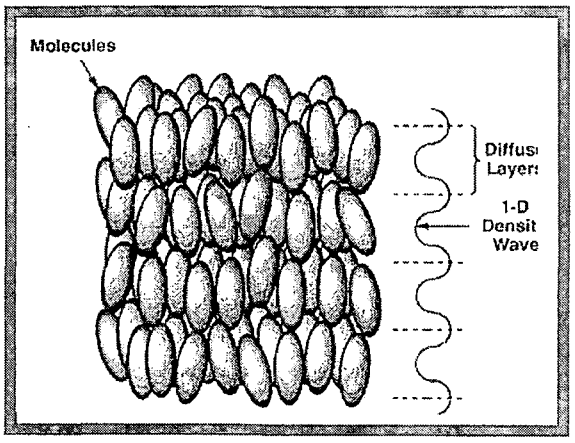

(b)

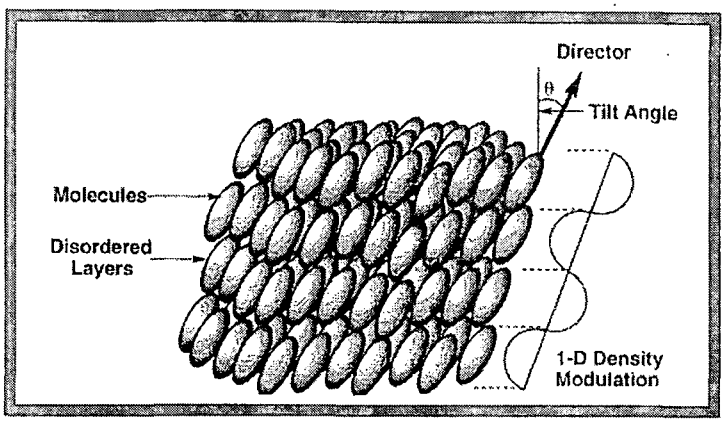

From [17]

(c)

Figure 1.4 The structure of the (a) nematic phase (b) orthogonal smectic A phase and (c) tilted smectic C phase.The arrow indicates the director **n**.

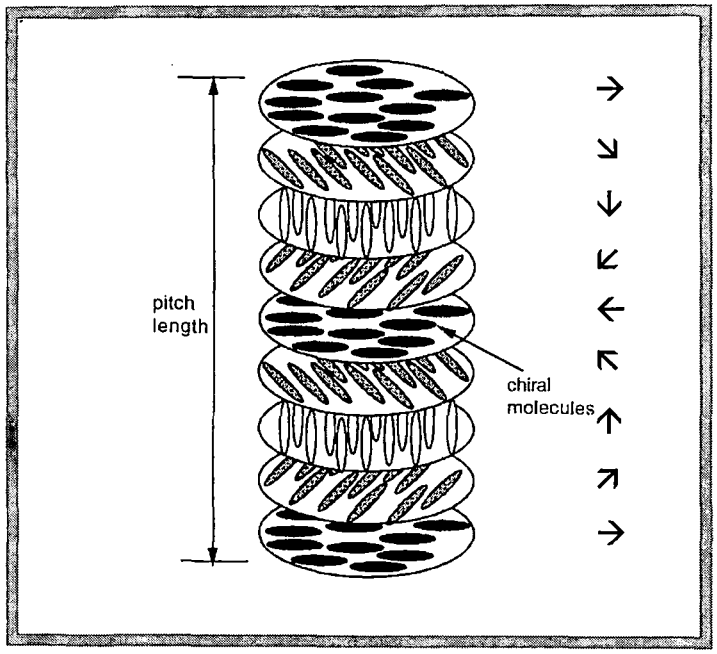

From [39]

Figure 1.5 Schematic representation of the helical structure of the cholesteric liquid crystals. The views represent imaginary slices through the structure and do not imply any type of layered structure. The arrows indicate the director **n**.

reflection of circularly polarised light and a rotatory power about a thousand times greater than that of an ordinary optically active substance [21]. Cholesterics of low pitch (less than about 0.5 μm) exhibit what are known as **blue phases** [99,100]. These phases exist over a small temperature range (~1°C) between the liquid crystal phase and the isotropic liquid. Three distinct blue phases (I, II and III) have been identified and occur in that order with increasing temperature.

1.2.2.3 *Smectic liquid crystal*

The smectic phase of a liquid crystal represents a higher state of ordering than nematics. In addition to the orientational ordering the molecules are arranged in layers. A great variety of smectic phases can be observed depending on the molecular arrangements in the layers[14, 17,18,24,25,101-108]. The molecules may be upright or inclined to the layers and may or may not have long range positional ordering in each layer, but long range orientational ordering is always present in all layers of the smectic liquid crystal. Some of the smectic liquid crystals have three

dimensional long range positional order as in a crystal while some others have three dimensional long range **'bond orientational order'** without any long range positional order [109,110]. The interlayer attractions are weaker than the lateral forces between molecules and hence the layers can easily slide over one another. Hence smectics have fluidity though these are much more viscous than nematics.

The stratified smectic phase is divided into four subgroups by considering first the extent of the in-plane positional ordering of the constituent molecules and then considering the tilt orientational ordering of the long axes of the molecules relative to the layer planes. Firstly, the two groups can be classified where the molecules on average are normal to the layers. The difference between these two groups is in the extent of positional ordering. For example, in the smectic A and hexatic B phases the molecules have only short range positional order [110], whereas the crystal B and crystal E phases are 'smectic-like' soft crystal modifications [111,112] where the molecules have long range positional ordering in three dimensions [101]. Secondly, in the two other classes the molecules are tilted with respect to the layer planes. In the smectic C, smectic I and smectic F phases the molecules have short range positional ordering [113,114], but in the crystal G, crystal H, crystal J and crystal K phases the molecules have long range three dimensional ordering [111,114]. X-ray diffraction techniques have been used to investigate the structures of the smectic modifications [111,115-119] and have been shown in Figure 1.6.

It may be mentioned here that previously all the above phases were termed as smectics. Some of these are now termed as crystals because of their long range orientational as well as long range 3-D positional ordering. These phases, however, have somewhat different properties from normal crystals, for example, their constituent molecules are reorientating on a time scale of 10^{11} times per second about their long axes[120,121].

Smectic A (SmA) phase:

In this phase the long axes of the molecules on average are perpendicular to the layer planes and within each layer the centres of mass of the molecules are

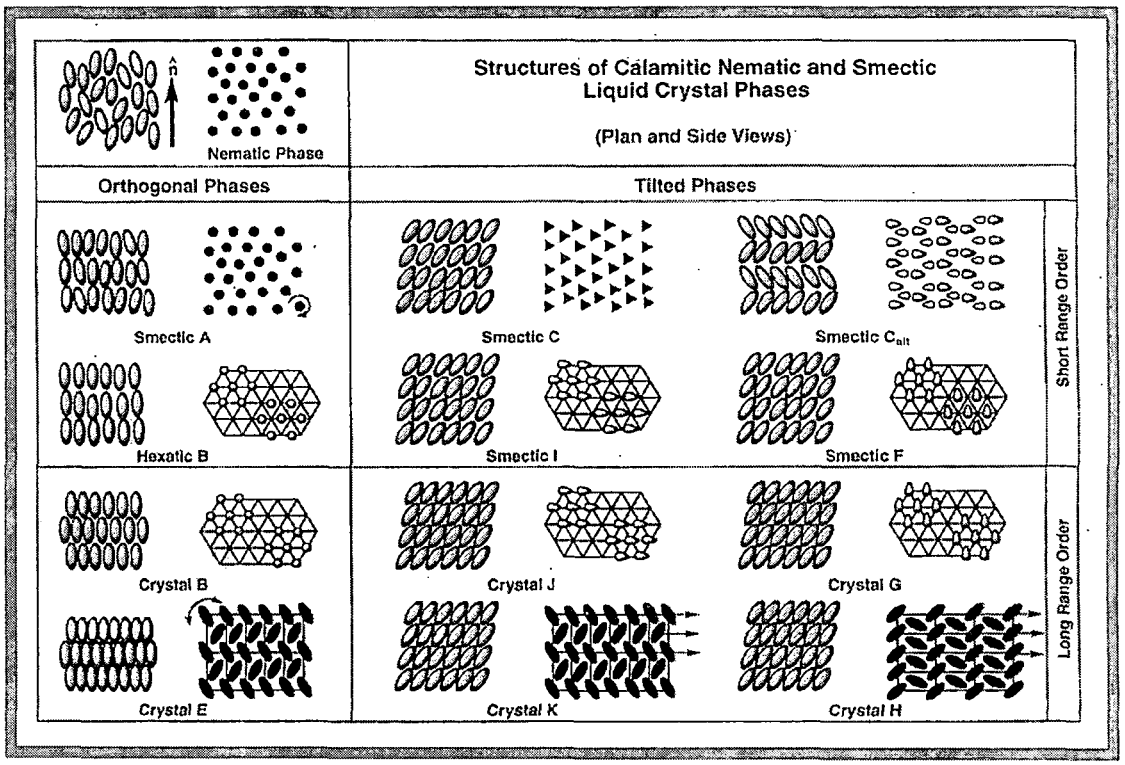

From [17]

Figure 1.6 The structures of the various liquid crystal mesophases. For each phase the side view is shown to the left and the plan view to the right. The rod-like molecules are shown as ellipses, their cross-sectional areas as circles, triangles or ellipses. The triangles and arrows are used to represent molecular tilt directions.

irregularly spaced in a liquid like fashion. Normal to the layers the molecules are essentially arranged in a one-dimensional density wave [101]. In this phase usually the layer spacing (d) is approximately equal to the molecular length (L). However, other modifications are also possible. The sub-phases of smectic A are described as monolayer smectic A (SmA_1), bilayer smectic A (SmA_2), partially bilayer smectic A (SmA_d) [101]. Partial bilayer ordering is typically caused either by interdigitation or pairing of the molecules with partial overlap [122,123] and found to happen in materials where the molecules have terminal polar groups. Another smectic modification called 'ribbon' or antiphase ((Sm~A) has also been reported [124,125] where an undulating bilayer is observed. Sub-structures of SmA phases is shown in Figure 1.7. Details regarding these polymorphism of smectic A have been reported by many authors [124-144].

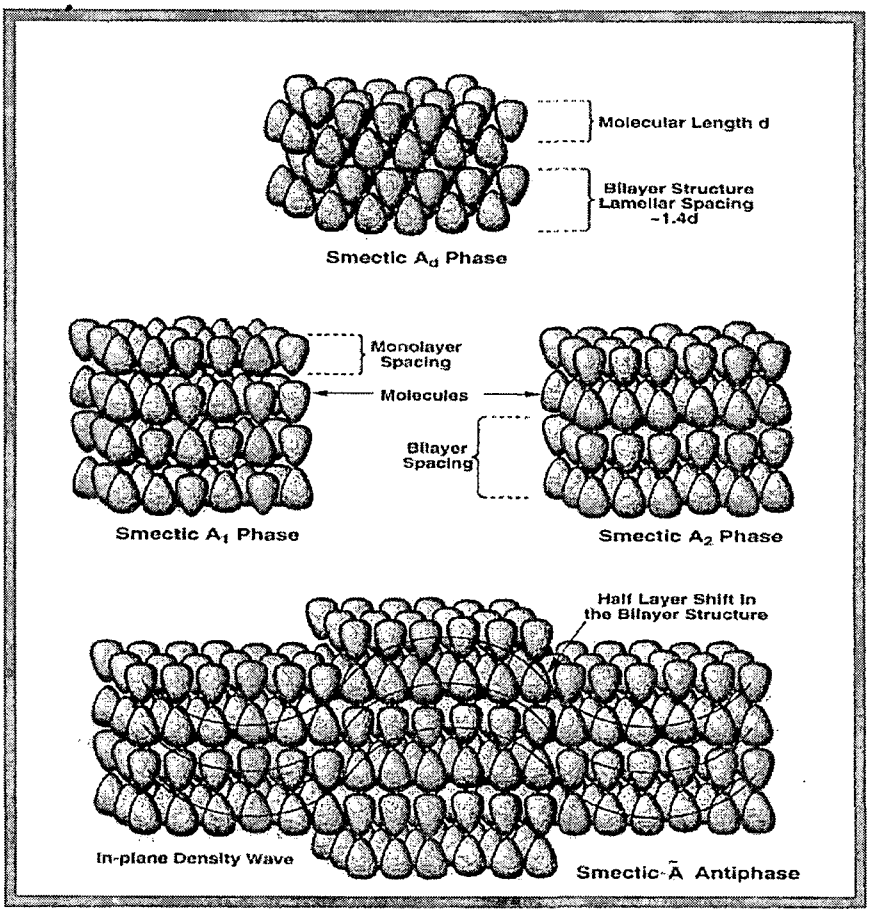

From [17]

Figure 1.7 Bilayer and monolayer structures of the smectic A phase.

Smectic C (SmC) phase:

The smectic C phase is a tilted form of the smectic A phase, i.e., the molecules are inclined with respect to the layer normal. The layer spacing (d) of this phase is less than the molecular length (L) due to this tilt. If β_t is the tilt angle with respect to the layer normal then the layer spacing is $d = L\cos\beta_t$. Depending upon the temperature dependence of the tilt angles attempts have been made to divide Sm_C phase in three subgroups [102,145]. The smectic C phase is optically biaxial [146,147]. A quadrupolar charge distribution in the molecules helps the formation of this phase, because the intermolecular electrostatic interaction is repulsive when the molecules are parallel to the layer normal, whereas it is reduced much when the molecules are tilted. From the consideration of the packing of the hydrocarbon

chains of the molecules it can be seen that tilted arrangement of molecules within the layers is energetically more favourable.

In SmC phase, when the constituent molecules are strongly axially polar, four sub phases are observed [119,148] identical to those of the SmA phase, except that the molecules are tilted with respect to the layer planes. In this case an additional subgroup has been found where the tilt direction appears to flip as one moves from one layer to the other and is called alternating smectic C (SmC_{alt}) [149-151].

Smectic B (SmB) phase:

Two distinct types of smectic B phase have been identified, one is called Hexatic B (SmB_{hex}) and the other one is Crystal B (B). In SmB_{hex} phase the molecular arrangement is close to that of the SmA phase, however, within a layer the molecules are arranged in close packed hexagonal symmetry [25,101, 110,152,153]. Although the positional ordering within the layer is short range, there is long range bond orientational order [109,154] in this phase. If the line joining the centres of mass of a molecule and its nearest neighbour is called a 'bond' then by 'long range bond orientational order' it is meant that the orientation of the hexagonal packing array is of long range. In Crystal B phase, additionally the molecules have long range positional order within the layers as well as along the layer normals [25,101,112,115]. However, in Crystal B phase the inter-layer stacking sequence may be of mono- (AAAA type), bi- (ABAB type) and tri- (ABCABC type) layers [155]. Even random ABCABC type packing is also reported[156]. Structures of SmB_{hex} and B phases have been shown in Figure 1.8.

Smectic E (SmE) phase:

The Smectic E phase is now designated as Crystal E (E) phase since it can also be considered as a 'soft' crystal like the B phase [157-160]. Doucet et al [158, 161] concluded that within the layers the molecules are packed in herringbone array with orthorhombic symmetry. The phase is, therefore, biaxial. The lath-like molecules rotate cooperatively about their long axes on a time scale of 10^{11} times

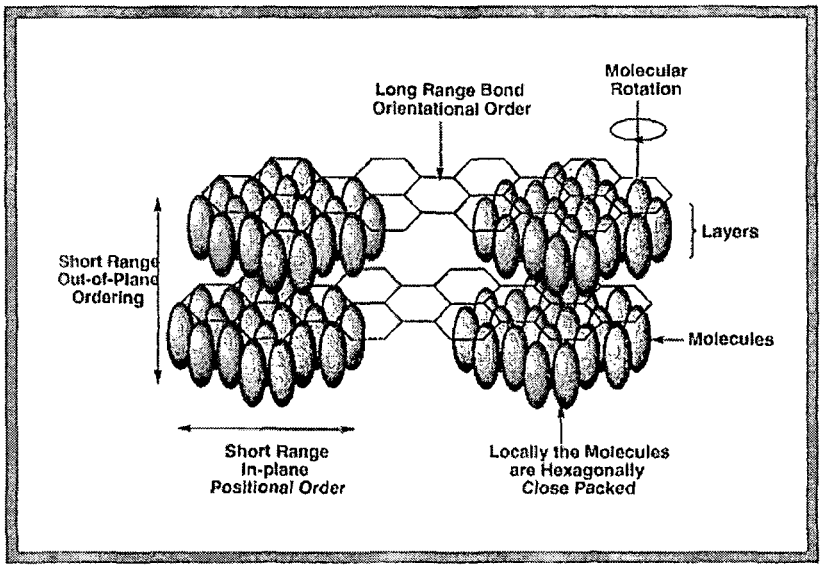

(a)

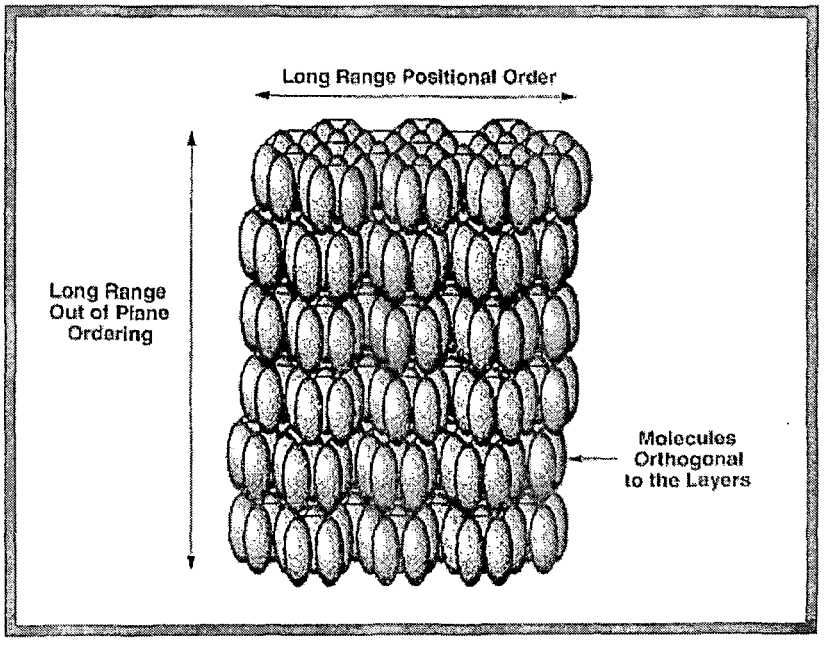

(b) From [17]

Figure 1.8 Structure of the (a) hexatic Smectic B phase, (b) Crystal B phase showing ABC packing.

per second [153,162] but unlike in B phase the motion is not full free rotation rather of an oscillatory nature. E phase is also found to have bilayer structure as in B phase [121].

Smectic I (SmI) and Smectic F (SmF) phases:

The structures of Smectic I phase is similar to SmB_{hex} but the molecules in this case are tilted within the layers, direction of tilt being towards an apex of the hexagonal packing net [113,118,163-166]. Thus it has short range in-plane and quasi-long range out-of-plane positional order as well as long-range bond orientational order in three dimension. The only difference in the molecular arrangement of Smectic F phase is that the tilt of the molecules is towards an edge of the hexagonal packing net [164,165]. In addition slightly longer correlation has been observed in the in-plane positional ordering than that found in Smectic I phase [167,168].

Smectic G, Smectic G′, Smectic H and Smectic H′ phases:

All these smectic phases are now termed respectively as Crystal G, Crystal J, Crystal H and Crystal K phase since they have long range three dimensional order [25,101,116,155,161,164,165,169,170] and they are like 'soft' crystals. In these cases the molecules are tilted with respect to the layer planes. The crystal J and G modifications are like the tilted Crystal B phase, direction of the tilt being that in SmI and SmF phases respectively (Figure 1.9). On the other hand the crystal H and K phases are like tilted Crystal E phase, the tilt direction is like that of SmI and SmF phases respectively. Thus the packing structure is pseudo-hexagonal in J and G whereas it is of monoclinic nature in H and K phases. Molecules are undergoing rapid reorientational motion about their long axes in J and G phases [25,101,155]. However, this motion is cooperative and oscillatory in nature in H and K phases like in the E phase [120,121].

The structural features of the phases observed in calamitic thermotropic type of liquid Crystals has been summarized in Table 1.1. No single liquid crystal

TABLE 1.1

Structural features of calamitic thermotropic liquid crystal phases.

Phase type	Molecular orientation	Molecular packing	Molecular orientational ordering	Bond orientational ordering	Positional ordering	
					Normal to the layer	within the layer
Isotropic	random	random	SRO	SRO	SRO	SRO
N	Parallelism of long molecular axis	random	LRO	SRO	SRO	SRO
SmA	orthogonal	random	LRO	SRO	QLRO	SRO
SmC	tilted	random	LRO	SRO	QLRO	SRO
SmB hex	orthogonal	hexagonal	LRO	LRO	QLRO	SRO
SmI	Tilt to apex of hexagon	pseudo hexagonal	LRO	LRO	QLRO	SRO
SmF	tilt to side of hexagon	pseudo hexagonal	LRO	LRO	QLRO	SRO
B	orthogonal	hexagonal	LRO	LRO	LRO	LRO
J	Tilt to apex of hexagon	pseudo hexagonal	LRO	LRO	LRO	LRO
G	tilt to side of hexagon	pseudo hexagonal	LRO	LRO	LRO	LRO
E	orthogonal	orthorhombic	LRO	LRO	LRO	LRO
K	tilted to longer side of cell	monoclinic	LRO	LRO	LRO	LRO
H	tilted to shorter side of cell	monoclinic	LRO	LRO	LRO	LRO

SRO→ short range order, LRO→ long range order, QLRO→ quasi-long range order

material is found to exhibit all the phases but many compounds are found to exhibit complex polymorphism, for example, the compound N-(4-n-pentyloxybenzylidene)-4'-n-hexylaniline possess the phases N, SmA, SmC, SmB, SmF and SmG phases (Figure 1.3). Current knowledge of phase sequencing with respect to temperature is found to be as follows [171]:

Isotropic, N_O, N_{SC} (or Ch), SmA, SmC, SmB_{hex}, SmI, SmF, B, J, G, E, K, H, Crystal

Decreasing temperature

Increasing order ⟶

1.2.2.4 *Ferroelectric Liquid Crystals*

The seven liquid crystal classes SmC, SmI, SmF, J, G , K and H are characterised by a tilt between the director and the normal to the smectic layers. If, additionally, the molecules are chiral, the material become optically active and show ferroelectric properties [42,45,172,173]. These phases are denoted by SmC*, SmI*, SmF*, J*, G* , K* and H*. By virtue of their symmetry, ferroelectric liquid crystals are piezoelectric too, because polarisation in these materials can be induced by mechanical stress. Antiferroelectric and ferrielectric liquid crystals phases have also been found. The constituent molecules of the antiferroelectric chiral smectic C (SmC^*_{anti}) phase have the tilted lamellar structure of the ferroelectric SmC* phase but the tilt direction alternates from layer to layer to give a zig-zag structure. Therefore, the spontaneous polarization of the phase is zero. The ferrielectric chiral smectic C (SmC^*_{ferri}) also has alternating tilted structure except that the alteration is not symmetrical and more layers are tilted in one direction than the other. Accordingly, the ferrielectric phase generates a spontaneous polarization which depends upon the degree of alternation of tilt directions. The study of ferroelectric liquid crystals has become important for their variety of applications such as in large area, high information content colour display devices and compounds having SmC* phase (both ferro and antiferro type) are mainly used for this purpose[174-178].

1.2.2.2 *Discotic Liquid Crystal*

Thermotropic mesomorphism has also been observed [179-181] in pure compounds consisting of simple disc-shaped molecules (one molecular axis is much shorter than the other two) and the mesophases formed by such compounds are called **discotic liquid crystals.** A large number of discotic compounds (also called **discogens**) have been synthesized and a variety of mesophases have been discovered [182-186]. A typical discotic liquid crystal molecule has been shown in Figure 1.10. Structurally most of the discotic liquid crystals fall into two distinct categories – the **columnar** and the **nematic.** In columnar phase, the disc-like molecules are stacked one on top of the other aperiodically to form liquid like

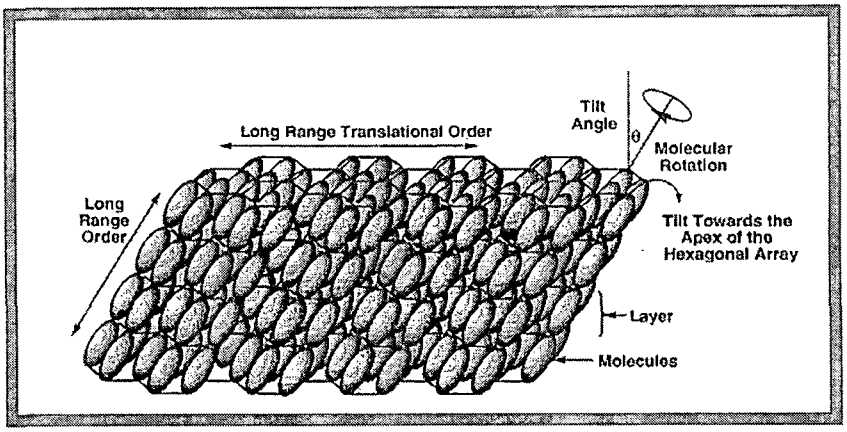

(a)

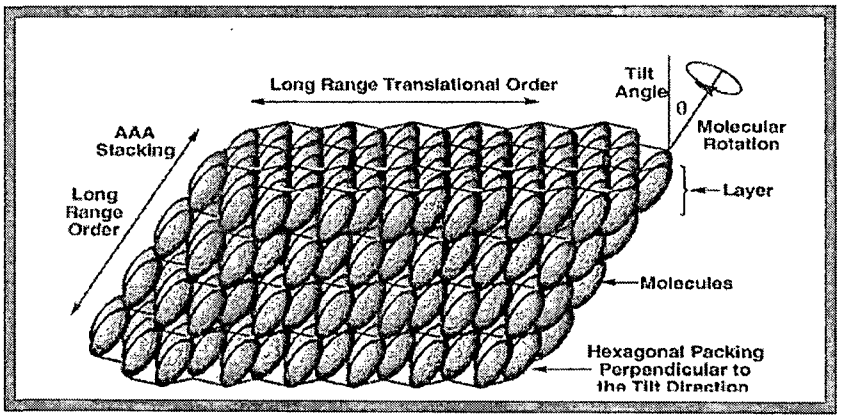

(b) From [17]

Figure 1.9 Structure of (a) crystal J phase and (b) crystal G phase.

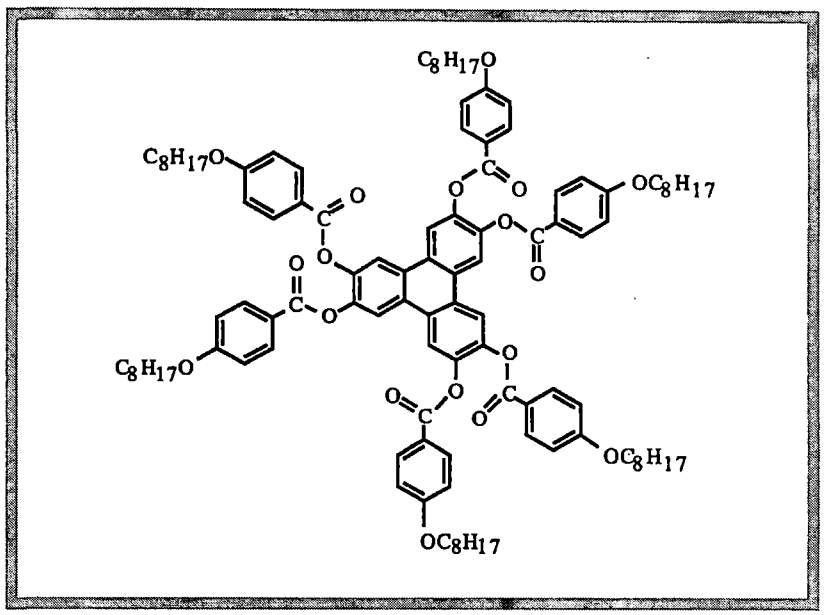

From [39]

Figure 1.10 Typical discotic liquid crystal molecule.

columns, the different columns constituting a two dimensional lattice. A number of variants of this structure have been identified: **hexagonal, rectangular** and **oblique** etc. The nematic discotic phase has an orientationally ordered arrangement of the discs without any long range translational order. This phase is optically negative. A cholesteric phase with disc-like molecules has also been identified [187,188]. A smectic-like lamellar phase of discotic liquid crystal has been reported [189-191] in the literature.

1.2.2.3 *Polymer Liquid Crystal*

Thermotropic liquid crystalline phases are also exhibited by some polymers [36,48,55,56]. The basic monomer units are lower molecular weight mesogens with rod-like or disc-like molecules, which are attached to the polymer backbone in the main chain, or as side groups (Figure 1.11). The nature of the mesophase depends rather sensitively on the backbone, the mesogenic unit and the spacers [192]. With rod-shaped repeating units in the polymers, mesophases similar to the nematic, cholesteric, smectic types of calamitic liquid crystals are observed [193-197],

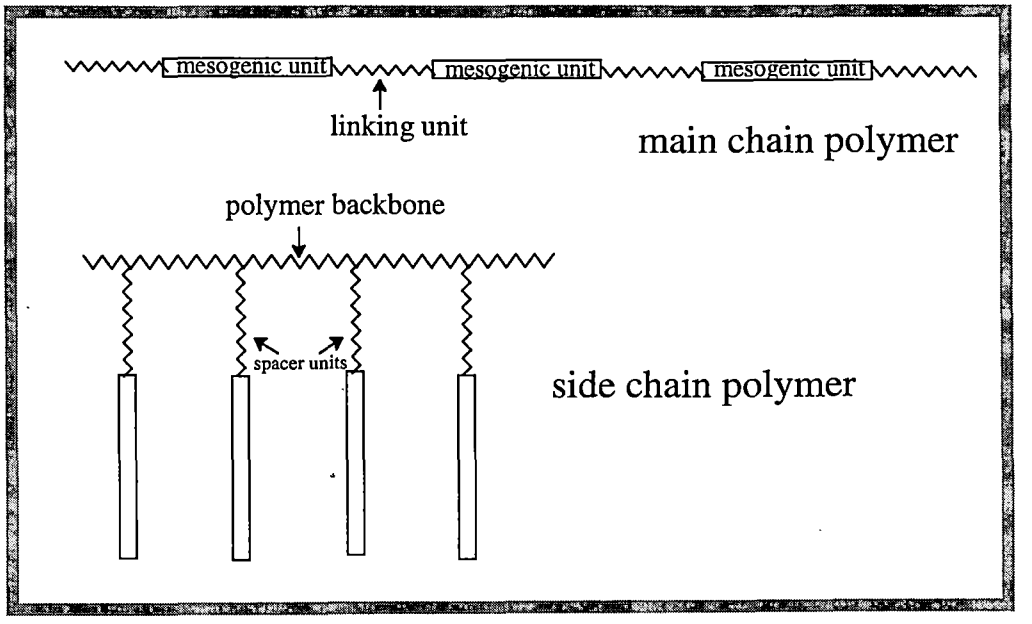

Figure 1.11 Schematic Polymer liquid crystal molecule (main and side chain).

whereas, with disc-shaped repeating units some new kinds of mesophase structures have been found [198-202] like **'sanidic'** (or board-like) nematic and **'columnar'** nematic phases.

Liquid crystals are also found to form with molecules other than the aforesaid molecular types viz. calamitic, chiral calamitic, discotic and polymeric . D. Demus has recently shown [10] in a review article that many different types of molecules can exhibit liquid crystallinity. For example, it has been shown that molecular shape may even be bowl-, sofa-, banana-, U-, H-, Y- and T-shaped[203-209]. A detailed discussion on liquid crystals in non-conventional materials like dimers, oligomers, dendrimers, plasmids, polycatenar, metallomesogens, charge-transfer systems, supramolecular hydrogen bonded systems have been made in reference [210]. Many other interesting liquid crystal phases have also been reported like frustrated chiral smectic A* or twist-grain boundary phase[211,212], reentrant phase [213-216], induced smectic phases [216-219] etc.

1.3 APPLICATIONS OF LIQUID CRYSTALS

Liquid crystals have got a wide range of scientific and technical applications due to their unique physical properties. There are several books and articles[28,30,42,48,49,50,220-240] which give an account of the applications of liquid crystals. General discussions on the principles of applications of liquid crystals have been given in references [232 - 240]. However, a brief outline of some of the applications of liquid crystals have been given here.

Since liquid crystals are very sensitive to even weak external perturbations they are used in measurement of temperature, pressure and chemical contamination. The helical pitch of cholesteric liquid crystals is highly sensitive to temperature and hence a slight change in temperature changes colour of the sample. Thus cholesteric liquid crystals have got interesting sensing applications[225, 226, 228,235]. One of these is the so called thermal mapping of components of electronic devices. The use of cholesteric liquid crystals as an investigative and diagnostic tool in medicine has become widespread. For example skin infections and malignant skin tumours may

From [39]

Plate 1 Privacy window using a polymer dispersed liquid crystal film.

From [39]

Plate 2 Portable computer with an active matrix colour liquid crystal display.

be detected and located by the use of cholesteric liquid crystals. It is possible due to the fact that the portion of the infected skin or tumour has higher temperature than the surrounding uninfected area.

The discovery of dynamic scattering mode in nematic liquid crystals [233,237-239] has opened a new area of electronic display technology. In thin layers nematic liquid crystals change their transmission properties for normal or polarised light when subjected to an electric field. This property is utilised for alphanumeric and analog display image converters and matrix type picture screens. Recently, ferroelectic liquid crystals (S_C*) are being used for a new generation of fast versatile liquid crystal devices [227,229,236]. Polymer dispersed liquid crystals (PDLC) form a relatively new class of materials which are used in many types of displays[227,231]. In practice liquid crystals are widely used in displays for watches, clocks, calculators, various digital panel meters, televisions, laptop computer monitors, note-book computers, mobile phone set, switchable windows and other light shutter devices [plate 1 and plate 2]. The relatively low optical contrast, low power consumption, light weight, etc. are the main advantages of liquid crystal displays (LCD's) over other types of displays. These facts have dramatically popularised the liquid crystal displays [240]. This trend will go up with the advent of better LC materials and improved technology paving a revolution in electronic communication system.

As the molecules of liquid crystals are oriented in magnetic field with optic axis parallel to the field, they are used as anisotropic solvents for nuclear magnetic resonance (NMR) measurements[227,234]. Liquid crystals are also used as solvents for the studies of infra red (IR) and ultra violet (UV) spectra of solute molecules in the form of liquid crystal films [231,234].

Liquid crystals are also used as solvents with stationary phases in gas liquid chromatography (GLC). Separation of compounds on the basis of molecular shape is the most promising practical application of liquid crystals in GLC [241,242]. The wider is the stationary mesophase range with higher molecular ordering the more effective is the liquid crystal in GLC.

1.4 NAME AND STRUCTURE OF THE INVESTIGATED COMPOUNDS

The name and structural formula of the nine compounds studied in the present work are given bellow. Abbreviated names are given within parentheses.

1. N, N′ –Bis (p-butoxybenzylidine)-α,α′ -bi-p-toluidine (BBBT)

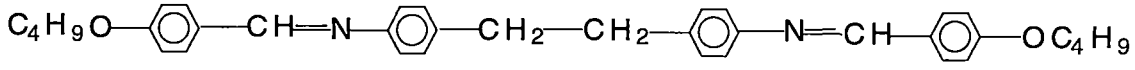

2. N, N′ –Bis (p-methoxybenzylidine)-α,α′ -bi-p-toluidine (BMBT)

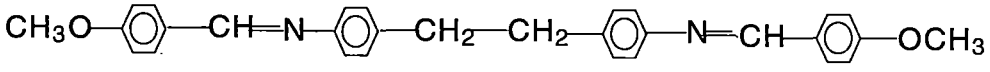

3. N-(4-n-hexyloxybenzylidene)-4′- phenylazoaniline (6OBPAA)

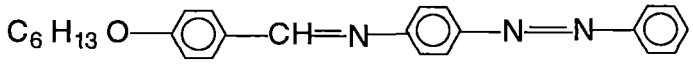

4. N-(4-n-octyloxybenzylidene)-4′- phenylazoaniline (8OBPAA)

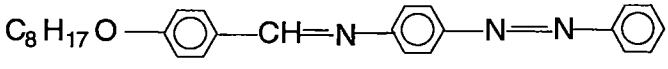

5. 4-n-ethyl 4′cyanobiphenyl (2CB)

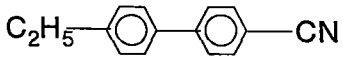

6. p-butoxyphenyl *trans*-4- propylcyclohexane carboxylate (BPPCC)

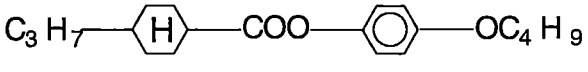

7. 5-(4-ethylcyclohexyl) -2- (4-Cyanophenyl) pyrimidine (ECCPP)

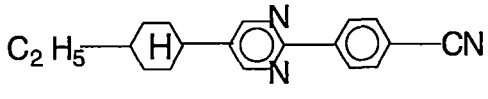

8. 5-(trans-4-pentylcyclohexyl)-2- (4-cyanophenyl) pyrimidine (PCCPP)

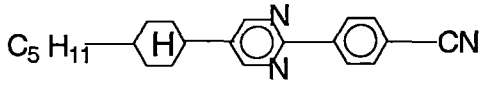

9. 5-(trans-4-heptylcyclohexyl)-2- (4-cyanophenyl) pyrimidine (HCCPP)

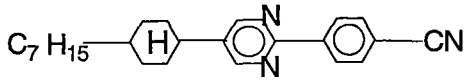

1.5 SCOPE AND AIM OF THE WORK

Liquid crystals have widespread scientific and technological applications for which identification of different phases, their different macroscopic and microscopic properties (like order parameters, dielectric constants, intermolecular interactions, etc.), crystal and molecular structure analysis are very important. Since, in commercial liquid crystal display devices multicomponent mixtures are always used to optimize the relevant physical parameters, studies on mixtures, in addition to the pure components, are also important. In view of this, texture studies by optical microscopy, DSC studies, X-ray diffraction studies, static dielectric anisotropy studies as well as crystal and molecular structural analysis and intermolecular interaction energy calculation on the above compounds and some binary mixtures are undertaken in the present dissertation. Results have been interpreted and tried to explain in the light of existing ideas and theories. Results obtained on the present systems have also been compared with those of structurally similar compounds to get better idea about structure-property relationship.

Texture and X-ray studies on, (a) BMBT and BBBT, (b) 6OBPAA, 8OBPAA and their equimolar mixture and (c) three binary mixtures of BPPCC and 2CB, are made for phase identification and determination of apparent molecular length, layer spacing, intermolecular distance, orientational order parameters of magnetically aligned samples. Temperature variation of some of the physical parameters have also been studied. The orientational order parameter values at different temperatures have been compared with those obtained from Maier-Saupe theory (for nematic

phase) and McMillan's theory (for smectic A phase). D.S.C. studies on BBBT and BMBT have also been carried out for evaluation of transition temperatures, transition enthalpies and entropies. Static dielectric studies on BPPCC and its mixtures with 2CB have also been made to determine the principal dielectric constants ($\varepsilon_{\parallel}$ and $\varepsilon_{\perp}$), dielectric anisotropy ($\Delta\varepsilon$) and mean dielectric constant ($\bar{\varepsilon}$) at different temperatures. Effective values of the molecular dipole moments in the mesophase have been calculated using Maier and Meier theory. Dipole-dipole correlation factors ($g_{\parallel}$ and $g_{\perp}$) for BPPCC have also been calculated.

The crystal and molecular structures of 2CB and BPPCC have been determined by direct methods from single crystal X-ray intensity data and attempts have been made to explain mesophase formation and stability in the light of the packing of the molecules in the crystalline state.

The pair intermolecular interaction energies of ECCPP, PCCPP and HCCPP have been calculated by atom-atom potential method taking into account the Van der Waals' and electrostatic interactions. The minimum energy configuration of dimers of these mesogens have been compared with the previous data obtained from crystal structure analysis and X-ray scattering studies in mesophases.

A brief review on different types of liquid crystal phases exhibited by different types of molecules has been made at the outset. Theoretical aspects relevant to the present work in brief and the experimental techniques and data analysis procedures in detail have also been described before presenting the results.

REFERENCES

1. F. Reinitzer, *Monatsh Chem.*, **9**, 421 (1888).
2. O. Lehmann, *Z. Physik.* Chem., **4**, 462 (1889).
3. O. Lehmann, *Z. Physik. Chem.*, **5**, 427 (1890).
4. H. Kelker, *Mol. Cryst. Liq. Cryst.*, **21**, 1 (1973).
5. G. Friedel, *Ann. Physique(Paris)*, **18**, 273 (1922).
6. G. Friedel and E. Friedel, *Z. Krist.*,**79**,1, (1931).
7. H. Kelker, , *Mol. Cryst. Liq. Cryst.*, **21**, 1 (1973)
8. H. Kelker and P. M. Knoll, Liquid. Cryst. **5**(1), 19 (1989).
9. G. W. Gray, *Liq. Cryst.*, **24**(1), 5 (1998).
10. D. Demus, *Mol. Cryst. Liq. Cryst.*, **364**, 25 (2001).
11. W. Kast, *Landolt - Börnstein Tables*, Vol. **II**, 6th edition, Part 2a p. 266, Springer - Verlag (1960).
12. H. Zocher, *Liquid crystals (2)*, Part-I, Ed. G. H. Brown, G. & B. Science Publishers, Inc., N.Y., (1969).
13. G. H. Brown, *J. Electronic Materials*, **2**, 403 (1973).
14. H. Kelker and R. Hatz, *Hand Book of Liquid Crystals*, Verlag - Chemie, Weinheim (1980).
15. D. Demus and H. Zaschke, *Flüssige Kristalle in Tabellen*, Vol. **II**, VEB Deutscher Verlag für Grundstoff industrie, Leipzig (1984).
16. V. Vill, Liq. Cryst. Database, Ver. 2.1, LC Publisher, GmbH, Humberg (1996).
17. D. Demus, J. Goodby, G.W. Gray, H.-W. Spiess and V. Vill, *Handbook of Liquid Crystals*, Vols. **1**, **2A**, **2B**, **3**, Wiley-VCH, Verlag GmbH, Weinheim, FRG (1998).
18. G. W. Gray, *Molecular Structure and the Properties of Liquid Crystals*, Academic Press, London (1962).
19. P. G. de Gennes, *The Physics of Liquid Crystals*, Clarendon Press, Oxford (1974). 2nd Ed., P. G. de Gennes and J. Prost (1993).
20. E. B. Priestley, P. J. Wojtowicz and P. Sheng, Eds., *Introduction to Liquid Crystals*, Plenum Press, NY, (1974).
21. S. Chandrasekhar, *Liquid Crystals*, 2nd edition, Cambridge University Press, Cambridge (1992).
22. G. W. Gray and P. A. Winsor, Eds., *Liquid Crystals and Plastic Crystals*, Vol. I and II, Ellis Horwood Limited (1974).
23. G. Vertogen and W. H. de Jeu, *Thermotropic liquid crystals: Fundamentals*, Springer – Verlag, Berlin (1988).
24. P. S. Pershan, *Structure of Liquid Crystals Phases*, World Scientific Lecture Note in Physics, Vol 23, World Scientific, Singapore (1988).

25. G. W. Gray and J. W. Goodby, Eds., *Smectic Liquid Crystals, Textures and Structures,* Leonard - Hill, Philadelphia(1984).

26. G. R. Luckhurst and G. W. Gray, Eds., *The Molecular Physics of Liquid Crystals*, Academic Press, New York (1979).

27. G. H. Brown, Ed., *Advances in Liquid Crystals,* Vols. I – VI, Academic Press (1975-1983).

28. B. Bahadur, Ed., *Liquid Crystals: Applications and Uses*, Vol I-III, World Scientific, Singapore (1990).

29. A. A. Sonin, *The Surface Physics of Liquid Crystals*, Gordon & Breach Publishers(1995).

30. G. Meier, E. Sackmann and J. G. Grabmaier, Eds., *Applications of Liquid* Crystals, Springer Verlag(1975)

31. L.Liebert, Ed., *Liquid Crystals*, Solid State Physics Suppl., **14**, AP(1978).

32. D. Demus and L. Richter, Eds., *Textures of Liquid Crystals*, Verlag Chemie(1978).

33. G. H. Brown and J. J. Wolken, Eds., *Liquid Crystals and Biological Structures*, AP(1979).

34. S. Chandrasekhar, Ed., *Liquid Crystals,* Proceedings of the International Conf., Bangalore, 1979, Heyden, London(1980).

35. W. H. de Jeu, *Physical properties of Liquid Crystalline materials*, G & B Pub., New York(1980).

36. A. Ciferri, W. R. Krigbaum and R. B. Meyer, Eds., *Polymeric Liquid Crystals,* AP, New York(1982).

37. A. L. Tsykalo, Ed.., *Thermophysical Properties of Liquid Crystals*, G & B(1991).

38. S. Kumar, Ed., *Liquid Crystals in the nineties and Beyond,* World Scientific(1995).

39. P. J. Collings and M. Hird, *Introduction to Liquid Crystals Chemistry and Physics,* Taylor & Francis(1998).

40. D. A. Dunmur, A. Fukuda and G. R. Luckhurst (Eds.), *Physical properties of liquid* crystals, INSPEC, London(2001).

41. N.V. Madhusudana, Ed., *Liquid Crystals and Other Soft Materials,* Indian Academy of Sciences, Bangalore (1999).

42. J. W. Goodby, R. Blinc, N. A. Clark, S. T. Lagerwall, M. A. Osipov, S. A. Pikin, T. Sakurai, K. Yoshino and B. Zeks, "*Ferroelectric Liquid Crystals: Principles, Properties and Applications*", Gordon and Breach, Philadelphia (1991).

43. L. M. Blinov, *Electro-optical and Magneto-optical Principles of Liquid Crystals*, Wiley, Chichester(1983).

44. L. M. Blinov and G. Chigrinov, *Electro-optic Effects in Liquid Crystal Materials*, Wiley, Chichester(1983).

45. A. Buka, *Modern topics in Liquid Crystals: From Neutron Scattering to Ferroelectricity*, World Scientific, Singapore(1993).

46. J. H. Clint, *Surfactant Aggregation*, Blackie, Glasgow(1991).

47. P. J. Collings, *Liquid Crystals: Nature's Delicate Phase of Matter,* Princeton Univ. Press, Princeton (1990).

48. A. A. Collyer, *Liquid Crystal Polymers: From Structures to Applications,* Elsevier, Oxford (1993).

49. R. Y. Dong, *Nuclear Magnetic Resonance of Liquid Crystals,* Springer-Verlag, New York(1994).

50. J. L. Ericksen and D. Kinderlehrer, Eds., *Theory and Applications of Liquid Crystals,* Springer-Verlag, New York(1987)

51. E. I. Kats and V. V. Lebedev, *Fluctuation Effects in the Dynamics of Liquid Crystals,* Springer-Verlag, New York(1994).

52. I. C. Khoo, Ed., *Physics of Liquid Crystalline Materials,* G & B, Amsterdam(1991).

53. I. C. Khoo and S. T. Wu, *Optics and non-linear optics of Liquid Crystals,* World Scientific, Singapore(1993).

54. S. Martelucci and A. N. Chester, Eds., *Phase Transitions in Liquid Crystals*, Plenum, New York(1992).

55. C. B. McArdle, *Side Chain Liquid Crystal Polymers*, Blackie, Glasgow(1989).

56. A. M. White and A. H. Windle, *Liquid Crystalline Polymers,* CUP, Cambridge(1992).

57. W. Helfrich and G. Heppke, *Liquid Crystals of One and Two Dimensional Order*, Springer–Verlag, New York(1980).

58. A. S. C. Lawrence, *Mol. Cryst. Liq. Cryst*, **7**, 1 (1960).

59. P. A. Winsor, *Chem. Rev.*, **68**, 1 (1968).

60. P. Ekwall, L. Mandell and K. Fontell, *Mol. Cryst. Liq. Cryst.*, **8,** 157 (1969).

61. V. Luzzati and F. Reiss-Husson, *Nature*, **210**, 1351 (1966).

62. V. Luzzati and A.Tardieu, *Annual Review of Physical Chemistry*, **25**, 79 (1974).

63. D. M. Small in *Liquid Crystals 2 – Part-I,* Ed. G. H. Brown, G. & B. Science Publishers, p. 209 (1969).

64. A. E. Skoulios and V. Luzzati, *Acta. Cryst.*, **14**, 278 (1961).

65. S. Friberg, *J. Am. Oil. Chem. Soc.*, **48**, 578 (1971).

66. F. B. Rosevear, *J. Soc. Cosmet. Chem.*, **19**, 581 (1968).

67. P. A. Winsor, *Mol. Cryst. Liq. Cryst.*, **12**, 141 (1971).

68. G. H. Brown, J. W. Doane and V. D. Neff, *A Review of the Structure and Physical Properties of Liquid Crystals*, Butterworths, London (1971).

69. V. Luzzati, A.Tardieu, T. Gulik – Krzywickyi, E. Rivas, and F. Reiss – Husson, *Nature,* **220**, 485 (1968).

70. K. D. Lawson and T. J. Flautt, *J. Am. Chem. Soc.*, **89**, 5489 (1967).

71. J. M. Seddon, *Biochim. et Biophys. Acta.*, **1031**, pp. 1 – 69 (1990).

72. C. Robinson, *Trans. Faraday Soc.*, **52**, 571 (1956).

73. D. Chapman, *Faraday Soc. Symp.*, No.5, 163 (1971).

74. L. J. Yu and A. Saupe, *Phys. Rev. Lett.*, **45**, 1000 (1980).

75. K. Praefcke, B. Kohne, B. Gundogan, D. Singer, D. Demus, S. Diele, G. Pelzl and U. Bakowsky, *Mol. Cryst. Liq. Cryst.*, **198**, 393 (1991).

76. S. Chandrasekhar, B. K. Sadashiva, S. Ramesha and B. S. Srikanta, *Pramana, J. Phys.*, **27**, L713 (1986).

77. S. Chandrasekhar, B. K. Sadashiva, B. R. Ratna and V. N Raja, *Pramana, J. Phys.*, **30**, L49 (1988).

78. K. Praefcke, B. Kohne, D. Singer, D. Demus, , G. Pelzl and S. Diele, *Liquid Crystals*, **7**, 589 (1990).

79. S. Chandrasekhar, B. R. Ratna, B. K. Sadashiva and V. N Raja, *Mol. Cryst. Liq. Cryst.*, **165**, 123 (1988).

80. S. Chandrasekhar V. N Raja and B. K. Sadashiva, *Mol. Cryst. Liq. Cryst. Lett.*, **7**, 65 (1990).

81. F. Hessel and H. Finkelmann, *Polymer Bull.*, **15**, 349 (1986).

82. A.H. Windle, C. Viney, R. Golombok, A.M. Donald and G.R. Mitchell, *Faraday Disc. Chem. Soc.*, **79**, 55 (1985).

83. A. M. Figueiredo Neto, A. M. Levelut, L. Liebert and Y. Galerne, *Mol. Cryst. Liq. Cryst.*, **129**, 191 (1985).

84. B. K. Sadashiva in *Handbook of Liquid Crystals*. Vol. **2B** "Low Molecular Weight Liquid Crystals II", Ed. D. Demus, J. Goodby, G. W. Gray, H.-W. Spiess and V. Vill, WILEY-VCH, Verlag GmbH, Weinheim, FRG 1998.

85. A. de Vries, *Mol. Cryst. Liq. Cryst.*,**10**, 31(1970).

86. A. de Vries, *Mol. Cryst. Liq. Cryst.*,**10**, 219 (1970).

87. A. de Vries, *Pramana Suppl. No.1*, pp. 93-113 (1975).

88. J. L. Fergason, *Sci. Am.*, **211**, 77(1964).

89. D. Demus, J. Goodby, G.W. Gray, H.-W. Spiess and V. Vill, *Handbook of Liquid Crystals*, Ch. IV and V, Vol. **2A**, Wiley-VCH, Verlag GmbH, Weinheim, FRG (1998).

90. F.D. Saeva, *Mol. Cryst. Liq. Cryst.*, **23**, 171 (1973).

91. G.H. Brown, *Am. Scientist*, **60**, 64 (1972).

92. T. Nakagiri, H. Kodama and K.K. Kobayashi, *Phys. Rev. Lett.*, **27**, 564 (1971).

93. I.G. Chistiyakov, *Sov. Phys. Usp.*, **9**, 551 (1967).

94. A.D. Buckingham, G.P. Ceaser and M.B. Dunn, *Chem. Phys. Lett.*, **3**, 540 (1969).

95. G.W. Gray, in '*The Molecular Physics of Liquid Crystals*', eds. G.R. Luckhurst and G.W. Gray , Academic Press (London), p.5 (1979).

96. A. Hochbaum, *Fluorescent Guest-Host in Scattering Liquid crystals and New Physical Phenomena in Thin Liquid Crystal Films* (Ph.D. Thesis), Temple University, p.5 (1980).

97. J.J. Wysocki, J. Adams and W. Hasse, *Phys. Rev. Lett.*, **20**, 1024 (1968).

98. H. Baessler and M.M. Labes, *Phys. Rev. Lett.*, **21**, 1791(1968).

99. P. Crooker, *Liq. Cryst.*, **5**, 571(1989).

100. H. Stegemeyer, *Liq. Cryst.*, **1**, 3(1986).

101. A. J. Leadbetter in *Thermotropic Liquid Crystals, Critical Reports on Applied Chemistry,* Vol. 22, G. W. Gray(Ed.),Wiley, Chichester(1987),p1

102. A. de Vries in *Liquid Crystals, The Fourth State of Matter*(Ed. F. D. Saeva), Marcell Dekker, New York(1972),p1.

103. A. de Vries, *Mol. Cryst. Liq. Cryst.*, **63**, 215(1981).

104. J. Doucet in *The Molecular Physics of Liquid Crystals* (Eds. G. R. Luckhurst and G. W. Gray), Academic Press, London (1979), p317.

105. L. V. Azaroff, *Mol. Cryst. Liq. Cryst.*, **60**, 73(1980).

106. D. Demus, J. W. Goodby, G. W. Gray and H. Sackmann, *Mol. Cryst. Liq. Cryst.*, **56**, 311(1980).

107. G. W. Gray, *Mol. Cryst. Liq. Cryst.*, **63**, 3(1981).

108. J. W. Goodby and G. W. Gray, *Mol. Cryst. Liq. Cryst.*, **41**, 145(1978).

109. R. J. Birgeneau and J. D. Litster, *J. de Physique Letters*, **39**, 399(1978)

110. R. Pindak, D. E. Moncton, S. C. Davey and J. W. Goodby, *Phys. Rev. Lett.*, **46**, 1135(1981).

111. P. S. Pershan, G. Aeppli, J. D. Litster and R. J. Birgeneau, *Mol. Cryst. Liq. Cryst.*, **67**, 205(1981).

112. D. E. Moncton, and R. Pindak, *Phys. Rev. Lett.*, **43**, 701(1979).

113. J. Budai, R. Pindak, S. C. Davey, J. W. Goodby, *J. Phys. (Paris) Lett.*, **41**, 1371(1980).

114. J. J. Benattar, F. Moussa, M. Lambert, *J. Chim. Phys.*, **80**, 99(1983).

115. A.J. Leadbetter, M.A. Mazid, B.A. Kelley, J.W. Goodby and G.W. Gray, *Phys. Rev. Lett.*, **43**, 630 (1979).

116. G. W. Gray in *The Molecular Physics of Liquid Crystals*, Eds. G. R. Luckhurst and G. W. Gray, Academic Press, London (1979), Ch. 12;
A.J. Leadbetter in *The Molecular Physics of Liquid Crystals*, Eds. G. R. Luckhurst and G. W. Gray, Academic Press, London (1979), ch.13;
J. Doucet in *The Molecular Physics of Liquid Crystals*, Eds. G. R. Luckhurst and G. W. Gray, Academic Press, London (1979), ch. 14.

117. J. J. Benattar, F. Moussa, M. Lambert, *J. Phys. (Paris) Lett.*, **45**, 1053(1984).

118. J. J. Benattar, F. Moussa, M. Lambert, A. M. Levelut, *Phys. Rev.*, **20A**, 2505(1979).

119. F. Hardouin, N.H. Tinh, M.F. Achard and A.M. Levelut, *J. Phys. Lett.* (Paris), **43**, L327 (1982).

120. R.M. Richardson, A.J. Leadbetter and J.C. Frost, *Mol. Phys.*, **45**,1163(1982).

121. A.J. Leadbetter, J.C. Frost, J.P. Gaughan, and M. A. Mazid, *J. Phys.* (Paris), **40**, C3-185 (1979).

122. A.J. Leadbetter, J.C. Frost, J.P. Gaughan, G.W. Gray and A. Mosley, *J. Phys.* (Paris), **40**, 375 (1979).

123. A. J. Leadbetter, J. L. Durrant and M. Rugman, *Mol. Cryst. Liq. Cryst. Lett.*, **34**, 231 (1977).

124. J. Prost, *Advances in Physics*, **33**, 1(1984).

125. J. Prost and P. Barois, *J. Chim. Phys.*, **80**, 65(1983).

126. S. Diele, P. Brand and H. Sackmann, *Mol. Cryst. Liq. Cryst.*, **16**, 105 (1972).

127. G. Sigaud, F. Hardouin, M.F. Achard and H. Gasparoux, *J. Phys.* (Paris), **40**, C3-356(1979).

128. B. R. Ratna, R. Shashidhar and V. N. Raja, *Phys. Rev. Lett.*, **55**(14), 1476(1985)

129. J. Prost, *J. de Physique*, **40**, 581(1979)

130. G.C. Fryberg, E. Gelerinter and D.L. Fishel, *Mol. Cryst. Liq. Cryst.*, **16**, 39(1972).

131. G.R. Luckhurst and A. Sanson, *Mol. Cryst. Liq. Cryst.*, **16**, 179 (1972).

132. A.M. Levelut, R.J. Tarento, F. Hardouin, M.F. Achard and G. Sigaud, *Phys. Rev.*, **A24**, 2180 (1981).

133. G. Sigaud, F. Hardouin, M.F. Achard and A.M. Levelut, *J. Phys.* (Paris), **42**,107 (1981).

134. C. Druon and J.M. Wacrenier, *Mol. Cryst. Liq. Cryst.*, **98**, 201 (1983).

135. I. Hatta, Y. Nagai, T. Nakayama and S. Imaizumi, *J. Phys. Soc. Jpn.*, **52**, Suppl. 47(1983).

136. F. Hardouin, A.M. Levelut, M.F. Achard and G Sigaud, *J. de Chemie Physique*, **80**, 53 (1983).

137. N.H. Tinh, P.Foucher, C. Destrade, A.M. Levelut and J. Malthete, *Mol. Cryst. Liq. Cryst.*, **111**, 277 (1984).

138. S. Diele, G. Pelzl, I. Latif and D. Demus, *Mol. Cryst. Liq. Cryst.*, **92**, 27 (1983).

139. N.A.P. Vaz, Z. Yaniv and J.W. Doane, *Mol. Cryst. Liq. Cryst.*, **92**, 75 (1983).

140. F. Hardouin, A.M. Levelut, J. Bennattar and G. Sigaud, *Solid State Comm.*, **33**, 337 (1980).

141. F. Hardouin and A.M. Levelut, *J. Phys.* (Paris), **41**, 41 (1980).

142. G. Sigaud, N.H. Tinh, F. Hardouin and H. Gasparoux, *Mol. Cryst. Liq. Cryst.*, **69**, 81 (1981).

143. G. J. Brownsey and A.J. Leadbetter, *Phys. Rev. Lett.*, **44**, 1608 (1980).

144. K.A. Suresh, R. Shashidhar, G. Heppke and R. Hopf, *Mol. Cryst. Liq. Cryst.*, **99**, 249 (1983).

145. A. de Vries, *J. Phys. (Paris)*, **C36**, Cl-1(1975).

146. T.R. Taylor, J.L. Fergason and S.L. Arora, *Phys. Rev. Lett.*, **24**, 359(1970).

147. T.R. Taylor, S.L. Arora and J.L. Fergason, *Phys. Rev. Lett.*, **25**, 722(1970).

148. N. H. Tinh, F. Hardouin and C. Destrade, *J. Phys.* (Paris), **43**, 1127 (1982).

149. A. M. Levelut, C. Germain, P. Keller, L. Liebert, J. Billard, *J. Phys.* (Paris), **44**, 623 (1983).

150. Y. Galerne and L.Liebert, *Phys. Rev. Lett.*, **64**, 906 (1990).

151. I. Nishiyama, J. W. Goodby, *J. Mater. Chem.*, **2**, 1015 (1992).

152. D. E. Moncton and R. Pindak in *Ordering in Two Dimensions* (Ed. S. K. Sinha), North Holland, New York (1980), p83.

153. A. J. Leadbetter, J. C. Prost, M. A. Mazid, *J. Phys. (Paris) Lett.*, **40**, 325 (1979).

154. B. J. Halperin and D. R. Nelson, *Phys. Rev. Lett.*, **41**, 121(1978).

155. A.J. Leadbetter, M.A. Mazid and R.M. Richardson, *Liquid Crystals*, Ed. S. Chandrasekhar, Heyden, London, p. 65(1980).

156. J. Collett, L. B. Sorensen, P. S. Pershan, J. D. Litster, R. J. Birgeneau and J. Als-Nielsen, *Phys. Rev. Lett.*, **49**, 553(1982).

157. S. Diele, P. Brand and H. Sackmann, *Mol. Cryst. Liq. Cryst.*, **17**, 163(1972).

158. J. Doucet, A.M. Levelut, M. Lambert, L. Lievert and L. Strzelecki, *J. Phys.* (Paris), Colloq. 36:Cl-13 (1975).

159. D. Coates, G.W. Gray and K.J. Harrison, *Mol. Cryst. Liq. Cryst.*, **22**, 99 (1973).

160. D.B. Chung, Ph.D. Dissertation, Kent State University, Kent, Ohio, p.75 (1974).

161. A. M. Levelut, J. Doucet and M. Lambert, *J. Phys. (Paris)*, **35**, 773(1974)

162. A. J. Leadbetter, R. M. Richardson C. J. Carlile, *J. Phys. (Paris)*, **37**, 65(1976)

163. J. W. Goodby and G. W. Gray, *J. Phys. (Paris)*, **40**, 27(1979)

164. A.J. Leadbetter, J.P. Gaughan, B. Kelley, G.W. Gray and J.W. Goodby, *J. Phys.* (Paris), **40**, 178 (1979).

165. P.A.C Gane, A.J. Leadbetter and P.G. Wrighton, *Mol. Cryst. Liq. Cryst.*, **66**, 247 (1981).

166. S. Diele, D. Demus and H. Sackmann, *Mol. Cryst. Liq. Cryst.* Lett. , **56**, 217 (1980).

167. J. J. Benattar, F. Moussa, M. Lambert, *J. Phys. (Paris) Lett.*, **41**, 1371(1980).

168. J. J. Benattar, F. Moussa, M. Lambert, *J. Phys. (Paris) Lett.*, **42**, 67(1981).

169. J. Doucet and A. M. Levelut, *J. Phys. (Paris) Lett.*, **38**, 1163(1977).

170. J. Doucet, P. Keller, A.M. Levelut and P. Porquet, *J. Phys. (Paris)*, **30**, 548 (1978).

171. D. Demus, J. Goodby, G.W. Gray, H.-W. Spiess and V. Vill, Eds., *Handbook of Liquid Crystals*, Vol.**2A**,Wiley-VCH, Verlag GmbH, Weinheim, FRG (1998), Ch1.

172. L. A. Beresnev, L. M. Blinov, M. A. Osipov and S. A. Pikin, *Mol. Cryst. Liq. Cryst.*, **158A**, 3(1988); K. Skarp and M.A. Handschy, *Mol. Cryst. Liq. Cryst.*, **165**, 439 (1988).

173. D. Demus, J. Goodby, G.W. Gray, H.-W. Spiess and V. Vill, *Handbook of Liquid Crystals*, Eds.,Vol.**2B**,Wiley-VCH, Verlag GmbH, Weinheim, FRG (1998), Ch VI.

174. N. A. Clark and S. T. Lagerwall, *Appl. Phys. Lett., 36,* 899(1980).

175. D. Armitage, J. I. Thakara and W. D. Eades, *Ferroelectrics,* **85**, 291(1988).

176. S. Matsumoto, H. Hatoh and A. Murayama, *Liq. Crystals,* **5**, 1345(1989).

177. J. Dijon in *Liquid Crystal Application and Uses* (Ed. B. Bahadur), Vol. I, World Scientific, Singapore (1990), p 305.

178. A. Fukuda in *Proceedings of the 15th International Display Research Conference,* pS6-1 (1995).

179. D. Demus, J. Goodby, G.W. Gray, H.-W. Spiess and V. Vill, Eds., *Handbook of Liquid Crystals*, Vol.**2B**,Wiley-VCH, Verlag GmbH, Weinheim, FRG (1998), Ch VIII.

180. S. Chandrasekhar, *Liquid Crystals*, 2nd edn, Cambridge University Press, Cambridge (1992),Ch 6.

181. S. Chandrasekhar, B.K. Sadashiva and K.A. Suresh, *Pramana*, **9**, 471 (1977).

182. A.M. Levelut, *J. Chim. Phys.*, **80**, 149 (1983).

183. C. Destrade, P. Foucher, H. Gasparoux, N.H. Tinh, A.M. Levelut and J. Malthete, *Mol. Cryst. Liq. Cryst.*, **106**, 121 (1984).

184. S. Chandrasekhar, in *Advances in Liquid Crystals*, Ed. G.H. Brown, Vol. 5, p. 47 Academic Press, NY (1982).

185. S. Chandrasekhar, *Phil. Trans. Roy. Soc. London*, **A309**, 93 (1983).

186. S. Chandrasekhar and G.S. Ranganath, *Rep. Prog. Phys.*, **53**, 57 (1990).

187. C. Destrade, N.H. Tinh, J. Malthete and J. Jacques, *Phys. Lett*, **79A**, 189 (1980).

188. J. Malthete, C. Destrade, N.H. Tinh and J. Jacques, *Mol. Cryst. Liq. Cryst. Lett.*, **64**, 233 (1981).

189. A.M. Giroud-Godquin and J. Billard, *Mol. Cryst. Liq. Cryst.*, **66**, 147 (1981).

190. K. Ohta, H. Muroki, A. Takagi, K.I. Hatada, H. Ema, I. Yamamoto and K. Matsuzaki, *Mol. Cryst. Liq. Cryst.*, **140**, 131 (1986).

191. A.C. Rebeiro, A.F. Martins and A.M. Giroud-Godquin, *Mol. Cryst. Liq. Cryst. Lett.*, **5**, 133 (1988).

192. P. J. Collings and M. Hird, *Introduction to Liquid Crystals Chemistry and Physics,* Taylor & Francis(1998), Ch 5.

193. A. Blumstein, Ed., *Liquid Crystalline Order in Polymers*, Academic Press, NY (1978).

194. H. Finkelman, J. Koldehoff, H. Ringsdorf, *Angew. Chem. Int. Ed. Engl.*, **17**, 935 (1978).

195. S.G. Kostromin, V.V. Sinitzyn, R.V. Talroze, V.P. Shibaev and N.A. Plate, *Macromol. Chem., Rapid Comm.*, **3**, 809 (1982).

196. H. Ringsdorf and A. Schneller, *Macromol. Chem., Rapid Comm.*, **3**, 557 (1982).

197. E.T. Samulski, *Physics Today*, **35**, 40 (1982).

198. O. Herrmann-Schönherr, J. H. Wendorff and H. Ringsdorff, *Macromol. Chem., Rapid Comm.*, **7**, 97 (1986).

199. O. Herrmann-Schönherr, J. H. Wendorff, H. Ringsdorff and P. Tschirner, *Macromol. Chem., Rapid Comm.*, **7**, 791 (1986).

200. M. Ebert, O. Herrmann-Schönherr, J. H. Wendorff, H. Ringsdorff and P. Tschirner, *Macromol. Chem., Rapid Comm.*, **9**, 445 (1988).

201. H. Ringsdorf, R. Wüsterfeld, E. Zerta, M. Ebert and J. H. Wendorff, *Angew. Chem. Int. Ed. Engl.*, **28**, 914 (1989).

202. H. Ringsdorf and R. Wüsterfeld, in *Molecular Chemistry for Electronics,* Eds. P. Day, D.C. Bradley and D. Bloor, The Royal Soc., London, p. 23 (1990); ibid, *Phil. Trans. Roy. Soc.*, **A330**, 95 (1990).

203. X. J. Wang, K. Tao, J. A. Zhaoand L. Y. Wang, *Liq. Crystals,* **5(2)**, 563 (1989).

204. T. Niori, T. Sekine, J. Watanabe, T. Furukawa and H. Takezoe, *J. Mater. Chem.,* **6**, 1231(1996).

205. W. Weissflog, Ch. Lischka, I. Benne, T. Scharf, G. Pelzl, S. Diele and H. Kruth, *SPIE*, **3319,** 14(1998).

206. M. A. Osipov and S. A. Pikin, *Mol. Cryst. Liq. Cryst. Lett.*, **103**, 57(1983).

207. L. A. Blinov, M. A. Osipov and S. A. Pikin, , *Mol. Cryst. Liq. Cryst. Lett.*, **158A**, 3 (1988).

208. J. Przedmojski, K. Czuprynski and E. Gorecka, *SPIE*, **3319**, 133(1998).

209. A. Pegenau, P. Goring, S. Diele and C. Tschierske, *SPIE*, **3319**, 70(1998).

210. D. Demus, J. Goodby, G.W. Gray, H.W. Spiess and V. Vill, Eds., *Handbook of Liquid Crystals*, Vol.**2B**,Wiley-VCH, Verlag GmbH, Weinheim, FRG (1998), Part 3, P 799.

211. J. W. Goodby, M. A. Waugh, S. M. Stein, E. Chin, R. Pindak and J. S. Patel, *Nature (London)*, **337**, 449(1989); *J. Am. Chem. Soc.*, **111**, 8119(1989).

212. G. Srajer, R. Pindak, M. A. Waugh, J. W. Goodby, and J. S. Patel, *Phys. Rev. Lett.*, **64**, 1545 (1990).

213. K. P. L. Moodithaya and N. V. Madhusudana in *"Liquid Crystals"*, Proc. Int. Liq. Cryst. Conf., Bangalore, (Dec. 1979), Ed. S. Chandrasekhar (Heyden, London.Philadelphia.Rheine 1980), p. 121.

214. P. E. Cladis, *Phys. Rev. Lett.*, **35**, 48 (1975).

215. P. E. Cladis in *"Liquid Crystals"*, Ed. S. Chandrasekhar, Heyden, London, p 105 (1980).

216. S. K. Giri, N. K. Pradhan, R. Paul, S. Paul, P. Mandal, R. Dabrowski, M. Brodzik and K. Czuprynski, *SPIE*, **3319**, 149 (1998).

217. M. Brodzik and R. Dabrowski, *Liq. Cryst.*, **18**, 61 (1995).

218. J. W. Park, C. S. Bak and M. M. Labes, *J. Amer. Chem. Soc.*, **97**, 4398 (1975).

219. C. S. Oh, *Mol. Cryst. Liq. Cryst.*, **42**, 1 (1977).

220. L.A. Goodman in *Introduction to Liquid Crystals*, Eds. E. B. Priestley, P. J. Wojtowicz and P. Sheng, Plenum Press, NY, (1974), ch. 12 and 14;
D.J. Channin in *Introduction to Liquid Crystals*, Eds. E. B. Priestley, P. J. Wojtowicz and P. Sheng, Plenum Press, NY, (1974), ch. 15.

221. T. Kallard, *Liquid Crystals and Their Applications*, Optoson. Press, NY (1970);

222. T. Kallard, *State of the Art Review, Vol.7: Liquid Crystal Devices*, Optoson. Press, NY (1973).

223. J.A. Castellano, in *Liquid Crystals : The Fourth State of Matter*, Eds. F.D. Saeva, M. Dekker, Inc., NY, Ch.12 (1979).

224. G.J. Sprokel, Ed., *The Physics and Chemistry of Liquid Crystal Devices*, Plenum Press (1980).

225. G.H. Brown, and J.J. Wolken, *Liquid Crystals and Biological Structures*, Academic Press (1979), ch. 12.

226. G.W. Gray and P.A. Winsor, Eds., *Liquid Crystals and Plastic Crystals*, Ellis Horwood Ltd., vol. 1 (1974), Ch. 7.

227. P. J. Collings and M. Hird, *Introduction to Liquid Crystals Chemistry and Physics,* Taylor & Francis(1998), Ch. 13.

228. P.L. Corrol, *Cholesteric Liquid Crystals, Their Technology and Applications*, Ovum Ltd., England (1979).

229. S. Kobayashi, H. Furue and T. Takahashi in *Liquid Crystals and Other Soft Materials,* Ed. N.V. Madhusudana, Indian Academy of Sciences, Bangalore (1999), p. 145;

230. T.N. Ruckmongathan in *Liquid Crystals and Other Soft Materials,* Ed. N.V. Madhusudana, Indian Academy of Sciences, Bangalore (1999), p. 199.

231. C.L. Khetrapal in *Liquid Crystals in the Nineties and Beyond,* Ed. S. Kumar, World Scientific (1995), p. 435.

232. H. Hirschmann and V. Reiffenrath in *Handbook of Liquid Crystals,*Eds. D. Demus, J. Goodby, G.W. Gray, H.-W. Spiess and V. Vill, Vol. **2A**, Wiley-VCH, Verlag GmbH, Weinheim, FRG (1998), p.199;
E. Kaneko in *Handbook of Liquid Crystals,*Eds. D. Demus, J. Goodby, G.W. Gray, H.-W. Spiess and V. Vill, Vol. **2A**, Wiley-VCH, Verlag GmbH, Weinheim, FRG (1998), p. 230.

233. B. Bahadur in *Handbook of Liquid Crystals,*Eds. D. Demus, J. Goodby, G.W. Gray, H.-W. Spiess and V. Vill, Vol. **2A**, Wiley-VCH, Verlag GmbH, Weinheim, FRG (1998), p. 243.

234. B. Bahadur in *Handbook of Liquid Crystals,*Eds. D. Demus, J. Goodby, G.W. Gray, H.-W. Spiess and V. Vill, Vol. **2A**, Wiley-VCH, Verlag GmbH, Weinheim, FRG (1998), p. 257.

235. H. Coles in *Handbook of Liquid Crystals,*Eds. D. Demus, J. Goodby, G.W. Gray, H.-W. Spiess and V. Vill, Vol. **2A**, Wiley-VCH, Verlag GmbH, Weinheim, FRG (1998), p. 335.

236. S.T. Lagerwall in *Handbook of Liquid Crystals,*Eds. D. Demus, J. Goodby, G.W. Gray, H.-W. Spiess and V. Vill, Vol. **2B**, Wiley-VCH, Verlag GmbH, Weinheim, FRG (1998), pp.515.

237. H. Kelker and R. Hatz, *Hand Book of Liquid Crystals*, Verlag - Chemie, Weinheim (1980), p. 604.

238. A. Sussman in *Liquid Crystals and Plastic Crystals*, Eds.,G.W. Gray and P.A. Winsor, Ellis Horwood Ltd., vol. 1 (1974), p. 338.

239. G.H. Heilmeier, L.A. Barton and L.A. Zanoni, *Proc. of IEEE*, **56**,1162(1968).

240. T. Geelhaar , *Liquid Crystals*, **24**, 91(1998).

241. J.P. Schroeder in *Liquid Crystals and Plastic Crystals*, Eds. G.W. Gray and P.A. Winsor, Ellis Horwood Ltd., Vol.1, p.356 (1974).

242. H. Kelker and E. Von-Schivizhoffen, *Adv. Chromat.*, **6**, 247 (1968).

Chapter II

THEORETICAL BACKGROUND AND EXPERIMENTAL TECHNIQUES

INTRODUCTION

After the existence of liquid crystals had been firmly established by the pioneering works of O. Lehmann, D. Vorländer, G. Friedel and others, scientists around the world were trying to develop theories to explain the behaviour of liquid crystals over many years. The most important problem to be solved by the theoreticians was to establish the relationship between the molecular structure and the properties of the liquid crystals. Some phenomenological theories were proposed in attempt to explain the behaviour of liquid crystals. There are many books [1-7] in the literature that describe the theories on liquid crystals in details. However, in this Chapter the main features of the mean-field theories of nematic and smectic A phases, developed by Maier and Saupe [7,8] and McMillan [9,10] respectively, have only been discussed, since some of the experimental results described in the thesis have been compared with these two theories only.

2.1 THEORIES OF LIQUID CRYSTALS

The first molecular field theory of the nematic phase was proposed in 1916 by M. Born [11]. He treated the liquid medium as an assembly of permanent electric dipoles and demonstrated the possibility of a transition from an isotropic phase to an anisotropic one as the temperature is lowered. But it is now well established that presence of permanent dipole moments is not necessary for the occurrence of the liquid crystalline phase. Moreover, the theory predicts that the aligned liquid crystal phase should be ferroelectric, which does not appear to be the case even when the molecules are polar.

The most widely used molecular field theory is the one due to Maier and Saupe [7,8] which nicely explains nematic-isotropic transition in terms of an orientational order parameter. A simple but elegant description of SmA phase was proposed by McMillan [9,10] in which he extended MS theory to include additional translational order parameter characterizing the layered structure. However, use of an approximate self-consistent mean molecular field neglects the effects of short-

range order and fluctuations of the order parameters [9,10]. The details of the McMillan, Wulf and de Gennes theories on smectic-C liquid crystals and the Meyer-McMillan theory on of Sm-C, -B, and –H liquid crystals are given in reference [7a]. Landau-de Gennes developed a phenomenological theory for N-I phase transition [12,13] that was subsequently extended to many other transitions including SmA-N transition.

Thermotropic liquid crystals have also been extensively studied by computer simulation techniques employing a variety of hard, soft and realistic models involving atom-atom potentials and using either Monte Carlo or molecular dynamics method [14-23].

2.1.1 Maier-Saupe Mean Field Theory of Nematic Phase

W. Maier and A. Saupe developed the theory with the idea that the existence of the nematic phase is caused by the anisotropic part of the attractive dispersion force between the molecules. Each molecule is assumed to experience the same force on average as any other molecule in the system. Further assumptions are:

- The nematic liquid crystal molecules are rigid cylindrical rods
- The molecules are, on the average, aligned along a preferred direction described by a unit vector **n,** called the director. The whole system is cylindrically symmetric about **n** such that **n** and –**n** are equivalent.
- The influence of permanent dipoles can be neglected as far as long-range nematic order is concerned.
- Only the effect of the induced dipole-induced dipole interaction is considered, the higher order terms are not thought to significantly affect the nematic order. No repulsive interaction is considered.

The degree of alignment of the molecules with respect to the director **n** is described by an orientational order parameter given by

$$S = \langle P_2(\cos\beta_i)\rangle = \frac{1}{2}\langle 3\cos^2\beta_i - 1\rangle \qquad (2.1)$$

where β_i is the angle between the long axis of the i^{th} molecule and the director **n** and $P_2(\cos\beta_i)$ is the second order Legendre polynomial. Here $\langle ... \rangle$ denotes statistical average over all β_i.

Since the distribution function is cylindrically symmetric about **n** and the directions **n** and -**n** are equivalent the potential energy of the i^{th} molecule may be assumed as

$$u_i(\cos\beta_i) \propto -\langle P_2(\cos\beta_i)\rangle P_2(\cos\beta_i)$$

so that,

$$u_i(\cos\beta_i) = -v\langle P_2(\cos\beta_i)\rangle P_2(\cos\beta_i) \qquad (2.2)$$

i.e.,

$$u_i(\cos\beta_i) = -\frac{A}{V^2}\langle P_2(\cos\beta_i)\rangle P_2(\cos\beta_i)$$

where V is the molar volume of the sample and A is taken to be a constant independent of pressure, volume and temperature. Also, $v = \frac{A}{V^2}$ is the coupling constant.

Humphries, James and Luckhurst [26] developed a more comprehensive concept by including higher order terms in the mean field potential for cylindrically symmetric molecules. Thus u_i was taken as

$$u_i(\cos\beta_i) = \sum_{L\,even} u_{Li}\langle P_L(\cos\beta_i)\rangle P_L(\cos\beta_i) \qquad (L\neq 0)$$

where $P_L(\cos\beta_i)$ is the L^{th} order Legendre polynomial.

2.1.1.1 *Orientational Distribution Function and Order Parameters*

If the system is in thermal equilibrium then the probability of a molecule being oriented at an angle β_i with the director **n** will be governed by the Boltzmann factor, so the orientational distribution function for the molecules of the system is given by

$$f(\cos\beta_i) = Z^{-1}\exp\left[\frac{-u_i(\cos\beta_i)}{kT}\right]$$

where k is the Boltzmann constant, T is temperature in absolute scale and Z being

the partition function for a single molecule. Z is given by

$$Z=\int_0^1 \exp\left[\frac{-u(\cos\beta)}{kT}\right]d(\cos\beta),$$

dropping the subscript 'i' for brevity.

The order parameter, S, is therefore written as

$$S = \langle P_2\rangle = \int_0^1 P_2(\cos\beta) f(\cos\beta) d(\cos\beta)$$

$$= \frac{\int_0^1 P_2(\cos\beta)\exp[v\langle P_2\rangle P_2(\cos\beta)/kT]d(\cos\beta)}{\int_0^1 \exp[v\langle P_2\rangle P_2(\cos\beta)/kT]d(\cos\beta)}$$

i.e., $$\langle P_2\rangle = \frac{\int_0^1 P_2(\cos\beta)\exp[\langle P_2\rangle P_2(\cos\beta)/T^*]d(\cos\beta)}{\int_0^1 \exp[\langle P_2\rangle P_2(\cos\beta)/T^*]d(\cos\beta)} \qquad (2.3)$$

where $T^* = kT/v$ is called the reduced temperature.

Thus we have a self-consistent equation for the determination of the temperature dependence of $\langle P_2\rangle$. It is observed that $\langle P_2\rangle = 0$ is a solution at all T showing a disordered phase, the normal isotropic liquid. Solving equation (2.3) numerically one observes that for $T^* < 0.22284$ two more solutions of $\langle P_2\rangle$ appear. One is positive $\langle P_2\rangle$ which tends to unity as $T\rightarrow 0$ and represent the nematic phase and the other one is negative $\langle P_2\rangle$ which corresponds to an unstable phase. The laws of thermodynamics demand that the stable phase will have the minimum free energy. Applying this condition, we get the region $0 \le T^* \le 0.22019$ where $\langle P_2\rangle$ is greater than zero corresponding to the anisotropic nematic phase and for $T^* > 0.22019$, the isotropic phase with $\langle P_2\rangle = 0$.

The order parameter $\langle P_2\rangle$ varies from 1 at $T^* = 0$ to 0.4289 at $T^* = 0.22019$ corresponding to nematic-isotropic transition point. Thus, according to Maier-Saupe theory the N-I transition is first order as has been observed experimentally.

Exactly the same way it is possible to obtain higher order parameter $\langle P_4\rangle$ using the 4th order Legendre polynomial

$$\langle P_4(\cos\beta)\rangle = \frac{1}{8}(35\langle\cos^4\beta\rangle - 30\langle\cos^2\beta\rangle + 3) \qquad (2.4)$$

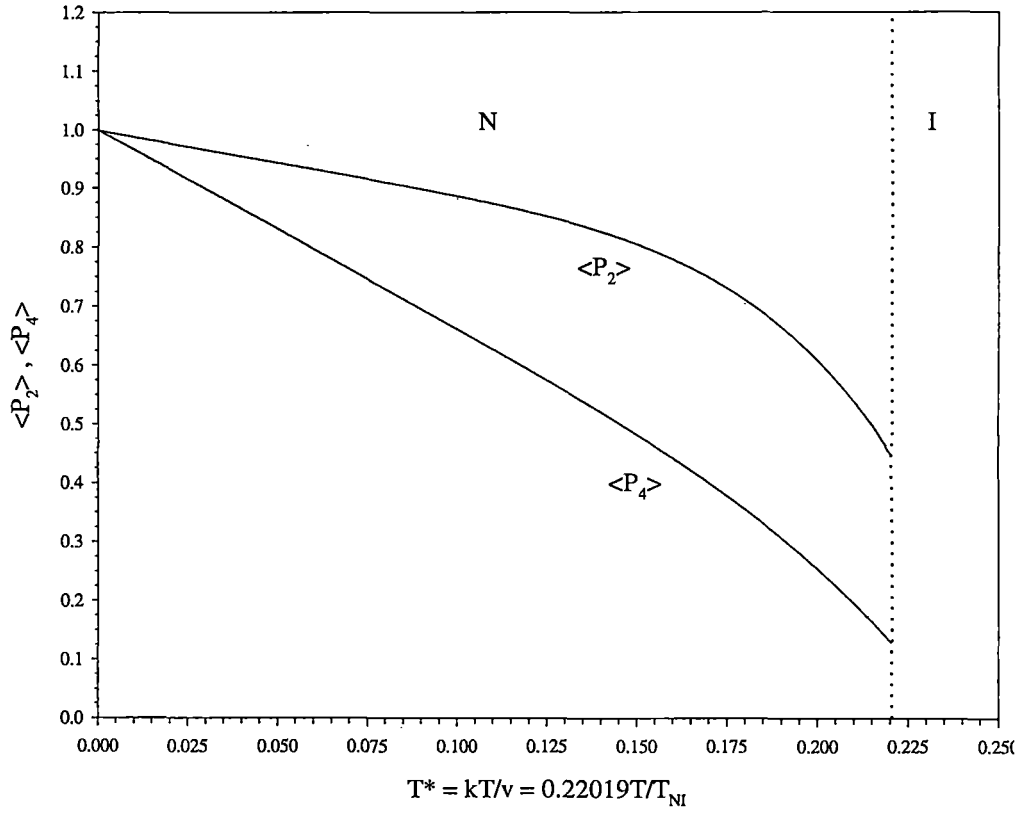

Figure 2.1 Temperature variation of order parameters $\langle P_2 \rangle$ and $\langle P_4 \rangle$ from Maier-Saupe theory.

in equation (2.3). Variation of $\langle P_2 \rangle$ and $\langle P_4 \rangle$ with temperature is shown in Figure 2.1. It is noted that nature of temperature variation of $\langle P_4 \rangle$ also indicates first order N-I transition. Moreover, temperature dependence of the order parameters is universal in character, there are no parameters that can be adjusted to allow for different order parameter behaviour of different compounds.

The Maier-Saupe theory has been extended by Humphries, James and Luckhurst [27] and by Palffy-Muhoray *et al.* [28], to investigate the properties of binary mixtures. The later treatment has led to some significant conclusions: For certain value of the parameters, it is possible to have a nematic-nematic coexistence region. Coexisting nematic phases have in fact been observed in mixtures of polymeric and low molecular weight nematogens as also in mixtures of rod-shaped and disc-shaped nematogens [2]. The order parameter of the mixture and its

variation with temperature agree very closely with the Maier-Saupe universal curve. However, the order parameters of the individual components of the mixture may differ appreciably [29,30]. The fact that the two components can have different order parameters is of practical importance in the design of dye displays. The dye molecules are chosen to have a high anisotropy, and hence a high order parameter which, in turn, improves the contrast ratio.

2.1.2 McMillan's Theory of Smectic A Phase

W.L. McMillan [9,10] extended the Maier-Saupe theory to describe the SmA–nematic transition in which an additional order parameter characterizing the 1-D translational periodicity of the layered structure is included.

If the periodicity of smectic layers is taken along the Z-axis, the normalised distribution function, for the present case, can be written as

$$f(z,\cos\beta) = \sum_{l\ \text{even}} \sum_{n} A_{l,n} P_l(\cos\beta)\cos\left(\frac{2\pi n z}{d}\right) \qquad (2.5)$$

with

$$\int_{-1}^{1} \int_{0}^{d} f(z,\cos\beta)\,dz\,d(\cos\beta) = 1$$

as normalising condition, d being the layer thickness.

McMillan developed the theory of smectic A liquid crystals starting from the Kobayashi [24,25] form of potential. For simplicity, neglecting higher order terms, McMillan wrote the mean field potential as

$$V_1(z,\cos\beta) = -v_0\left[\delta\alpha\tau\cos\left(\frac{2\pi z}{d}\right) + \left\{S + \sigma\alpha\cos\left(\frac{2\pi z}{d}\right)\right\}P_2(\cos\beta)\right] \qquad (2.6)$$

Here we have,

Orientational order parameter, $S = \frac{1}{2}\langle 3\cos^2\beta - 1\rangle$;

Translational order parameter, $\tau = \langle\cos\left(\frac{2\pi z}{d}\right)\rangle$;

Mixed order parameter, $\sigma = \langle P_2(\cos\beta)\cos\left(\frac{2\pi z}{d}\right)\rangle$

and v_0 and δ are constants characterising respectively the strengths of the anisotropic and isotropic parts of the interaction, α is a parameter which depends on the core length and the molecular length. Obviously it reduces to MS potential when the two adjustable parameters δ and α become zero.

The distribution function in this case is

$$f_1(z,\cos\beta) = Z^{-1}\exp\left[-\frac{V_1(z,\cos\beta)}{kT}\right] \tag{2.7}$$

where the single molecular partition function Z is given by

$$Z = \int_0^d dz \int_0^1 \exp\left[-\frac{V_1(z,\cos\beta)}{kT}\right] d(\cos\beta)$$

The various order parameters are, therefore, given by,

$$\left.\begin{aligned} S &= \int_0^1\int_0^d P_2(\cos\beta) f_1(z,\cos\beta)\,dz\,d(\cos\beta) \\ \tau &= \int_0^1\int_0^d \cos\left(\frac{2\pi z}{d}\right) f_1(z,\cos\beta)\,dz\,d(\cos\beta) \\ \sigma &= \int_0^1\int_0^d P_2(\cos\beta)\cos\left(\frac{2\pi z}{d}\right) f_1(z,\cos\beta)\,dz\,d(\cos\beta) \end{aligned}\right\} \tag{2.8}$$

These self-consistent equations can be solved numerically to find the temperature dependence of the three order parameters.

Out of several solutions, the equilibrium state is identified by the minimum value of free energy. In general we get the following three cases with S, σ and τ:

i) $\tau = \sigma = S = 0$, no order characteristic of the isotropic liquid phase;

ii) $\tau = 0$, $\sigma = 0$, $S \neq 0$, orientational order only, the theory reduces to the Maier-Saupe theory for the nematic phase; and

iii) $\tau \neq 0$, $\sigma \neq 0$, $S \neq 0$, orientational and translational order characteristic of the smectic A phase.

One can also predict the nature of the smectic to nematic phase transition observing McMillan ratio (T_{NA}/T_{NI}). If (T_{NA}/T_{NI})>0.87 then the SmA – N

transition is of first order and if $(T_{NA}/T_{NI}) < 0.87$ then it is of the second order. Here T_{NA} and T_{NI} are the SmA – N and N – I transition temperature respectively.

2.2 X-RAY DIFFRACTION FROM LIQUID CRYSTALS

X-ray diffraction is a very useful technique in investigating the microscopic structure of all kinds of crystalline materials including liquid crystals. Studies of the properties of the liquid crystals and further development in the theory of liquid crystalline state are based on the results of structural investigations and in particular, X-ray structure analysis. An X-ray experiment provides Fourier image of the electron density function and analysis of the scattering data yields information both on the mutual arrangement of the molecules in a liquid crystal and the specific features of the orientational and translational long range order [31]. X-ray diffraction studies on mesophases have been reviewed by many authors [32-40].

Let us consider a basic scattering situation as shown in Figure 2.2. For elastic scattering, magnitude of incident ($\mathbf{K}_i$) and scattered wave vector ($\mathbf{K}_s$) must be equal, i.e., $|\mathbf{K}_s| = |\mathbf{K}_i| = 2\pi / \lambda$, where λ is the wavelength of the incident radiation.

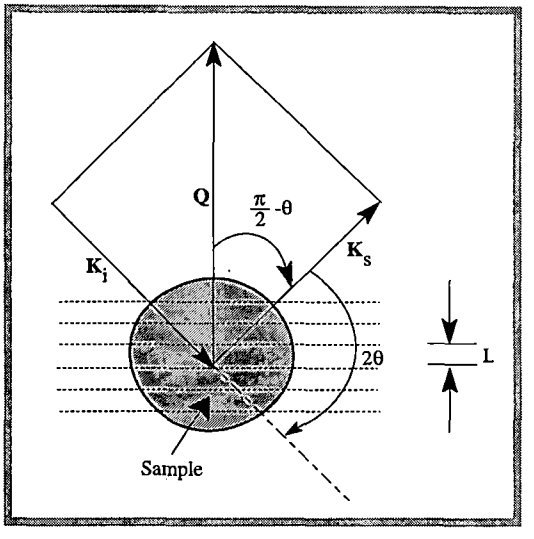

Figure 2.2 Typical scattering geometry showing the incident ($\mathbf{K}_i$), scattered ($\mathbf{K}_s$) and scattering ($\mathbf{Q}$) wave vectors. L is layer spacing.

The magnitude of the scattering vector $\mathbf{Q} = \mathbf{K}_s - \mathbf{K}_i$ is given by

$$Q = |\mathbf{Q}| = \frac{4\pi}{\lambda}\sin\theta \qquad (2.9)$$

where 2θ is the angle between $\mathbf{K}_s$ and $\mathbf{K}_i$. The scattering of incident radiation by a point scattering centre at $\mathbf{r}$ is described (relative to the initial amplitude) by the scattering amplitude

$$f \exp(i\mathbf{Q}.\mathbf{r}),$$

where f is the scattering power and $i=\sqrt{-1}$. Generalized to N centres the scattering amplitude is written as

$$F(\mathbf{Q}) = \sum_{j=1}^{N} f_j \exp(i\mathbf{Q}.\mathbf{r}_j) \qquad (2.10)$$

where $\mathbf{r}_j$ denotes the position of scattering centre j. For a continuous distribution of scattering centers characterized by the electron density function $\rho(\mathbf{r})$ one writes

$$F(\mathbf{Q}) = \int \rho(\mathbf{r}) \exp(i\mathbf{Q}.\mathbf{r}) d\mathbf{r} \qquad (2.11)$$

If the integration is carried over all space then F is Fourier transform of the electron density and provides the link between the real ($\mathbf{r}$) and the reciprocal ($\mathbf{Q}$) space.

For an isolated atom this assumes the form

$$f(\mathbf{Q}) = \int \rho_a(\mathbf{r}) \exp(i\mathbf{Q}.\mathbf{r}) d\mathbf{r}$$

and is called the atomic scattering amplitude. For a group of atoms, for which

$$\rho(\mathbf{r}) = \sum_{j=1}^{N} \rho_j(\mathbf{r} - \mathbf{r}_j),$$

this leads to

$$F(\mathbf{Q}) = \sum_{j=1}^{N} f_j(\mathbf{Q}) \exp(i\mathbf{Q}.\mathbf{r}_j) \qquad (2.12)$$

This is almost identical to equation (2.10), but in this case the atoms are considered as extended object and the variation of the atomic scattering amplitude with $\mathbf{Q}$ has been considered.

The scattered intensity at a particular point in $\mathbf{Q}$-space is given by

$$I(\mathbf{Q}) = |F(\mathbf{Q})|^2$$

For molecular liquids it is convenient to separate the amplitude due to the molecular structure from the total scattering amplitude [32]. Accordingly (2.12) can be written as

$$F(\mathbf{Q}) = \sum_{k,m} f_{km}(\mathbf{Q}) \exp[i\mathbf{Q}.(\mathbf{r}_k - \mathbf{R}_{km})] \qquad (2.13)$$

where $\mathbf{r}_k$ is the centre of mass of the k^{th} molecule, and $\mathbf{R}_{km}$ is the position of the m^{th} atom in the k^{th} molecule, f_{km} is the atomic scattering factor of the m^{th} atom in the k^{th} molecule.

Therefore, the general formula for the scattering intensity from a system of molecules is

$$I(\mathbf{Q}) = \sum_{k,l,n,m} \langle f_{k,m}(\mathbf{Q}) f_{ln}^*(\mathbf{Q}) \exp[i\mathbf{Q}.(\mathbf{r}_k - \mathbf{r}_j)] \exp[i\mathbf{Q}.(\mathbf{R}_{ln} - \mathbf{R}_{km})] \rangle \qquad (2.14)$$

where the brackets indicate statistical average.

The intensity can be written as

$$I(\mathbf{Q}) = I_m(\mathbf{Q}) + D(\mathbf{Q})$$

where $I_m(\mathbf{Q})$ is the molecular structure factor and $D(\mathbf{Q})$ is called the interference function which are respectively given by

$$I_m(\mathbf{Q}) = \sum_k \langle \sum_{m,n} f_{km}(\mathbf{Q}) f_{kn}^*(\mathbf{Q}) \exp[i\mathbf{Q}.(\mathbf{R}_{kn} - \mathbf{R}_{km})] \rangle$$

$$= N \langle \left| \sum_m f_{km} \exp(-i\mathbf{Q}.\mathbf{R}_{km}) \right|^2 \rangle \qquad (2.15)$$

and $$D(\mathbf{Q}) = \langle \sum_{k \neq l} \exp(i\mathbf{Q}.\mathbf{r}_{kl}) \sum_{m,n} \langle f_{km}(\mathbf{Q}) f_{ln}^*(\mathbf{Q}) \exp[\mathbf{Q}.(\mathbf{R}_{ln} - \mathbf{R}_{km})] \rangle \rangle \qquad (2.16)$$

with $\mathbf{r}_{kl} = \mathbf{r}_k - \mathbf{r}_l$

The term $I_m(\mathbf{Q})$ gives the scattered intensity which would be observed from a random distribution of identical molecules. $D(\mathbf{Q})$ is the term containing information about correlation in both positional and orientation of different molecules.

$D(\mathbf{Q})$ contains information regarding :

- Apparent molecular length

- Layer thickness in smectics
- Average lateral distance between the molecules
- Correlation lengths
- Tilt angle
- Molecular packing
- Orientational distribution function
- Order parameters $\langle P_2 \rangle$, $\langle P_4 \rangle$ ... etc.
- Bond orientational order parameter
- Layer order parameters τ and $\langle z^2 \rangle$ in SmA
- Critical exponents.

Procedure of determination of some of these parameters relevant to the present study has been described later.

2.2.1 Experimental Techniques for X-ray Diffraction Studies and Method of Data Analysis

Set-up used for X-ray diffraction studies is shown in Figure 2.3 schematically which was designed and fabricated in our laboratory earlier [41,42]. Small angle X-ray photographs are taken using Nickel-filtered CuK_α radiation. By capillary action the sample is filled in a thin walled (~0.05 mm) Lindemann glass capillary of 1 mm diameter and is aligned by slow cooling from the isotropic phase to the desired temperature in presence of a magnetic field of about 5 KGauss. All photographs are taken with X-rays perpendicular to the magnetic field direction. The temperature of the sample is regulated within ±0.5°C by a controller, Indotherm 401-D2 (India).

Different types of diffraction patterns are obtained depending upon the type of the mesophases [42-51]. In Figure 2.4 typical X-ray photographs for nematic and SmA phases are shown. Evidently two characteristic distances, parallel and perpendicular to **n** (or **H**) are present. However, an unoriented nematic sample shows diffraction pattern as obtained from an isotropic liquid viz. two uniform halo, at low and high angles. This is due to the fact that, generally an unoriented liquid crystal sample consists of a large number of domains and within each domain

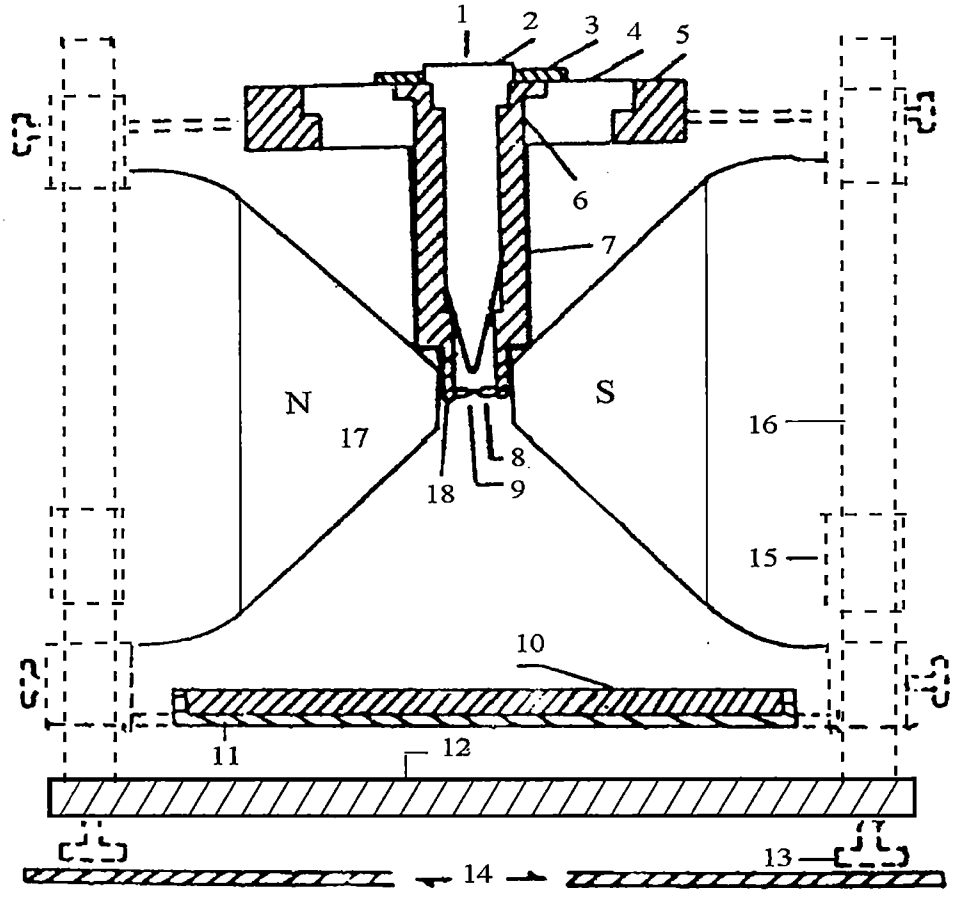

Figure 2.3 Schematic diagram of the X-ray Diffraction set up.

Different components of the set up:

1 →Entrance of x-ray beam
2 →Collimator
3 →Brass ring
4 →Ring of syndanyo board
5 →Brass ring
6 →Cylindrical Brass chamber
7 →Asbestos insulation and heater winding
8 →Specimen holder and thermocouple
9 →Sample position
10→Film cassette
11→Film cassette holder
12→Base plate
13→Leveling screw
14→Brass plates over the coils of the electromagnet
15→Removable spacer
16→Supporting brass stand
17→Pole pieces
18→Asbestos insulation

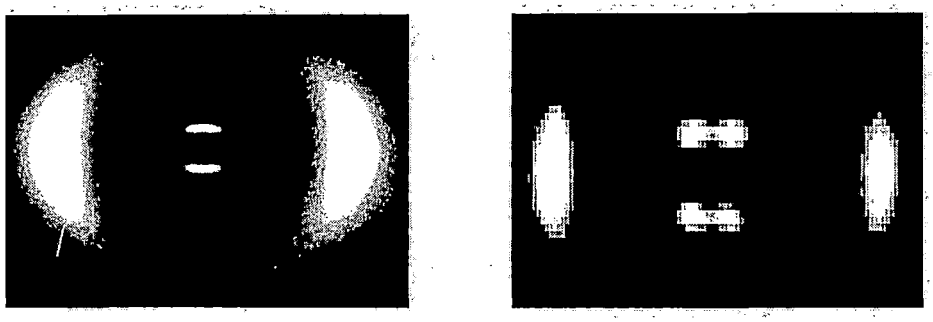

Ordinary Nematic phase Cybotactic Nematic phase

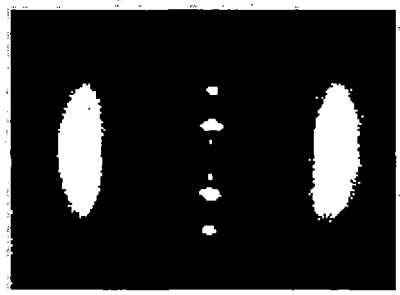

Smectic A phase

Figure 2.4 Typical X-diffraction photographs for nematic and smecticA phase.

the molecules are aligned in a preferred direction, but there is no preferred direction for the sample as a whole and naturally, X-ray diffraction pattern will have a symmetry of revolution around the direction of X-ray beam. For an aligned nematic sample the diffraction feature at larger angle is splitted into two crescents having maxima along the equatorial direction ($\perp$ to **n**). This feature is a result of intermolecular scattering and the corresponding diffraction angle is the measure of average intermolecular distance (D). These distances lie between 3.5Å and 6.5Å, lateral dimensions of a typical mesogenic molecule and the average intermolecular distance is found to be around 5Å.

Along the meridional direction ($\parallel$ to **n**), the inner halo also has two crescents with maxima at much lower angle. This diffraction peak must arise from correlations in the molecular arrangement along the director **n**. So by measuring the corresponding diffraction angles one gets the value of the apparent molecular length

(l) in nematic phase or the layer spacing (d) in the smectic phase. For skewed cybotactic nematic phase the inner halo splits into four spots as shown in Figure 2.5(c). Occasionally it also appears as dumbbell shaped. In smectic A phase, often the inner pattern appears as sharp spots, sometimes second order spots are found. From these second order spots the translational order parameter τ can also be determined.

The diffraction photograph is scanned linearly by an optical microdensitometer (Carl Zeiss Jena MD 100, Germany) equipped with auto chart drive facility and the Bragg angle corresponding to the equatorial and the meridional peaks are determined. The apparent molecular length in nematic phase and layer thickness in smectic phase are calculated using the Bragg equation but the average intermolecular distance (D) is determined using a modified Bragg formula $D=1.117\lambda/2\sin\theta$ derived by de Vries [52,53] on the arguments of cylindrical symmetry. The interplanar spacing (l) of cybotactic group [32,52,54,55] is calculated using Bragg relation and length of the building unit (L') is calculated using the relation $\beta_t = \cos^{-1}(l/L')$, where β_t is the tilt angle of the molecules (Figure 2.6). Sometimes it is possible to measure β_t directly from the film (Figure 2.5 (c)). When β_t cannot be measured from the film one calculates it using the above relation and assuming $L = L'$, where L is the model length of the molecules. Tilt angle of the molecules in smectic C phase is also determined in a similar way.

Orientational distribution function $f(\beta)$ and order parameters $\langle P_L \rangle$ are calculated from the azimuthal intensity distribution of the outer halo of the diffraction pattern following a procedure described below.

The X-ray photographs are scanned circularly at an interval of 5 degrees of the azimuthal angle ψ. These OD data are converted to intensity using a calibration curve and following the procedure of Klug and Alexander[56]. The experimental intensity values are then corrected for background intensity values arising due to air scattering. Thus one gets the angular intensity distribution curve of $I(\psi)$ vs. ψ. Position of the maximum OD along the equator of the outer halo is considered as $\psi=0$ (Figure 2.5). The orientational distribution function $f(\beta)$ is calculated from the

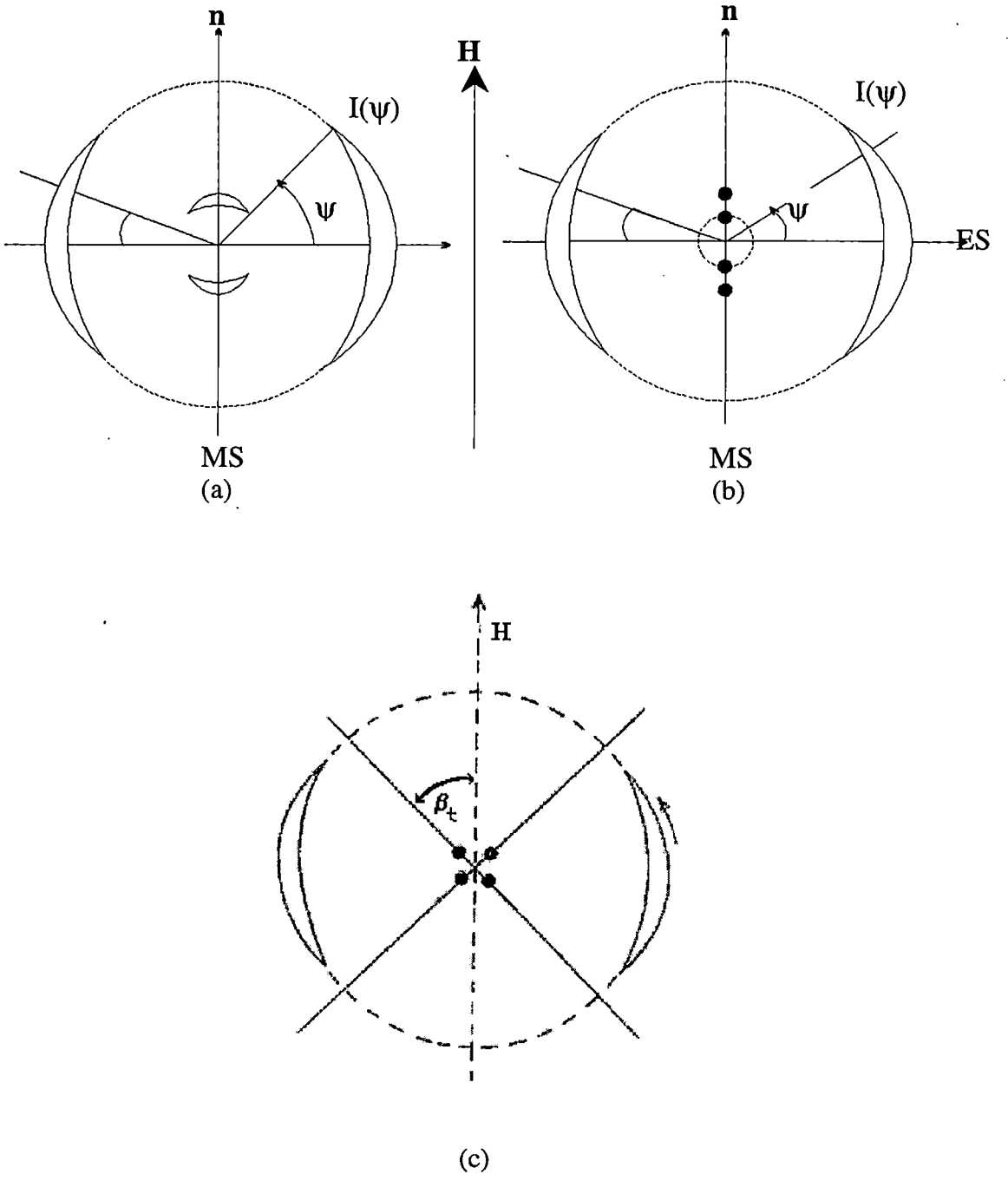

Figure 2.5. Schematic representation of the X-ray diffraction pattern of an oriented (a) nematic, (b) smectic A and (c) skewed cybotactic nematic phase. ES- equatorial section, MS- meridional section, β_t – tilt angle, ψ - azimuthal angle (see text)

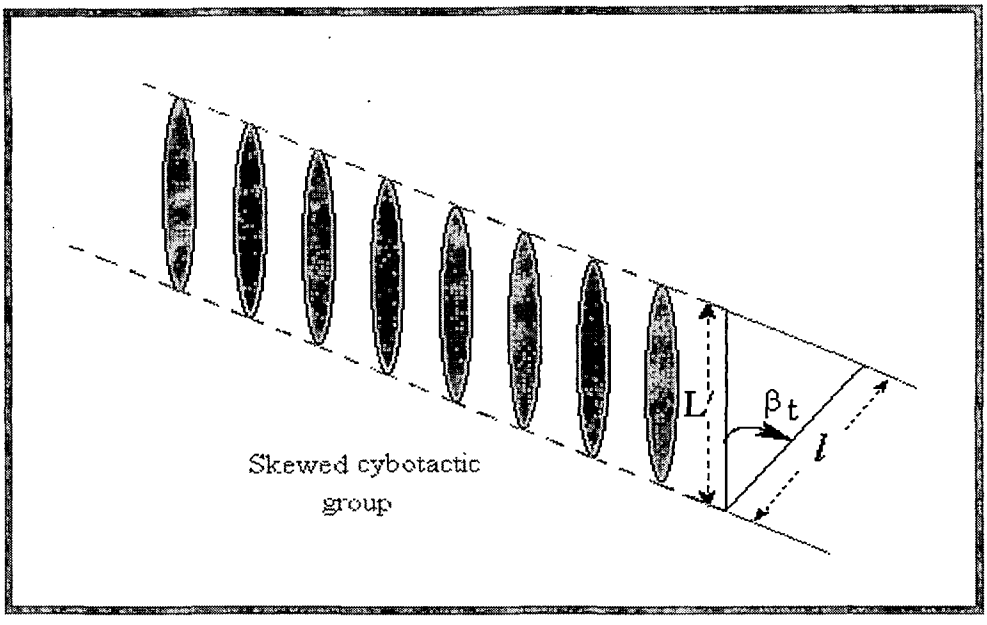

Figure 2.6 Showing tilt angle β_t in the skewed cybotactic nematic phase.

intensity distribution $I(\psi)$ using the following relation given by Leadbetter and Norris[32]:

$$I(\psi) = C\int_{\beta=\psi}^{\frac{\pi}{2}} f(\beta)\sec^2\psi[\tan^2\beta - \tan^2\psi]^{-\frac{1}{2}}\sin\beta d\beta \qquad (2.17)$$

Obviously to get $f(\beta)$ equation (2.17) needs to be inverted numerically. Since the molecular distribution in the nematic phase is centrosymmetric, the distribution function and the intensity can be expanded as even powered cosine series

$$I(\psi) = \sum_{n=0}^{r} a_{2n}\cos^{2n}\psi \qquad (2.18)$$

$$f(\beta) = \sum_{n=0}^{r} b_{2n}\cos^{2n}\beta \qquad (2.19)$$

It is observed that if eight terms are retained in the series, a reasonably good fitting of the $I(\psi)$ values is obtained by least squares method. The coefficients thus determined are used to calculate the coefficients b_{2n} of the equation (2.19) using the relation

$$b_{2n} = a_{2n}\frac{(2n+2)!}{2^{2n}(n!)^2} \qquad (2.20)$$

Orientational order parameter $\langle P_2 \rangle$ and $\langle P_4 \rangle$ are then calculated using the following equation

$$\langle P_L \rangle = \frac{\int_0^1 P_L(\cos\beta)\, f(\beta)\, d(\cos\beta)}{\int_0^1 f(\beta)\, d(\cos\beta)} \qquad (2.21)$$

Necessary computer program have been developed for this purpose in our laboratory. The uncertainties in l, D and β_t values are estimated to be $\pm$ 0.1, $\pm$ 0.01, $\pm$ 0.1 respectively and those in $<P_2>$ and $<P_4>$ values are $\pm$0.02.

To find the exact distance between the sample and the X-ray film, powder photograph of aluminium is taken. The Bragg angle corresponding to the (hkl) reflecting plane for aluminium is calculated using the relation [57]

$$\sin\theta' = \frac{\lambda}{2a}\sqrt{h^2 + k^2 + l^2} \qquad (2.22)$$

where a is its lattice constant. Measuring the diameter of the diffraction rings corresponding to (111) and (222) reflections, the actual distance between the sample and the film is found out from the relation

$$\tan 2\theta' = \frac{\text{radius of the ring}}{\text{sample to film distance}} \qquad (2.23)$$

Using this distance the Bragg angle (θ) for the peak corresponding to the parameter l (or D) of the liquid crystal sample are then calculated using the same relation.

2.3 CHARACTERIZATION OF MESOPHASES:

As described earlier, there are a variety of liquid crystal phases and often the distinction between two phases is very subtle. Several techniques are, therefore, used to identify a particular phase. These are (1) mutual miscibility of same phases of different mesogens, (2) differential scanning calorimetry, (3) textures in optical polarising microscopy, (4) X-ray diffraction, etc. The most widely used technique for liquid crystal phase identification is to study the optical texture as a function of temperature under a polarizing microscope. Phase transition temperatures are also determined during the process. Though some phases reveal distinct textures, but

often phase identification only by texture study is difficult. Detailed description of various textures and their photographs are given in the books by Demus and Richter [58], Slaney *et al.* [59], Bouligand [60].

Differential Scanning Calorimetry (DSC) is nearly always employed as a complementary tool to optical microscopy and reveals the transition temperatures by measuring the enthalpy change associated with a transition. Though DSC cannot identify the type of liquid crystal phase, the level of enthalpy change does give some information about the degree of molecular ordering within a mesophase. Solid to liquid phase transition involves high enthalpy change (around 30 to 40 $kJmol^{-1}$). But LC to LC and LC to isotropic liquid transitions are accompanied much smaller enthalpy changes (1 to 2 $kJmol^{-1}$). X-ray diffraction technique, as described before, is used to find the structure of a phase thus identifying it uniquely. However, good quality photograph from aligned samples are needed for the purpose. Alignment of the sample often becomes a problem, especially for higher order smectic phases. Other techniques used to find the nature of a mesophase include neutron scattering[61], nuclear magnetic resonance[29,30,61-63], IR, Raman, UV-Visible spectroscopic studies [64], Fabry-Perot Etalon method[65] etc.

2.4 DIELECTRIC PERMITTIVITY OF MESOPHASES

Dielectric studies of nematic liquid crystals have proved to be a valuable source of information on molecular organization, intermolecular interactions and molecular dynamics and relaxation mechanisms. Moreover, there is considerable practical importance of the study of temperature dependence of the permittivity of liquid crystals. The threshold voltage and other operational parameters of liquid crystal display devices depend on the anisotropy of the permittivity [66] and the multiplexity of matrix displays may be limited by the temperature dependence of the permittivity. Also, an understanding of the factors that determine the dielectric behaviour of liquid crystals will aid the development of new materials having better display properties. So, the dielectric permittivities of nematic liquid crystals have extensively been studied both experimentally and theoretically [67-72].

W. Maier and G. Meier [73] combined the Onsager description [74] of dielectric liquids with the Maier-Saupe mean field theory [8] of the nematic phase and formulated their well known theory for the dielectric properties of nematic liquid crystals. This theory predicts that the temperature dependence of the magnitude of dielectric anisotropy is similar to that of the order parameter, while the mean permittivity decreases with increasing temperature and is continuous at the nematic to isotropic transition [67]. In defining the reaction field and cavity field, the theory neglected the macroscopic anisotropy of the permittivity

Specific dipole-dipole interactions are included in the Kirkwood-Frölich theory of liquid dielectrics and Bordewijk [75] has extended this theory to anisotropic dielectrics. This theory may be used in conjunction with known values of molecular properties to evaluate dipole-dipole correlation factors for liquid crystals.

2.4.1 Maier and Meier theory of dielectrics for nematic liquid crystals

W. Maier and G. Meier [73] extended the Onsager's theory [74] for isotropic liquid dielectrics to nematics to correlate the dielectric properties with molecular parameters. Essentially, they consider a molecule with polarizabilities $\alpha_{\parallel}$ and $\alpha_{\perp}$ and dipole components $\mu_{\parallel} = \mu\cos\beta$ and $\mu_{\perp} = \mu\sin\beta$; μ being the dipole moment of the molecule making an angle β with the long molecular axis. The symbols $\parallel$ and $\perp$ respectively refer to the directions parallel and perpendicular to the molecular long axis. The molecules are considered to be in a spherical cavity surrounded by a continuum with macroscopic properties of the dielectric. The following relations were obtained for the dielectric components $\varepsilon_{\parallel}$ and $\varepsilon_{\perp}$:

$$\varepsilon_{\parallel} = 1 + 4\pi NhF\left\{\bar{\alpha} + \frac{2}{3}\Delta\alpha S + F\frac{\langle\mu_{\parallel}^2\rangle}{kT}\right\} \tag{2.24}$$

and

$$\varepsilon_{\perp} = 1 + 4\pi NhF\left\{\bar{\alpha} - \frac{1}{3}\Delta\alpha S + F\frac{\langle\mu_{\perp}^2\rangle}{kT}\right\} \tag{2.25}$$

with

$$\langle\mu_{\parallel}^2\rangle = \frac{\mu^2}{3}\left[1 - (1 - 3\cos^2\beta)S\right]$$

and

$$\langle\mu_{\perp}^2\rangle = \frac{\mu^2}{3}\left[1 + \frac{1}{2}(1 - 3\cos^2\beta)S\right].$$

So that, $$\Delta\varepsilon = \varepsilon_{\parallel} - \varepsilon_{\perp} = 4\pi NhF\left\{\Delta\alpha - F\frac{\mu^2}{2kT}(1-3\cos^2\beta)\right\}S, \quad (2.26)$$

and $$\bar{\varepsilon} = \frac{\varepsilon_{\parallel} + 2\varepsilon_{\perp}}{3} = 1 + 4\pi NhF\left\{\bar{\alpha} + F\frac{\mu^2}{3kT}\right\} \quad (2.27)$$

Also, for isotropic state, when S=0, one gets the permittivity

$$\varepsilon_{iso} = 1 + 4\pi NhF\left\{\alpha_{iso} + F\frac{\mu^2}{3kT}\right\} \quad (2.28)$$

where N = the particle density = $\rho N_A/M$, ρ = mass density, N_A=Avogadro's number, M = Molecular weight, S= the order parameter and $\bar{\alpha}$= mean polarizability given by

$$\bar{\alpha} = \frac{\alpha_{\parallel} + 2\alpha_{\perp}}{3} \quad (2.29)$$

$\Delta\alpha$ = polarizability anisotropy = $\alpha_{\parallel}$-$\alpha_{\perp}$,

α_{iso} being the polarizability in the isotropic state; h and F are respectively the cavity field factor and the reaction field factor and are given by

$$h = \frac{3\bar{\varepsilon}}{2\bar{\varepsilon}+1} \quad \text{and} \quad F = \frac{1}{(1-\bar{\alpha}f)}$$

Here, the factor f, called Onsager factor, is given by

$$f = \frac{8\pi}{3}N\frac{\bar{\varepsilon}-1}{2\bar{\varepsilon}+1}$$

The above expressions for $\varepsilon_{\parallel}$ and $\varepsilon_{\perp}$ are often used to find effective dipole moment of the molecules in the nematic phase and its orientation with the molecular long axis. Alternatively, one may find the order parameter S when all remaining quantities are known.

2.4.2 Dipole-Dipole Correlation Factor

Further insight into the phase structure may be obtained if the dipole-dipole correlation factor (g_λ), as defined below, is calculated

$$g_\lambda = \frac{\langle \sum_{i\neq j} (\mu_\lambda)_i (\mu_\lambda)_j \rangle}{\langle \mu_\lambda^2 \rangle}. \quad (2.30)$$

This factor g_λ takes into account the correlation between the neighbouring dipole moments only and the subscript λ refers to axes || and $\perp$ to the nematic director. The ensemble averages of the || and $\perp$ components of the molecular dipole moments are calculated following the procedure of Bata and Buka [76].

As noted earlier, short-range dipole-dipole interactions are not considered in Maier-Meier theory [73]. The Kirkwood-Fröhlich theory for isotropic liquid dielectrics [69,77] provides a formula in which these short-range effects are considered. Bordewijk and de Jeu [78-81] extended this idea to anisotropic media with uniaxial symmetry and used it to find dipole-dipole correlation factor for nematic liquid crystals. Their model was based on the observation that the square of birefringence (Δn^2) and the product of the density (ρ) and order parameter (S) is linearly proportional. Bata and Buka [76] later obtained the following relation between the low and high frequency dielectric constants:

$$\varepsilon_\lambda - \varepsilon_{\infty\lambda} = \frac{4\pi N \varepsilon_\lambda (\varepsilon_{\infty\lambda}+2)^2}{9kT\,(2\varepsilon_\lambda + \varepsilon_{\infty\lambda})} \langle \mu_\lambda^2 \rangle f_\lambda(\varepsilon, \Omega_\lambda^\varepsilon) g_\lambda \qquad (2.31)$$

where

$$f_\lambda(\varepsilon, \Omega_\lambda^\varepsilon) = \frac{2\varepsilon_\lambda + \varepsilon_{\infty\lambda}}{\varepsilon_\lambda - (\varepsilon_\lambda - \varepsilon_{\infty\lambda})\Omega_\lambda^\varepsilon} \qquad (2.32)$$

Here $\Omega^\varepsilon_\lambda$ is a factor which depends on the dielectric anisotropy of the system.

For positive dielectric anisotropy [79] one has

$$\Omega_{||}^\varepsilon = \frac{\varepsilon_{||}}{\varepsilon_{||} - \varepsilon_\perp} - \frac{\varepsilon_{||} \cdot \varepsilon_\perp^{\frac{1}{2}}}{(\varepsilon_{||} - \varepsilon_\perp)^{3/2}} \tan^{-1}\left(\frac{\varepsilon_{||} - \varepsilon_\perp}{\varepsilon_\perp}\right)^{\frac{1}{2}} \qquad (2.33)$$

and

$$\Omega_\perp^\varepsilon = \frac{\varepsilon_{||}\varepsilon_\perp^{\frac{1}{2}}}{2(\varepsilon_{||} - \varepsilon_\perp)^{3/2}} \tan^{-1}\left(\frac{\varepsilon_{||} - \varepsilon_\perp}{\varepsilon_\perp}\right)^{\frac{1}{2}} - \frac{\varepsilon_\perp}{2(\varepsilon_{||} - \varepsilon_\perp)} \qquad (2.34)$$

For negative dielectric anisotropy

$$\Omega_{||}^\varepsilon = \frac{\varepsilon_{||}\varepsilon_\perp^{\frac{1}{2}}}{2(\varepsilon_\perp - \varepsilon_{||})^{3/2}} \left(\ln \frac{\varepsilon_\perp^{\frac{1}{2}} + (\varepsilon_\perp - \varepsilon_{||})^{\frac{1}{2}}}{\varepsilon_\perp^{\frac{1}{2}} - (\varepsilon_\perp - \varepsilon_{||})^{\frac{1}{2}}} \right) - \frac{\varepsilon_{||}}{\varepsilon_\perp - \varepsilon_{||}} \qquad (2.35)$$

and

$$\Omega_\perp^\varepsilon = \frac{\varepsilon_\perp}{2(\varepsilon_\perp - \varepsilon_{||})} + \frac{\varepsilon_{||}\varepsilon_\perp^{\frac{1}{2}}}{4(\varepsilon_\perp - \varepsilon_{||})^{3/2}} \left(\ln \frac{\varepsilon_\perp^{\frac{1}{2}} - (\varepsilon_\perp - \varepsilon_{||})^{\frac{1}{2}}}{\varepsilon_\perp^{\frac{1}{2}} + (\varepsilon_\perp - \varepsilon_{||})^{\frac{1}{2}}} \right). \qquad (2.36)$$

Hence, for both cases

$$\Omega_{\perp}^{\varepsilon} = \frac{1}{2}(1-\Omega_{\parallel}^{\varepsilon})$$

Average components of the effective dipole moment, $< \mu^2_{\parallel} >$ and $< \mu^2_{\perp} >$, appearing in equation (2.31) are evaluated from the following relations [76]:

$$\langle \mu_{\parallel}^2 \rangle = \frac{1}{3}\left\{(2S+1)\left[\frac{\varepsilon_{\infty\parallel} + (1-\varepsilon_{\infty\parallel})\Omega_{\parallel}^{sh}}{\varepsilon_{\infty\parallel}}\right]^2 \mu_{m\parallel}^2 + (1-S)\left[\frac{\varepsilon_{\infty\perp} + (1-\varepsilon_{\infty\perp})\Omega_{\perp}^{sh}}{\varepsilon_{\infty\perp}}\right]^2 \mu_{m\perp}^2 \right. \tag{2.37}$$

$$\langle \mu_{\perp}^2 \rangle = \frac{2}{3}\left\{(1-S)\left[\frac{\varepsilon_{\infty\parallel} + (1-\varepsilon_{\infty\parallel})\Omega_{\parallel}^{sh}}{\varepsilon_{\infty\parallel}}\right]^2 \mu_{m\parallel}^2 + \frac{1}{2}(S+2)\left[\frac{\varepsilon_{\infty\perp} + (1-\varepsilon_{\infty\perp})\Omega_{\perp}^{sh}}{\varepsilon_{\infty\perp}}\right]^2 \mu_{m\perp}^2 \right\} \tag{2.38}$$

where the cavity field factor is calculated taking into account the shape factors (Ω_{λ}^{sh}) of ellipsoidal molecules with semi-major axis a and semi-minor axis b (Figure 2.7):

$$\Omega_{\parallel}^{sh} = 1-\omega^2 + \frac{1}{2}\omega(\omega^2-1)\ln\frac{\omega+1}{\omega-1} \tag{2.39}$$

and

$$\Omega_{\perp}^{sh} = \frac{1}{2}\omega^2 - \frac{1}{4}\omega(\omega^2-1)\ln\frac{\omega+1}{\omega-1} \tag{2.40}$$

So,

$$\Omega_{\perp}^{sh} = \frac{1}{2}(1-\Omega_{\parallel}^{sh})$$

where

$$\omega^2 = \frac{a^2}{a^2-b^2} \tag{2.41}$$

The value of 2a is taken to be equal to apparent molecular length l obtained from X-ray study and b is calculated by using the relation:

$$b = \frac{1}{2}\left[\frac{6M}{\pi N_A l \rho}\right]^{\frac{1}{2}} \tag{2.42}$$

on the assumption that the volume occupied by a molecule in the LC phase is equal to the geometrical volume of the molecule[81]. They also used $\varepsilon_{\parallel\infty} = 1.05\ n_{\parallel}^2$ to take into account the atomic polarization factor. Since, according to Kirkwood-Fröhlich theory, the effective value of molecular dipole moment is given by:

$$\mu_{eff.\parallel}^2 = \frac{9kT}{4\pi N}\frac{(\varepsilon_{\parallel}-\varepsilon_{\infty\parallel})(2\varepsilon_{\parallel}+\varepsilon_{\infty\parallel})}{\varepsilon_{\parallel}(\varepsilon_{\infty\parallel}+2)^2} \tag{2.43}$$

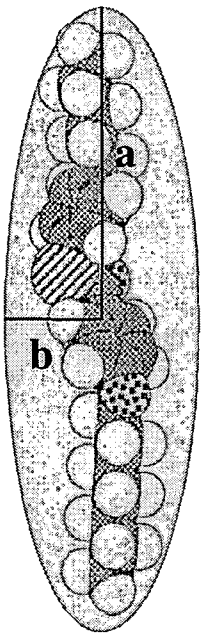

Figure 2.7 Model of ellipsoid of revolution having semi-major axis 'a' and semi-minor axis 'b' for space filling model of a liquid crystal molecule

So, with the help of equation (2.31) we can rewrite equation (2.43) as

$$\mu^2_{\text{eff}\,\parallel} = f_{\parallel}(\varepsilon,\Omega_{\parallel})g_{\parallel}(\varepsilon,T_{\parallel})\langle\mu^2_{\parallel}\rangle \tag{2.44}$$

so that,

$$g_{\parallel} = \frac{\mu^2_{\text{eff}\,\parallel}}{f_{\parallel}\langle\mu^2_{\parallel}\rangle} \tag{2.45}$$

Similarly for the perpendicular component we have:

$$\mu^2_{\text{eff}\,\perp} = \frac{9kT}{4\pi N}\frac{(\varepsilon_{\perp} - \varepsilon_{\infty\perp})(2\varepsilon_{\perp} + \varepsilon_{\infty\perp})}{\varepsilon_{\perp}(\varepsilon_{\infty\perp} + 2)^2} \tag{2.46}$$

and

$$g_{\perp} = \frac{2\mu^2_{\text{eff}\,\perp}}{f_{\perp}\langle\mu^2_{\perp}\rangle} \tag{2.47}$$

where the factor 2 arises due to rotational symmetry.

Equations (2.45) and (2.47) are used to calculate $g_{\parallel}$ and $g_{\perp}$ for uniaxial liquid crystals. Necessary computer program has been written for this purpose.

For uniaxial liquid crystals de Jeu *et al.*[82,83] obtained the following equation for short range order parameter (T_λ)

$$T_\lambda = (1 - g_\lambda)\frac{kT}{4\pi N\langle \mu_\lambda^2 \rangle} \tag{2.48}$$

2.4.3 Experimental Set up for Measurement of Permittivity Components

A schematic diagram of the experimental set up designed and fabricated for dielectric measurements is shown in Figure 2.8. A cell is constructed using two ITO coated conducting glass plates (coating thickness 7000Å and conductivity 10.5–11.1 Ω^{-1}/cm) separated by glass spacers of thickness ~190 μm. A small area of the lower plate is marked to keep the effective area of the liquid constant. Two glass plates are sealed together on three sides by using a high temperature adhesive and the cell is baked in an oven for several hours. The conducting glass plates were donated by Dr Murray Bennet, Solarix Thin Film Division, USA. The LC sample is inserted into the cell as an isotropic melt and the sample-filled cell is cooled at a rate of approximately 1°C/min to the desired temperature. The temperature of the cell is controlled within ±0.5°C by means of a temperature controller. Magnetic field is used to align the sample. The cell is rotated by 90° with respect to the magnetic field such that a homeotropic alignment of the sample is achieved from a homogeneous one.

By applying electric field parallel and perpendicular to the director of the LC sample and measuring capacitances C_e, C_b and C_x of the cell filled with air, benzene (as standard materials) and the liquid crystal sample respectively as the dielectric, one can determine $\varepsilon_{\parallel}$ and $\varepsilon_{\perp}$, the parallel and perpendicular components of dielectric permittivity, using the following expression:

$$\varepsilon_x = 1 + \frac{(C_x - C_e)}{(C_b - C_e)}(\varepsilon_b - 1) \tag{2.49}$$

where ε_b and ε_x are the relative permittivities of benzene and mesogenic substance; and that of air is taken as unity.

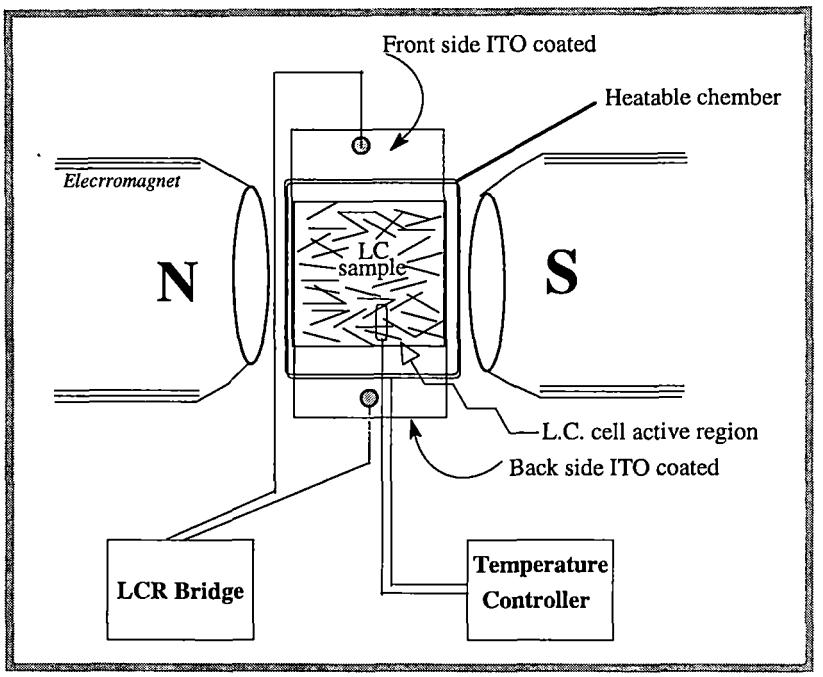

Figure 2.8 Schematic diagram of experimental arrangement for dielectric constant measurement.

The capacitance values are measured at a field frequency of 10kHz using a digital LCR meter bridge (Model VLCR7, VASAVI Electronics, India) with precision of 0.1 pF. The bridge voltage across the sample was low (~300 mV) enough to produce any electric-field-induced instabilities. The cell constants were determined at room temperature with benzene, p-xylene and carbon tetrachloride and the measured permittivity values agreed with 2% of the standard values.

2.5 X-RAY DIFFRACTION BY CRYSTALS

With the discovery of x-rays and Von Laue's experiment on x-ray diffraction by single crystals brought forth a revolution in the concept of the structure of crystalline solids [84]. The idea of regularity in external geometrical shape to be the basic feature and characteristic of the crystallinity of solids was then replaced by the regularity in the arrangement of atoms and molecules in space. This new idea of crystallinity established, due to Bragg [85,86], that X-rays are capable of diffraction by crystals and interpretation of the diffraction pattern

could bring their inside structures out. It is now well established that for a proper understanding and interpretation of several physical properties of liquid crystals, knowledge of the crystal and molecular structure of the compounds is very useful as the molecular conformation and packing in the crystalline state predetermines the molecular organisation in the mesophase. Since the discovery of liquid crystals a number of useful rules concerning their chemical constitution have been stated, yet much less is known about the relationship between molecular packing in the solid state and the possible occurrence of mesomorphism after melting. Though the first attempt to correlate the molecular arrangement in mesophase with the crystal structure of mesogenic material was undertaken by Bernal and Crowfoot [87] in the early 1930's, further studies had been very few for many years. Up to 1974 only seven crystal structures had been determined [88]. The situation changed drastically with the advent of computer programs in the late 1970's making three dimensional structural analysis of moderately large organic compounds much easier. As a result, a large number of structures have been determined, most of them being nematic, a few with different types of smectic precursors. Crystal structures determined earlier by the co-workers are given in references [89-97]. In a typical nematogenic crystal the molecules are found to be packed in a parallel imbricated manner whereas in a smectogenic crystal the constituent molecules are usually found to be arranged in layers. Although the above picture is true in large number of known cases, the generalization must be made with caution [98]. A review on the present knowledge of the structure-property relationship is given by Bryan [99] and more recently by Haase and Athanassopoulou [100].

2.5.1 Theory of Crystal Structure Analysis

In a crystal the constituent atoms/molecules are arranged in a regular fashion with long range three dimensional order. In real space a unit cell may be constructed with three non-coplanar vectors **a, b, c**; repetition of this cell in 3-D will fill up the space completely. If the j-th atom is at point $\mathbf{r}_j$ and if there are N

such atoms within the cell, then the amplitude of the radiation scattered from the array of planes represented by the Miller indices (hkl) is given by [101],

$$F_{hkl} = \sum_{j=1}^{N} f_j \exp 2\pi i(hx_j + ky_j + lz_j) \tag{2.50}$$

F_{hkl} is known as the structure factor for the reflection hkl. This may also be written as

$$F_{\mathbf{H}} = \sum_{j=1}^{N} f_j \exp\left(2\pi i \mathbf{H}.\mathbf{r}_j\right) \tag{2.51}$$

Equation (2.51) is identical to equation (2.12), only difference is that the reciprocal lattice vector **Q** has now been replaced by $2\pi\mathbf{H}$.

Evidently the structure factor $F_{\mathbf{H}}$, is a complex number and it may be written in terms of its magnitude and phase as

$$F_{\mathbf{H}} = |F_{\mathbf{H}}| \exp(i\phi_{\mathbf{H}}) \tag{2.52}$$

Since the as x-rays are scattered by the electrons of an atom, so far as X-ray diffraction is concerned, the crystal may also be thought as periodic distribution of electrons in three dimensions. The electron density $\rho(\mathbf{r})$ at position **r** in the crystal may, therefore, be represented as a Fourier series in three dimensions with structure factors as the Fourier coefficients:

Or,

$$\left.\begin{aligned} \rho(r) &= \frac{1}{V}\int_S F_H \exp(-2\pi i H.r)\,ds \\ \rho(r) &= \frac{1}{V}\sum_h \sum_k \sum_l F_H \exp(-2\pi i H.r) \end{aligned}\right\} \tag{2.53}$$

So, if one sums up the Fourier series for a fine enough grid of points spanning the entire unit cell, the structure is obtained. But measurement of intensities of the reflections provides us with $|F_{\mathbf{H}}|^2$ and hence $|F_{\mathbf{H}}|$, but not the phase $\phi_{\mathbf{H}}$ which is lost.

This is the well-known **Phase Problem** in the crystallography. To overcome this problem, we generally take help of four methods viz., (1) *Patterson function*, (2) ***Direct methods***, (3) *Isomorphous replacement technique* and (4)

Anomalous scattering method. Salient features of only the direct methods [102] have been discussed below since the two crystal structures, described in the present dissertation, were solved by applying the direct methods.

2.5.1.1 *Direct Methods*

Direct methods try to evaluate the phases $\phi_{\mathbf{H}}$ directly from the observed intensities (I_{obs}) through purely mathematical techniques. The goal of the direct methods is to find phases of few reflections and then generate phases of other reflections through some phase relationship such as Σ_2 phase relations (described later in this chapter). Now let us see how direct methods calculate phases from observed structure factor magnitudes even though the amplitude and phase of a wave are physically independent quantities. $|F_{\mathbf{H}}|$ and $\phi_{\mathbf{H}}$ are linked through a knowledge of the electron density $\rho(\mathbf{r})$. Since $\rho(\mathbf{r})$ is related to structure factors by a Fourier transformation, constraints on the electron density impose corresponding constraints on the structure factors. As the structure amplitudes are known, most constraints restrict the values of structure factor phase or, more precisely, the phases of structure invariants and seminvariants. In most cases, these constraints are sufficient to determine the phase values directly. The direct methods are now so efficient in solving crystal structures especially of low molecular weight organic compounds that in 1985 Herbert Hauptman and Jerome Karle was awarded Nobel Prize in chemistry for their pioneering work in this field.

Structure Invariants and Seminvariants:

A structure invariant is a quantity, the value of which remains unchanged for any shift of the origin of the unit cell [102]. A simple example is the intensity of a reflection, or F^2 because it can be measured and therefore is independent of any shift of the origin. The structure factor F is not a structure invariant since for any shift in the origin by, say, $\Delta\mathbf{r}$ the phase of 'F' changes by $2\pi\mathbf{H}.\Delta\mathbf{r}$ radians. However, if the sum of the indices of the structure factors equals zero then it can

easily be shown that the product of these structure factors is a structure invariant. Since $-\mathbf{H} + \mathbf{K} + \mathbf{H}-\mathbf{K} = 0$, sum of their phases viz.,

$$\phi_{-\mathbf{H}} + \phi_{\mathbf{K}} + \phi_{\mathbf{H}-\mathbf{K}} = \phi(\mathbf{H},\mathbf{K}) = \phi_3 \quad \text{(say)} \qquad (2.54)$$

is an invariant as well as the product $F_{-\mathbf{H}}F_{\mathbf{K}}F_{\mathbf{H}-\mathbf{K}}$ in all space groups. The value of a structure invariant is not, however, always known, even though it can only be a function of other structure invariants, e.g., intensities.

The structure seminvariants [102] are those linear combinations of the phases whose values are uniquely determined by the crystal structure alone, when the choice of origin is restricted within permissible values. It originates from space group symmetry. For example in space group P $\bar{1}$, the linear combination $2\phi_{-\mathbf{H}} + \phi_{2\mathbf{H}}$ is a structure invariant for any reciprocal vector **H.** For each space group they have to be derived separately. In any space group any structure invariant is also a structure seminvariant, but reverse is always not true. A complete theory concerning this topic is given in a series of papers by Hauptman and Karle[103-105] and in a book by Schenk [106].

Software Packages Based on Direct Methods:

Different computer programs are available for solving crystal structures by direct methods viz., MULTAN [107], SIMPEL [108], SHELX[109], XTAL[110], SIR 92 [111], NRCVAX [112], SAPI [113], MITHRIL[114] etc. Some of these have been described by Gilmore [115].

A systematic account of the development of the direct methods is beyond the scope of this thesis. Only the basic principles and some working formulae will be discussed here.

Steps to Solve the Structure:

In order to solve the crystal structure a set of intensity data is required which is collected using a single crystal X-ray diffractometer and monochromatic X-radiation. The intensity data is then corrected for Lorentz Polarisation factor [116]. Then by a method introduced by Wilson [117] the scale factor is determined

to convert the intensities into structure factors on an absolute scale. A temperature factor is also obtained during the process that takes into account the thermal vibrations of the real atoms. Then one has to undergo the following steps:

1. Estimation of normalised structure factors |E|'s from observed F_{obs} structure factor values
2. Set up of phase relationships via structure invariants and seminvariants, starting phase determination, phase extension and refinement
3. Calculation of figure of merit
4. Production of E-map by Fourier method and their interpretation
5. Refinement of structures through Fourier synthesis, Difference Fourier synthesis and Least-square refinement techniques.

Estimation of |E|'s from $|F_{obs}|$ values:

Since in direct methods the phases of the structure factors are estimated directly from the structure amplitudes, it becomes necessary that the structure amplitudes be judged on their intrinsic merit where the decrease of the atomic scattering factor with increasing scattering angle is allowed. Ordinarily, the amplitudes of the different structure factors, F_H, cannot be compared directly, since the scattering factor decreases with increasing reflection angle θ. The observed $|F_H|$ is therefore modified so that they correspond to the hypothetical diffracted wave which would be obtained if atoms were stationary point atoms. This modified structure factor is called 'Normalised structure factor' (E_H) and is defined as,

$$|E_H|^2 = \frac{|F_H|^2}{\varepsilon \sum_{j=1}^{N} f_j^2} = \frac{I_h}{\langle I \rangle}$$

and $$\left\langle |E_H|^2 \right\rangle = 1$$

where ε is an integer characteristic of the space group symmetry.

Set up of phase relationships, starting phase determination, phase extension and refinement:

At the initial stage, phases of only the strongest reflections are determined. In practice a suitable number of reflections (4 x no. of independent atoms + 100) are chosen. If the crystal is non-centrosymmetric, more reflections may be required.

The most commonly used phase relation is a three phase structure invariants based on positivity of electron density criterion, as proposed by Karle and Karle[105]:

$$\phi_{\mathbf{H}} \approx \phi_{\mathbf{K}} + \phi_{\mathbf{H}-\mathbf{K}} \tag{2.55}$$

which for centrosymmetric structure is expressed by signs as

$$S(\mathbf{H}) \approx S(\mathbf{K})\, S(\mathbf{H}-\mathbf{K}) \tag{2.56}$$

Relation (2.55) is used to generate phases $\phi_{\mathbf{H}}$ when the values of the phases on the right-hand side are known and it is used in a cyclic manner to propagate the phases to all the selected reflections. These relations are probability relations and the probability is high when the reflections have large |E| values in addition to satisfying the criterion $\mathbf{H} + \mathbf{K} + \mathbf{L} = 0$. These are called Σ_2 phase relations. Probability of the phase of **H** being equal to the sum of the phases of **–H** and **H-K** is given by the following relations:

Centrosymmetric case [118]:

$$P_{+}(\mathbf{H},\mathbf{K}) = \frac{1}{2} + \frac{1}{2}\tanh\left[\frac{1}{2}k(\mathbf{H},\mathbf{K})\right] \tag{2.57}$$

Non-centrosymmetric case [119]:

$$P[\phi(\mathbf{H},\mathbf{K})] = \frac{\exp\{k(\mathbf{H},\mathbf{K})\cos[\phi(\mathbf{H},\mathbf{K})]\}}{2\pi I_0\{k(\mathbf{H},\mathbf{K})\}} \tag{2.58}$$

where I_0 is a zero-order modified Bessel function of the first kind.

Now the question arises about finding the overall estimate of a particular phase, if there are several pairs of known phases, the estimate from each of which might be well different. The answer to this important problem was given by Karle and Hauptman[120] in 1956. They introduced the tangent formula

$$\tan\phi_{\mathbf{H}} \approx \frac{\sum_{\mathbf{K}} k(\mathbf{H},\mathbf{K}) \sin\left(\phi_{\mathbf{K}} + \phi_{\mathbf{H}-\mathbf{K}}\right)}{\sum_{\mathbf{K}} k(\mathbf{H},\mathbf{K}) \cos\left(\phi_{\mathbf{K}} + \phi_{\mathbf{H}-\mathbf{K}}\right)} = \frac{B(\mathbf{H})}{A(\mathbf{H})} \qquad (2.59)$$

where $k(\mathbf{H},\mathbf{K}) = 2\sigma_3\sigma_2^{-\frac{3}{2}} |E_{\mathbf{H}}||E_{\mathbf{K}}||E_{\mathbf{H}-\mathbf{K}}|$

$$\sigma_n = \sum_{j=1}^{N} Z_j^n$$

Z_j being the atomic number of the j^{th} atom in a unit cell containing a total of N atoms. For identical atoms

$$\sigma_3\sigma_2^{-\frac{3}{2}} = N^{-\frac{1}{2}}.$$

In order to use the tangent formula to obtain a new phase, the value of some phases have to be known and put into the right -hand side of the tangent formula. The set of the known phases is called a starting set from which the tangent formula derives more and more new phases and refines them in a self-consistence manner. But in this way all phases cannot be determined with acceptable reliability. It is therefore useful at this stage to eliminate about 10% of these reflections whose phases are most poorly defined by the tangent formula (2.59). An estimate of the reliability of each phase is obtained from $\alpha(\mathbf{H})$:

$$\alpha(\mathbf{H}) = \left\{A(\mathbf{H})^2 + B(\mathbf{H})^2\right\}^{\frac{1}{2}} \qquad (2.60)$$

when (2.60) contains only one term, as it may in the initial stages of the phase determination, then $\alpha(\mathbf{H}) = k(\mathbf{H},\mathbf{K})$.

The larger the value of $\alpha(\mathbf{H})$, the more the reliable is the phase estimate. The relation between $\alpha(\mathbf{H})$ and the variance is given by Karle and Karle[105], in 1966, as

$$\sigma^2(\mathbf{H}) = \frac{\pi^2}{3} + 4\sum_{t=1}^{\infty} \frac{(-1)^t}{t^2} \frac{I_t\{\alpha(\mathbf{H})\}}{I_0\{\alpha(\mathbf{H})\}}$$

From (2.60) it can be seen that $\alpha(\mathbf{H})$ can only be calculated when the phases are known. However, an estimate of $\alpha(\mathbf{H})$ can be obtained from the known distribution of three phase structure invariants [119]. The estimated $\alpha(\mathbf{H})$ at the initial stage is given approximately by

$$\alpha_{est}(\mathbf{H}) = \sum_{\mathbf{K}} k(\mathbf{H},\mathbf{K}) \frac{I_1\{k(\mathbf{H},\mathbf{K})\}}{I_0\{k(\mathbf{H},\mathbf{K})\}} \qquad (2.61)$$

As the tangent phasing process is usually initiated with a few 'known' phases so to fix the origin and enantiomorphs is the first step in phase extension. This is done imposing the condition in terms of structure factor seminvariant phases. The selection of starting phases is critical to the success of the multisolution methods. The generator reflections are sorted by a convergence-type process by Germain, Main and Woolfson [107], which maximises the connection between starting phases. At the end of the convergence procedure a number of reflections, sufficient to fix the origin and the enantiomorphs whose phases are known, are obtained. A number of few other reflections to which different phase values are assigned (either numerically or symbolically) to create different starting points for phase extension through Σ_2 relations. The strength of convergence procedure is that it ensures, as far as possible, that the initial phases will develop through strong and reliable phase relationships. For each starting phase set, phases of all the selected strong reflections are generated and refined as explained in earlier section. Thus we get a multiple phase set.

Calculation of figure of merit of the generated phase sets:

When a number of sets of phases have been developed, it is necessary to rank them according to some Figure-of-Merit (FOM), prior to computing a Fourier map (i.e., E-map). Combining all weights from various FOM viz., Absolute Figure-of-Merit (ABSFOM), Relative Figure-of-Merit (RFOM), R-factor Figure-of-Merit (RFAC), Psi (zero) Figure-of-Merit (PSIO) etc. Combined Figure-of-Merit (CFOM) are calculated for each set. The most likely correct sets of phases are those with the highest value of CFOMs.

E-map calculation and interpretation:

Using the best phase set, E-maps are calculated using equation (2.53) at a large number of grid points covering the entire unit cell. The complete interpretation of the maps is done in three stages:

i. peak search
ii. separation of peaks into potentially bonded clusters
iii. application of simple stereochemical criteria to identify possible molecular fragments.

The molecular fragments thus obtained can be compared with the expected molecular structure. The computer can thus present the user with a list of peaks and their interpretation in terms of the expected molecular structure can be done quite automatically. It is also common practice to have an output of the picture of the molecule as an easy check on the structure the computer has found.

Refinement of structures through Fourier synthesis, Difference Fourier synthesis and Least-squares refinement techniques:

Generally for refinement of a model structure (partial or complete) obtained from E-map we use following three methods, e.g., 1) Fourier synthesis, 2) Difference Fourier synthesis and 3) Least squares refinement[121,122] .

The Fourier synthesis gives the refined co-ordinates of the atoms and also tends to reveal the position of any atom that is not included in computing the structure factors using equation (2.50). The Difference Fourier map is very useful for correcting the position of an atom used in structure factor calculation. This is also very useful in locating H-atoms towards the final stages of refinement procedure.

An analytical method of refinement of great power and generality is that based on the principle of least squares. In brief, least-squares refinement consists in using the square of the difference between observed and calculated values as a measure of their disagreement and adjusting the parameters so that the total disagreement is a minimum.

An agreement between the calculated structures factors F_c and those observed, F_o, indicates the degree of refinement. The most common method of assessing the agreement is calculating the residual or reliability index of the form

$$R = \frac{\sum(|F_o| - |F_c|)}{\sum|F_o|} \qquad (2.62)$$

the summation being over all the reflections. Evidently, the lower the value of R, the better is the agreement. Another form of the residual of common use is

$$R_w = \left[\frac{\sum w\left(\left|F_o - F_c\right|^2\right)}{\sum w\left|F_o\right|^2} \right]^{\frac{1}{2}} \qquad (2.63)$$

where the frequently used weight is,

$$w = \frac{1}{\sigma^2(F_o)}$$

$\sigma(F_o)$ being the standard deviation of F_o.

REFERENCES

1. E.B. Priestly, P.J. Wojtowicz and P. Sheng (Eds.), *Introtuction to Liquid Crystals,* Plenum,NY (1974).

2. S. Chandrasekhar, *Liquid Crystals*, second edn., , Cambridge University Press, Cambridge(1992).

3. G. Vertogen and W.H. de Jeu, *Thermotropic Liquid Crystals: Fundamentals,* Springer-Verlag, Berlin (1988).

4. G.R. Luckhurst and G.W. Gray (Eds.), *The Molecular Physics of Liquid Crystals*, Academic Press, London(1979).

5. P.G. de Gennes, *The Physics of Liquid Crystals*;, Clarendon Press, Oxford (1974); P.G. de Gennes and J. Prost, *The Physics of liquid crystals* , second edn.,., Clarendon Press, Oxford (1993).

6. P.J. Collings and M. Hird, *Introtuction to Liquid Crystals Chemistry and Physics,* Taylor & Francis Ltd., London (1997).

7. W. Maier and A. Saupe, *Z. Naturforsch* **13a**, 564 (1958); *ibid.*, **14a**, 882 (1959); *ibid.,* **15a**, 287 (1960).
7a. R. B. Meyer and W. L. McMillan, *Phys. Rev. A*, **9**, 899(1974).

8. A. L. Tsykalo, *Thermophysical Properties of Liquid Crystals,* Gordon and Breach Science Publishers (1991), p27.

9. W. L. McMillan, *Phys. Rev.*, **A4**, 1238(1971).

10. W. L. McMillan, *Phys. Rev.*, **A6**, 936(1972).

11. M. Born, *Sitzb. kgl. preuss, Ak. d. Wiss., phys. math. Klasse v. 25.5.1916,* **XXX**, 614 (1916).

12. P. J. Collings and M. Hird, *Introduction to Liquid Crystals - Chemistry and Physics,* Taylor & Francis, London (1998), p245.

13. P.G. de Gennes, *The Physics of Liquid Crystals*;, Clarendon Press, Oxford (1974), p48.

14. C. Zannoni in *The Molecular Physics of Liquid Crystals,* G.R. Luckhurst and G.W. Gray (Eds.), Academic Press, London(1979), Ch. 9.

15. C. Dasgupta in *Liquid Crystals in the nineties and beyond*, S. Kumar (Ed.), World Scientific, Singapore(1995), p 81.

16. R. Hasim, G. R. Luckhurst and S. Romano, *J. Chem. Soc. Farad. Trans.*, **91**(14), 2141(1995).

17. G. R. Luckhurst, S. Romano and H. B. Zewdie, , *J. Chem. Soc. Farad. Trans.*, **92**(10), 1781(1996).

18. D. Frenkel in *Phase Transitions in Liquid Crystals*, S. Martellucci and A. N. Chester (Eds.), Plenum Press, NewYork (1992).

19. R. R. Netz and A. N. Berker, *Phys. Rev. Lett.*, **68**, 333(1992).

20. D. Frenkel and R. Eppenga, *Phys. Rev.*, **A31**, 1776(1985).

21. S. G. Dunn and T. C. Lubensky, *J. Phys. (Paris),* **42**, 1201(1981).

22. I. M. Jiang, S. N. Huang, J. Y. Ko, T. Stoebe, A. J. Jin and C. C. Huang, *Phys. Rev.*, **E48**, 3240(1993).

23. D. Frenkel, *J. Phys. Condensed Mat.*, **2(SA)**, 256(1990).

24. K. K. Kobayashi, J. Phys. Soc. Jpn., **29**, 101(1970).

25. K. K. Kobayashi, *Mol. Cryst. Liq. Cryst.*, 13, 137 (1971)

26. R. L. Humphries, P. G. James and G. R. Luckhurst, *J. Chem. Soc., Faraday Trans. 2*, **68**, 1031(1972).

27. R. L. Humphries, P. G. James and G. R. Luckhurst, *Symp. Faraday Soc.*, no. **5**, 107, (1971).

28. P. Palffy-Muhoray, D. A. Dunmur, W. H. Muller and D. A. Balzarini, in *Liquid Crystals and Ordered Fluids*, Vol.**4**, ed. A. C. Griffin and J. F. Johnson, Plenum, NY, p. 615 (1984).

29. G. R. Luckhurst, *Quart. Rev.*, **22**, 179 (1968).

30. G. R. Luckhurst, *Mol. Cryst. Liq. Cryst.*, **21**, 125 (1973).

31. B. L. Ostrovskii, Sov. Sci. Rev. A12, 85(1989).

32. A. J. Leadbetter and E. K. Norris, *Mol. Phys.*, **38**, 669(1979).

33. B. K. Vainstein, *Diffraction of X-rays by Chain Molecules*, Elsevier, Amsterdam, (1966).

34. A. J. Leadbetter in *The Molecular Physics of Liquid Crystals*, G.R. Luckhurst and G.W. Gray (Eds.), Academic Press, London (1979).

35. I. G. Chistyakov, *Sov. Phys. Usp.*, **9**, 551(1967).

36. L. V. Azaroff, *Mol. Cryst. Liq. Cryst.*, **60**, 73(1980).

37. J. Falguerettes and P. Delord in *Liquid Crystals and Plastic Crystals,* G. W. Gray and P. A. Winsor(Eds.), Ellis Horwood(1974), **Vol. 2**, Ch. 3.

38. H. Kelkar and R. Hatz, *Handbook of Liquid Crystals,* Verlag Chemie(1980), Ch. 5.

39. P. S. Pershan, *Structure of Liquid Crystalline Phases,* World Scientific, Singapore(1988).

40. G. Ungar in *Physical properties of liquid* crystals, D. A. Dunmur, A. Fukuda and G. R. Luckhurst (Eds.),INSPEC, London(2001), Ch. 4.1

41. B. Jha and R. Paul, *Proc. Nucl. Phys. and Solid State Phys. Symp., India* . **19C**, 491 (1976).

42. B. Jha, S. Paul, R. Paul and P. Mandal, *Phase Transitions*, **15**, 39 (1989).

43. S. Diele. P. Brand and H. Sackmann, *Mol. Cryst. Liq. Cryst.*, **16**, 105 (1972).

44. A. de Vries, *Pramana, Suppl. No.* **1**, 93 (1975).

45. A. de Vries, A. Ekachi and N. Sielberg, *J. de Phys.*, **40**, C3-147 (1979).

46. A. J. Leadbetter, J. Prost, J. P. Gaughan and M. A. Mazid, J. de Phys., **40**, C3-185 (1979).

47. A. J. Leadbetter and P. G. Wrighton, J. de Phys., **40**, C3-234 (1979).

48. V. M. Sethna, A. de Vries and N. Spielberg, *Mol. Cryst. Liq. Cryst.*, **62**, 141 (1980).

49. L.V. Azaroff and C. A. Schuman, *Mol. Cryst. Liq. Cryst.*, **122**, 309 (1985).

50. A. de Vries, *Mol. Cryst. Liq. Cryst.*, **131**, 125 (1985).

51. P. Mandal, M. Mitra, S. Paul and R. Paul, *Liq. Cryst.*, **2**, 183 (1987).

52. A. de Vries, *Mol. Cryst. Liq. Cryst.*, **10**, 219 (1970).

53. A. de Vries, *Mol. Cryst. Liq. Cryst.*, **11**, 261 (1970).

54. I. G. Chistyakov, and W. M. Chaikowsky, *Mol. Cryst. Liq. Cryst.*, **7**, 269 (1969).

55. A. de Vries, *Mol. Cryst. Liq. Cryst.*, **10**, 31 (1970).

56. H. P. Klug and L. E. Alexander, *"X-ray Diffraction procedures"*, John Wiley and Sons, N. Y., p. 114 and 473 (1994).

57. C. Kittle, *Intro to Solid State Physics*, Wiley Eastern, Chapter 2 (1976).

58. D. Demus and L. Richter, *Textures of Liquid Crystals*, Verlag Chemie, NY(1978).

59. A. J. Slaney, K. Takatohi and J. W. Goodby in *The Optics of Thermotropic Liquid Crystals*. Ed. S. Elston and R. Sambles, Taylor & Francis (1998).

60. Y. Bouligand in *Handbook of Liquid Crystals*. Vol. **1** (Fundamentals), Ed. D. Demus, J. Goodby, G. W. Gray, H.-W. Spiess and V. Vill, WILEY-VCH, Verlag GmbH, Weinheim, FRG (1998).

61. G. Vertogen and W. H. de Jeu (Eds.), *Thermotropic Liquid Crysatals Fundamentals.*, Springer-Verlag 1988. p-207.

62. G. R. Luckhurst in *Liquid Crystals & Plastic Crystals* (Eds. G. W. Gray and P. A. Winsor), Ellis Horwood Limited(1974), Vol **2,** p-144.

63. C. L. Khetrapal and A. C. Kunwar in *Advances in Liquid Crystals* Vol. **1-6**, Ed. Glenn H. Brown, AP (1983). p-173.

64. V. D. Neff in *Liquid Crystals & Plastic Crystals* (Ed. G. W. Gray and P. A. Winsor), Ellis Horwood Limited(1974), Vol **2**, p-231.

65. S. J. Gupta, R. A. Gharde and A. R. Tripathi, , *Mol. Cryst. Liq. Cryst.*, **364**, 461 (2001).

66. K. Toriyama, K. Suzuki, T. Nakagomi, T. Ishibashi and K. Odawara, *J. de Phys*, **40**, C3-317 (1979).

67. D. A. Dunmur and W. H. Miller, *Mol. Cryst. Liq. Cryst.*, **60**, 281 (1980).

68. R. E. Michel and G. W. Smith, J. Appl. Phys. **45**, 3234(1974).

69. *Theory of Electric Polarization*, Vol I (1973). 2nd edition Ed. C. J. F. Böttcher. and Vol II, 2nd edition Ed. C. J. F. Böttcher and P. Bordewijk. Elsevier Scientific Publishing Co. (1978).

70. W. H. de Jeu and T. W. Lathouwers, *Z. Naturforsch* **29a**, 905 (1974).

71. H. Kresse in *Handbook of Liquid Crystals*, Vols. **2A**, (Eds. D. Demus, J. Goodby, G.W. Gray, H.-W. Spiess and V. Vill, Wiley-VCH, Verlag GmbH, Weinheim, FRG (1998), p 91.

72. S. Urban and H, Kresse in *Physical properties of liquid* crystals, (Eds. D. A. Dunmur, A. Fukuda and G. R. Luckhurst), INSPEC, London(2001), Ch 6.1 and 6.2

73. W. Maier and G. Meier, *Z. Naturforsch*, **16a**, 262 (1961),

74. L. Onsager, *Ann. N.Y. Acad. Sci.*, **51**, 627 (1949); *ibid, J. Am. Chem. Soc.*, **58**, 1486 (1936); *ibid, Phys. Rev.*, **62**, 558 (1942).

75. P. Bordewijk, *Physica*, **75**, 146 (1974).

76. L. Bata and A. Buka, *Mol. Cryst. Liq. Cryst*, **63**, 307 (1981).

77. H. Frohlich, *Theory of Dielectrics*. Clarendon Press (Oxford, 1949); H. Frohlich, *J. Chem. Phys.*, **22**, 1804 (1954).

78. P. Bordewijk, *Physica*, **69**, 422 (1973).

79. P. Bordewijk, *Physica*, **75**, 146 (1974).

80. P. Bordewijk and W. H. de Jeu, *J. Chem. Phys.* **68(1)**, 116(1978).

81. W. H. de Jeu and P. Bordewijk, *J. Chem. Phys.* **68(1)**, 109(1978).

82. W. H. de Jeu, T. W. Lathouwers and P. Bordewijk, *Phys. Rev. Lett.* **32**, 40 (1974).

83. W. H. de Jeu, J. W. A. Goosens and P. Bordewijk, *J. Chem. Phys.* **61**, 1985(1974).

84. M. V. Laue, "Sitzungberichte der (kgl) Bayerische Akademic der Wissenschaften", p. 308 (1982).

85. W. L. Bragg, Proc. Camb. Phil. Soc., **17**, 43 (1913).

86. W. L. Bragg, *Proc. Roy. Soc.*, **A89**, 249 (1913).

87. J. D. Bernal and D. Crowfoot, *Trans. Farad. Soc.*, **29**, 1032(1933).

88. D.B. Chung, Ph.D. Dissertation, Kent State University, Kent, Ohio(1974), p38.

89. P. Mandal and S. Paul, *Mol. Cryst. Liq. Cryst.*, **131**, 223 (1985).

90. P. Mandal, S. Paul, H. Schenk and K. Goubitz, *Mol. Cryst. Liq. Cryst.*, **135**, 35 (1986).

91. P. Mandal, B. Majumdar, S. Paul, H. Schenk and K. Goubitz, *Mol. Cryst. Liq. Cryst.*, **168**, 135 (1989).

92. P. Mandal, S. Paul, C. H. Stam and H. Schenk, *Mol. Cryst. Liq. Cryst.*, **180B**, 369 (1990).

93. S. Gupta, P. Mandal, S. Paul, M. de Wit, K. Goubitz and H. Schenk, *Mol. Cryst. Liq. Cryst.*, **195**, 149 (1991).

94. P. Mandal, S. Paul, H. Schenk and K. Goubitz, *Mol. Cryst. Liq. Cryst.*, **210**, 21(1992).

95. P. Mandal, S. Paul, K. Goubitz and H. Schenk, *Mol. Cryst. Liq. Cryst.*, **258**, 209(1995).

96. A. Nath, S. Gupta, P. Mandal, S. Paul and H. Schenk, *Liq. Crystals.*, **20**, 765(1996).

97. Pranab Sarkar, Parimal Sarkar, Pradip Mandal and T. Manisekaran, *Mol. Cryst. Liq. Cryst.*, **325**, 91(1998).

98. A. J. Leadbetter and M. A. Mazid, *Mol. Cryst. Liq. Cryst.*, **65**, 265(1981).

99. R. F. Bryan, Proceedings of the Pre-Congress Symposium on Organic Crystal Chemistry, Poznan, Poland, 105(1979); *J. Structural Chem.*, **23**, 128(1982).

100. W. Haase and M.A. Athanassopoulou, *Liquid Crystals*, D.M.P. Mingos(Ed.), Springer-Verlag, Vol. I, pp. 139-197 (1999).

101. B. K. Vainshtein, *Diffraction of X-rays by Chain Molecules*, Elsevier, Amsterdam, (1966), p12.

102. M. F. C. Ladd and R. A. Palmer, *"Theory and practice of Direct methods in Crystallography"*, Plenum Pub. Co., N. Y., (1980).

103. H. Hauptman and J. Karle, *Acta Cryst.*, **9**, 45 (1956); ibid., **12**, 93 (1959).

104.J. Karle and H. Hauptman, *Acta Cryst.*, **14**, 217 (1961).

105.J. Karle and I. L. Karle, *Acta Cryst.*, **21**, 849 (1966).

106.H. Schenk (Ed), *Direct Methods in Solving Crystal Structures,* NATO ASI Series, Plenum Press, New York (1991).

107.G. Germain, P. Main and M. M. Woolfson, *Acta Cryst.*, **B26**, 274 (1970).

108.H. Schenk and C. T. Kiers, *Simpel 83, an automatic direct method program package,* University of Amsterdam, 1983; H. Schenk, *Recl. Trav. Chim. Pays-bas,* **102**, 1(1983).

109.G. M. Sheldrick, *Direct method package program,* University of Gottingen, Germany (1993).

110.S. R. Hall and J. M. Stewart, *XTAL,* University of Western Australia and Maryland (1989).

111.A. Altomere, G. Cascarano, C. Giacovazzo, A. Guagliardi, M. C. Burla, G. Polidori and M. Camalli, *The SIR 92 Programme,* (1992).

112.P. S. White, *PC Version of NRCVAX(88),* University of New Brunswick, Canada (1988).

113.Yao Jia-Xing, Zheng Chao-de, Quian Jin-Zi, Han Fu-Son, Gu Yuan-Zin and Fan Hai-Fu, *SAPI: A Computer Program for Automatic Solution of Crystal Structures from X-ary Data,* Institute of Physics, Academia Sinica, Beijing (1985).

114.C. J. Gilmore, *J. App. Cryst.*, **17**, 42 (1984).

115.C. J. Gilmore in *Direct Methods in Solving Crystal Structures,* H. Schenk (Ed), NATO ASI Series, Plenum Press, New York (1991), p177.

116.G. H. Stout and L. H. Jensen, *X-ray Structure Determination*, Macmillan, New York(1968), p195.

117.A. J. C. Wilson, Nature, **150**, 152(1942).

118.W. Cochran and M. M. Woolfson, *Acta Cryst.*, **8**, 1(1955).

119.W. Cochran, *Acta Cryst.*, **8**, 473 (1955).

120.J. Karle and H. Hauptman, *Acta Cryst.*, **9**, 635 (1956).

121.G. H. Stout and L. H. Jensen, *X-ray Structure Determination*, Macmillan, New York(1968), p353.

122.M. J. Buerger, *Crystal Structure Analysis,* Wiley, New York (1960).

Chapter III

DSC AND SMALL ANGLE X-RAY SCATTERING STUDIES ON SMECTIC AND NEMATIC PHASES OF TWO BI-SCHIFF'S BASES

Part of this work has been published in *Mol. Cryst. Liq. Cryst.*, **265**, 249 (1995)

3.1 INTRODUCTION

Liquid crystals with low melting points are used in various electro-optical devices. High-temperature melting liquid crystals, therefore, attracted little attention till it was suggested that such systems might be used in gas-liquid chromatography (GLC). Use of liquid crystals in GLC was reviewed by Kelker and Von Schivizhoffen [1] and Schroeder [2]. The main aim was to use high-melting nematic liquid crystals for the gas-liquid chromatographic separation of geometric isomers of various systems like underivatized steroid epimers [3], drug isomers [4], 3-5 ring polycyclic aromatic hydrocarbon (PAH) isomers [5] etc. which is not attainable by conventional GLC liquid phases. With this aim Janini *et al.* [6] synthesised the di-Schiff's base compound N, N′ –Bis (p-methoxybenzylidine)-α, α′ -bi-p-toluidine (BMBT) and found that it can be used in the analysis of high-boiling solute classes having a broad based interest to biochemical and ecological research. For example, separation of PAH isomers by GLC using BMBT has direct application in carcinogenesis research and in environmental evaluation of human exposure to PAH. They later found that the butoxy member of the series (BBBT) is more effective than BMBT [7,8]. General conclusion was that for members of a homologous series, the higher the temperature T_{NI} and the order parameter $\langle P_2 \rangle$, the more effective it is in GLC separation. BMBT, BBBT and several other members of the series were studied by Janini *et al.* [6-8] to determine the transition temperatures by optical microscopy and thermodynamic parameters at transition points by DSC study, phases were identified by the optical textures. To the best of our knowledge no X-ray diffraction study on the compounds has been done so far. We have, therefore, undertaken the study of BMBT and BBBT by small angle X-ray scattering technique to determine various physical and molecular properties in both the smectic and nematic phases. Molecular and crystal structure of the compound BBBT was also reported from our laboratory earlier [9]. Packing of the molecules in the liquid crystalline as well as in the crystalline state has been discussed. Different properties of BMBT and BBBT have been compared with other structurally related compounds like mono- and di-Schiff's bases.

3.2 EXPERIMENTAL

The title compounds, BMBT and BBBT, were obtained from Eastman Kodak and used without further purification. Phase transition temperatures were determined by studying textures under polarizing microscope (150X). Mettler FP82 hot stage and FP80 control system were used.

Small angle X-ray photographs of both non-aligned and magnetically aligned samples were taken throughout the mesomorphic range. A high temperature camera, described in Chapter II, was used. The sample was taken in Lindemann glass capillary of ~ 1.0 mm diameter and a temperature controller (Indotherm 401-D2) was used to control the temperature within ±0.5°C. We tried to get monodomain sample in smectic phase by very slow and regulated cooling from isotropic to smectic phase using only the capillary surface effect and also applying magnetic field of 0.5 Tesla. Attempt was also made to align the sample by slow heating to smectic phase in presence of magnetic field. But only partial alignment could be achieved. All photographs were taken with X-rays perpendicular to the magnetic field direction. In order to determine various parameters the photographs were scanned linearly and circularly by an optical densitometer (Carl Zeiss, Jena, Model MD100). Details of the experimental procedure have been described in Chapter II.

3.3 RESULTS AND DISCUSSIONS

An unspecified variety of mosaic texture in the smectic region and marbled texture in the nematic phase were observed in texture study. Nematic droplets were observed at N-I transition both during heating and cooling. Pre-transition effect was observed both before Cr-Sm and N-I transitions. Structural formula of the compounds, observed phase sequence with transition temperatures (in °C) and thermodynamic parameters are given below:

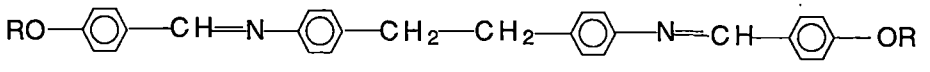

BMBT:	Cr	179.3 (181) ⟷		N	309.4 (337) ⟷	I
(R=CH_3)		145.1				
ΔH (kJ/mole)		**50.4 (43.5)**			**1.1 (7.2)**	
ΔS (J/mole.K)		**111.4 (96.0)**			**1.9 (11.7)**	

BBBT :	Cr	159.0(159) ⟷		Sm	188.0 (188) ⟷	N	293.0 (303) ⟷ I
(R=C_4H_9)		145.0			172.0		
ΔH (kJ/mole)		**26.53 (24.7)**			**12.04 (12.2)**		**5.01 (8.5)**
ΔS (J/mole.K)		**61.39 (57.2)**			**26.11 (26.5)**		**8.85 (14.7)**

Transition temperatures and the thermodynamic parameters at the transition points obtained by Janini *et al.* [6,7,8] are given within parentheses for comparison. It is observed that the transition temperatures, determined from texture studies, agreed with reported values except T_{NI} which was 28° (for BMBT) and 10° (for BBBT) less than the reported values. Repeated observations yielded same values. Supercooling effect was also observed by us at N-Cr, N-Sm and Sm-Cr transitions which was not reported earlier. Though it is unusual to have a hysteresis effect at transitions within different mesophases but such observation has been reported recently [10]. The DSC study at a heating rate of 5°C/min, made with Mettler thermosystem FP84, showed transition temperatures almost identical to those observed by texture study. Calculated transition enthalpies (ΔH) and entropies (ΔS) during heating are shown above. Values obtained by Janini *et al.* [8] are shown within parentheses. The maximum discrepancy in thermodynamic parameters is also observed at T_{NI}. It might be noted that Janini *et al.* [7,8] made DSC study at a scan rate of 10 or 20°C/min. This high scan rate may be one of the reasons of discrepancy in T_{NI} and thermodynamic parameters. Moreover, they were not sure about the purity of the compound. Also to find the accuracy of their results they measured ΔH value at T_{NI} of PAA and found it to be 0.72 kJ/mole [8]. They observed that this was in good agreement with values reported in [11]. However, Chandrasekhar [12] quoted ΔH value at T_{NI} of PAA as 0.574 kJ/mole (measured by Arnold [13]). This is about 26% less than the measured value of Janini *et al.* [8]. For BBBT during

cooling the N-Sm transition was detected by DSC at 171.1°C as against 172.0°C by texture study; the Sm-Cr transition was observed at 120.2°C whereas by texture study the transition was observed at 145.0°C. X-ray study (described below) reveals that this was actually CrII-CrI transition, so by DSC study we could not detect Sm-Cr transition. This may not be very unusual if it is considered that the smectic phase is actually a highly ordered 'soft' crystalline state as described later.

Janini *et al.* [8] observed that the first two members of the series were pure nematogens, the next two members showed both nematic and smectic phases, members with n=5-8 showed two smectic types and a nematic region while the tenth member exhibited only one smectic phase. However, as noted earlier, they identified the phases only by texture study, so could not characterize the phases explicitly. A representative X-ray diffraction photograph of BMBT at 165°C is shown in Figure 3.1. This is a typical nematic photograph except that the inner ring is weak. X-ray photographs of BBBT in smectic phase at 160°C are shown in Figures 3.2(a) for non-aligned sample and in Figure 3.2(b) for magnetically aligned sample. From the X-ray photographs the phase apparently appears to be a crystalline phase rather than smectic. It shows two very closely spaced outer rings with 'd' values of 4.44 and 4.55 Å; there are four inner rings with 'd' spacings of 11.97, 13.55, 21.47 and 29.90 Å, not multiple of each other (Table 3.1). These data are obtained from aligned sample. Both the photographs were taken during cooling from isotropic phase. Evidently though monodomain sample could not be obtained, partial alignment could be achieved by applying magnetic field which is not expected in crystalline phase. Moreover, comparison of photographs at 158°C, one obtained during heating (Figure 3.3(a)) and the other during cooling (Figure 3.3(b)), suggests that the former photograph is in crystalline phase while the latter is in smectic phase. Since the innermost ring originates from the density variation along the smectic layers, the smectic layer thickness would be 29.90Å at 160°C.The model length of BBBT in all *trans*-conformation is found to be 34.3 Å. So the molecules are tilted within the smectic layers, the tilt angle being 29.3°. This tilt angle is found to decreases with temperature (shown later) and it is not expected in a perfect

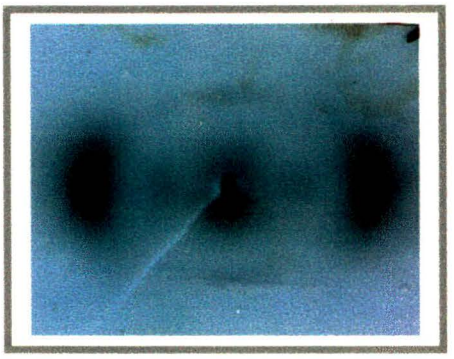

Figure 3.1 X-ray diffraction photograph of BMBT at 165°C in nematic phase.

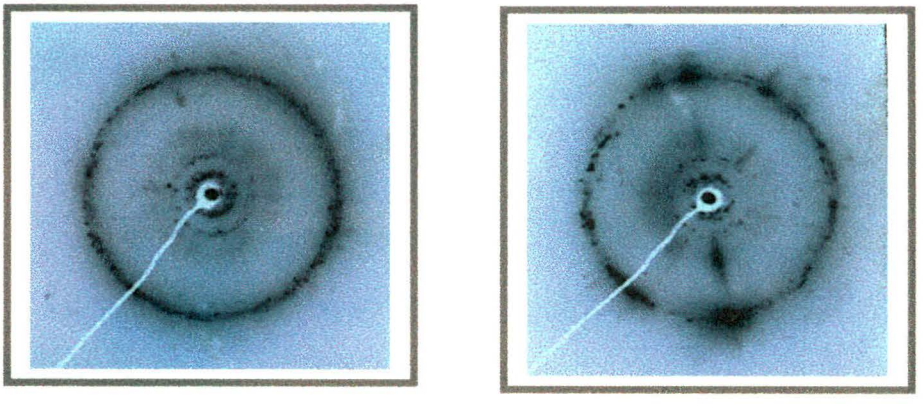

(a) (b)

Figure 3.2 X-ray diffraction photographs of BBBT in smectic phase: (a) non aligned and (b) aligned at 160°C.

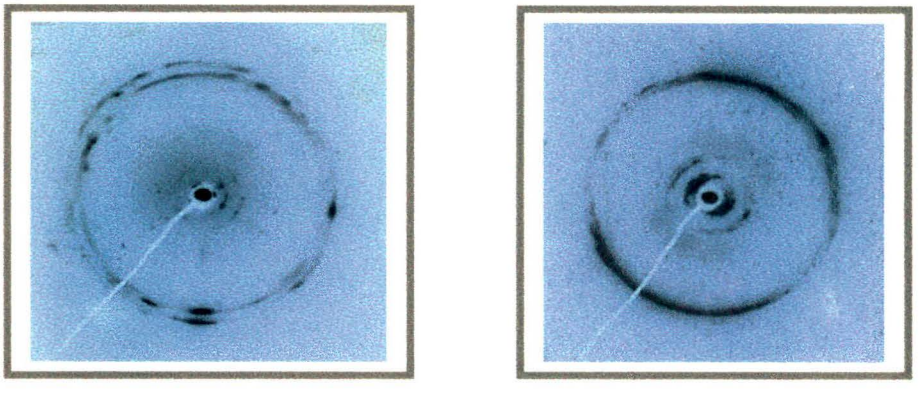

(a) (b)

Figure 3.3 X-ray diffraction photographs of BBBT at 158°C: (a) during heating and (b) during cooling.

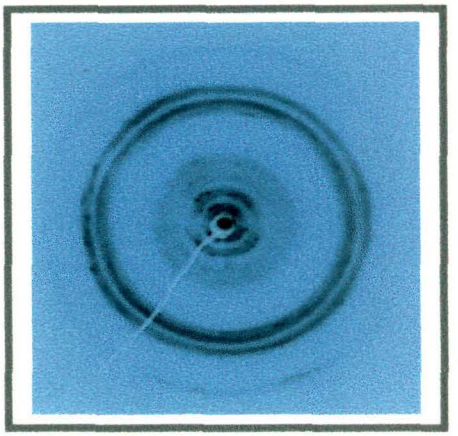

Figure 3.4 X-ray diffraction photographs of BBBT at room temperature (25 °C).

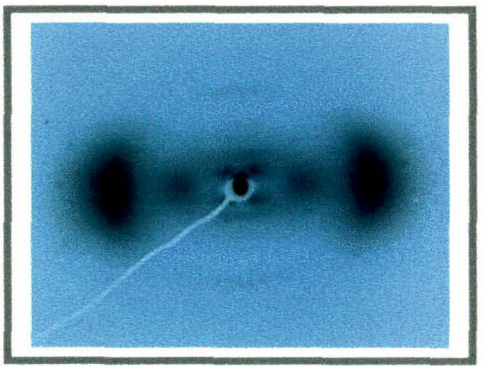

Figure 3.5 X-ray diffraction photograph of BBBT in nematic phase at 183 °C.

crystalline phase. However, presence of two closely spaced sharp outer rings indicates that there is long range positional ordering within the layers. Doucet [14] and Vertogen [15] noted the appearance of closely spaced several rings in Sm G and Sm H phases in powder pattern of TBBA and PPP. Probably, because of very high degree of thermal agitation higher order outer rings are not visible in our case. All these features along with the observed texture and DSC data suggest that the above phase is a tilted version of Crystal B or Crystal E phase. So the phase may be SmG/SmG'/SmH/SmH' which are now termed as Crystal G/J/H/K phases [16,17]. For precise identification of the phase, one, however, needs to index a photograph obtained from a mono-domain sample with X-rays parallel to the smectic layer normal. As far as the extent of positional ordering is concerned these modifications are crystalline i.e. there is long range order within and perpendicular to the smectic layers; however, the molecules are undergoing rapid reorientational motion about their long axes normally not observed in crystals[17]. So they are also called smectic like 'soft' crystals. It may be of interest to point out that Crystal G phase was observed in mono-Schiff's base compounds *p-n-alkoxybenzylidene-p'-n-alkylaniline (nO.m)* [18,19] and as mentioned before, in a pyrimidine compound 2-(4-n-*pentylphenyl)-5-(4-n-pentyloxyphenyl) pyrimidine* (PPP) [20]. Both the Crystal G and Crystal H phases were observed in directly coupled di-Schiff's base compound *Terephthalylidene-bis-(p-butylaniline)* (TBBA) [21,22].

X-ray photograph of BBBT at room temperature is shown in Figure 3.4. Measured 'd' spacings reveal that this phase is different from the crystalline phase observed at 158°C during heating (Figure 3.3(a)). Thus there are two crystalline modifications in the sample. In DSC study this CrII-CrI transition is observed at 120.2°C. Presence of two or more crystalline modifications is not uncommon in mesophase forming compounds, for example three crystalline modifications have been observed in OOBPD [23]. For many nCB and nOCB members it was observed that slow or delayed cooling gives rise to a lower melting crystalline ploymorphic form which then slowly converts into the higher melting stable crystalline structure [24-27]. These polymorphic crystalline forms result from a subtle balance of intermolecular interactions [28].

It is also observed that the diffraction photograph of BBBT at 150°C during cooling is not of smectic phase, as was expected from texture study, rather it shows Cr-II phase. The 'd' spacings obtained from this photograph are similar to those observed at 158°C during heating. Thus though the texture study indicates supercooling of the smectic phase till 145°C, but X-ray studies show that the supercooling is not extended even upto 150°C. Different container geometry, sample thickness and external alignment field in the two experimental situations may be responsible for this type of anomalous behaviour.

Aligned X-ray photograph in the nematic phase of BBBT is given in Figure 3.5. This photograph is qualitatively different from the nematic phase photograph of BMBT (Figure 3.1). In addition to the outer crescents it is observed that the inner crescent, in this case, splits into four distinct spots symmetrically about the meridional direction. Unlike the ordinary nematic phase in BMBT, this phase is, therefore, identified as skewed cybotactic nematic phase where the molecules are arranged in 'cybotactic groups' such that the ends of the rod-like molecules constitute more or less a well-defined boundary plane which is tilted to the average direction of the molecules in the group (Figure 2.6). Such phase has been observed in mono-Schiff's base compound 4O.4 [19]; in several members of the series bis-(4'-n-alkoxybenzal)-2-chloro-1,4-phenylinediamine [29-34]. Cybotactic nematic phase has also been observed by the author (and co-workers) in pentyl and octyl members (and in their binary mixtures) of the series *p-pentylphenyl-2-chloro-4-(p-pentylbenzoyloxy)-benzoate* [35] (Though a substantial amount of work was done by the author, results of this work are not presented in this dissertation since those results were presented by the first author Parimal Sarkar in his thesis).

Variations of different molecular parameters, determined from X-ray photographs, with temperature have also been studied. The outer equatorial arc in the nematic phase arises from the intermolecular distances perpendicular to the director. Finding the peak position the average intermolecular distance, D, is calculated using a modified Bragg's relation, $2D\sin\theta=1.117\lambda$, obtained on the assumption of cylindrical symmetry of the molecules [29,30]. In BMBT the D

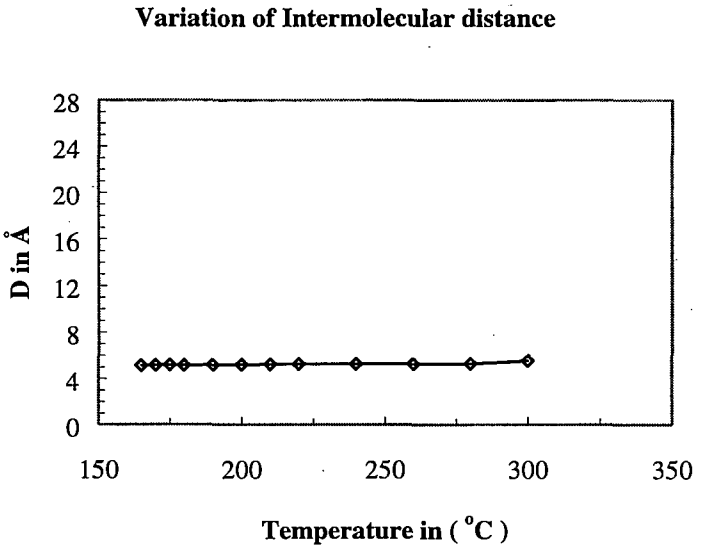

Figure 3.6 Temperature variation of D in the nematic phase of BMBT.

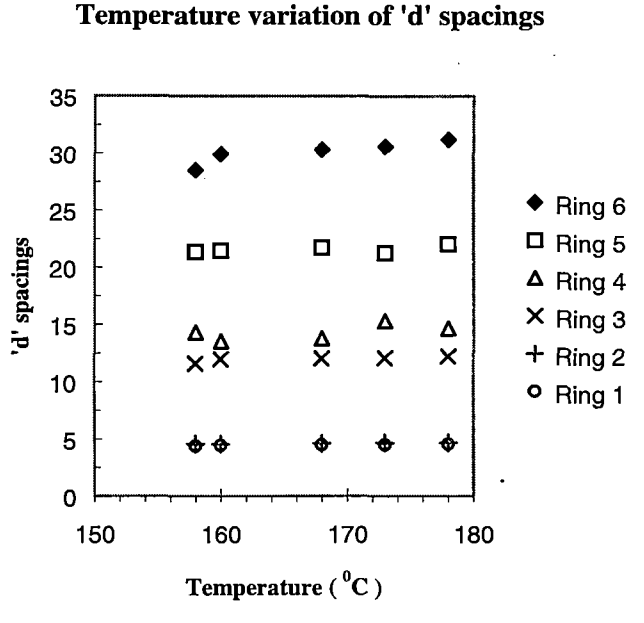

Figure 3.7 Temperature variation of 'd' spacings in smectic phase of aligned BBBT. Outermost ring is labeled as ring 1.

values are found to increase slightly with temperature, D_{min}= 5.12 Å and D_{max}= 5.53 Å (Table 3.2). The temperature dependence of D is shown in Figure 3.6.

The meridional scattering amplitude is obtained from the density variation along the director and gives information about the apparent molecular length, *l*, of the molecules in the nematic phase. In this case unmodified Bragg's relation is used. In BMBT the inner ring is observed to be very weak throughout the nematic phase. So it is very difficult to find the peak positions, necessary to calculate the apparent molecular length (*l*). Only at 165°C, peak positions could be found approximately and corresponding *l* value is found to be 24.3 Å. However, the model length (L) of BMBT in all *trans*-conformation is found to be 26.4 Å. Thus the molecules are tilted at an angle 23.3° at 165°C. Of course, change of conformation of the molecules in the nematic phase may also result in *l* values less than the model length.

In the smectic phase of BBBT the d-spacings corresponding to the intermolecular distances (related to the two outer most rings) do not change appreciably with temperature as shown in Figure 3.7. However, the d-spacing corresponding to the smectic layer spacing (related to the innermost ring) increases with temperature appreciably. If the tilt angle (β_t) of the molecules within the smectic layer is defined as $\beta_t = \cos^{-1}(d/L)$, where d is the layer spacing and L is the model length of the molecules in all *trans* conformations, it is observed that β_t decreases from 33.8° to 24.6° with temperature (Table 3.3). This is shown graphically in Figure 3.8.

The temperature dependence of the average intermolecular distance (D) in the nematic phase of BBBT is shown in Figure 3.9. With temperature D is found to increase slightly, D_{min}= 5.02 Å and D_{max}= 5.24 Å (Table 3.4). On the other hand, it is observed that the value of the apparent molecular length (*l*) increases by 3.7 Å from a value of 22.2 Å to a value of 25.9 Å as the temperature changes from 178°C to 278°C (Table 3.4). This variation is also shown in Figure 3.9. Corresponding change in the tilt angle of the molecules is from 49.8° to 41.1° (Table 3.4), with a mean value of 46.0° and is depicted graphically in Figure 3.10. Value of β_t measured directly from the photograph is found to be about 45° at 183°C, almost

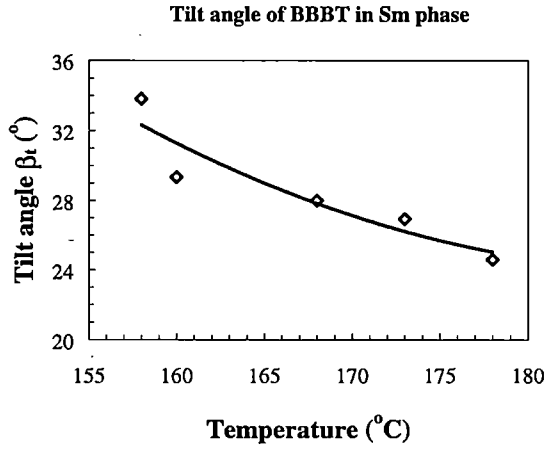

Figure 3.8 Tilt angle β_t (°) as a function of temperature in smectic phase of BBBT.

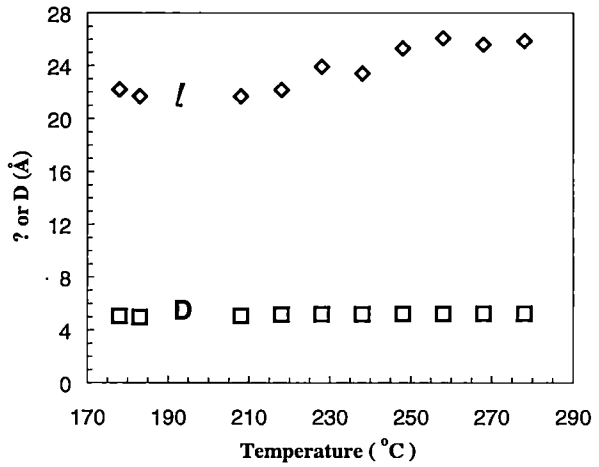

Figure 3.9 Variation of *l* and D with temperature in the nematic phase of BBBT.

equal to the calculated mean value of β_t. However, the tilt angle in this case is almost double the value found in case of BMBT which exhibits an ordinary nematic phase in contrast to the skewed cybotactic nematic phase in BBBT. Following Vainshtein and Chistyakov as described in [35], the size (b) of the cybotactic group was calculated using the relation $b=0.8L/\tan\beta_t$ and found to be about 27 Å. Thus the transverse correlation in the cybotactic group extends not beyond 5 molecular diameters.

Although the nature of temperature variation of the respective molecular parameters *l*, D and β_t is same in the Sm and the N phase, it is observed that there is an abrupt change in those parameters at temperature T_{Sm-N} signifying a first order phase transition. Measured ΔH and ΔS values also support this observation.

Though it is not yet possible to predict with certainty the occurrence of a particular mesophase from the knowledge of the molecular shape and nature of intermolecular interactions, it is argued that knowledge about the molecular packing in the crystalline state may provide an insight in understanding the solid - mesophase transitions [36-38]. It had been shown earlier by co-workers [9] that in the crystalline state BBBT molecules are arranged in layers and within a layer the molecules are tilted with respect to the layer normal. This arrangement is the classical solid state precursor of smectic phase. It may be mentioned here that in BOCP, another di-Schiff's base compound which exhibits only skewed cybotactic nematic phase, parallel imbricated mode of molecular packing was observed [37,39]. For comparison molecular packing diagrams of BBBT and BOCP have been reproduced in Figure 3.11.

Mandal *et al.* [9] observed that BBBT molecules crystallize in triclinic system with cell parameters *a*=6.116Å, *b*=7.916 Å, *c*=31.421 Å and α=92.39°, β=92.35°, γ=96.59° and space group $P\bar{1}$. Also, it is found that the molecular long axis, defined as a best fitted line through all the atoms, makes an angle 32° with the layer normal. Comparing these values with the d-values and the tilt angle of the molecules in the smectic phase it may be inferred that Crystal-Smectic transition is essentially of displacive type [40] contrary to reconstitutive type usually observed at this transition.

In order to get an idea about the intermolecular forces responsible for mesophase stability, all the intermolecular distances less than 3.65Å were calculated. Distances between few carbon atoms of centro-symmetrically related molecules are found to be less than the sum of their van der Waals' radii. Packing fraction of the structure, calculated using method of Kitaigorodsky [41], is found to be 0.73. It may thus be inferred that dispersion forces resulting from van der Waals

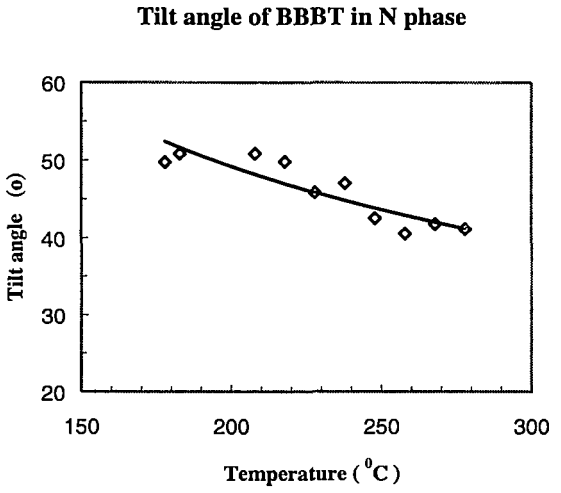

Figure 3.10 Tilt angle β_t (°) as a function of temperature in nematic phase of BBBT.

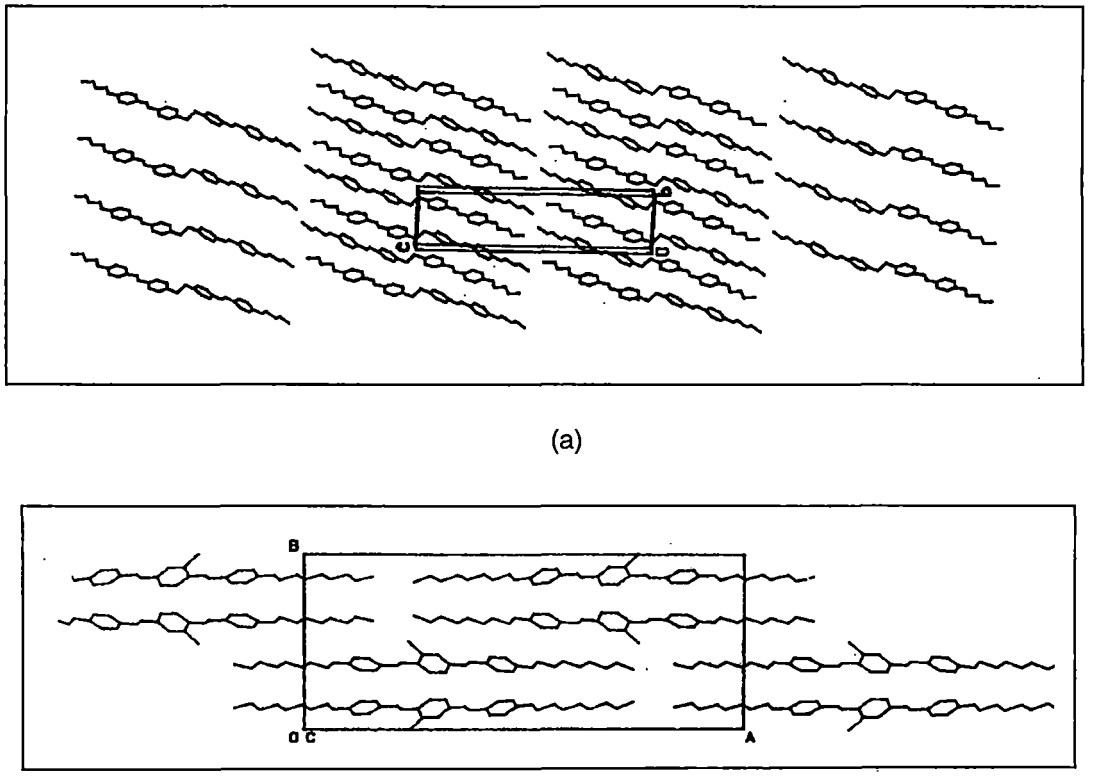

Figure 3.11 Crystal structure of (a) BBBT viewed along X-axis and (b) BOCP viewed along Z-axis.

interactions give rise to very efficient packing of the molecules. High melting point and very large thermal stability of the mesophases may be the result of this packing. No intermolecular contact is found to exist between the transverse dipole moments though the tilting of the molecules within the smectic layers may be favoured by the longitudinal component of the dipoles [42].

Both the orientational order parameters, $\langle P_2 \rangle$ and $\langle P_4 \rangle$, have been determined in the nematic phase by measuring the circular intensity distribution at the peak position of the equatorial crescents. The detailed procedure is given in Chapter II. Measured intensity values $I(\psi)$ as a function of ψ are fitted to an even-powered cosine series (equation 2.18). It is observed that with 8 terms in the series the fitting is quite good. The orientational distribution function f (β) is calculated from the fitted $I(\psi)$ values using equations (2.19) and (2.20) in Chapter II. Measured and fitted intensity values $I(\psi)$ as a function of ψ and the distribution function $f(\beta)$ as a function of β are presented in Table 3.5 for BBBT at temperature of 183°C. Variation of measured and fitted $I(\psi)$ with ψ has been shown in Figure 3.12(a) and that of $f(\beta)$ against β in Figure 3.12(b) at this temperature. As a representative set the observed and fitted $I(\psi)$ as well as the calculated $f(\beta)$ values have been presented only for one temperature (183°C). For brevity these quantities will not be shown even in subsequent chapters.

The temperature variations of the calculated order parameters, $\langle P_2 \rangle$ and $\langle P_4 \rangle$, in N phase of BMBT and BBBT have been shown in Figure 3.13 (and in table 3.6) and Figure 3.14 (and in table 3.7) respectively. Order parameter values were also calculated according to Maier and Saupe [43] mean field theoretical approach (using equation 2.3) and have been depicted in the above figures for comparison. In BMBT both the order parameters are not found to be in good agreement with the MS values. On the other hand, for BBBT, it is seen that $\langle P_2 \rangle$ values agree nicely with theoretical values, however, $\langle P_4 \rangle$ values at higher temperatures are found to be significantly lower than the theoretical values. Such behaviour of $\langle P_4 \rangle$ has been observed in mono-Schiff's base compounds BBBA and APAPA [19,44] and in several other compounds of different molecular structures [45-49]. This discrepancy

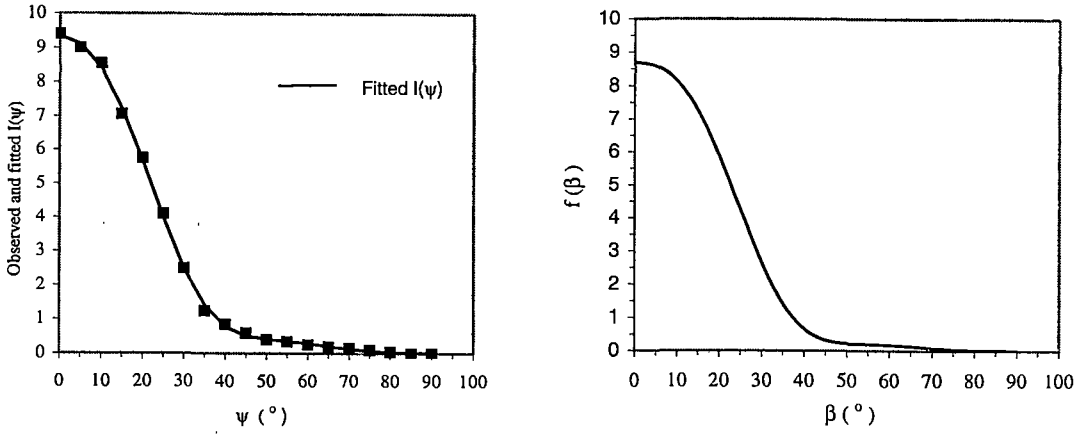

(a) (b)

Figure 3.12 Plot of (a) observed and fitted intensities I(ψ) against ψ and (b) distribution function f(β) against β of BBBT in N phase at 183°C.

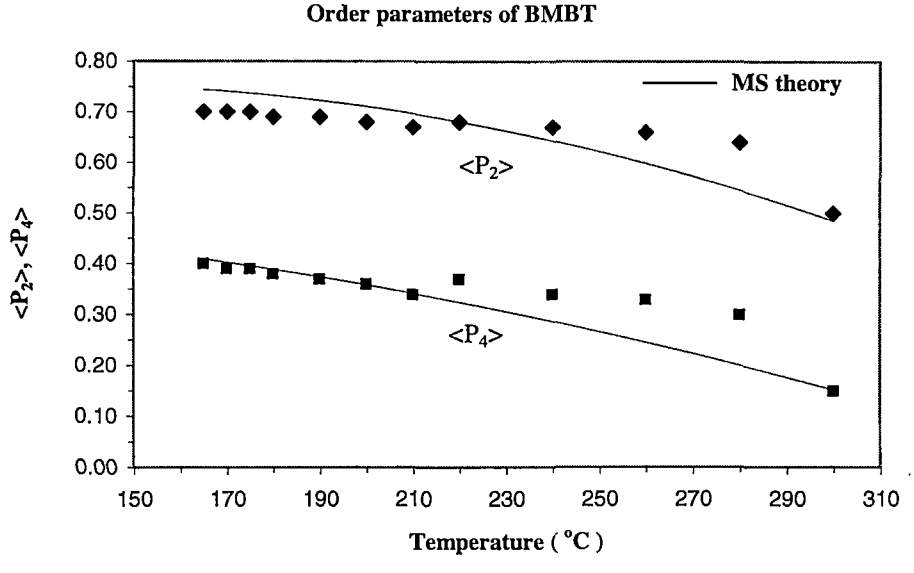

Figure 3.13 Experimental and theoretical order parameters $\langle P_2 \rangle$ and $\langle P_4 \rangle$ plotted against temperature in N phase of BMBT.

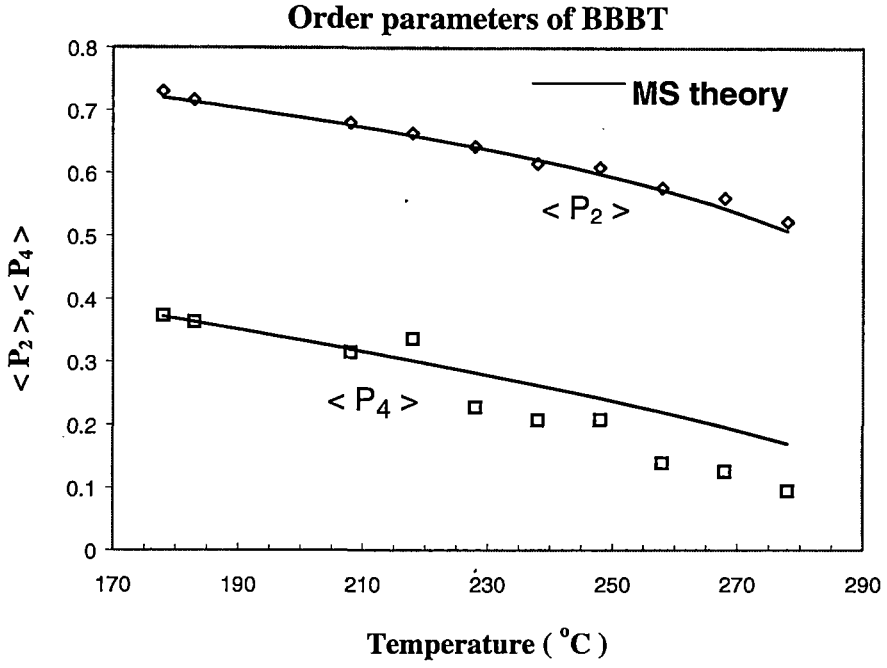

Figure 3.14 Variation of orientational order parameters with temperature in N phase of BBBT.

remains unexplained. According to Faber's continuum theory [50] the parameter $\ln\langle P_2\rangle/\ln\langle P_4\rangle$ should have a universal value of 0.30. In case of BMBT it varies from 0.37-0.39 with mean value of 0.38 whereas in BBBT it varies from 0.27-0.32 with mean value of 0.30 (the value 0.39 at 218°C is ignored). Thus excellent agreement is observed in BBBT but in BMBT the agreement is not good though the values are less spread in this case. Paul [51] and Parimal Sarkar *et al.* [52] also showed that for a large number of nematic compounds the agreement is impressive.

J. W. Goodby [17] has commented that for a typical nematic phase the order parameter has a value in the region of 0.4 - 0.7. Obviously, value of $\langle P_2\rangle$ has been referred here. Order parameters determined for a large number of compounds [51] from this laboratory agree with that observation but values higher than 0.60 are rare. In the two mono-Schiff's base compound APAPA [44] and BBBA [19] the $\langle P_2\rangle$ values are respectively found to be in the range 0.49 - .60 and 0.52-0.61. Range of $\langle P_2\rangle$ values in case of BMBT and BBBT are respectively 0.50-0.70 and 0.52-0.73. Comparable values of $\langle P_2\rangle$ were found in the cybotactic nematic phase of BHeCP,

BOCP and BdeCP [39]. The respective ranges are: 0.55-0.70, 0.60-0.74 and 0.56-0.72. But melting point of these materials is below 100°C. It may be reasonably assumed that high order parameter values of BMBT and BBBT increase their ability in GLC phase separation, as noted in the introduction. High melting point and quite a long range of the nematic phase stability (more than 100°C) are added advantage. Since the order parameters of BBBT are of higher value than those of BMBT, the former may be more effective in GLC separation technique than the latter.

TABLE 3.1

d-spacings of BBBT within smectic phase.

Sample to film distance =4 .92 cm
Wavelength of X-ray used λ=1.5418 Å
Measurements made on aligned sample

Temperature (in °C)	d-spacings (in Å) (Outermost ring is labeled as ring 1)					
	Ring 1	Ring 2	Ring 3	Ring 4	Ring 5	Ring 6
158	4.39	4.55	11.58	14.33	21.34	28.50
160	4.44	4.55	11.97	13.55	21.47	29.90
168	4.50	4.62	12.05	13.80	21.75	30.29
173	4.50	4.68	12.10	15.32	21.29	30.58
178	4.56	4.68	12.22	14.68	22.05	31.19

TABLE 3.2

Intermolecular distances (D) in nematic phase of BMBT

Sample to film distance = 6.92 cm
Wavelength of X-ray used λ=1.5418 Å
Measurements made on aligned sample

Temperature in °C	Intermolecular distance D in Å
165	5.12
170	5.15
175	5.17
180	5.15
190	5.17
200	5.20
210	5.24
220	5.27
240	5.27
260	5.27
280	5.29
300	5.53

TABLE 3.3

Tilt angle (β_t) of BBBT in smectic phase.
Model length of BBBT molecule L=34.3Å

Temperature in °C	Tilt angle β_t in degrees
158	33.8
160	29.3
168	28.0
173	26.9
178	24.6

TABLE 3.4

Intermolecular distance (D), apparent molecular length (*l*)
and tilt angle (β_t) of BBBT in N phase.

Sample to film distance =4.92 cm Wavelength of X-ray used λ=1.5418 Å

Temp. in °C	D in Å	*l* in Å	β_t in degrees
178	5.02	22.2	49.7
183	4.99	21.7	50.8
208	5.04	21.7	50.8
218	5.13	22.1	49.8
228	5.16	23.9	45.8
238	5.18	23.4	47.0
248	5.21	25.3	42.5
258	5.2	26.1	40.5
268	5.23	25.6	41.8
278	5.24	25.9	41.1

TABLE 3.5

Observed and fitted intensities I(ψ) and orientational distribution functions f(β)
Sample: BBBT Temperature: 183°C

Azimuthal angle ψ (°)	X-ray intensity I(ψ) (arbitrary unit)		Orientational angle β (°)	Orientational distribution function f(β) (arbitrary unit)
	Measured	Fitted		
0	9.40	9.34	0	8.70
5	9.00	9.11	5	8.58
10	8.55	8.41	10	8.15
15	7.05	7.23	15	7.27
20	5.75	5.68	20	5.90
25	4.10	4.00	25	4.26
30	2.50	2.50	30	2.66
35	1.25	1.42	35	1.42
40	0.85	0.79	40	0.66
45	0.60	0.51	45	0.32
50	0.40	0.42	50	0.22
55	0.35	0.36	55	0.20
60	0.25	0.29	60	0.17
65	0.20	0.21	65	0.13
70	0.15	0.13	70	0.08
75	0.10	0.07	75	0.04
80	0.05	0.04	80	0.02
85	0.00	0.02	85	0.01
90	0.00	0.02	90	0.01

TABLE 3.6

Orientational order parameters of BMBT in N phase

Temperature (°C)	Order parameters from X-ray data		Maier-Saupe theoretical order parameters	
	$\langle P_2 \rangle$	$\langle P_4 \rangle$	$\langle P_2 \rangle$	$\langle P_4 \rangle$
165	0.70	0.40	0.75	0.41
170	0.70	0.39	0.74	0.40
175	0.70	0.39	0.74	0.40
180	0.69	0.38	0.73	0.39
190	0.69	0.37	0.72	0.37
200	0.68	0.36	0.71	0.36
210	0.67	0.34	0.69	0.34
220	0.68	0.37	0.68	0.32
240	0.67	0.34	0.65	0.29
260	0.66	0.33	0.60	0.25
280	0.64	0.30	0.55	0.20
300	0.50	0.15	0.48	0.15

TABLE 3.7

Orientational order parameters of BBBT in N phase

Temperature in °C	Order parameters from X-ray data		Maier-Saupe theoretical order parameters	
	<P2>	<P4>	<P2>	<P4>
178	0.73	0.37	0.72	0.37
183	0.72	0.36	0.71	0.36
208	0.68	0.32	0.68	0.32
218	0.66	0.34	0.66	0.30
228	0.64	0.23	0.64	0.28
238	0.62	0.21	0.62	0.26
248	0.61	0.21	0.60	0.24
258	0.58	0.14	0.57	0.22
268	0.56	0.13	0.54	0.20
278	0.52	0.09	0.51	0.17

REFERENCES

1. H. Kelker and E.Von Schivizhoffen, *Advances in chromatography*, Vol. 6,(J. C. Giddings and R. A. Keller, Eds.), Marcel Dekker, N. Y., 1968, p. 247.
2. J. P. Schroeder, *Liquid Crystals and Plastic Crystals*, Vol. 1 (G. W. Gray and P. A. Winsor, Eds.), Ellis Harwood, Chichester, England, 1974, p. 356.
3. W. L. Zielinski, Jr., K. Johnston and G. M. Muschik, *Anal. Chem.*, **48**, 907 (1976).
4. M. Hall and D. N. B. Mallen, *J. Chromatog.*, **118**, 268 (1976).
5. P. E. Strup, R. D. Giammer, T. B. Stanford and P. W. Jones in *Carcinogenesis - A comprehensive Survey*, Vol. 1 (R. Freudenthal and P. W. Jones, Eds.), Raven Press, N. Y., 1976.
6. G. M. Janini, K. Johnston and W. L. Zielinski, Jr., *Anal. Chem.*, **47**, 670 (1975).
7. G. M. Janini, G. M. Muschik and W. L. Zielinski, Jr., *Anal. Chem.*, **48**, 809 (1976).
8. G. M. Janini, G. M. Muschik and C. M. Hanlon, *Mol. Cryst. Liq. Cryst.*, **53**, 15 (1979).
9. P. Mandal, S. Paul, K. Goubitz and H. Schenk, *Mol. Cryst. Liq. Cryst.*, **258**, 209 (1995).
10. J. P. F. Lagerwall, P. Rudquist, S. T. Lagerwall and F. Giebelmann, *Liq. Crystals*, **30**, 399(2003)
11. N. Barall II and J. Johnson, *Liquid Crystals and Plastic Crystals*, Vol. 2 (G. W. Gray and P. A. Winsor, Eds.), Ellis Harwood, Chichester, England, 1974, p 255.
12. S. Chandrasekhar, *Liquid Crystals*, 2nd Ed., *Cambridge*, UK, 1992, p26.
13. H. Arnold, *Z. Phys. Chem.*, (Leipzig), **226**, 146 (1964).
14. J. Doucet, The Molecular Physics of Liquid Crystals (G. R. Luckhurst and G. W. Gray, Eds.), Academic Press, London, 1979, p 317.
15. G. Vertogen and W. H. de Jeu, *Thermotropic Liquid Crystals, Fundamentals*, Springer Verlag, Berlin, 1987, p 45.
16. P. S. Pershan, *Structure of Liquid Crystal Phases*, World Scientific, USA, 1988, p 62.
17. J. W. Goodby, *Handbook of Liquid Crystals, Low Molecular Liquid Crystals I*, Vol. 2A (D. Demus, J. Goodby, G. W. Gray, H. W. Spiess and V. Vill, Eds.), Wiley-VCH, Weinheim,1998, Ch. I., p3.
18. L. Richter, D. Demus and H. Sackmann, *J. Phys. (Paris)*, **37**, C3-41 (1976).
19. P. Mandal, M. Mitra, S. Paul and R. Paul, *Liquid Crystals*, **2**, 183 (1987)
20. D. Demus, S. Diele, M. Klapperstuck, V. Link and H. Zaschke, *Mol. Cryst. Liq. Cryst.*, **15**, 161 (1971).
21. J. Doucet, A. M. Levelut and M. Lambert, *Mol. Cryst. Liq. Cryst.*, **24**, 317 (1974)
22. J. Doucet, A. M. Levelut and M. Lambert, *Phys. Rev. Lett.*, **32**, 301 (1974).
23. P. Mandal, R. Paul and S. Paul, *Mol. Cryst. Liq. Cryst.*, **131**, 299 (1985).
24. D.S. Hulme and E.P. Raynes, *J. Chem. Soc., Chem. Commun.*, 98 (1974).
25. K. Hori and H. Wu, *Liquid Crystals*, 26, 37 (1999).
26. K. Hori, M. Kurosaki, H. Wu and K. Itoh, *Acta Cryst.*, C52, 1751 (1996).
27. M. Kuribayashi and K. Hori, *Liquid Crystals*, 26, 809 (1999).
28. A. Jakli, I. Janossy and A. Vajda, *Liquid Crystals*, **27**, 1035(2000).
29. A. de Vries, *Mol. Cryst. Liq. Cryst.*, **10**, 31 (1970).

30. A. de Vries, *Mol. Cryst. Liq. Cryst.*, **10**, 219 (1970).

31. A. de Vries, *Liquid Crystals, The Fourth State of Matter* (F. D. Saeva, Ed.), Marcel Dekker, New York, 1979, p. 15.

32. L. V. Azaroff, *Proc. Nat. Acad. Sci.*, **77**, 1252 (1980).

33. V. M. Sethna, A. de Vries and N. Spielberg, *Mol. Cryst. Liq. Cryst.*, **62**, 141 (1980).

34. L. V. Azaroff and C. A. Schumann, *Mol. Cryst. Liq. Cryst.*, **122**, 309 (1985).

35. Parimal Sarkar, Pranab K. Sarkar, Sukla Paul and Pradip Mandal, *Phase Transitions*, **71**, 1 (2000).

36. R. F. Bryan, *J. Struc. Chem.*, 23, 128(1982).

37. P. Mandal, S. Paul, H. Schenk and K. Goubitz, *Mol. Cryst. Liq. Cryst.*,**210**, 21 (1992) and references therein.

38. W. Haase and M.A. Athanassopoulou, *Liquid Crystals*, D.M.P. Mingos(Ed.), Springer-Verlag, Vol. I, pp. 139-197 (1999).

39. B. Jha, S. Paul, R. Paul and P. Mandal, *Phase Transitions*, **15**, 39(1989).

40. R. F. Bryan and P. G. Fourier, *Mol. Cryst. Liq. Cryst.*, **60**, 133 (1980).

41. A. I. Kidaigorodsky, *Molecular Crystals and Molecules*,Academic Press, New York, 1973, p 18.

42. N. V. Madhusudana, *Liquid Crystals —Applications and Uses* (B. Bahadur, Ed.), World Scientific, Singapore, 1990, p. 76.

43. W. Maier and A. Saupe, *Z. Natureforsch.*, **14a**, 882 (1959); Ibid, **15a**, 287 (1960).

44. P. Mandal, M. Mitra, K. Bhattacharjee, R. Paul and S. Paul, *Mol. Cryst. Liq. Cryst.*, **149**, 203 (1987).

45. B. Bhattacharjee, S. Paul and R. Paul, *Molec. Phys.*, **44**, 1391 (1981).

46. B. Bhattacharjee, S. Paul and R. Paul, *Mol. Cryst. Liq. Cryst.*, **89**, 181 (1982).

47. S. Jen, N. A. Clark, P. S. Pershan and E. B. Priestley, *Phys. Rev. Lett.*, **31**, 1552 (1973)

48. S. Kobinata, Y. Nakajima, H. Yoshida and S. Maeda, *Mol. Cryst. Liq. Cryst.*, **66**, 387 (1981)

49. J. P. Heagen, *J. Phys. Lett. (Paris)*, **36**, 209 (1975).

50. T. E. Faber, *Proc. Royal Soc. London A*, **353**, 247(1977).

51. R. Paul, *Liquid Crystals*, **9**, 239 (1991).

52. P. Sarkar, P. Mandal, S. Paul, R. Paul, R. Dabrowski and K. Czyprinski, *Liq. Crystals,* **30**, 507(2003).

Chapter IV

X-RAY STUDIES ON HEXYLOXYBENZYLIDENE PHENYLAZOANILINE, OCTYLOXYBENZYLIDENE PHENYLAZOANILINE AND THEIR MIXTURE

4.1 INTRODUCTION

Schiff's base compounds were the first room temperature liquid crystals with high thermal stability[1]. But, because the azomethine linkage (-CH=N-) imparts colour to the material and is found to be susceptible to water causing degradation in the physical properties, the materials are not used in commercial display devices[2,3]. However, such compounds, specifically N-(4-n-alkoxybenzylidene)-4'-alkylanilines (nO.m series) have extensively been studied because they also exhibit rich smectic polymorphism and as a result has been the subject of considerable structural work [4,5]. For example, 5O.6 is found to exhibit N, SmA, SmC, SmF, SmB, SmH [5] (the last two phases are now termed as Crystal phases as described in Chapter I). In this connection we have undertaken the study on hexyl and octyl members of the series N-(4-n-alkoxybenzylidene)-4'-phenylazoaniline by X-ray diffraction techniques. Henceforth, the compounds will respectively be referred to as 6OBPAA and 8OBPAA. In these compounds one alkyl chain of the nO.m series is replaced by an azophenyl group enhancing the rigidity of the molecules. Arora and Fergason [6] and Fishel and Patel [7] reported the transition temperatures and the phases observed by DTA and optical microscopy. K. R. K. Rao *et al.* [8] studied the temperature dependence of density and ultrasonic velocity of the hexyl member. Sakagami and Nakamizo [9] explored the possibility of using the compounds in GLC study. No X-ray study is reported so far to investigate the nature of molecular organizations in the smectic and nematic phases of the compounds. Moreover, equimolar mixture of the two compounds have also been studied to see if there is any change in physical properties with relation to the properties of the pure compounds.

4.2 EXPERIMENTAL

The compounds were synthesised by Prof. R. A. Vora, University of Vadodara, India and were kindly donated to us. We studied the compounds without further purification. Phase transition temperatures were determined by studying textures under polarizing microscope (150X) using Mettler FP80 control system and

FP82 hot stage. Typical mosaic texture in smectic B phase and marble texture in the nematic phase was observed in both the pure compounds and the mixture [10]. Near T_{NI} typical schlieren texture, consisting entirely of 4-brush |s|=1 disclinations, were found in all cases indicating uniaxial character of the nematic phase [11]. In smectic A phase broken fan shaped texture was observed in 6OBPAA, while in 8OBPAA and in the binary mixture typical fan shaped texture was observed. Since no photographic facility was available with the polarizing microscope, photomicrograph of the textures cannot be depicted. Fishel and Patel [7] did not specify the type of observed textures, only mentioned that criteria of Sackmann and Demus [12] was used for preliminary classification. DSC studies on the compounds could not be made because of the non-availability of the samples after the X-ray work. The structural formula of the compounds and observed phase sequence with transition temperatures (in °C) are given below. Supercooling effect was observed in crystallization temperature.

6OBPAA: 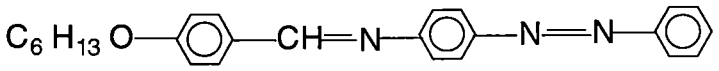

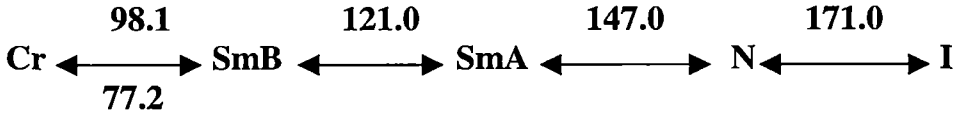

8OBPAA: 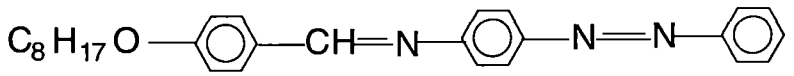

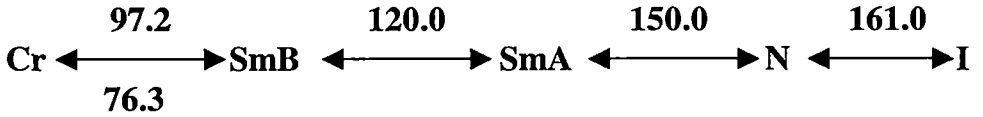

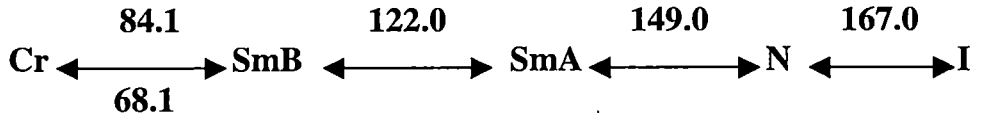

Transition temperatures observed by us differ by few degrees from those reported earlier [6,7,8], values reported by different workers are also found to be

different. K. R. K. Rao *et al.* [13] found transition enthalpies (kJ/mole) as 6.795 (K-SmB at 110°C), 2.254 (SmB-SmA at 124.5°C), 1.307 (SmA-N at 148°C) and 0.016 (N-I at 177°C) in 6OBPAA. Thus no change in phase sequence or no appreciable change in transition temperatures is observed between the two homologues except that the temperature T_{NI} is 10°C less in 8OBPAA than in 6OBPAA. In the equimolar binary mixture of the two compounds all the transition temperatures are

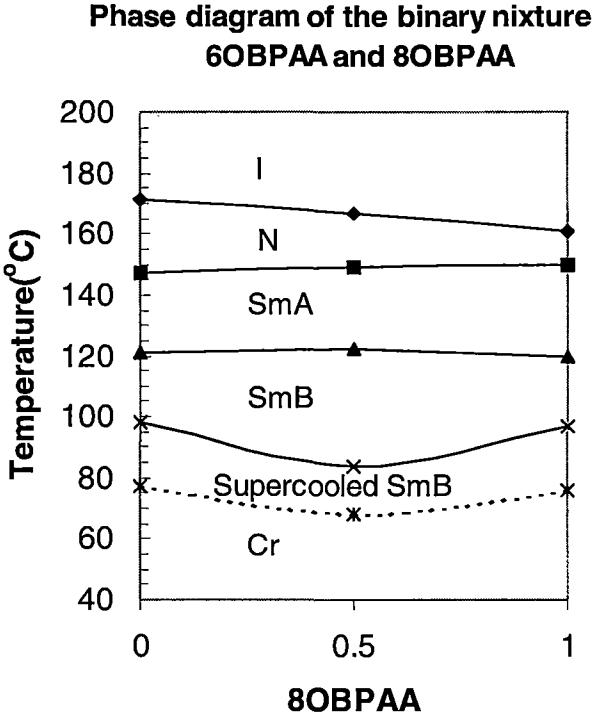

Figure 4.1 Phase diagram of the equimolar mixture of 6OBPAA + 8OBPAA.

found to vary linearly with concentration, however, there is enhancement of the SmB phase by about 15°. Phase diagram of the mixture is shown in Figure 4.1.

Phase behaviour of two related Schiff's bases may be compared at this stage. The compound 6O.4 (structural formula: $C_6H_{13}O$ –C_6H_4 – CH = N – C_6H_4 – C_4H_9) shows the phase behaviour [5] : Cr 30 SmH 57.6 SmB 58.9 SmA 69.6 N 77.8 I; and the compound 4O.4 exhibits the phase behaviour [14] : Cr ~8 SmG 41 SmB 45 SmA 45.5 N_{OC} 59 N_O 74 I. Thus it is observed that replacement of the flexible butyl chain of 6O.4 (or 4O.4) by a rigid azophenyl group in 6OBPAA or in 8OBPAA

increases the transition temperatures and the stability of the different phases substantially, however, the SmH/SmG phase is suppressed altogether.

X-ray diffraction photographs were taken throughout the mesomorphic range, both types of samples were used - non-aligned and magnetically aligned. The details of the high temperature camera and experimental procedure have been described in Chapter II. The sample was taken in a Lindemann glass capillary of ~ 1.0 mm diameter and a temperature controller (Indotherm 401-D2) was used to control the temperature within ±0.5°C. We tried to get monodomain sample by very slow and regulated cooling from isotropic state to the desired temperature using only the capillary surface effect and also applying magnetic field of 0.5 Tesla. Attempt was also made to align the sample by slow heating to the mesophase in presence of magnetic field. But only partial alignment could be achieved. All photographs were taken with X-rays perpendicular to the magnetic field direction. In order to determine various physical parameters, the X-ray photographs were scanned linearly and circularly by an optical densitometer (Carl Zeiss, Jena, Model MD100) and analyzed according to the procedure described in Chapter II and in Chapter III.

4.3 RESULTS AND DISCUSSIONS

X-ray diffraction photographs of the magnetically aligned samples are shown in Figure 4.2(a-e) for 6OBPAA, in Figure 4.3(a-d) for 8OBPAA and in Figure 4.4(a-d) for the mixture. Figures 4.2(a), 4.3(a) and 4.4(a) depict typical nematic phase pattern, not like cybotactic nematic as was observed in Chapter III. Similarly Figures 4.2(b), 4.3(b) and 4.4(b) are of typical SmA phase photographs, where in some cases second order spots, which arise from correlation among smectic layers, are also visible. In figures 4.2(c), 4.3(c) and 4.4(c) typical photographs of SmB phase are shown. The available magnetic field was not sufficient to produce monodomain sample in 8OBPAA. The incident X-ray beam was parallel to the smectic layers, so the equatorial maxima did not show six spots as is expected when molecules within smectic layers are in hexagonal symmetry. The photographs, instead, showed elongated bars of relatively intense diffuse scattering on both sides

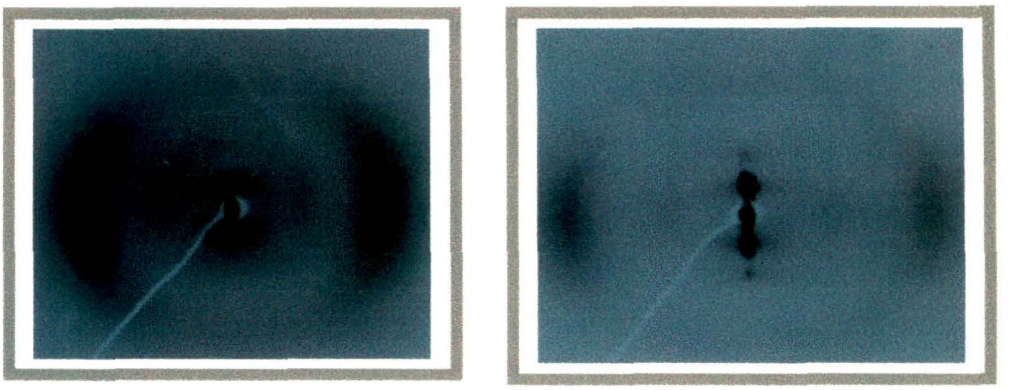

(a) (b)

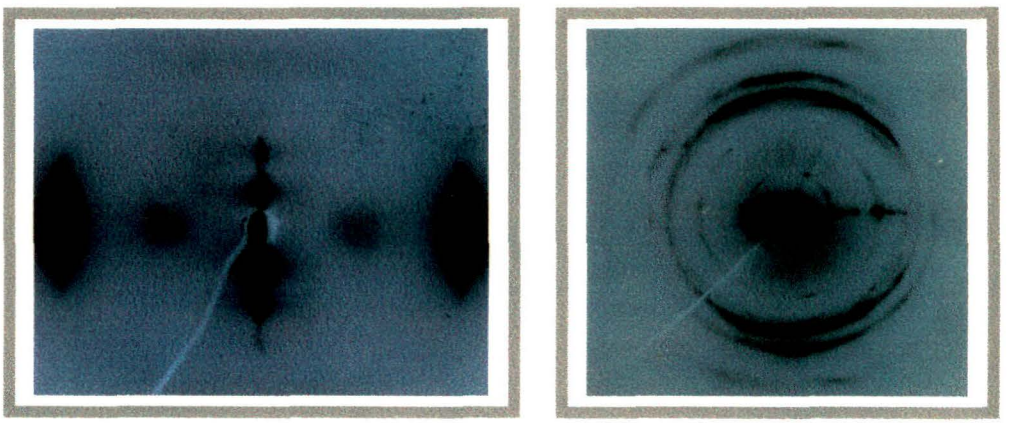

(c) (d)

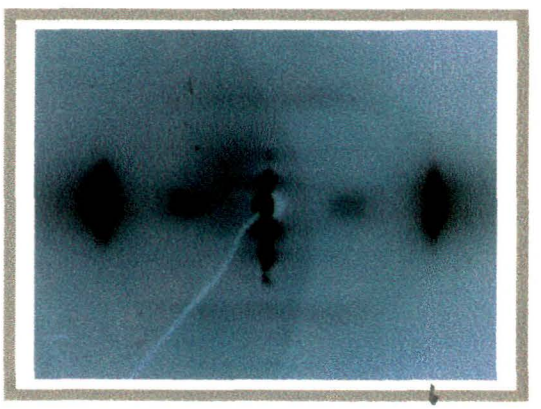

(e)

Figure 4.2 X-ray diffraction photographs of 6OBPAA at (a) 165°C in nematic phase, (b) 145°C in smectic A phase, (c) 100°C in smectic B phase, (d) 90°C in solid phase (during heating) and (e) 80°C in supercooled smectic B phase.

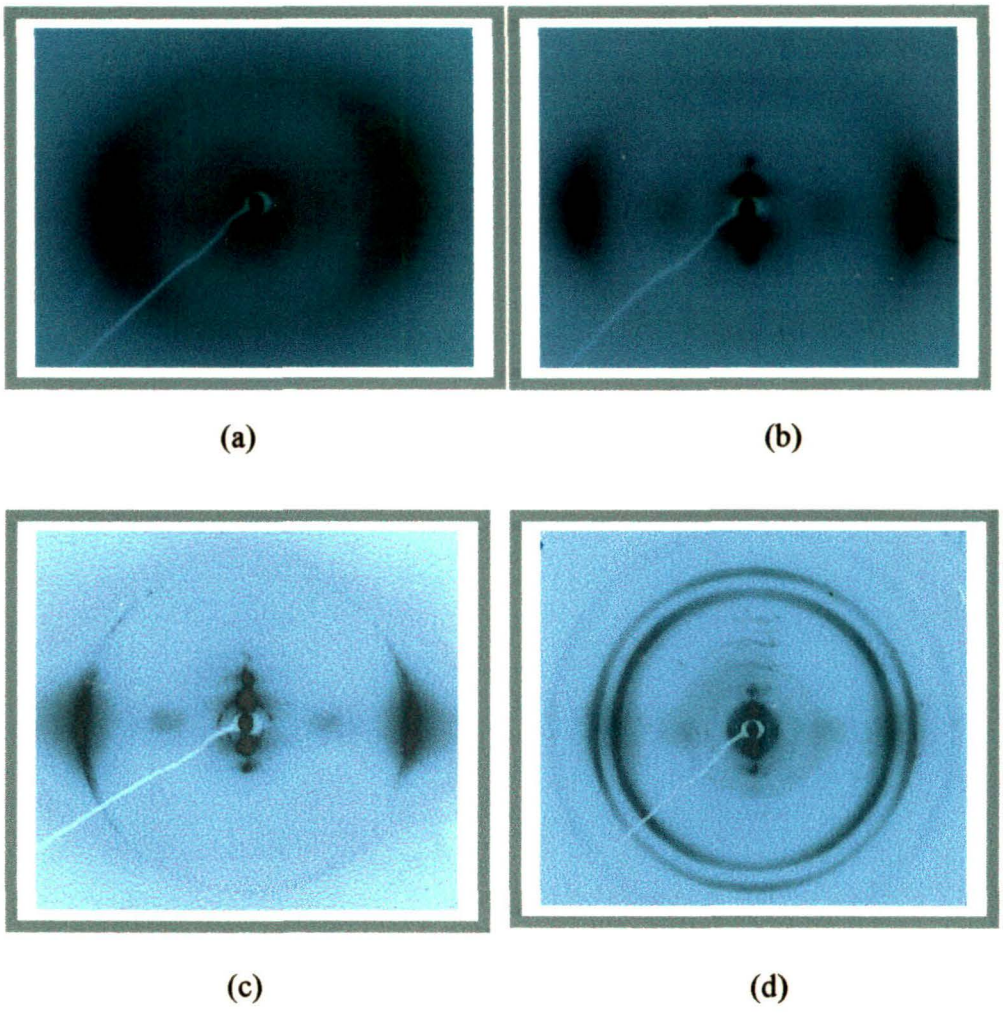

Figure 4.3 X-ray diffraction photographs of 8OBPAA at (a) 151°C in nematic phase, (b) 130°C in smectic A phase, (c) 90°C in supercooled smectic B phase and (d) 75°C in solid phase (during cooling).

of the equator symmetrically. The width of the bars is quite sharp compared to SmA phase but not as sharp as observed in crystal phase. It is therefore assumed that the smectic phase is Hexatic B type rather than a crystal B phase. It might be mentioned that in some case even third order inner spots are also visible signifying stronger correlation among layers in this phase than in SmA phase. It has been described in detail in Chapter I that in hexatic B phase the positional order within and normal to layer is respectively short range and quasi long range while in crystal B phase both are of long range. The soft smectic like crystal phase is different from true crystals in that the molecules are undergoing rapid reorientational motion about their

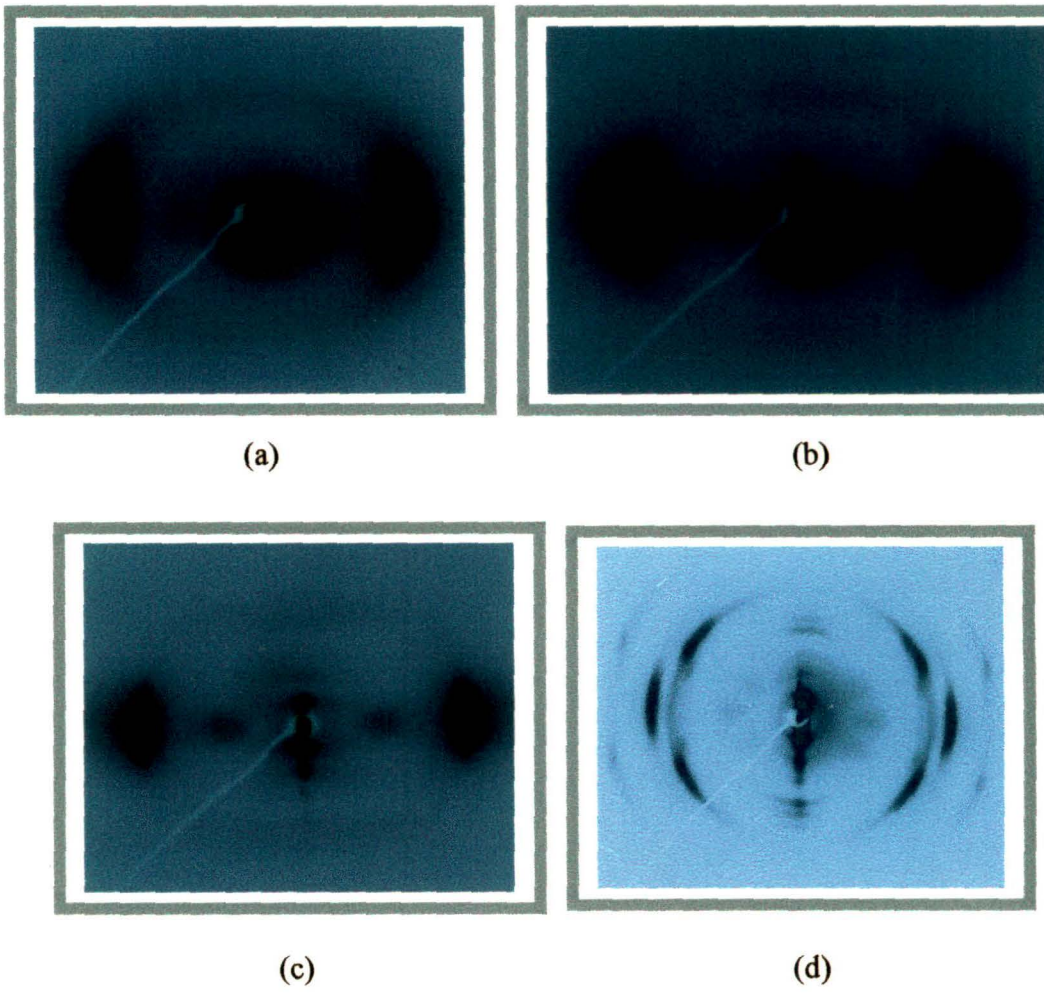

Figure 4.4 X-ray diffraction photographs of the mixture at (a) 150°C in nematic phase, (b) 130°C in smectic A phase, (c) 100°C in smectic B phase and (d) 40°C in solid phase (during cooling).

long axes [15,16]. In Figures 4.2(d)-4.4(d) the powder pattern of solid phases are shown for comparison. Figure 4.2(e) is given to show the SmB phase in the supercooled region (80°C) of 6OBPAA to compare with solid phase photograph at 90°C during heating.

Intermolecular distance (D) and apparent molecular length (l) in the nematic phase and layer spacing (d) in the smectic phase are calculated as described in Chapter II and III. These data are given in Tables 4.1-4.3. Temperature variations of these parameters are shown in Figures 4.5-4.7. Within experimental uncertainty all the parameters are found to be temperature independent in a particular phase for all the compounds. In 6OBPAA average values of d or ℓ are 29.5 Å, 27.8 Å, 26.2 Å

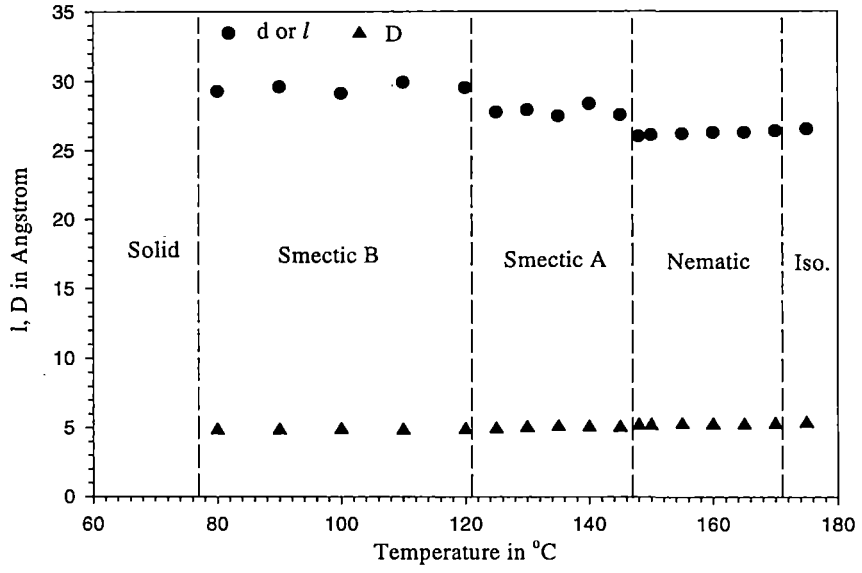

Figure 4.5 Temperature variation of d, *l* and D in different phases of 6OBPAA.

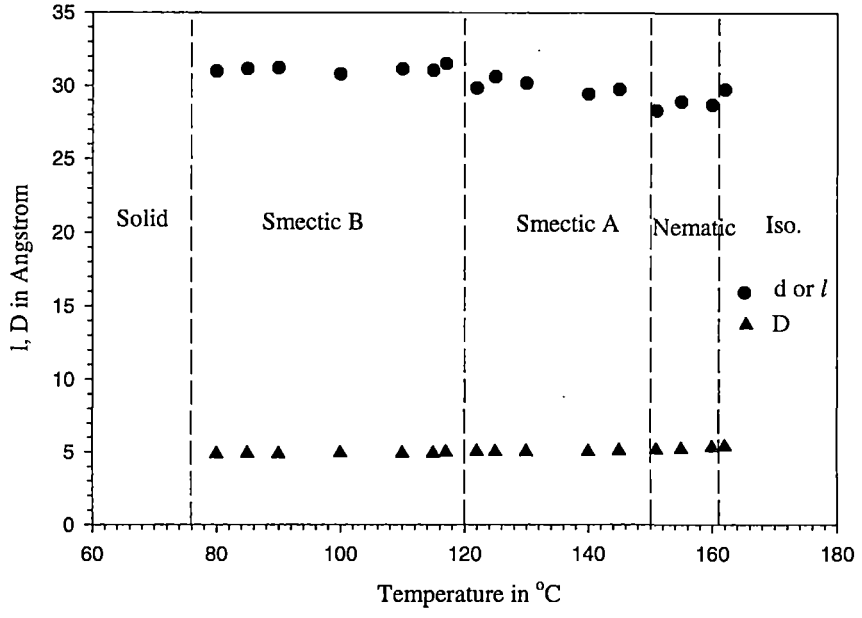

Figure 4.6 Temperature variation of d, *l* and D in different phases of 8OBPAA.

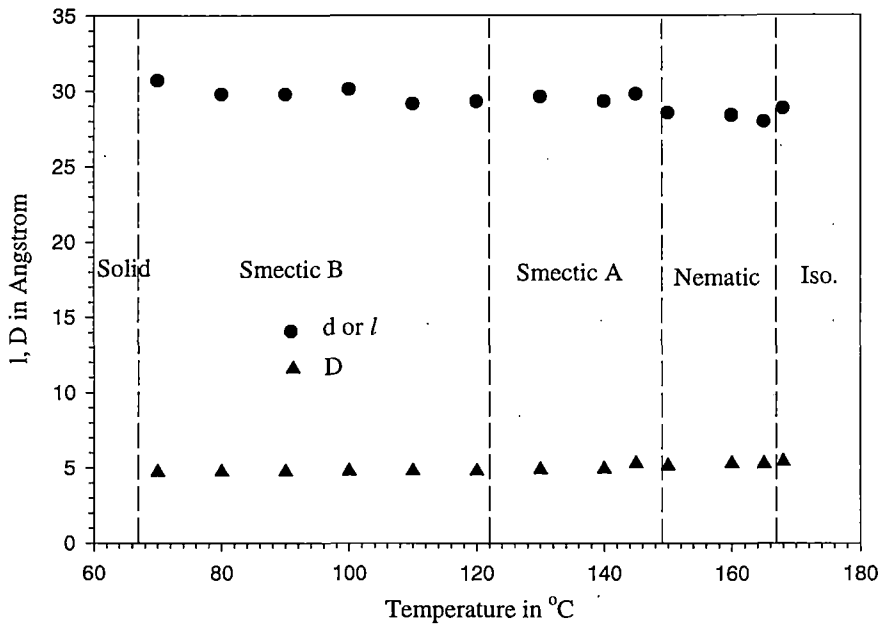

Figure 4.7 Temperature variation of d, *l* and D in different phases of the mixture.

and 26.5 Å respectively in SmB, SmA, N and I phases. Corresponding values of D are 4.82 Å, 4.98 Å, 5.19 Å and 5.31 Å. Thus d or *l* decreases as one moves from SmB to N phase, reverse trend is observed in D values. In 8OBPAA average values of d or *l* are 31.1 Å, 30.0 Å, 28.6 Å and 29.8 Å respectively in SmB, SmA, N and I phases. Corresponding values of D are 4.88 Å, 5.02 Å, 5.22 Å and 5.36 Å. Thus it is observed that all the molecular parameters - *l*, d and D - exhibit similar behaviour as observed in the lower homologue 6OBPAA. As the number of carbon atoms in the alkoxy chain increases (6OBPAA → 8OBPAA) all these parameters increase, the effect, however, is more prominent in d or *l* than in D. Though this is true for the two compounds but for all members of the series it must be stated with caution since in many physical properties 'odd-even' effect is observed. A review on this for nCHBT series has recently been published by co-workers [17]. On the other hand, in the equimolar mixture, average values of d or *l* are found to be 29.8 Å, 29.6 Å, 28.3 Å and 28.8 Å respectively in SmB, SmA, N and I phases. Corresponding values of D are 4.76 Å, 5.03 Å, 5.23 Å and 5.41 Å. These values are collected in

Table 4.4 for comparison. Thus the molecular parameters - *l* and d - in the mixture show intermediate values compared to the values observed in the two pure compounds. D values, however, does not show such behaviour. Similar behaviour of *l* was reported earlier from this laboratory in a binary mixture of benzoate systems [18]. In the compound 4O.4 the D-values are found to increase systematically as one moves from the high to low ordered phases, however, d or *l* values do not show such behaviour [14].

In all the compounds systematic increment of D values from SmB to I phase suggests that the molecules are most efficiently packed in SmB phase and in isotropic phase the packing is least efficient. Moreover, increase of chain length results in less efficient packing. In the mixture, where 50% molecules of 8OBPAA are replaced by 6OBPAA molecules with smaller chain length, efficiency of packing does not improve except in SmB phase.

The lengths of the molecules (L) were determined employing geometry optimization technique through energy minimization procedure using the software HYPERCHEM [19] and are found to be 26.2 Å and 28.3 Å respectively in 6OBPAA and 8OBPAA. In the mixture the effective molecular length is taken as 27.3 Å, the mean value of the pure component lengths. Ratio of smectic layer spacing to model length (d/L) or apparent molecular length to model length (*l*/L) is found to be slightly more than 1, the maximum value being 1.13. Since the molecules possess high dipole moments (3.14 D in 6OBPAA and 3.74D in 8OBPAA, determined using HYPERCHEM), anti-parallel bimolecular association may occur in the mesophases. Almost complete overlap of the paired molecules would results in such apparent molecular lengths. This type of bimolecular association has been observed in many systems with various degrees of overlap. For example, in a previous communication from this laboratory [17,20], it was shown that in nCHBT series, like the present members, the ratio varies between 1.04 and 1.16. In nCB series, however, the observed ratio is about 1.4 [21,22]. The nCB molecules possess stronger axial dipole moment (around 5.0 D in 8CB [23]) than nCHBT molecules (3.50D in 6CHBT [17,24]) or the molecules under investigation. Thus in nCB dimers molecular overlap is much less than in these compounds or in

nCHBT. Dielectric studies of 6CHBT in CCl_4 show the presence of both monomers and dimers [24,25] but the association is weaker than that observed in the solution of 5CB in C_6H_6 [26,27]. Therefore, a lower dimer concentration may as well be the reason of smaller (l /L) ratio.

Orientational order parameters, $<P_2>$ and $<P_4>$, have been determined in SmA and N phase from the circular intensity distributions along the peak position of the outer crescents. Details of the calculation procedure have been described in Chapter II and Chapter III. For brevity, no observed and fitted intensities $I(\psi)$ and the calculated distribution function $f(\beta)$ values are given in this chapter. Temperature dependence of these parameters is shown in Figures 4.8-4.10. Order parameter values calculated from Maier-Saupe mean field theory [28] in the nematic phase and from McMillans theory [29,30] in SmA-N phase have also been calculated and depicted in the above figures. Calculation details have been given in Chapter II. All the experimental and calculated order parameters are shown in Tables 4.5-4.7. It is observed that in all cases both $<P_2>$ and $<P_4>$ values more or less agree with the MS theoretical values in nematic phase, except in 8OBPAA near the transition temperature T_{NI}. In many systems such behaviour of $<P_2>$ and $<P_4>$ has been reported earlier [14,31]. In the nematic phase of 4O.4 [14] the behaviour of $<P_2>$ and $<P_4>$ is found to be similar to that found in 8OBPAA. However, in none of these compounds and also in the compounds described in Chapter III negative $<P_4>$ values are observed as was found from Raman scattering studies first in a Schiff's base MBBA and then in several nCB compounds [32-34]. From MS theoretical consideration also negative $<P_4>$ cannot be accounted for [35].

From the graphs it is also observed that in 6OBPAA, both in SmA and N phase, order parameters reasonably agree with values predicted from McMillan's model. However, in 8OBPAA, observed order parameter values are slightly less than McMillan's values (more in $<P_4>$ than $<P_2>$, specially near T_{NI}). On the other hand, in the mixture behaviour of $<P_2>$ is similar to that in 6OBPAA and $<P_4>$ behaves like 8OBPAA. In calculating the order parameter values, the adjustable parameters, δ and α in McMillan's theory, were set at δ=0.18 and α=0.665 in

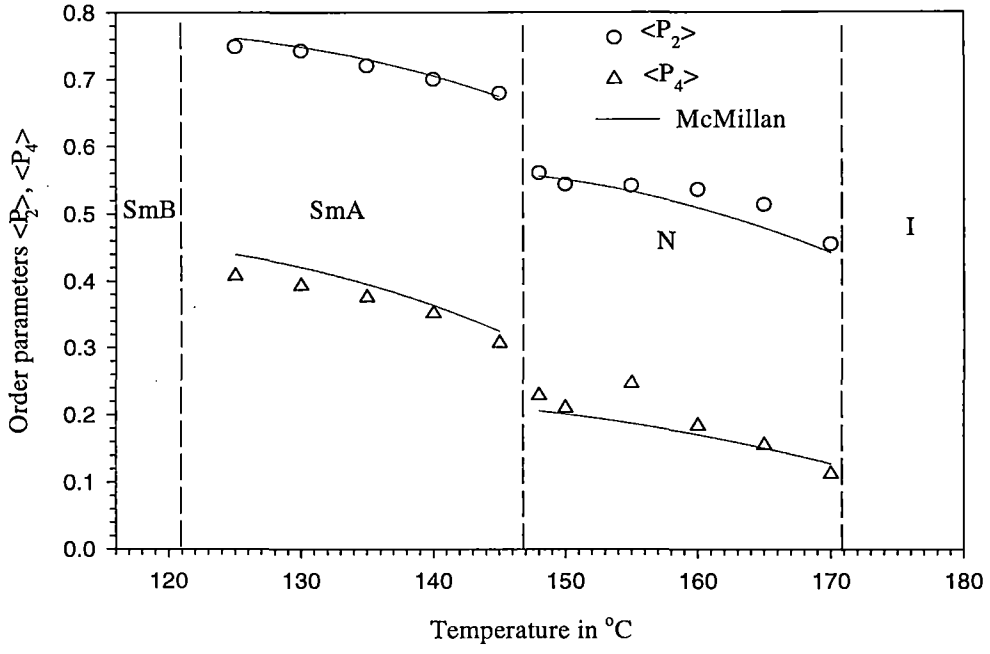

Figure 4.8 Temperature variation of order parameters in SmA and N phase of 6OBPAA. In N phase MS theoretical curve coincides with McMillan's curve with δ=0.18 and α=0.665.

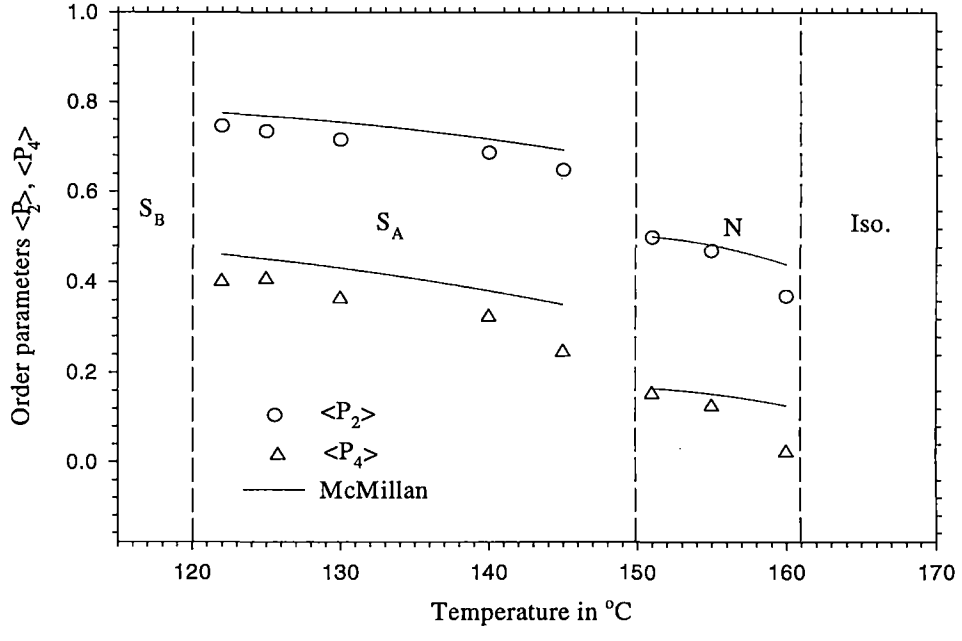

Figure 4.9 Temperature variation of order parameters in SmA and N phase of 8OBPAA. In N phase MS theoretical curve coincide with McMillan's curve with δ=0.175 and α=0.715.

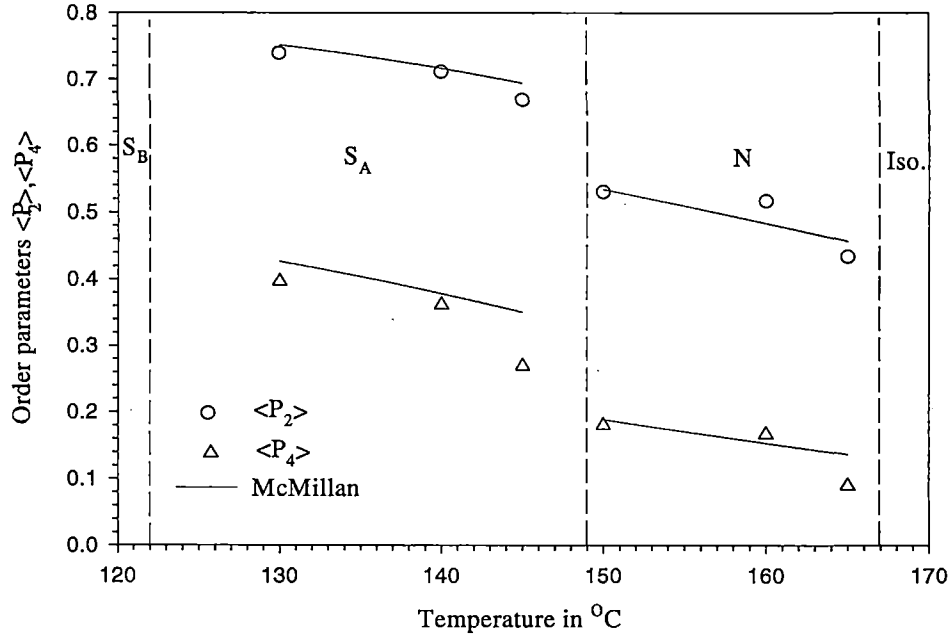

Figure 4.10 Temperature variation of order parameters in SmA and N phase of the mixture. In N phase MS theoretical curve coincides with McMillan's curve with δ=0.178 and α=0.69.

6OBPAA; δ=0.175 and α=0.715 in 8OBPAA; δ=0.178 and α=0.69 in the mixture. Thus, as predicted in the theory, α values are found to increase with chain length while for the mixture intermediate value of α is observed. Moreover, for the above parameters SmA-N transition occurs at 145.4°C, 149.8°C and 147.6°C in 6OBPAA, 8OBPAA and the mixture respectively, excellent agreement with observed values. However, the calculated T_{NI} values are 177.7, 167.5 and 173.6°C respectively, about 6°C more than the observed values. R. Paul *et al.* [36] observed in a mixture that for δ=0.05 and α=0.73 both the T_{SmA-N} and T_{NI} can be reproduced along with a reasonable fit to the experimental order parameters in SmA and N phase. However, in other reported systems agreement is not that good [37-39]. From McMillan's theory the translational order parameters can also be calculated as described in Chapter II. These are found to be 0.62-0.42 in 6OBPAA, 0.67-0.51 in 8OBPAA and 0.61-0.49 in the mixture.

It is also observed that value of $\ln\langle P_2\rangle/\ln\langle P_4\rangle$ lies in the range 0.31-0.34 in SmA phase and in the range 0.35-0.39 (except at one temperature) in nematic phase of all the compounds. Applying continuum theory of disorder in nematic liquid crystals Faber [40] showed that the above parameter $\ln\langle P_2\rangle/\ln\langle P_4\rangle$ should have a universal value of 0.30. Thus observed values are close to it, surprisingly, however, closer in SmA phase than in nematic phase. Paul [31] and Parimal Sarkar *et al.* [17] also showed that for a large number of nematic compounds the agreement is impressive.

In all the compounds nature of transition of $\langle P_2\rangle$ at $T_{SmA\text{-}N}$ and T_{NI} is first order.. Behaviour of l and D also supports this inference though the observed enthalpy at T_{NI} is very small. Moreover, the observed ratio of $T_{N\text{-}SmA}/T_{NI}$ is 0.95, 0.96 and 0.97 respectively in the three compounds. Therefore, according to McMillan's theory, as noted in Chapter II, the SmA-N transition should be of first order since the ratio is much higher than 0.87. K. R. K. Rao *et al.* [8] observed first order type discontinuity in density and in adiabatic compressibility at all the transitions in 6OBPAA. Some disagreement is found in the literature on whether the SmA-N transition is of first order or second order. Theoretically the problem was investigated by Kobayashi [41] and McMillan [29,30]. On the other hand from DSC measurements Cabane and Clark [42] showed first order SmA-N transition and de Jeu [43] reported the said transition as first-, weakly first- and second-order.

TABLE 4.1

Layer spacing (d), apparent molecular length (*l*) and average intermolecular Distance (D) in 6OBPAA

Sample to film Distance= 5.92 cm. Wavelength of X-ray used =1.5418 Å

Temperature in °C	Phase	Layer spacing (d) or Apparent molecular length (*l*) in Å	Average Intermolecular distance(D) in Å
80	SmB	29.3	4.80
90		29.6	4.81
100		29.1	4.83
110		29.9	4.80
120		29.5	4.85
		Av 29.5	**Av 4.82**
125	SmA	27.8	4.88
130		27.9	4.98
135		27.5	5.05
140		28.4	5.01
145		27.6	4.99
		Av 27.8	**Av 4.98**
148	N	26.0	5.14
150		26.1	5.14
155		26.2	5.23
160		26.3	5.19
165		26.3	5.19
170		26.4	5.24
		Av 26.2	**Av 5.19**
175	I	26.5	5.31

TABLE 4.2

Layer spacing (d), apparent molecular length (*l*) and average intermolecular Distance (D) in 8OBPAA

Sample to film Distance= 5.92 cm. Wavelength of X-ray used =1.5418 Å

Temperature in °C	Phase	Layer spacing (d) or Apparent molecular length (*l*) in Å	Average Intermolecular distance(D) in Å
80	SmB	31.0	4.84
85		31.1	4.87
90		31.2	4.84
100		30.8	4.90
110		31.1	4.88
115		31.0	4.88
117		31.5	4.97
		Av 31.1	**Av 4.88**
122	SmA	29.8	5.02
125		30.6	4.99
130		30.2	5.00
140		29.4	5.01
145		29.8	5.07
		Av 30.0	**Av 5.02**
151	N	28.3	5.15
155		28.9	5.19
160		28.7	5.31
		Av 28.6	**Av 5.22**
162	I	29.8	5.36

TABLE 4.3

Layer spacing (d), apparent molecular length (*l*) and average intermolecular Distance (D) in the mixture

Sample to film Distance= 5.92 cm. Wavelength of X-ray used =1.5418 Å

Temperature in °C	Phase	Layer spacing (d) or Apparent molecular length (*l*) in Å	Average Intermolecular distance(D) in Å
70	SmB	30.7	4.71
80		29.8	4.73
90		29.8	4.74
100		30.1	4.78
110		29.1	4.78
120		29.3	4.79
		Av 29.8	**Av 4.76**
130	SmA	29.6	4.88
140		29.3	4.92
145		29.8	5.28
		Av 29.6	**Av 5.03**
150	N	28.5	5.14
160		28.4	5.27
165		27.9	5.27
		Av 28.3	**Av 5.23**
168	I	28.8	5.41

TABLE 4.4

Average d, *l* and D values of 6OBPAA, 8OBPAA and the Mixture in the SmB, SmA, N and I phases. The d/L or *l*/L ratio is also given.

	SmB		SmA		N		I	
	d	**d/L**	**d**	**d/L**	***l***	***l*/L**	***l***	***l*/L**
6OBPAA	29.5	1.13	27.8	1.06	26.2	1.0	26.5	1.01
8OBPAA	31.1	1.10	30.0	1.06	28.6	1.01	29.8	1.05
Mixture	29.8	1.09	29.6	1.08	28.3	1.04	28.8	1.05
	D		D		D		D	
6OBPAA	4.82		5.18		5.18		5.31	
8OBPAA	4.88		5.02		5.22		5.36	
Mixture	4.76		5.03		5.23		5.41	

TABLE-4.5

Experimental, MS and McMillan theoretical order parameters of 6OBPAA.

Phase	Temperature in °C	T*	Experimental value		McMillan theoretical Value[#]	
			$\langle P_2 \rangle$	$\langle P_4 \rangle$	$\langle P_2 \rangle$	$\langle P_4 \rangle$
SmA	125	0.19738	0.75	0.41	0.7667	0.4490
	130	0.19986	0.74	0.39	0.7502	0.4249
	135	0.20234	0.72	0.38	0.7369	0.4063
	140	0.20482	0.70	0.35	0.7099	0.3704
	145	0.20730	0.68	0.31	0.6793	0.3325
N	148	0.20878	0.56	0.23	0.5570 0.5575	0.2063 0.2067
	150	0.20978	0.54	0.21	0.5504 0.5497	0.2011 0.2005
	155	0.21226	0.54	0.25	0.5338 0.5286	0.1883 0.1845
	160	0.21473	0.54	0.18	0.5060 0.5044	0.1683 0.1672
	165	0.21721	0.51	0.15	0.4836 0.4755	0.1532 0.1479
	170	0.21969	0.46	0.11	0.4410 0.4384	0.1267 0.1252

[#]**In N phase MS theoretical values are shown in the lower line.**

TABLE-4.6

Experimental, MS and McMillan theoretical order parameters of 8OBPAA.

Phase	Temperature in °C	T*	Experimental value		McMillan theoretical Value[#]	
			<P2>	<P4>	<P2>	<P4>
S_A	122	0.20040	0.75	0.40	0.7264	0.3846
	125	0.20193	0.73	0.41	0.7155	0.3705
	130	0.20446	0.72	0.36	0.7031	0.3550
	140	0.20954	0.69	0.32	0.6617	0.3071
	145	0.21207	0.65	0.25	0.6137	0.2579
N	151	0.21512	0.50	0.15	0.5040 0.5003	0.1669 0.1644
	155	0.21715	0.47	0.12	0.4839 0.4764	0.1533 0.1485
	160	0.21968	0.37	0.02	0.4410 0.4386	0.1268 0.1254

[#]In N phase MS theoretical values are shown in the lower line.

TABLE-4.7

Experimental, MS and McMillan theoretical order parameters of the mixture.

Phase	Temperature in °C	T*	Experimental value		McMillan theoretical Value[#]	
			<P2>	<P4>	<P2>	<P4>
S_A	130	0.20167	0.74	0.40	0.7518	0.4284
	140	0.20668	0.71	0.36	0.7123	0.3748
	145	0.20918	0.67	0.27	0.6829	0.3381
N	150	0.21168	0.58	0.24	0.5345 0.5337	0.1889 0.1883
	160	0.21669	0.52	0.17	0.4836 0.4822	0.1532 0.1522
	165	0.21919	0.43	0.09	0.4567 0.4470	0.1361 0.1303

[#]**In N phase MS theoretical values are shown in the lower line.**

REFERENCES

1. H. Kelker, B. Scheurle, R. Hatz and W. Bartsch, *Angew. Chem.*,**82**, 984 (1970).

2. D. Coates, *Liquid Crystals: Application and Uses*, Vol. I (B. Bahadur, Ed.), World Scientific, Singapore, 1990, Ch. 3.

3. Christopher J. Booth in *Handbook of Liquid Crystals*, Eds. D. Demus, J. Goodby, G.W. Gray, H.-W. Spiess and V. Vill, Vol. **2A**, Wiley-VCH, Verlag GmbH, Weinheim, FRG (1998), p. 313.

4. A. J. Leadbetter, M. A. Mazid, B. A. Kelly, J. W. Goodby and G. W. Gray, *Phys. Rev. Letts.*, **43**, 630 (1979).

5. A. J. Leadbetter, M. A. Mazid and R. M. Richardson, *Liquid Crystals* (S. Chandrasekhar, Ed.), Heyden, London, p 65 (1980).

6. S. L. Arora and J. L. Fergason, *Symp. Faraday Soc.*, **5**, 97 (1971).

7. D. L. Fishel and P. R. Patel, *Mol. Cryst. Liq. Cryst.*, **17**, 139 (1972).

8. K. R. K. Rao, J. V. Rao, P. Venkatacharyulu and V. Baliah, *Mol. Cryst. Liq. Cryst.*, **136**, 307 (1986).

9. S. Sakagami and M. Nakamizo, *J. Chromatogr.*, **234**, 357 (1982).

10. D. Demus and and L. Richter, *Textures of Liquid Crystals*, Verlag Chemie, Weinheim, 1978.

11. S. Chandrasekhar, G. G. Nair, D. S. Sankar Rao, S. Krishnaprasad, K. Praefcke and D. Blunk, *Liquid Crystals*, **24**, 67 (1998).

12. H. Sackmann and D. Demus, *Fortschr. Chem. Forsch.*, **12**, 349 (1969).

13. K. R. K. Rao, J. V. Rao, P. Venkatacharyulu, S. V. Chiranjeevi Rao and V. Baliah, *Cryst. Res. Technol.*, **22**, 1211 (1987).

14. P. Mandal, M. Mitra, S. Paul and R. Paul, *Liq. Crystals*, **2**, 183(1987).

15. P. S. Pershan, *Structure of Liquid Crystal Phases*, World Scientific, USA, 1988, p 62.

16. J. W. Goodby, *Handbook of Liquid Crystals, Low Molecular Liquid Crystals I*, Vol. 2A (D. Demus, J. Goodby, G. W. Gray, H. W. Spiess and V. Vill, Eds.), Wiley-VCH, Weinheim,1998, Ch. I., p3.

17. P. Sarkar, P. Mandal, S. Paul, R. Paul, R. Dabrowski and K. Czyprinski, *Liq. Crystals*, **30**, 507(2003).

18. P. Sarkar, P. K. Sarkar, S. Paul and P. Mandal, *Phase Transitions*, **71**, 1(2000).

19. Hyperchem Release 6.03 for Windows, Hypercube Inc, Florida, USA(2001).

20. P. Sarkar, P. Mandal, S. Paul, R. Paul, R. Dabrowski and K. Czyprinski, *Mol. Cryst. Liq. Cryst.*, **330**, 159(1999).

21. A. J. Leadbetter, M. A. Mazid and R. M. Richardson, *J. Phys. (Paris)*, Suppl. **36**, C1, 37 (1975).

22. J. E. Lydon, an C. J. Coakley, *J. de Physique*, **36**, C1, 45 (1975).

23. K. P. Gueu, E. Megnassan and A. Proutierre, *Mol. Cryst. Liq. Cryst.*, **132**, 303 (1986).

24. P. Kedziora and J. Jadzyn, *Mol. Cryst. Liq. Cryst.*, **192**, 31 (1990).

25. P. Kedziora and J. Jadzyn, *Acta Physica Polonica*, **A77(5)**, 605 (1990).

26. D. A. Dunmur and K. Toriyama, *Liquid Crystals*, **1**(2), 169 (1986).

27. K. Toriyama and D. A. Dunmur, *Mol. Cryst. Liq. Cryst.*, **139**, 123 (1986).

28. W. Maier and A. Saupe, *Z. Natureforsch.*, **14a**, 882 (1959); Ibid, **15a**, 287 (1960).

29. W. L. McMillan, *Phys. Rev.*, **A4**, 1238(1971).

30. W. L. McMillan, *Phys. Rev.*, **A6**, 936(1972).

31. R. Paul, *Liquid Crystals*, **9**, 239 (1991).

32. S. Jen, N. A. Clark, P. S. Pershan and E. B. Priestley, *Phys. Rev. Letts.*, **31**(26), 1552 (1973).

33. K. M. Miyano, *J. Chem. Phys.*, **69**, 4807 (1978).

34. S. N. Prasad and S. Venugopalan, *J. Chem. Phys.*, **75**, 3035 (1981).

35. P. J. Wojtowicz, *Introduction to Liquid Crystals* (E. B. Priestley, P. J. Wojtowicz and P. Sheng, Eds.), Plenum Press, New York, 1975, p56.

36. R. Paul, B. Jha and D. A. Dunmur, *Liq. Crystals,* **13**, 629(1993).

37. M. Mitra, S. Paul and R. Paul, *Z. Naturforsch*, **46a**, 858(1991).

38. S. Gupta, B. Majumdar, P. Mandal, R. Paul and S. Paul, *Phase Transitions*, **40**, 73(1992).

39. M. K. Das and R. Paul, *Phase Transitions*, **46**, 185(1994).

40. T. E. Faber, *Proc. Royal Soc. London A*, **353**, 247(1977).

41. K. K. Kobayashi, *J. Phys. Soc. Japan*, **29**, 101(1970).

42. B. Cabane and W. G. Clark, *Solid State Commn.,* **13**, 129(1973).

43. W. H. de Jeu, *Solid State Commn.,* **13**, 1521(1973).

Chapter V

X-RAY AND DIELECTRIC STUDIES ON BINARY MIXTURES OF A CARBOXYLATE AND A CYANOBIPHENYL

5.1 INTRODUCTION

For many years aromatic compounds based on phenyl(s) were the most common unit for liquid crystals, partly because of their easier synthesis and partly because the link between highly polarizable π-electron systems and mesogenecity was over-emphasized. Later it was realized that saturated systems are also excellent units when placed appropriately in relation to other planar or high polarizability regions of the cores or when the cores are entirely saturated [1]. Moreover, the presence of ester linking group results in an increase in flexibility of the core and its electron-withdrawn nature increases the core polarity. Since the ester group is intrinsically asymmetric, exchange of substituents attached to the ester group sometimes give rise to a notable change in liquid crystalline properties [2]. Phase behaviour of some such compounds is shown in Table 5.1. Data were collected from [3]. It is observed that 3CB exhibits monotropic nematic phase [4] but when the alkyl phenyl group is replaced by alkyl cyclohexyl group (3PCH) enantiotropic nematic phase sets in [5]. When both the phenyl groups are replaced by cyclohexyl groups (CCH3) stability of nematic phase is doubled and smectic phases appear while cooling [6]. On the other hand if an ester linkage group is introduced between the phenyl groups (CPPB) [7] situation does not change much from 3CB. Replacement of the phenyl by the cyclohexyl group in addition (CPPCC) increases the thermal stability of nematic phase [8]. When the highly polar cyano group is changed by a less polar and more flexible butoxy group (BPPCC) [8] thermal stability of the enantiotropic nematic is increased by about four fold compared to 3CB. Increment of number of carbon atoms by two at the cyclohexyl end and one at the butoxy end (PPPCC) results in both cybotactic and ordinary nematic phase as well as a smectic phase [8]. In this context X-ray diffraction studies were made on CPPCC and its next homologue CPBCC as well as on the above BPPCC and PPPCC; measurement of density, refractive indices, magnetic susceptibility anisotropy and elastic constants were also made by co-worker [9]. To see the effect of BPPCC guest molecules in the host 2CB matrix, binary mixtures of three different

TABLE 5.1.

Phase behaviour of some structurally related compounds (Temperatures in °C).

3CB	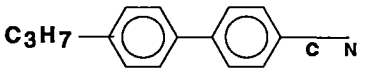	Cr 67 N (25.5) I
3PCH	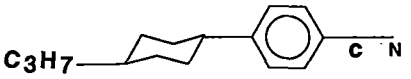	Cr 35.7 N 46 I
CCH3		Cr 58 Sm (18) Sm (44) Sm (57) N 80 I
CPPB	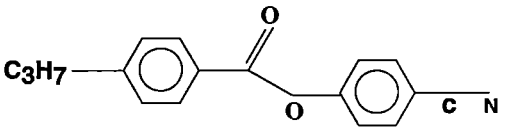	Cr 100 N (46) I
CPPCC	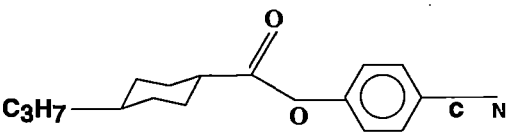	Cr 54.5(47) N 70 I
BPPCC	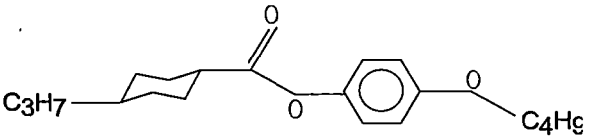	Cr 43(28) N 72 I

concentrations have been studied by optical microscopy, X-ray diffraction technique and by static dielectric constants measurements. These results are presented in this chapter. Crystal and molecular structures of BPPCC and 2CB have also been determined by single crystal diffractometry to study the influence of molecular arrangement in the crystalline state on the phase behaviour of the mesomorphic state. These results have been described in subsequent chapters.

RESULTS AND DISCUSSIONS

Transition temperatures of the pure components determined by texture studies are given below.

I. p-butoxyphenyl *trans*-4-propyl cyclhexane carboxylate (**BPPCC** in short)

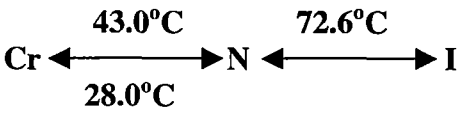

II. 4-n-Ethyl-4'-cyanobiphenyl (**2CB** in short)

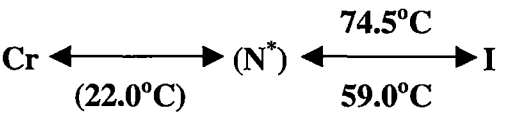

Three mixtures were prepared with 0.25, 0.5 and 0.75 of mole fraction (x) of BPPCC. By agitating the heated mixture in the isotropic phase for at least 24 hours formation of homogeneous mixture was ensured. Observed transition temperatures are as follows:

Mixture I: $x_{BPPCC} = 0.25$

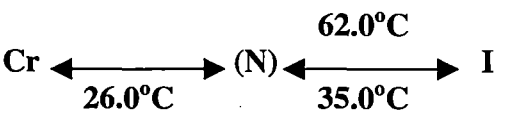

Mixture II: $x_{BPPCC} = 0.50$

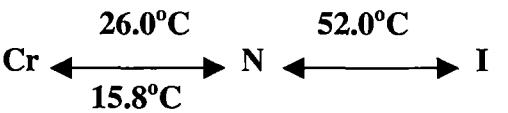

Mixture III: $x_{BPPCC} = 0.75$

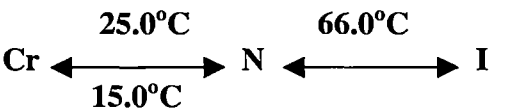

In all cases, with crossed polarizers, marble texture was observed in the nematic phase. The compound **2CB**, according to BDH literature, shows only virtual nematic phase at 22.0°C (i.e. nematic transition temperature is obtained by

extrapolation of data from mixtures with other nematogens). In **Mixture I**, where only 25% **2CB** molecules are replaced by **BPPCC** molecules, the melting point drops down to 62.0°C and monotropic nematic phase is observed within 26-35°C. However, replacement of 50% or more **2CB** molecules by **BPPCC** molecules (**Mixture II and III**) results in enantiotropic nematic phase. Thermal stability of

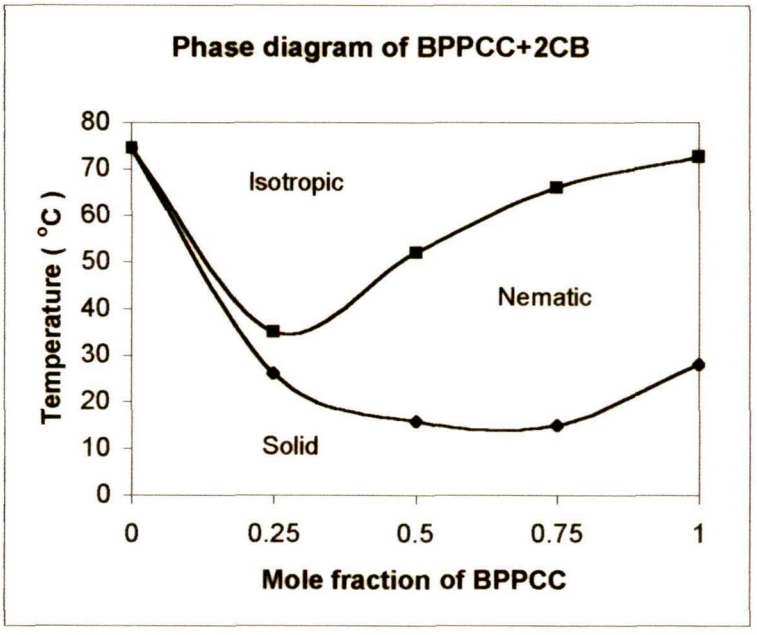

Figure 5.1 Phase diagram of BPPCC+2CB mixture

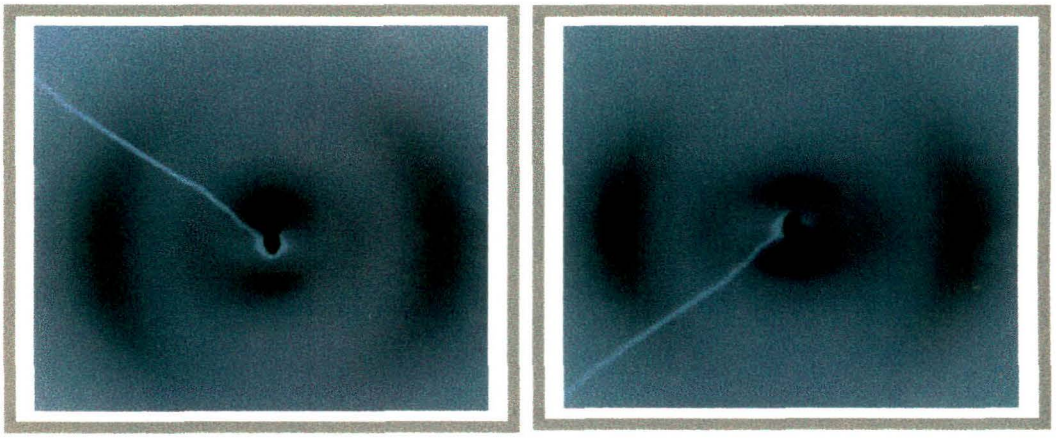

Figure 5.2 X-ray diffraction photographs in nematic phase of (a) the mixture with x_{BPPCC}=0.50 at 45°C and (b) the mixture with x_{BPPCC}=0.75 at 26°C.

N phase in **Mixture III** is increased by about 17°C from that of pure **BPPCC.** Thus the **Mixtures II and III**, being nematic at ambient temperature because of the supercooling effect and having ranges respectively 36° and 51°, are expected to be useful in commercial display devices. The phase diagram of the mixtures is shown in Figure 5.1. Smectic A_d phase was found to induce in a binary mixture (ME60.5 + 5CB, an ester/biphenyl mixture) in some compositions [10], no such phenomenon is observed in this case though the gross molecular structures are similar.

X-ray diffraction photographs confirmed the presence of ordinary nematic phase in all cases. No cybotactic nematic phase is observed in this case though one homologue (PPPCC) of BPPCC exhibits such phase [9]. Two representative magnetically aligned photographs, one each of **Mixture II** and **Mixture III**, have been presented in Figure 5.2. However, in **Mixture I**, no aligned N phase photograph could be recorded even after several attempts. But optical textures indicated that the phase is nematic and dielectric measurements confirmed that the phase is anisotropic. Therefore only **Mixture II** and **Mixture III** have been studied in detail by X-ray scattering technique. X-ray photographs were taken throughout the mesomorphic range, however, it was not possible to take photographs in the supercooling region since no arrangement for taking low temperature photographs was available.

The apparent molecular length (l) and the average intermolecular distance (D) over the entire mesomorphic range have been determined respectively from the low and high angle diffraction features following procedures described in Chapters II and III. These values are given in Table 5.2. Both l and D are found to increase very slowly with temperature as depicted in Figure 5.3.

Mean value of D is found to be 5.13 Å in **Mixture II and** 5.19 Å in **Mixture III** which are more than the value 5.0 Å usually found in N phase of nCB compounds [11]. Though X-ray study on **BPPCC** was done [9] previously but no D value was reported. But in two other nematogenic compounds, containing carboxylate group and lateral chloride group, the D value are found to be 5.09 Å [12]. At $0.98T_{NI}$ on average the D value is found to be 5.09 Å for n=3-12 members of the nCHBT series containing a cyclohexyl group and a –NCS group [13]. Thus it

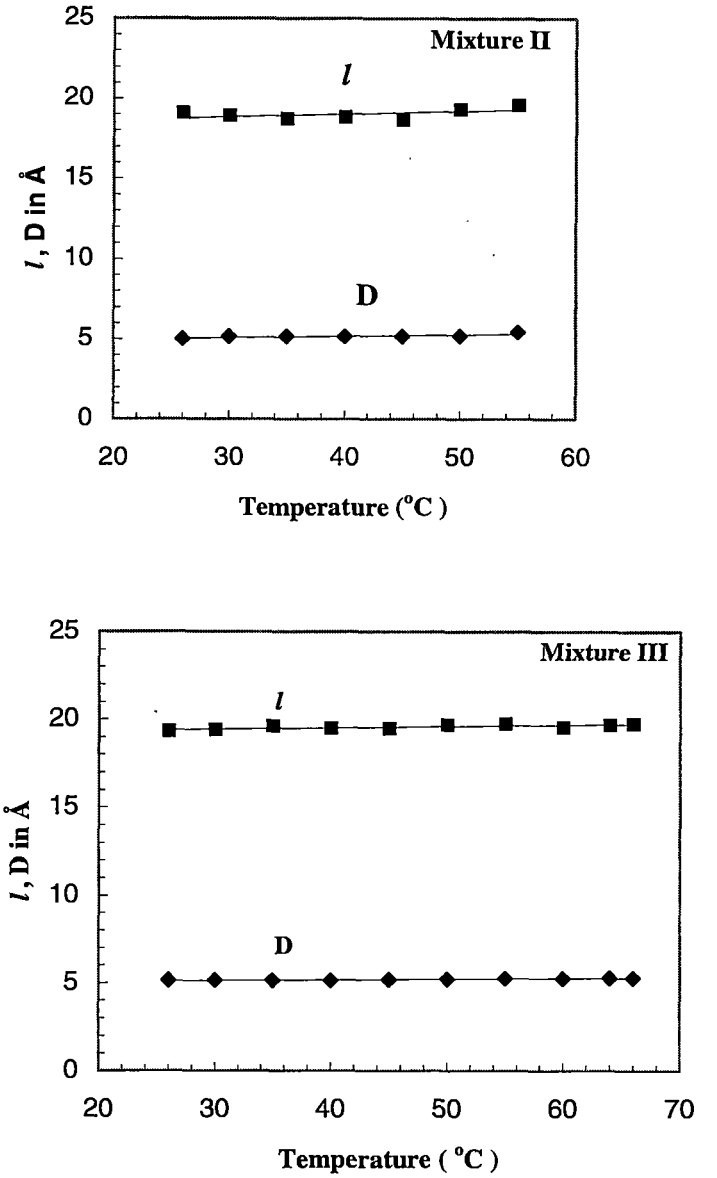

Figure 5.3 Temperature variation of *l* and D in Mixture II and Mixture III.

might be inferred that the packing of the dissimilar molecules in the mixtures is less efficient than that in the pure components.

The length L, measured from a stereo model, of **BPPCC** molecule is found to be 19.15 Å and that of molecule **2CB** is found to be 12.85 Å which have been confirmed by crystal structure analysis of the compounds (Chapter VI and VII). From simple additive rule [$l = x_{BPPCC} \cdot L_{BPPCC} + x_{2CB} \cdot L_{2CB}$] one expects that the apparent lengths in **Mixture II** and **Mixture III** would be 16.0 Å and 17.58 Å.

However, the average *l* of the molecules is found to be 19.6 Å in both the **Mixtures**, considerably different from the expected value. In pure **BPPCC** mean value of the observed *l* is about 20.87 Å and *l*/L ratio is about 1.09 [9]. Though for pure **2CB** this data is not available but for many homologues of the nCB series it is observed [11] that *l*/L ratio is about 1.4. Even cyanocompounds with ester linkage group (CPPCC and CPBCC) showed similar result [9]. In both cases it is assumed that existence some sort of bimolecular association is the cause of *l*/L greater than 1. In BPPCC the molecules of the pair are in almost complete overlap configuration whereas in nCB molecules the extent of overlap is much less. If the associated length of the pairs is taken as the effective lengths of the molecules within nematic phase, then the calculated *l* values in the mixtures become 20.15 Å and 19.43 Å respectively, very close to the observed value (19.6 Å). Thus bimolecular association within same type of molecules (homo dimmers) is likely to be present in the mixtures as well. In a binary mixture of dodecyloxy cyanobiphenyl and a four-ring carboxylate molecule, where both the molecules have strong axial dipole moments and much longer molecular lengths [L_{12OCB}=26.0 Å and L_{7CBB}=31.5 Å], both homo- and hetero- dimmers are found to be present [14].

Orientational order parameters, $\langle P_2 \rangle$ and $\langle P_4 \rangle$, have been determined from the intensity distribution of the outer halo of the X-ray photographs following the procedure described in Chapters II and III. Order parameter values are given in Tables 5.3-5.4. Variation of the order parameters with temperature is shown in Figure 5.4. It is observed that for both the mixtures order parameters $\langle P_2 \rangle$ and $\langle P_4 \rangle$ agree well with the values predicted by Maier-Saupe theory. Only for the **Mixture III** at low temperature region $\langle P_2 \rangle$ values are lower than MS values. Moreover, in this system the molecules are found to be less ordered than in systems described in previous two chapters. However, the molecules of the previous systems are longer and less rigid than the present molecules and therefore, expected to be less ordered.

For pure BPPCC, observed $\langle P_2 \rangle$ and $\langle P_4 \rangle$ values [9] are also found to be consistent with MS theory and in the mixtures no significant change in order parameters is observed. For example, $\langle P_2 \rangle$ and $\langle P_4 \rangle$ values at $(T_{NI} - 12)$ °C are

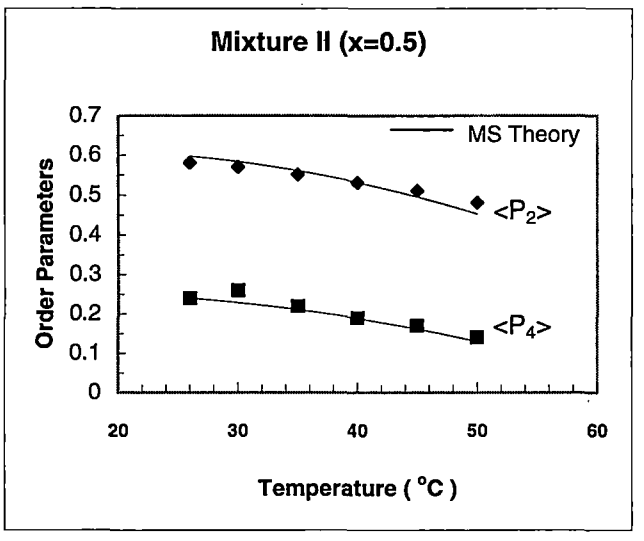

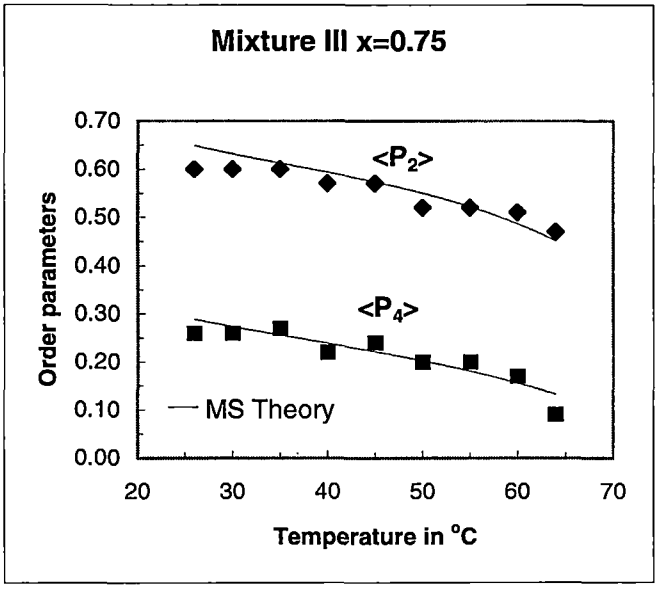

Figure 5.4 Orientational order parameters of Mixture II and Mixture III

found to be (0.53, 0.19), (0.52, 0.20) and (0.54, 0.18) respectively in **Mixture II**, **Mixture III** and **BPPCC**.

Static dielectric permittivities, $\varepsilon_{\parallel}$ and $\varepsilon_{\perp}$, have been measured parallel and perpendicular to the molecular axis following the procedure described in Chapter II.

Using cells made of ITO coated conducting glass plates dielectric parameters were measured at 10 KHz by an LCR bridge. Magnetic field of about 5 KGauss was applied to align the samples in homeotropic (for $\varepsilon_{\parallel}$ measurement) and homogeneous (for $\varepsilon_{\perp}$ measurement) geometry. Average permittivity $\bar{\varepsilon}$ and the anisotropy in permittivities $\Delta\varepsilon$ have also been calculated. Since no dielectric data for **BPPCC** was reported earlier dielectric measurements have been made on pure **BPPCC** as well. Values of the dielectric parameters, $\varepsilon_{\parallel}$, $\varepsilon_{\perp}$, $\bar{\varepsilon}$ and $\Delta\varepsilon$, are collected in Table 5.5 for BPPCC and in Tables 5.6-5.8 for all three mixtures. Variations of dielectric parameters have been shown in Figures 5.5-5.6. The compound **BPPCC** shows small ($\Delta\varepsilon$=-1.1 at 29.5°C) but negative anisotropy because of the presence of non-axial dipole moment of the ester group in the molecule. $\Delta\varepsilon$=-1.26, -1.20 and –1.05 (at low end of nematic range) have been reported for the homologues EPPCC, EPBCC and MPBCC of the BPPCC series [15]. However, all the three mixtures show large positive anisotropy. Since **2CB** is only virtually nematic no mesophase data for **2CB** is available. All members of the **nCB** series show large positive dielectric anisotropy, for example $\Delta\varepsilon$=8.0 for 8CB at $0.98T_{NI}$ [13]. Thus the dielectric behaviour of the mixtures is dominated by the **2CB** component. Even when only 25% of the **BPPCC** molecules are replaced by the **2CB** molecules (Mixture III) substantial positive anisotropy (maximum value is about 2.73) is yielded. Replacement of 50% and 75% **BPPCC** molecules by **2CB** molecules results in larger $\Delta\varepsilon$.

In all the **mixtures** dielectric permittivity in the isotropic phase ε_{iso} is found, from the above figures, to be larger than $\bar{\varepsilon}$ in the nematic phase, no such jump is observed in **BPPCC**. These suggest presence of some sort of anti-parallel dipolar association within nematic phase of the mixtures. This dipolar association breaks down completely or partially in the isotropic phase resulting in increased effective dipole moment of the molecules and thereby increased permittivity. In **BPPCC** probably no such change of molecular associations takes place during the **N-I** transition, though from X-ray study anti-parallel dipolar association is found to exist in N phase.

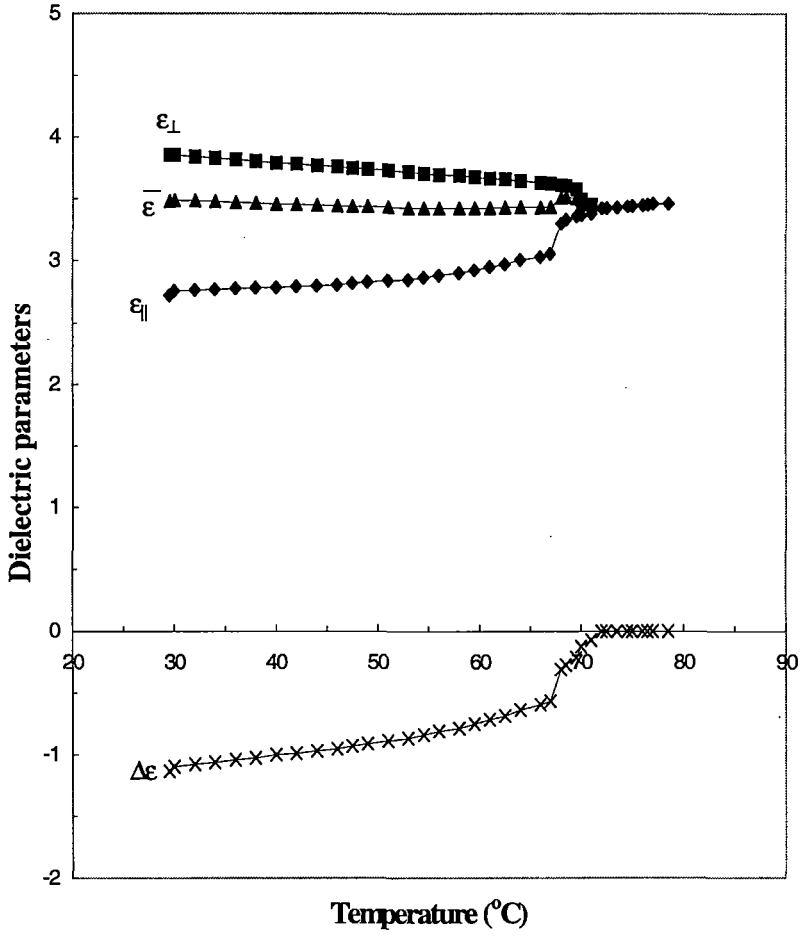

Figure 5.5 Temperature variation of dielectric parameters of BPPCC.

It is also observed that in pure BPPCC the values of $\varepsilon_\perp$ decrease very slowly with temperature while $\varepsilon_\parallel$ and $\Delta\varepsilon$ values are found to increase very slowly. In the mixtures, however, $\varepsilon_\parallel$ and $\Delta\varepsilon$ values are found to decrease with temperature as expected for a Debye type liquid.

It is also clear from the graphs that all the dielectric parameters are substantially higher in the **mixtures** than that in pure **BPPCC** suggesting, as noted earlier, that dielectric behaviour of the mixtures is dominated by the strongly axial polar component 2CB.

Using the expressions for $\varepsilon_\parallel$ and $\varepsilon_\perp$ of Maier and Meier [Equations 2.24 and 2.25], which were obtained by extending Onsager's theory of isotropic liquid to

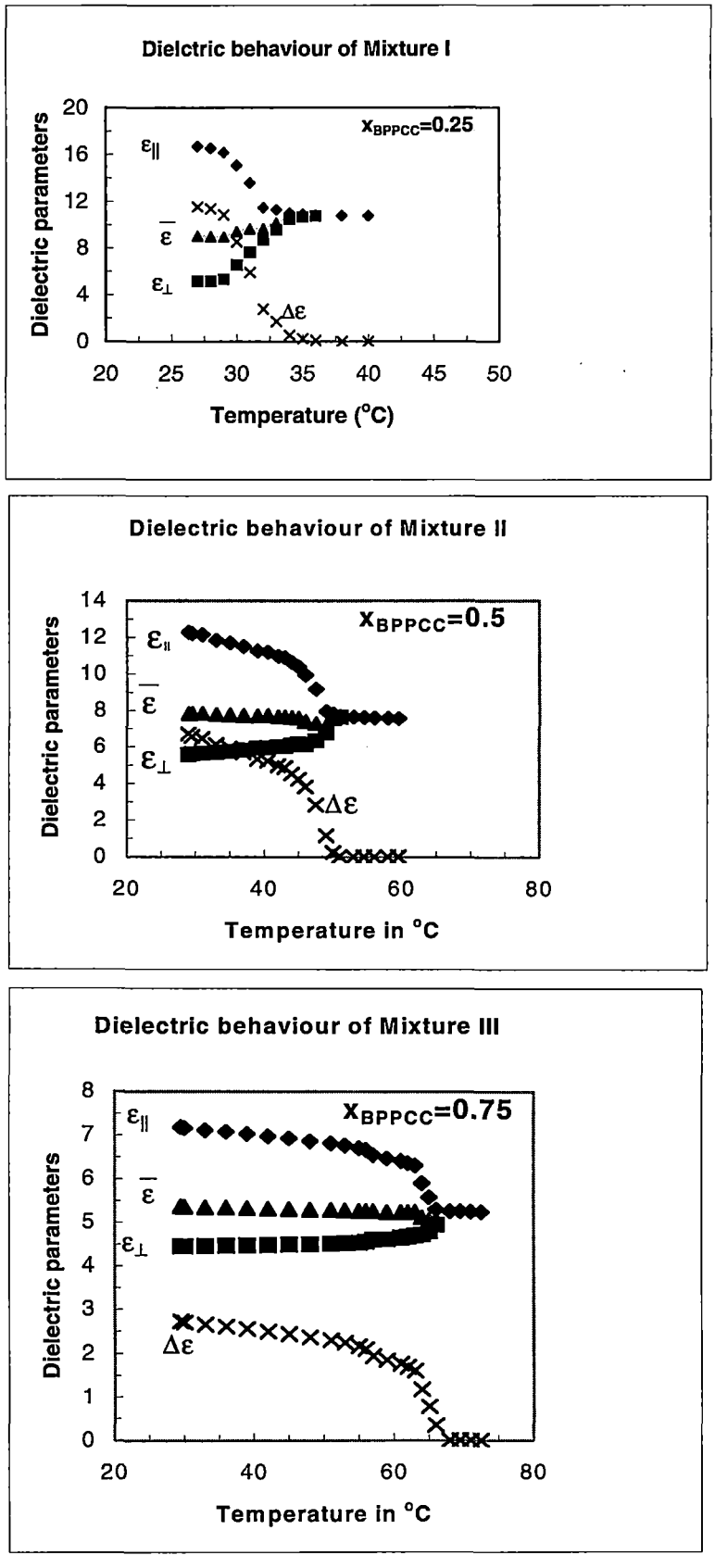

Figure 5.6 Temperature variation of dielectric parameters of the mixtures.

nematics, effective value of the dipole moment μ and the angle β which it makes with the molecular long axis are calculated at various temperatures for BPPCC. The calculation procedure has been described in detail in Chapter II. Mean field order parameters $<P_2>$ and densities, average molecular polarizability and polarizability anisotropy values [9] estimated from refractive indices using Neaugebauer's method [16] were used in this calculation. Since the above data were not available for the mixtures and we could not determine those values for want of sufficient sample, μ and β could not be calculated for the mixtures. Calculated values of μ and β have been given in Table 5.9. Both are found to increase slowly with temperature except near T_{NI}. Dipole moment of the free BPPCC molecules is not available but for few homologues of the series (with C_1 or C_2 at the alkoxy end and C_3 or C_5 at the alkyl end) reported μ values are 2.08D, 2.17D and 2.23D [15]. It was also shown previously for nCB series that free molecule dipole moment does not vary appreciably with chain length [17,18]. Therefore, it may be reasonably assumed that the free molecule dipole moment of BPPCC will be around 2.15 Debye. Effective value of the dipole moment within nematic phase is, therefore, about 20% less than the above free molecule value, again suggesting the presence of antiferroelectric type short range order between the neighbouring molecules. This type of result has also been tried to explain assuming the presence of both monomer and dimer molecules [10, 19-22]. Moreover, it is observed that the effective dipole moment is at large angle (β_{min}=74.6°and β_{max}=83.9°) with the molecular long axis and BPPCC molecules, therefore, exhibit negative dielectric anisotropy. Kali *et al.* [15] reported that the value of β, calculated from the known group dipole moments [23], is about 72° in the lower homologues. Thus observed low temperature β value agrees reasonably well with this data. However, it is observed that the calculated β values increase by 1-2° if $<P_2>$ determined from refractive indices data are used in the calculation instead of MS $<P_2>$ values, though this produces no change in the values of μ.

A quantitative measure of the above dipolar correlation is possible to determine using Bordewijk [24] theory of anisotropic dielectrics which is an

extension of Kirkwood-Fröhlich theory [25] where, unlike Maier-Meier theory, short range dipole-dipole interaction was considered explicitly. Correlation factor (g_λ), called Kirkwood correlation factor, are calculated taking into account the correlation between neighbouring dipole moments only where the suffix λ refers to $\parallel$ and $\perp$ to the nematic director. The ensemble average of the $\parallel$ and $\perp$ components of the molecular dipole moments were calculated following the procedure of Bata and Buka [26] and has been described in detail in Chapter II. Obviously, $g_\lambda = 1$ signifies no correlation (monomeric system), $g_\lambda = 0$ means perfect antiparallel correlation and $g_\lambda = 2$ means perfect parallel correlation. Calculated values are shown in Table 5.9. Values of $g_\parallel$ is found to be 0.35 and 0.83 at the low and high temperature end of the nematic phase while corresponding values of $g_\perp$ are 1.15 and 1.17. These values suggest parallel components of the molecular dipole moments are strongly correlated in antiferroelctric fashion at low temperatures but at high temperatures this correlation is almost negligible. Over the entire nematic range the correlation of the perpendicular component is ferroelectric type but almost negligible. No such data are available for BPPCC or its homologues. However, in a nematogenic compound, containing two carboxylate groups, moderate $g_\parallel$ but similar $g_\perp$ values were observed [27].

In the isotropic phase, the effective dipole moment was calculated by Kirkwood-Fröhlich relation [25] and found to be 1.87 Debye at 73.0°C. Corresponding dipole correlation factor (g_{iso}) is 0.76. Thus antiparallel dipolar correlation is found to exist even in the isotropic phase. It is also observed that μ value does not change appreciably at T_{NI}, similar phenomenon was noticed earlier while comparing the values of ε_{iso} and $\bar{\varepsilon}$ below T_{NI}. Thus X-ray and dielectric study suggests the presence of anti-parallel molecular association in **BPPCC** in both nematic and isotropic phases and no effective change in molecular associations takes place during the **N-I** transition.

Since the threshold voltage and other operational parameters of liquid crystal display devices depend on $\Delta\varepsilon$ and since the multiplexability of matrix displays may be limited by the temperature dependence of $\Delta\varepsilon$ and since multicomponent mixtures

are used in commercial display devices, the results presented above on pure compound and mixtures are of interest from application point of view in addition to the general interest of understanding the basic science.

TABLE 5.2

D and *l* values at different temperatures

Mixture II			Mixture III		
Temp.(°C)	**D** (Å)	*l* (Å)	**Temp.**(°C)	**D** (Å)	*l* (Å)
26	4.99	19.1	26	5.12	19.3
30	5.16	18.9	30	5.14	19.4
35	5.14	18.7	35	5.15	19.6
40	5.15	18.9	40	5.14	19.5
45	5.16	18.7	45	5.18	19.5
50	5.19	19.3	50	5.2	19.7
55	5.44	19.6	55	5.25	19.8
			60	5.23	19.5
			64	5.29	19.7
			66	5.3	19.8

TABLE 5.3

Orientational order parameters of Mixture II

Temperature (°C)	$\langle P_2 \rangle$	$\langle P_4 \rangle$	MS Value	
			$\langle P_2 \rangle$	$\langle P_4 \rangle$
26	0.58	0.24	0.60	0.24
30	0.57	0.26	0.58	0.23
35	0.55	0.22	0.56	0.21
40	0.53	0.19	0.53	0.19
45	0.51	0.17	0.50	0.16
50	0.48	0.14	0.45	0.13

TABLE 5.4

Orientational order parameters of Mixture III

Temperature (°C)	$\langle P_2 \rangle$	$\langle P_4 \rangle$	MS Value	
			$\langle P_2 \rangle$	$\langle P_4 \rangle$
26	0.60	0.26	0.65	0.29
30	0.60	0.26	0.63	0.27
35	0.60	0.27	0.61	0.26
40	0.57	0.22	0.60	0.24
45	0.57	0.24	0.57	0.22
50	0.52	0.20	0.55	0.20
55	0.52	0.20	0.52	0.18
60	0.51	0.17	0.49	0.16
64	0.47	0.09	0.45	0.13

TABLE 5.5

Dielectric parameters for BPPCC

BPPCC				
Temp.(°C)	$\varepsilon_{\parallel}$	$\varepsilon_{\perp}$	$\bar{\varepsilon}$	$\Delta\varepsilon$
71	3.380	3.451	3.427	-0.071
70	3.368	3.493	3.451	-0.125
69.5	3.362	3.576	3.504	-0.214
68.5	3.332	3.605	3.514	-0.273
68	3.303	3.611	3.508	-0.309
67	3.053	3.623	3.433	-0.570
66	3.030	3.629	3.429	-0.599
64	3.006	3.647	3.433	-0.641
62.5	2.970	3.659	3.429	-0.688
61	2.947	3.665	3.425	-0.718
59.5	2.923	3.676	3.425	-0.754
58	2.899	3.688	3.425	-0.789
56	2.881	3.694	3.423	-0.813
54.5	2.863	3.706	3.425	-0.843
53	2.846	3.718	3.427	-0.872
51	2.840	3.730	3.433	-0.890
49	2.828	3.742	3.437	-0.914
47.5	2.816	3.748	3.437	-0.932
46	2.804	3.760	3.441	-0.955
44	2.798	3.771	3.447	-0.973
42	2.792	3.783	3.453	-0.991
40	2.786	3.789	3.455	-1.003
38	2.780	3.807	3.465	-1.027
36	2.774	3.819	3.471	-1.044
34	2.769	3.831	3.477	-1.062
32	2.763	3.843	3.483	-1.080
30	2.757	3.855	3.489	-1.098
29.5	2.721	3.855	3.477	-1.134

TABLE 5.6

Dielectric parameters for Mixture I

Mixture I				
Temp.(°C)	$\varepsilon_{\parallel}$	$\varepsilon_{\perp}$	$\bar{\varepsilon}$	$\Delta\varepsilon$
36	10.828	10.739	10.768	0.089
35	10.887	10.656	10.733	0.231
34	10.988	10.454	10.632	0.534
33	11.285	9.581	10.149	1.703
32	11.463	8.709	9.627	2.754
31	13.552	7.647	9.615	5.905
30	15.065	6.543	9.384	8.522
29	16.157	5.309	8.925	10.848
28	16.519	5.154	8.942	11.365
27	16.661	5.142	8.982	11.519

TABLE 5.7

Dielectric parameters for Mixture II

Mixture II				
Temp.(°C)	$\varepsilon_{\parallel}$	$\varepsilon_{\perp}$	$\bar{\varepsilon}$	$\Delta\varepsilon$
51	7.670	7.635	7.647	0.036
50	7.801	7.564	7.643	0.237
49	7.949	6.792	7.178	1.157
47.5	9.166	6.347	7.287	2.819
46	9.937	6.127	7.397	3.810
45	10.383	6.169	7.574	4.214
44	10.626	6.110	7.615	4.516
43	10.887	6.021	7.643	4.866
42	10.970	6.003	7.659	4.967
40.5	11.196	5.967	7.710	5.228
39	11.255	5.926	7.702	5.329
37	11.498	5.831	7.720	5.668
35	11.688	5.765	7.740	5.923
33	11.848	5.712	7.758	6.136
31	12.139	5.665	7.823	6.475
29.5	12.204	5.635	7.825	6.570
29	12.276	5.576	7.809	6.700

TABLE 5.8

Dielectric parameters for Mixture III

Mixture III				
Temp.(°C)	$\varepsilon_{\parallel}$	$\varepsilon_{\perp}$	$\bar{\varepsilon}$	$\Delta\varepsilon$
66	5.297	4.952	5.067	0.344
65	5.576	4.798	5.057	0.777
64	5.902	4.727	5.119	1.175
63	6.311	4.703	5.239	1.608
62	6.365	4.674	5.237	1.691
61	6.412	4.650	5.237	1.763
59	6.466	4.620	5.235	1.846
57	6.543	4.608	5.253	1.935
56	6.662	4.561	5.261	2.101
55	6.703	4.537	5.259	2.166
53	6.768	4.525	5.273	2.243
51	6.816	4.513	5.281	2.303
48	6.863	4.501	5.289	2.362
45	6.929	4.490	5.303	2.439
42	6.976	4.478	5.310	2.498
39	7.030	4.472	5.324	2.558
36	7.077	4.466	5.336	2.611
33	7.113	4.460	5.344	2.653
30	7.160	4.454	5.356	2.706
29.5	7.184	4.454	5.364	2.730

TABLE 5.9

Effective dipole moment (μ), angle (β) and correlation factors of BPPCC

Temperature (°C)	μ	β	$g_{\parallel}$	$g_{\perp}$
43	1.73	74.6	0.35	1.15
48	1.75	75.8	0.43	1.15
51	1.76	76.6	0.5	1.16
55	1.77	78.3	0.59	1.16
60	1.8	83.2	0.83	1.16
63	1.82	83.9	0.96	1.17
68	1.9	66	0.89	1.24
70	1.86	60.5	0.83	1.17
73	1.87 iso		0.76 iso	

REFERENCES

1. D. Demus, J. Goodby, G.W. Gray, H.-W. Spiess and V. Vill, *Handbook of Liquid Crystals*, Vols. **2A**, Wiley-VCH, Verlag GmbH, Weinheim, FRG (1998), p48
2. T. Tasaka, H. Okamoto, V. F. Petrov and S. Takenaka, *Liq. Crystals*, **28**, 1025(2001).
3. V. Vill, Liq. Cryst. Database, Ver. 2.1, LC Publisher, GmbH, Humberg (1996).
4. G. W. Gray, K. J. harrison and J. A. Nash, *Electron Lett.*, **9**, 130(1973) and BDH literature data.
5. R. Eidenschink, D. Erdmann, J. Krause and L. Pohl, *Angew. Chem*, **89**, 103(1977).
6. R. Eidenschink, D. Erdmann, J. Krause and L. Pohl, *Angew. Chem*, Int. Ed. Engl. **17**, 133(1978).
7. A. Boller and H. Scherrer, *Ger. Offen*, **2.306**, 739(1972); C. A. **79**, 146267y (1973).
8. Hoffmann-La Roche Catalogue data.
9. N. K. Pradhan, Ph.D. Thesis, University of North Bengal, Siliguri - 734430, India (1998).
10. S. K. Giri, P. K. Mandal and S. Paul, *Mol. Cryst. Liq. Cryst.*, **330,** 343(1999).
11. A. J. Leadbetter, R. M. Richardson and C. N. Cooling, *J. de Phys. (Paris)*, Colloque, **36**, Cl-37(1975).
12. P. Sarkar, P. K. Sarkar, S. Paul and P. Mandal, *Phase Transitions, 71*, 1(2000).
13. P. Sarkar, P. Mandal, S. Paul, R. Paul, R. Dabrowski and K. Czuprinski, *Liq. Crystals,* **30**, 507(2003).
14. S. K. Giri, N. K. Pradhan, R. Paul, S. Paul, P. Mandal, R. Dabrowski and K. Czuprinski, *SPIE,* **3319**, 149(1998).
15. K. Kali, S. Sen and S. K. Roy, *Bull. Chem. Soc. Jpn.*, **58**, 3576(1985).
16. H. E. J. Neaugebauer, *Can. J. Phys.*, **32**,1(1954).
17. E. Megnassan and A. Proutierre, *Mol. Cryst. Liq. Cryst.*, **108,** 245(1984).
18. K. P. Gueu, E. Megnassan and A. Proutierre, *Mol. Cryst. Liq. Cryst.*, **132,** 303(1986).
19. D. A. Dunmur and K. Toriyama, Liq. Cryst. **1**(2) 169 (1986).
20. P. Kedziora and J. Jadzyn, Acta Phys. Pol. **A77**(5), 605 (1990).
21. P. Kedziora and J. Jadzyn, Mol. Cryst. Liq. Cryst., **192**, 31 (1990).
22. S. Y. Yakovenko and J. Pelzl, Mol. Cryst. Liq. Cryst., **366**, 27 (2001).
23. V. I. Minkin, O. A. Osipov and Y. A. Zhadanov, *Dipole Moments in Organic Chemistry*, Plenum Press, New York(1970).
24. P. Bordewijk, *Physica*, **75**, 146 (1974).
25. C. J. F. Bottcher, *Theory of Electric Polarization*, 2nd edition (Elsevier, Amsterdam, 1973), Vol. **1**, chapter 6.
26. L. Bata and A. Buka, *Mol. Cryst. Liq. Cryst*, **63**, 307 (1981).
27. P. Sarkar, S. Paul and P. Mandal, *Mol. Cryst. Liq. Cryst.*, **330,** 87(1999).

Chapter VI

MOLECULAR STRUCTURE AND PACKING IN THE CRYSTALLINE STATE OF 4-n-ETHYL-4'-CYANOBIPHENYL (2CB) BY SINGLE CRYSTAL X-RAY DIFFRACTOMETRY

Part of this work has been published in *Mol. Cryst. Liq. Cryst.*, **325**, 91 (1998)

6.1 INTRODUCTION

Both the homologous series; 4-n-alkyl-4´-cyanobiphenyl (*n*CB) and 4-n-alkoxy-4´-cyanobiphenyl (*n*OCB) are particularly interesting and useful family of mesogens. These systems have been studied extensively from different angles using various experimental techniques. Several of them are used as components in commercially available liquid crystal mixtures [1]. In both the series the first four homologous compounds show monotropic nematic phase whereas the eight higher ones form enantiotropic nematic and/or smectic phases. Knowledge of molecular conformation and packing in the crystalline state gives better insight in understanding their structure and properties in the mesophase [2,3] as has been discussed in Chapter II. With this view crystal and molecular structures of the 3rd, 4th, 6th and 7th members of the *n*CB-series [4-6] and first to eighth members of the *n*OCB-series[7-10] were reported earlier. Crystal and molecular structures of a large number of liquid crystal compounds including the 5th member of the nOCB series [8,11-17] have been determined by co-workers and mechanism of transition to mesomorphic phase has been tried to explain in relation to the molecular organization in the crystalline state. In continuation of this program the crystal and molecular structure of the second member of the *n*CB series (2CB) have been determined and described in this chapter.

6.2 EXPERIMENTAL

6.2.1 Crystal Data

Transparent needle shaped crystals were grown by slow evaporation technique from a solution in acetone. A single crystal of dimensions .23×.18×.28 mm was used to collect intensity data using Enraf-Nonious CAD4 diffractometer. MoK_α radiation, monocromated by graphite monocromator, was used for data collection. The unit cell parameters were obtained using the method of short vector followed by least-squares refinement of 25 reflections in the interval $8 < \theta < 18^\circ$. All the 25 reflections could be indexed with respect to a monoclinic cell. The reflections

0k0 with k=2n+1 were found to be systematically absent indicating that the space group is $P2_1$. All together 1153 independent reflections were measured in the interval $4 < 2\theta < 50^\circ$ of which 557 were taken as observed reflections with $I>2\sigma(I)$. Lorentz and polarization corrections were applied but no absorption correction was made. Data were collected in ω-2θ scan mode. Important crystallographic data of the compound are given in Table 6.1

6.2.2 Structure Determination and Refinement:

The structure was solved by direct methods using the PC version of the crystallographic package program SIR92 [18]. Details of the direct method have been described in Chapter II. In SIR92 package estimation of structure invariants and structure seminvariants is based on Representation Theory developed by Giacovazzo [19,20]. Stereochemically best suited model obtained from E-map was refined by full-matrix block least-squares method. Anisotropic thermal parameters for the non-hydrogen atoms were used during refinement while the hydrogen atoms were attributed isotropic thermal parameters of the parent C-atoms. Positions of hydrogen atoms were calculated theoretically. SHELXL-93 computer program [21] was used for refinement. The final residual structure factor R(F) is 0.079. A difference Fourier map at this stage showed no electron density maxima greater than $\pm 0.3 Å^{-3}$. The atomic scattering factors were taken from the International Table for Crystallography [22]. For brevity calculated and observed structure factors are not produced here and also in Chapter VII.

6.3 RESULTS AND DISCUSSIONS

6.3.1 Molecular Conformation

Perspective view of 2CB molecule is shown in figure 6.1. Final positional and anisotropic thermal parameters of all non-hydrogen atoms are listed in Tables 6.2 and 6.3 using the numbering scheme of atoms shown in figure 6.1. Their bond lengths and bond angles are given in Table 6.4. Positions of the hydrogen atoms with their isotropic temperature factors are given in Table 6.5. Average C-C bond

distance in cyanophenyl ring is 1.375(11) Å and that in alkyl phenyl ring is 1.374(10) Å, about 0.02 Å less than the expected value [23]. Mean C-C bond lengths in the phenyl rings were found to be 1.383 Å and 1.40 Å in 3CB and 4CB molecules respectively [4,5]. Moreover, the C2-C3 bond distance is found to be 1.358(13) Å, quite less than the expected value. Such shortening of bond lengths has, however, been observed in other mesogens [8,24,25]. But average C-C-C bond angle in the phenyl rings is 120.0(7)° as expected. The distance C14-C15 in the ethyl chain is 1.390(13) Å, quite less than the expected value 1.541 Å [23]. In fact the terminal atom C15 is found to have a temperature factor almost double than that of other atoms. Hence we ignored the methyl hydrogen atoms in final stages of refinement. It is noted that 4CB molecule also showed [5] disordering in the last two C atoms of the butyl chain and such disordering in terminal chain was observed in other mesogenic structures [26-28] as well. The C1-N bond distance is found to be 1.159(7) Å somewhat larger than 1.142(5) Å in 3CB and 1.130(2) Å in 4CB and 1.132Å in 5OCB [4,8]. The angle N-C1-C2 is 179.6(8)° close to the value observed in other cyanophenyl compounds.

To get an idea about the conformation of the molecule least-squares planes through different fragments of 2CB and the dihedral angles between the planes have been calculated and given in Table 6.6. As expected both the phenyl rings are highly planar. The cyano group atoms C1 and N are displaced downward from the phenyl group by 0.10 Å and 0.18 Å respectively. The two phenyl rings are inclined to each other at an angle 1.46° unlike the 3CB and 4CB molecules where the angle is 40.5° and 42.8° respectively. Though few biphenyl mesogenic compounds [5,7] show the

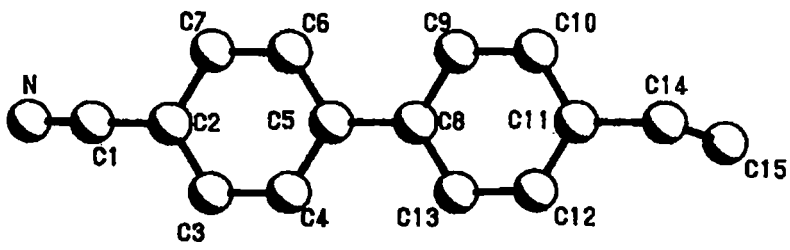

Figure 6.1: Perspective view of 2CB molecule along with atomic numbering scheme.

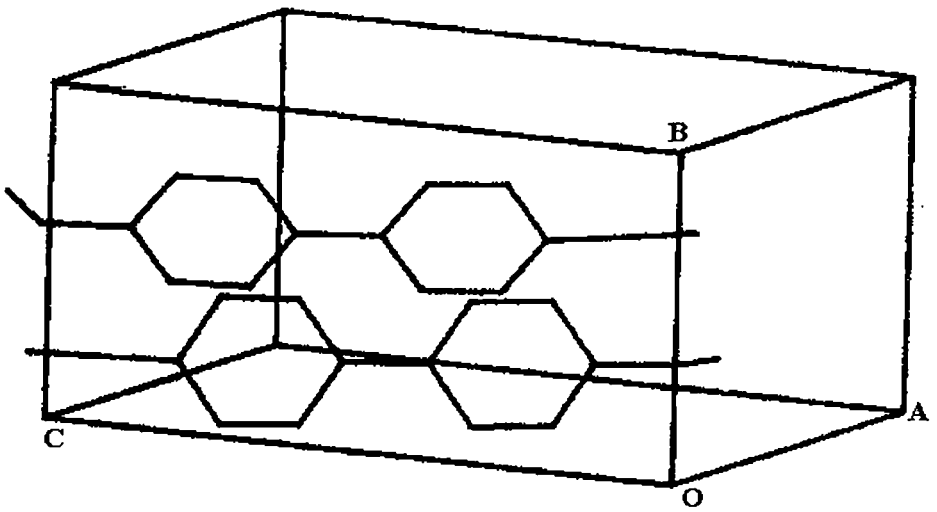

Figure 6.2: Packing of 2CB molecules in the unit cell.

above dihedral angle around 40° but a wide range of values namely 0-50° have also been observed [7]. Interestingly, all the first eight *n*OCB members show large dihedral angles only exception is 5OCB [8] where this angle was found to be 0.82°. Length of the molecule (N-C15) in the crystalline state is found to be 11.83 Å and when methyl group hydrogen bond length is included it becomes 12.85 Å in good agreement with the model length of the molecule in *all-trans* configuration.

6.3.2 Crystal Packing:

Different views of the packing of 2CB molecules in the crystalline state are shown in figures 6.2-6.4. The molecules are extended parallel to each other with their long axis making an angle of ~23° with [001] direction. Antiparallel pairs of molecules, related by the symmetry element two fold screw axis (2_1), are arranged in layers by translational symmetry along [100] and [010] and the layers are stacked along [001] direction. The thickness of these layers is equal to the length of crystallographic *c*-axis.

In order to discuss the molecular association in the crystalline state, which might be interpreted either as a precursor or as a result of liquid crystalline state, we

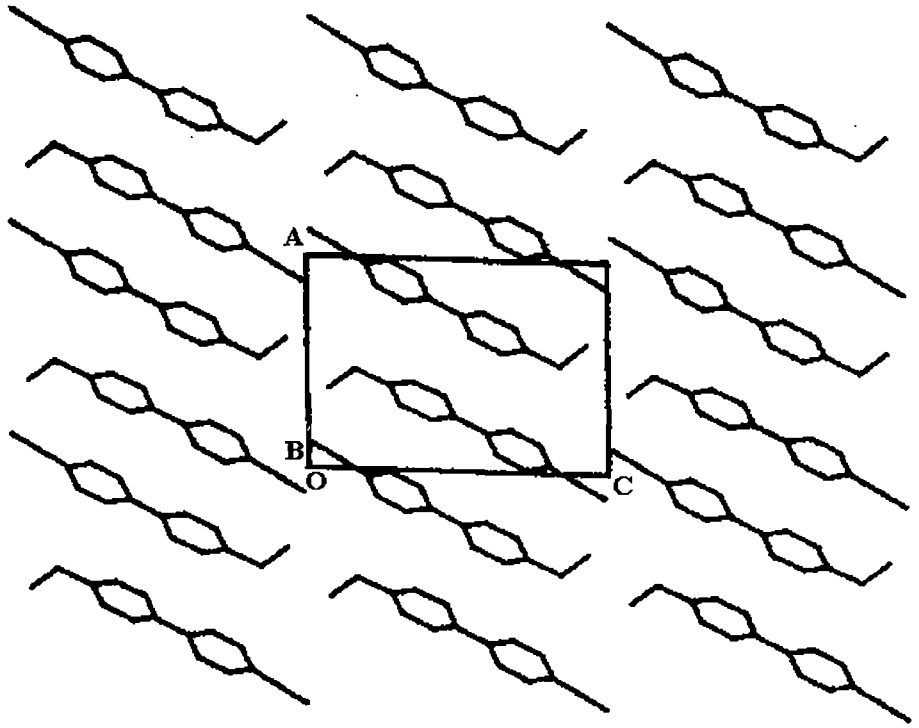

Figure 6.3: Crystal structure of 2CB projected in ac-plane.

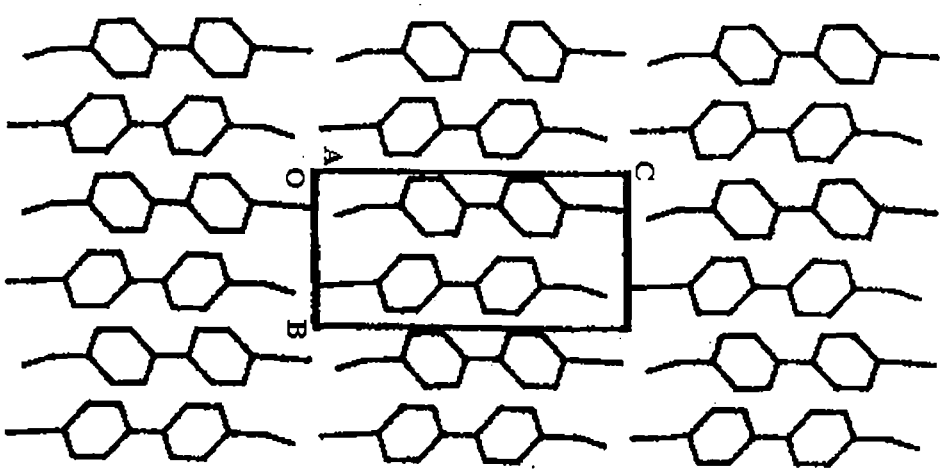

Figure 6.4: Crystal structure of 2CB projected in bc-plane.

have calculated the intermolecular distance between the atoms of the neighbouring molecules. No dipole-dipole contact is observed in this case. However van der Walls' type of contact is found to exist between atoms N-C15 (3.52 Å), C4-C8 (3.74

Å) and C12-C2 (3.79 Å) of the 2_1 symmetry related molecules. The length of such paired molecules is found to be 14.47 Å which is 1.13 times the single molecule length (L=12.85 Å). Thus the neighbouring molecules overlap almost completely. Due to van der Walls' type or dipole-induced dipole type contact, however, both the 3CB and 4CB molecules show different type of overlapping. In 3CB the overlapping is between cyano group of one molecule with the phenyl ring of the neighbouring molecule related by inversion symmetry. On the other hand, in 4CB overlapping is between the cyano group of one molecule with either the cyanophenyl group of centrosymmetric molecule or with the alkyl phenyl group of 2_1 symmetry related molecule. In case of the first four members of nOCB series, which also exhibit monotropic nematic phase, the overlapping of the neighbouring molecules is either of 3CB type or of 4CB type. In 4OCB no cyano-cyano or cyano-phenyl interaction is observed as in 2CB. The three higher homologues (n = 5,6,7), which exhibit enantiotropic nematic phase, show dipole-dipole interaction and overlapping is between opposing cyano groups. The length of the paired molecules, often called dimmer, is found to be in the range $L \leq l \leq 2L$. In the nematic or smectic phase l is found to be 1.4 times L [29,30].

Finally, some comment might be made on the appearance of virtual monotropic nematic phase in 2CB. Though the 2CB molecules are arranged in parallel fashion but the packing is not of imbricated type as is assumed necessary for a precursor to nematic phase. Observed packing is in fact precursor to the tilted smectic type. Moreover van der Walls' type of contact encompasses all the molecules within a layer. So the melting point is well above the range of thermal stability of the nematic phase. However, while cooling from isotropic melt, dipole-dipole interaction may give rise to parallel imbricated mode of packing as observed in the fifth member onwards of nOCB series of compounds and this in turn may sets in nematic phase.

TABLE 6.1

Important Crystallographic Data

Identification code	2CB
Empirical formula	$C_{15}H_{13}N$
Formula weight	207.26 g/mol
Crystal system	Monoclinic
Space group	$P2_1$
Form/habit	Needle shaped
a = 8.584(4) Å	α = 90.00(3) deg.
b = 5.865(3) Å	β = 92.30(3) deg.
c = 11.833(3) Å	γ = 90.00(4) deg.
Volume	595.3(4) $Å^3$
Z	2
Density (calculated)	1.156 Mgm^{-3}
Absorption coefficient	0.067 mm^{-1}
F(000)	220
Wavelength	0.71073 Å
Data collected within θ	2.37° to 24.98°
Index ranges	$0 \le h \le 10$, $0 \le k \le 6$, $-14 \le l \le 14$
Independent reflections	1153
Refinement method	Full-matrix-block least-squares on F^2
Final R index [$I>2\sigma(I)$]	R = 0.0787
Largest diff. peak and hole	0.265 and -0.179 $e.Å^{-3}$

TABLE 6.2

Atomic co-ordinates ($\times 10^4$) and equivalent isotropic displacement parameters ($Å^2 \times 10^3$) with e.s.d's in parentheses for the non-hydrogen atoms. U(eq) is defined as one third of the trace of the orthogonalized Uij tensor.

Atom	x	y	z	U(eq)
N	-1173(8)	2280(24)	9871(6)	137(3)
C1	-496(8)	2177(24)	9045(6)	107(3)
C2	350(7)	2053(18)	8031(5)	85(2)
C3	124(9)	343(16)	7268(7)	107(3)
C4	863(9)	351(14)	6266(6)	100(2)
C5	1840(6)	2110(12)	5960(4)	64(2)
C6	2033(8)	3842(17)	6736(6)	100(3)
C7	1304(9)	3878(19)	7736(6)	111(3)
C8	2619(6)	2123(13)	4862(4)	68(2)
C9	3598(7)	3871(15)	4575(5)	82(2)
C10	4273(8)	3946(16)	3536(6)	94(2)
C11	4076(7)	2197(18)	2770(5)	88(2)
C12	3144(8)	466(17)	3064(6)	104(3)
C13	2434(8)	372(15)	4093(6)	93(2)
C14	4827(9)	2250(23)	1619(6)	123(3)
C15	3838(15)	2829(40)	705(9)	226(10)

TABLE 6.3

Anisotropic displacement parameters ($Å^2 \times 10^3$) for the non-hydrogen atoms with e.s.d's in parentheses. The anisotropic displacement factor exponent takes the form: $-2\pi^2 [h^2 a^{*2} U11 + ... + 2 h k a^* b^* U12]$

Atom	U11	U22	U33	U23	U13	U12
N	137(5)	154(7)	124(5)	40(6)	52(4)	10(6)
C1	101(5)	125(7)	96(4)	25(6)	23(4)	-4(6)
C2	72(4)	101(6)	82(4)	17(5)	11(3)	-5(5)
C3	101(5)	100(6)	122(6)	-13(6)	39(5)	-33(6)
C4	108(5)	87(5)	107(5)	-15(6)	23(4)	-24(6)
C5	55(3)	69(4)	68(3)	4(5)	0(2)	-3(5)
C6	94(5)	113(6)	95(5)	-26(6)	22(4)	-39(6)
C7	113(5)	124(7)	100(5)	-33(6)	33(4)	-34(7)
C8	54(3)	69(4)	81(4)	-3(5)	-3(3)	3(5)
C9	77(4)	83(5)	85(4)	-9(5)	8(3)	-14(6)
C10	82(4)	98(6)	104(5)	-3(6)	10(4)	-9(6)
C11	68(4)	111(6)	85(4)	-4(6)	7(3)	-4(6)
C12	101(5)	115(7)	97(5)	-30(6)	7(4)	0(7)
C13	102(5)	85(5)	92(4)	-14(5)	15(4)	-15(6)
C14	135(6)	156(9)	78(4)	-3(7)	10(4)	23(9)
C15	196(10)	327(30)	159(9)	102(14)	42(8)	59(16)

TABLE 6.4

Bond lengths (Å) and bond angles (°) involving non-hydrogen atoms with e.s.d's in parentheses.

N-C1	1.159(7)	N-C1-C2	179.6(8)
C1-C2	1.429(9)	C3-C2-C7	117.9(6)
C2-C3	1.358(13)	C3-C2-C1	122.1(10)
C2-C7	1.401(13)	C7-C2-C1	119.5(11)
C3-C4	1.367(9)	C2-C3-C4	121.0(8)
C4-C5	1.387(10)	C3-C4-C5	122.4(8)
C5-C6	1.375(10)	C6-C5-C4	115.6(5)
C5-C8	1.485(6)	C6-C5-C8	122.3(6)
C6-C7	1.360(9)	C4-C5-C8	122.1(6)
C8-C13	1.377(10)	C7-C6-C5	123.1(8)
C8-C9	1.377(10)	C6-C7-C2	119.9(9)
C9-C10	1.380(8)	C13-C8-C9	116.6(5)
C10-C11	1.375(12)	C13-C8-C5	122.0(6)
C11-C12	1.347(13)	C9-C8-C5	121.4(6)
C11-C14	1.530(8)	C8-C9-C10	121.7(7)
C12-C13	1.385(9)	C11-C10-C9	121.2(8)
C14-C15	1.390(13)	C12-C11-C10	116.8(6)
		C12-C11-C14	121.4(9)
		C10-C11-C14	121.8(9)
		C11-C12-C13	122.9(8)
		C8-C13-C12	120.5(8)
		C15-C14-C11	115.6(8)

TABLE 6.5

Hydrogen co-ordinates ($\times 10^4$) and isotropic displacement parameters ($Å^2 \times 10^3$) with e.s.d's in parentheses for the non-hydrogen atoms.

Atom	x	y	z	U(eq)
H14A	5944	3523	1576	59
H14B	5344	459	1424	91
H3	-545(9)	-852(16)	7429(7)	128
H4	706(9)	-868(14)	5772(6)	120
H6	2692(8)	5044(17)	6570(6)	120
H7	1440(9)	5113(19)	8223(6)	134
H9	3810(7)	5032(15)	5094(5)	98
H10	4873(8)	5203(16)	3352(6)	113
H12	2968(8)	-719(17)	2552(6)	125
H13	1827(8)	-884(15)	4267(6)	112

TABLE 6.6

Equations of the least-squares planes, distances (Å) of the atoms from them and dihedral angles (°) between them.

Plane no.	Equation of the plane	Atom	Distance	Atom	Distance
1	6.56111X - 2.82276Y + 4.70957Z	C2	.0153	C5	.0015
	= 3.41708	C3	-.0096	C6	.0047
		C4	.0011	C7	-.0129
	Other atoms	C1	-.0972	N	-.1815
2	6.67844X - 2.80266Y + 4.45162Z	C8	-.0167	C11	.0044
	= 3.33514	C9	.0195	C12	-.0021
		C10	-.0133	C13	.0082
	Other atoms	C4	-.0678	C14	-.0213
3	6.59860X - 2.81335Y + 4.63595Z	C2	.0025	C8	.0109
	= 3.37398	C3	-.0192	C9	.0321
		C4	.0016	C10	-.0253
		C5	.0096	C11	-.0183
		C6	.0094	C12	-.0100
		C7	-.0182	C13	.0250
	Other atoms	C1	-.1205	N	-.2133
		C14	-.0713	C15	-1.3105
4	7.09265X - 2.95778Y + 2.57269Z	C8	-.2174	C12	.1825
	= 2.69782	C9	-.1138	C13	-.0285
		C10	.0754	C14	.4768
		C11	.2560	C15	-.6310
5	6.42531X - 2.81915Y + 5.04445Z	N	-.0468	C4	-.0134
	= 3.62978	C1	.0005	C5	-.0359
		C2	.0675	C6	-.0087
		C3	.0195	C7	.0172

Dihedral angles between planes:

1 & 2, 1 & 3, 1 & 4, 1 & 5, 2 & 3, 2 & 4, 2 & 5, 3& 4, 3 & 5 and 4 & 5 are respectively 1.462°, .437°, 10.908°, 1.828°, 1.027°, 9.542°, 3.279°, 10.512°, 2.254° and 12.710°.

REFERENCES

1. D. Demus, *Mol. Cryst. Liq. Cryst.*, **364**, 25 (2001).
2. R. F. Bryan, *J. Struc. Chem.*, **23**, 128 (1982).
3. W. Haase and M. A. Athassopoulou, *Struct. Bonding*, **94**, 140(1999).
4. W. Haase, H. Paulus and R. Pendzialec, *Mol. Cryst. Liq. Cryst.*, **100**, 211(1983).
5. G. V. Vani, *Mol. Cryst. Liq. Cryst.*, **99**, 21 (1983).
6. M. Kuribyashi and K. Hori, *Liq. Cryst.*, **26**, 809(1999).
7. L. Walz, H. Paulus and W. Haase, *Zeitchrift für Cryst.*, **180**, 97 (1987).
8. P. Mandal and S. Paul, *Mol. Cryst. Liq. Cryst.*, **131**, 223 (1985).
9. K. Hori, Y. Koma, A. Uchida and Y. Ohashi, *Mol. Cryst. Liq. Cryst.*, **225**, 15 (1993).
10. K. Hori, Y. Koma, M. Kurosaki, K. Itoh, H. Uekusa, Y. Takenaka and Y. Ohashi, *Bull. Chem. Soc. Japan*, **69**, 891 (1996).
11. P. Mandal, S. Paul, H. Schenk and K. Goubitz, *Mol. Cryst. Liq. Cryst.*, **135**, 35 (1986).
12. P. Mandal, B. Majumdar, S. Paul, H. Schenk and K. Goubitz, *Mol. Cryst. Liq. Cryst.*, **168**, 135 (1989).
13. P. Mandal, S. Paul, C. H. Stam and H. Schenk, *Mol. Cryst. Liq. Cryst.*, **180B**, 369 (1990).
14. S. Gupta, P.Mandal, S. Paul, M. Wit, K. Goubitz and H. Schenk, *Mol. Cryst. Liq. Cryst.*, **195**, 149 (1991).
15. P. Mandal, S. Paul, H. Schenk and K. Goubitz, *Mol. Cryst. Liq. Cryst.*, **210**, 21 (1992).
16. P. Mandal, S. Paul, K. Goubitz and H. Schenk, *Mol. Cryst. Liq. Cryst.*, **258**, 209 (1995).
17. A. Nath, S. Gupta, P. Mandal, S. Paul and H. Schenk, *Liq. Cryst.*, **20**, 765 (1996).
18. A. Altomare, G. Cascarano, C.Giacovazzo, A.Guagliardi, M.C. Burla, G. Polidori and M. Camalli, *The SIR92 Programme* (1992).
19. C. Giacovazzo, *Acta Cryst.*, **A33**, 933 (1977).
20. C. Giacovazzo, *Acta Cryst.*, **A36**, 362 (1980).
21. G. M. Sheldrick, *Programme for crystal structure refinement,* University of Göttingen, Germany (1993).
22. *International Tables for X-ray Crystallography,* Birmingham, Kynoch Press (1974), Vol. **IV.**
23. *International Tables for X-ray Crystallography,* Birmingham, Kynoch Press (1974), Vol. **III.**
24. A. J. Leadbetter and M. A. Mazid, *Mol. Cryst. Liq. Cryst.*, **51**, 85 (1979).
25. W. Haase, H. Paulus and H. T. Muller, *Mol. Cryst. Liq. Cryst.*, **97**, 131 (1983).
26. G. V. Vani and K. Vijayan, *Mol. Cryst. Liq. Cryst.*, **51**, 253 (1979).

27. J. Doucet, J. P. Mornon, R. Chevalier and A. Lifchitz, *Acta Cryst.*, **B33**, 1701 (1977).

28. M. Cotrait, C. Destrade and H. Gasparaux, *Acta Cryst.*, **B31**, 2704 (1975).

29. A. J. Leadbetter, R. M. Richardson and C. N. Cooling, *J. Phys. (Paris)*, **36**, 37(1975).

30. B. Bhattacharjee, S. Paul and R. Paul, *Mol. Cryst. Liq. Cryst.*, **89**, 181 (1982).

Chapter VII

CRYSTAL AND MOLECULAR STRUCTURE OF THE NEMATOGENIC COMPOUND P-BUTOXYPHENYL trans-4- PROPYL CYCLOHEXANE CARBOXYLATE

Part of this work was accepted for presentation at the 19th ILCC, Edinburgh,2002 (Ref. No. ILCC 2002-133). Has been communicated for publication in *Mol. Cryst. Liq. Cryst.*

7.1 INTRODUCTION

The crystal structure determination of mesogenic materials is a useful way to obtain general information about the conformation and packing of the molecules in the solid state that in turn can throw light on the understanding of their properties and behaviour in liquid crystal state. In this chapter results of the X-ray structural analysis of the compound p-butoxyphenyl *trans* -4- propyl cyclohexane carboxylate (BPPCC) have been presented. The compound has the following phase sequence and transition temperatures:

$$\text{Solid} \xleftrightarrow{43^\circ\text{C}} \text{Nematic} \xleftrightarrow{72.6^\circ\text{C}} \text{Isotropic}$$

As described in Chapter V several physical properties of BPPCC and few other homologues in the liquid crystalline state have been studied by co-workers by means of density, X-ray diffraction, optical birefringence, elastic constants and magnetic susceptibility anisotropy measurements [1,2]. From the structural analysis of BPPCC an attempt has been made, in this chapter, to explain the molecular organization in the nematic phase in relation to the molecular packing in the crystalline state.

7.2 EXPERIMENTAL

A transparent plate shaped single crystal suitable for X-ray analysis was obtained from a solution of the compound in acetone by slow evaporation. X-ray intensity data were collected with Enraf-Nonius CAD4 diffractometer using CuK_α radiation and graphite monochromator. A total of 7052 independent reflections were measured in the interval $2.55^\circ<\theta<67.90^\circ$ (h from -13 to 13, k from 0 to 24 and l from 0 to 21) of which 2447 were taken as observed reflections with $I > 2\sigma(I)$. Lorentz and polarization corrections were applied, but no absorption correction was made. Intensity data were taken in ω–2θ scan mode. From the systematic absence conditions of $h0l$ reflections with h odd and $0k0$ reflections with k odd the space group was uniquely determined to be $P2_1/a$. From the calculation of density the

number of independent molecules per unit cell was found to be 2. Important crystallographic data are given in Table 7.1.

TABLE 7.1

Important Crystallographic Data

Identification code	BPPCC
Molecular formula	$C_{20}H_{30}O_3$
Molecular weight	318.46
Crystal system	Monoclinic
Space group	$P2_1/a$
Form / habit	Plate shaped
a = 11.2483(22) Å	α = 90.000(10)°
b = 20.2968(44)Å	β = 100.342 (11)°
c = 17.6311(14)Å	γ = 90.000(10)°
Cell volume (V)	3959.8640 $Å^3$
Z	8
Density (calculated)	1.0684 gcm^{-3}
Absorption coefficient	0.551
F (000)	1392
Wavelength (λ)	1.5418Å
Data collected within (θ)	2.55° to 67.90°
Index range	$-13 \leq h \leq 13, 0 \leq k \leq 24, 0 \leq l \leq 21$
Number of independent reflections	7052
Number of observed reflections	2447
Refinement method	Block diagonal least squares
Final R-index [I>2σ(I)]	0.106

7.3 STRUCTURE DETERMINATION AND REFINEMENT

The structure was determined by means of direct method using the PC version of the NRCVAX package program [3]. Phase set with highest combined figure of merit (CFOM), obtained by multisolution direct method MULTAN, was used to calculate the E-map. The detailed procedure has been described in Chapter II. Sites of only 40 non-hydrogen atoms of the two independent molecules could be located from the E-map. The positions of the remaining six non-hydrogen atoms were located by using successive Fourier and difference Fourier synthesis. The structure thus obtained was refined by block diagonal least-squares method with individual isotropic temperature factor for each non-hydrogen atom and the resulting R-value was 0.22. Introduction of individual anisotropic temperature factors for the non-hydrogen atoms reduced the R-value to 0.18. At this stage it was observed that bond lengths and bond angles for some atoms in the terminal alkyl chains were having unusual values, thermal vibrations were also found to be very large. Discarding their positions difference Fourier synthesis was computed again and those atoms were relocated. After several attempts the structure refined to an R-value of 0.15. Some of the atoms in the flexible alkyl chains still had very large values of temperature factors and unusual bond lengths. Attempts were also made to refine the structure by varying the occupancy of these atoms but no improvement was achieved. The hydrogen atoms in the structure were generated from the known geometry around the respective carbon atoms. These atoms were given isotropic temperature factors of the corresponding non-hydrogen atoms to which they were attached and included in the refinement process but kept them fixed. The R-value thus obtained was 0.12. The non-hydrogen atoms were then kept fixed and the positions as well as the temperature factors of the hydrogen atoms were varied for further refinement. The structure could be refined to a minimum R-value of 10.2%. Eight hydrogen atoms at this stage showed unusual bond lengths and angles. Those atoms were removed with final R-value of 10.6%. Such a high R-value may be due to disorder in the terminal alkyl chains which is not uncommon in mesogenic crystals and even higher R-values have been reported earlier [4-6].

7.4 RESULTS AND DISCUSSIONS

7.4.1 Molecular conformation

The two independent molecules (A and B) in the unit cell are shown in figure 7.1. Final positional coordinates with equivalent isotropic thermal parameter (B_{iso}), anisotropic thermal parameters (u_{ij}), bond distances and bond angles of the non-hydrogen atoms, whose numbering scheme has been shown in figure7.1, are listed in Tables 7.2 – 7.5. The average C–C bond distances in the phenyl ring of molecules A and B are respectively 1.369Å and 1.374 Å which are about 0.02 Å less than the expected value [7]. Some of the bond angles in the phenyl ring of the molecules A and B differ considerably from the mean value of 120° indicating a degree of strain because of the presence of carboxylic linkage group. The average C–C bond lengths are 1.491 Å and 1.500 Å in the cyclohexyl group of A and B molecules. These are

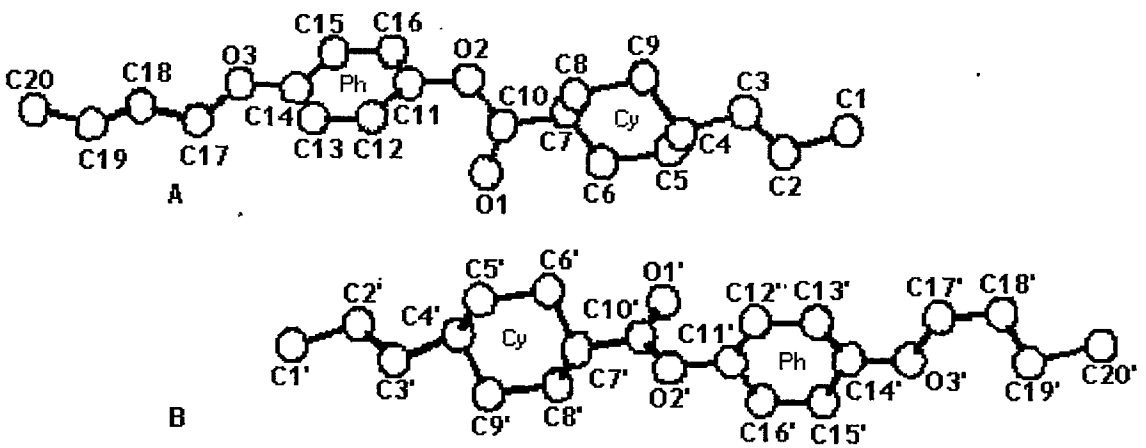

Figure 7.1: Perspective view of molecules A and B of BPPCC and their atom numbering scheme.

slightly less than the values observed in the cyclohexyl group(s) of 4-(1"-pentenyl)-4'-(cyano)-1,1'-bicyclohexane[8], 4-(3"-Pentenyl)-4'-(cyano)-1,1'-bicyclohexane[9], 4-(3"-pentenyl)-4'-(ethoxy)-1,1'-bicyclohexane [10], 5-(*trans*-4-heptyl cyclohexyl)-

2-(4-cyanophenyl) pyrimidine [11] and *trans, trans*-4'-pentyl bicyclohexyl-4-carbonitrile [12]. For example, the average C–C bond length in the two cyclohexyl groups of 4-(1"-pentenyl)-4'-(cyano)-1,1'-bicyclohexane[8] are 1.528Å and 1.525Å. The maximum and minimum bond angles in the cyclohexyl ring are found, respectively, to be 115.2° and 110.2° in A and 119.4° and 110.3° in B which are slightly more than the reported values in other cyclohexane compounds [8-12]. The length of the C=O bond is 1.20 Å in molecule A and 1.17 Å in B. Similar values are observed in 4'-cyanophenyl-4-*n*-pentylbenzoate [13], 4-cyanophenyl-4'-*n*-heptylbenzoate [14], 4'-cyanophenyl-4-*n*-pentoxybenzoate [15] and agree well with the standard dimensions in Cambridge Crystallographic Database [16]. The length of the C–O bond attached to the carbonyl group in both the molecules is less than the reported values, however, the other C–O bonds in the molecules are as expected [13-16]. Some of the bond lengths and bond angles in the chain part of both the molecules differ significantly from the standard values. For example the C2–C3, C18'–C19' and C19'–C20' bond lengths are 1.25 Å, 1.23 Å and 1.71 Å. Associated thermal parameters of the chain atoms are also very high compared to remaining atoms. Even same type of bonds of the two molecular conformations, such as C2–C3 and C2'–C3', are found to be quite different. These may be due to some conformational disorder in the chain parts of both the molecules; such disorder is not uncommon in the crystalline state of mesogenic compounds [9,17-22].

To describe the molecular conformation we have calculated the least-squares planes through different fragments of BPPCC and the dihedral angles between the planes. Selected data are given in Tables 7.6–7.7. The phenyl, alkoxy, carboxylic and the alkyl groups of both the molecules are planar and the R.M.S. displacements of the atoms from the respective planes are given in Table 7.6. Both the cyclohexyl rings are in chair conformation. In molecule A the dihedral angle between the phenyl group and the alkoxy group is only 6.5°, however, the phenyl group makes angle 81.7° and 108.6° respectively with the carboxylic and the cyclohexyl groups. The corresponding dihedral angles in molecule B are 4.8°, 95.6° and 13.8°. Thus in both the molecules the carboxylic group is in a plane almost perpendicular to that of

the phenyl group, while the alkoxy group is nearly coplanar with it. The cyclohexyl group of molecule A is nearly perpendicular to the phenyl group but in molecule B they are nearly coplanar. In three nematogenic bicyclohexylnitrile compounds [8,9,23] the dihedral angle between two adjacent cyclohexyl rings were reported as 80.3°, 4.05° and 34°.

The lengths of the molecules A and B in the crystalline state are found to be 19.09 Å and 18.85 Å, whereas the model length of the molecule in all *trans* conformation is 19.15 Å. Thus both the molecules are in their most extended conformations.

7.4.2 Molecular packing and relation to the nematic phase

Molecular long axis of the molecule A, defined as the least-squares fitted line through all the atoms, makes angles 45.9°, 88.4° and 135.9° respectively with the *a*, *b* and *c* axes. The corresponding angles for the molecule B are 44.1°, 89.9° and 134.1°. Thus the long axes of the molecules lie almost in the ac-plane. The views of molecular packing projected in XY, YZ and XZ-plane are shown in Figures 7.2-7.4. To make the packing diagrams clearer different colours are used to depict the two independent molecules in the unit cell and also their symmetry related ones. It is evident that the molecules are arranged in a parallel-imbricated manner. Centro symmetrically related molecules are packed in ABAB..... form in XZ-plane while in XY-plane the packing is AABBAABB... type. The molecular packing in BPPCC, thus, corresponds to that observed in the crystalline state of many nematogens [24,25]. On heating the molecules can easily undergo a transition to the nematic state, which is characterized by an orientational ordering but having no positional correlation. The transition may thus be of displacive type [6,26,27], possibly accompanied by rotation only about the molecular long axis. Since both 2CB and BPPCC molecules undergo diaplacive type of transition at $T_{Cr\text{-}N}$, their mixtures are also expected to behave similarly and thus gives rise to nematic phase at around the same melting point.

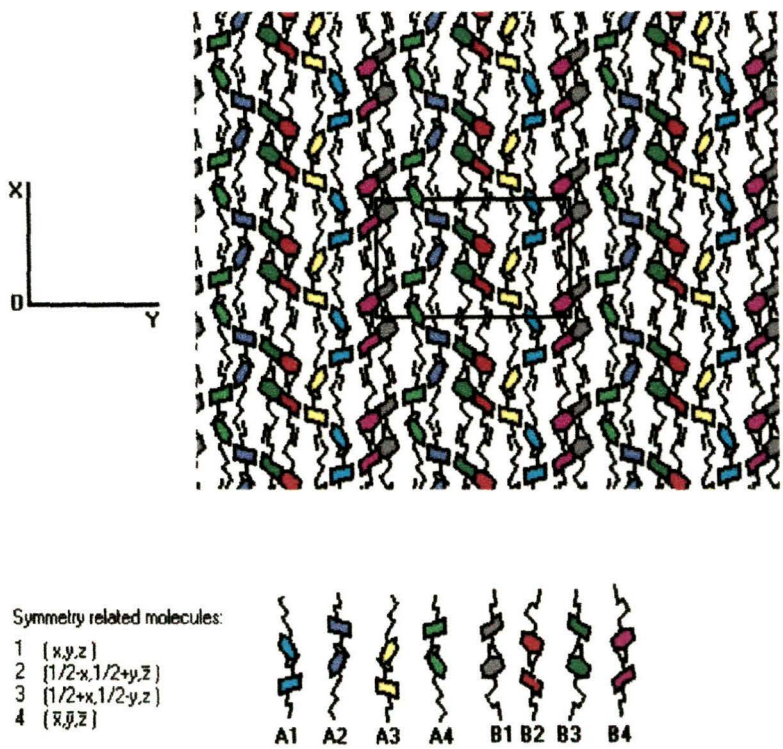

Figure 7.2: The view of molecular packing of BPPCC projected on XY plane.

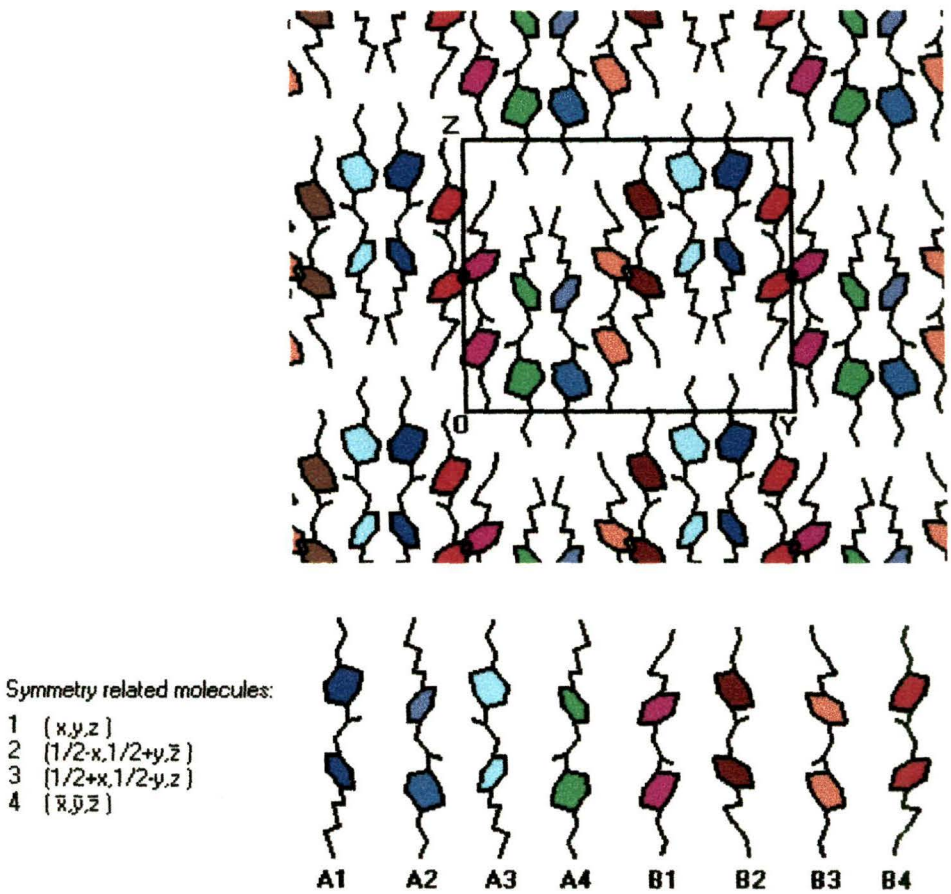

Figure 7.3: The view of molecular packing of BPPCC on YZ plane.

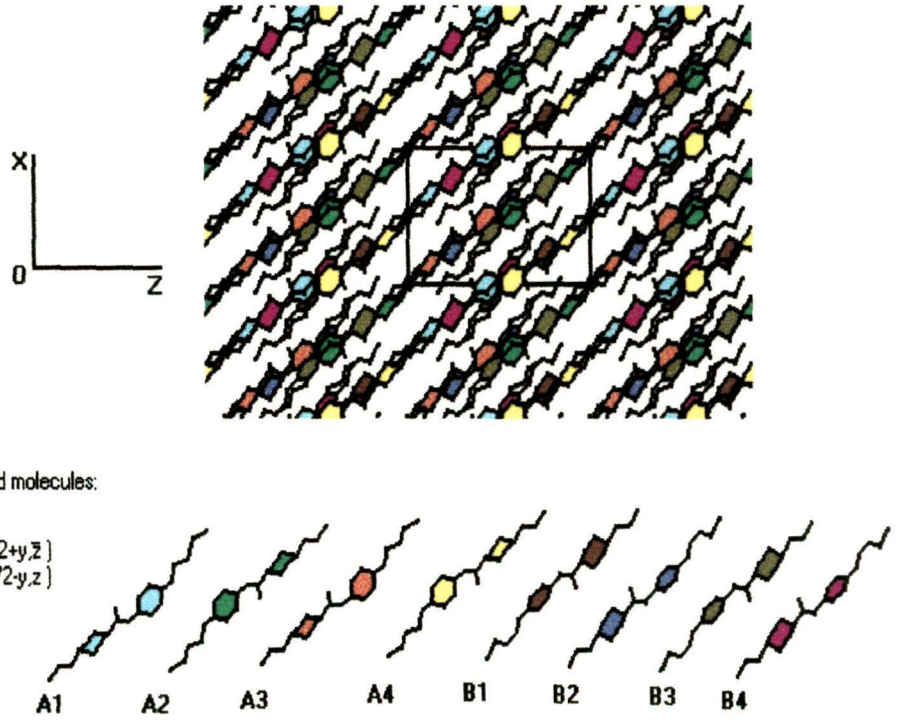

Figure 7.4: The view of molecular packing of BPPCC projected on XZ plane.

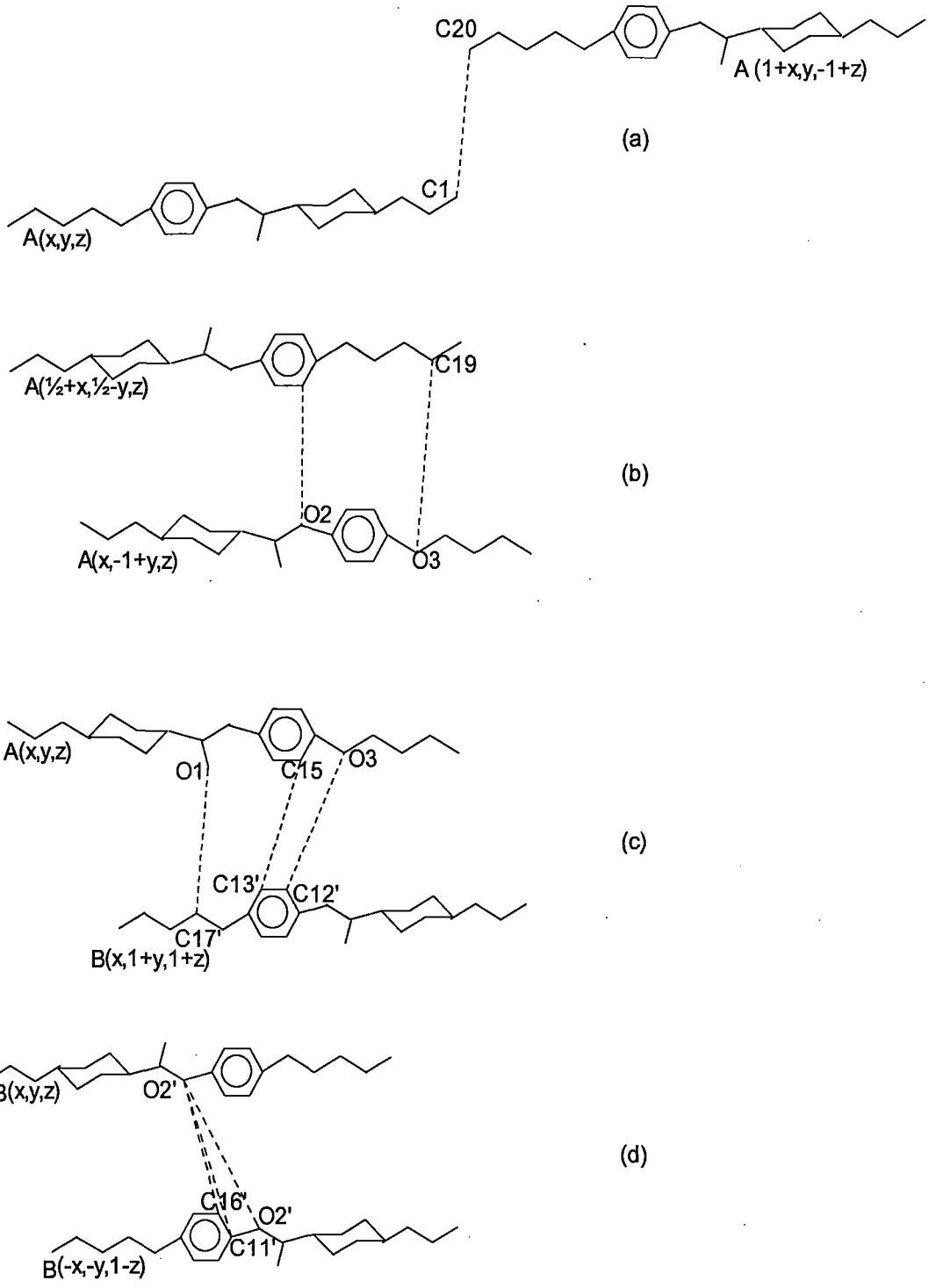

Figure 7.5: Models of various types of associations of molecules A and B. Intermolecular inter-atomic distances smaller than 3.7Å are indicated by dashed lines: (a) between A(x,y,z) and A(1+x,y,-1+z); (b) between A(½+x,½-y,z) and A(x,-1+y,z); (c) between A(x,y,z) and B(x,1+y,1+z); (d) between B(x,y,z) and B(-x,-y,1-z).

To have an idea about the nature of molecular associations we have calculated the distance between the non-hydrogen atoms of all the neighbouring molecules. Some intermolecular C-C or C-O distances are observed to be less than the sum of their van der Waals' radii. This type of intermolecular short contact distances are often found in mesogenic compounds [11,18,26,28-32]. All such contact distances less than 3.7 Å in BPPCC are listed in Table VIII, These suggest two types of AA molecular associations due to weak van der Waals interactions. In one such case, there is no molecular overlap at all and the length of the associated molecules is found to be 39.54 Å. In the other case, the overlap is from cyclohexyl to phenyl groups, the associated length being 23.08 Å. AB type of molecular association is also observed with similar overlap and the length of this pair is found to be 23.89 Å. Only one type of BB molecular association is observed, the length of the pair is 21.02 Å and so almost complete overlapping of the molecules is necessary. Individual lengths of the molecules A and B and lengths of various associated pairs are given in Table 7.9. Models of these molecular associations are shown in Figure 7.5. It was mentioned in chapter 5 that the apparent molecular length of BPPCC in the nematic phase increases from 20.70 Å to 21.33 Å over the temperature range of 43.0°C to 72.6°C, the mean length being 20.87 Å [1]. Since this mean length was 1.09 times the model length presence of some kind of bimolecular association was, therefore, assumed. The length of BB type pair almost corresponds to the mean length in the nematic phase. It is also noted that slight increase of overlapping in AA (second type) and AB pairs on heating may also result in similar length. Thus it may be inferred that as a result of van der Waals' interactions bimolecular associations exist in crystalline state as well as in nematic phase and play a dominant role in the mesophase stability.

TABLE 7.2

Final fractional co-ordinates and B_{iso} of the non-hydrogen atoms (E.S.D's.are in the parentheses and refer to the last digit)

Molecule	Atom	x	y	z	B_{iso}
A	C1	0.8574(17)	0.8098(11)	0.8697(10)	20.5(15)
	C2	0.7623(21)	0.8239(12)	0.9232(10)	23.1(18)
	C3	0.7825(14)	0.8001(9)	0.9897(8)	15.6(11)
	C4	0.6844(11)	0.8087(6)	1.0409(6)	10.4(8)
	C5	0.6603(16)	0.8722(8)	1.0635(9)	16.1(12)
	C6	0.5695(22)	0.8712(8)	1.1240(11)	21.4(17)
	C7	0.6046(10)	0.8297(5)	1.1889(6)	8.9(6)
	C8	0.6262(13)	0.7676(6)	1.1701(7)	12.2(9)
	C9	0.7271(14)	0.7655(7)	1.1120(8)	14.6(11)
	C10	0.5173(8)	0.8306(5)	1.2451(6)	8.4(6)
	C11	0.4834(7)	0.8047(4)	1.3681(5)	5.7(4)
	C12	0.3813(8)	0.7672(4)	1.3656(5)	6.5(5)
	C13	0.3199(7)	0.7722(4)	1.4269(4)	5.6(4)
	C14	0.3615(6)	0.8116(4)	1.4851(4)	4.5(4)
	C15	0.4686(7)	0.8474(4)	1.4884(5)	5.7(4)
	C16	0.5302(7)	0.8447(4)	1.4275(5)	5.6(4)
	C17	0.1997(8)	0.7885(4)	1.5522(5)	6.9(5)
	C18	0.1702(12)	0.8069(6)	1.6308(7)	11.6(9)
	C19	0.0785(13)	0.7665(7)	1.6525(8)	12.9(9)
	C20	0.0493(13)	0.7870(8)	1.7333(7)	14.1(10)
	O1	0.4308(7)	0.8660(4)	1.2354(4)	12.5(5)
	O2	0.5496(5)	0.7955(3)	1.3057(3)	7.5(3)
	O3	0.3115(5)	0.8212(3)	1.5510(3)	6.6(3)
B	C1'	-0.2518(17)	0.0576(11)	0.9937(11)	20.2(15)
	C2'	-0.1469(14)	0.0684(8)	0.9456(8)	14.9(11)
	C3'	-0.1748(14)	0.0427(12)	0.8700(9)	20.1(16)
	C4'	-0.0651(10)	0.0510(7)	0.8270(6)	12.1(8)
	C5'	0.0000(11)	-0.0081(9)	0.8103(8)	14.5(11)
	C6'	0.0889(11)	0.0023(6)	0.7506(8)	11.3(8)
	C7'	0.0302(7)	0.0402(4)	0.6853(5)	6.0(4)
	C8'	-0.0352(10)	0.0991(5)	0.6981(8)	10.7(8)
	C9'	-0.1239(11)	0.0865(6)	0.7579(8)	11.7(9)
	C10'	0.1222(8)	0.0568(5)	0.6348(5)	7.4(5)
	C11'	0.1699(7)	0.0366(4)	0.5120(5)	6.0(4)
	C12'	0.2477(8)	-0.0106(4)	0.5016(5)	6.0(5)
	C13'	0.3131(7)	0.0005(4)	0.4407(5)	6.1(5)
	C14'	0.2965(7)	0.0547(4)	0.3974(5)	5.7(4)
	C15'	0.2132(8)	0.1030(4)	0.4062(5)	6.5(5)
	C16'	0.1492(7)	0.0910(5)	0.4673(5)	6.5(5)
	C17'	0.4513(10)	0.0198(7)	0.3248(7)	11.7(9)
	C18'	0.5283(15)	0.0459(10)	0.2730(10)	18.2(14)
	C19'	0.482 (3)	0.0776(16)	0.2160(16)	31.8(28)
	C20'	0.5882(16)	0.0934(10)	0.1605(10)	19.2(14)
	O1'	0.2109(6)	0.0879(5)	0.6523(4)	12.6(5)
	O2'	0.0922(5)	0.0288(3)	0.5681(3)	7.7(3)
	O3'	0.3618(5)	0.0677(3)	0.3377(4)	7.8(3)

B_{iso} is the mean of the principal axes of the thermal ellipsoid.

TABLE 7.3

Anisotropic thermal parameters of non-hydrogen atoms (values multiplied by 100); E.S.D.'s in the parentheses. The temperature factor is of the form: $Exp[-2\pi^2(u_{11}h^2a^{*2} + u_{22}k^2b^{*2} + u_{33}l^2c^{*2} + 2u_{12}hka^*b^* + 2u_{13}hla^*c^* + 2u_{23}klb^*c^*)]$

Molecule	Atom	u_{11}	u_{22}	u_{33}	u_{12}	u_{13}	u_{23}
A	C1	26.1(19)	38.0(27)	18.7(16)	-7.9(19)	17.4(15)	-7.9(17)
	C2	38.1(28)	37.6(28)	17.1(16)	9.4(23)	19.1(19)	4.7(17)
	C3	21.3(15)	27.2(19)	13.8(11)	-3.6(14)	12.0(11)	-0.5(12)
	C4	16.6(11)	14.7(11)	10.3(9)	-0.2(9)	7.6(8)	-2.6(8)
	C5	27.0(19)	22.9(18)	14.1(13)	0.4(15)	11.0(13)	4.9(12)
	C6	49.6(32)	15.1(14)	23.5(19)	14.9(18)	25.7(22)	8.5(13)
	C7	15.5(10)	9.4(8)	9.8(8)	3.8(7)	5.1(7)	1.5(6)
	C8	22.1(14)	12.6(11)	14.2(10)	-0.8(10)	10.4(10)	0.7(9)
	C9	22.8(15)	16.5(13)	20.7(14)	4.6(12)	15.9(13)	1.5(11)
	C10	9.0(7)	13.2(9)	10.7(8)	2.9(7)	4.0(6)	1.9(7)
	C11	5.4(5)	9.3(7)	8.1(6)	1.8(5)	4.1(4)	2.4(5)
	C12	8.2(6)	8.7(7)	8.2(6)	-1.3(5)	2.1(5)	-2.3(5)
	C13	7.8(6)	7.3(6)	6.6(5)	-2.7(5)	2.2(4)	-2.3(5)
	C14	5.2(5)	5.8(5)	6.2(5)	0.4(4)	1.6(4)	-0.0(4)
	C15	6.2(5)	7.0(6)	8.5(6)	-0.4(5)	1.8(5)	-1.4(5)
	C16	5.6(5)	7.2(6)	7.8(6)	-0.0(4)	-0.3(4)	-1.0(5)
	C17	10.7(7)	7.3(7)	10.0(7)	-0.6(5)	6.5(6)	0.2(6)
	C18	19.7(13)	12.7(10)	15.2(11)	-3.5(9)	12.4(10)	-2.4(8)
	C19	20.6(14)	15.8(12)	15.4(11)	-2.9(11)	10.4(10)	-3.0(10)
	C20	20.8(14)	3.9(17)	11.2(10)	-0.1(13)	8.9(10)	-3.4(11)
	O1	16.8(7)	21.0(9)	11.3(6)	9.9(7)	6.3(5)	5.4(6)
	O2	8.7(4)	11.7(5)	8.8(4)	3.1(4)	3.3(3)	3.1(4)
	O3	6.9(4)	9.7(5)	8.8(4)	-0.8(3)	2.5(3)	-1.9(3)
B	C1'	24.9(17)	38.9(27)	17.2(14)	7.5(19)	15.4(14)	9.6(17)
	C2'	22.3(15)	21.9(16)	15.6(13)	2.5(13)	11.6(12)	3.4(12)
	C3'	16.4(14)	48.9(32)	13.2(13)	-7.6(18)	8.5(11)	-1.4(17)
	C4'	12.5(9)	27.2(16)	7.8(8)	-9.8(10)	6.1(7)	-5.1(9)
	C5'	11.9(10)	28.9(19)	16.3(13)	2.1(11)	7.3(9)	8.3(13)
	C6'	12.0(9)	16.0(12)	16.3(12)	2.5(8)	6.0(8)	6.6(10)
	C7'	7.3(6)	8.8(7)	7.3(6)	-2.7(5)	2.4(5)	-3.0(5)
	C8'	13.1(9)	10.4(9)	20.1(13)	2.9(7)	10.5(9)	4.5(9)
	C9'	15.5(11)	11.8(10)	20.8(14)	-0.1(8)	13.3(10)	-0.6(9)
	C10'	8.1(6)	13.1(9)	7.4(6)	-4.0(6)	2.9(5)	-3.2(6)
	C11'	6.5(5)	9.2(7)	6.8(6)	-3.6(5)	0.0(4)	-0.9(5)
	C12'	7.1(6)	7.5(6)	8.2(6)	-0.3(5)	1.6(5)	-1.2(5)
	C13'	7.3(6)	6.8(6)	9.5(7)	-0.3(5)	2.2(5)	-0.2(5)
	C14'	7.0(5)	7.0(6)	7.5(6)	-3.0(5)	1.1(4)	-2.0(5)
	C15'	8.6(6)	5.6(6)	10.4(7)	-0.1(5)	1.9(5)	-0.4(5)
	C16'	4.1(5)	10.5(8)	10.1(7)	0.6(5)	0.9(4)	-3.0(6)
	C17'	10.9(9)	23.9(15)	10.9(9)	2.0(9)	5.4(7)	0.9(9)
	C18'	21.2(16)	29.7(22)	22.2(18)	5.3(16)	14.5(14)	9.6(16)
	C19'	39.2(34)	49.6(44)	30.7(32)	-4.8(33)	2.6(26)	21.8(32)
	C20'	26.1(19)	31.9(23)	19.6(16)	5.1(17)	17.2(15)	11.8(16)
	O1'	11.9(6)	25.9(10)	11.0(6)	-13.0(6)	4.9(4)	-8.2(6)
	O2'	7.1(4)	13.9(6)	9.0(4)	-5.2(4)	3.8(3)	-3.4(4)
	O3'	10.4(5)	10.3(5)	9.6(5)	-1.7(4)	3.3(4)	-0.2(4)

TABLE 7.4

Bond distances of the non-hydrogen atoms(Å) with E.S.D.'s in parentheses

Molecule A		Molecule B	
C(1) – C(2)	1.573(19)	C(1') – C(2')	1.587(18)
C(2) – C(3)	1.252(23)	C(2') – C(3')	1.414(23)
C(3) – C(4)	1.556(15)	C(3') – C(4')	1.569(15)
C(4) – C(5)	1.390(21)	C(4') – C(5')	1.463(22)
C(4) – C(9)	1.535(19)	C(4') – C(9')	1.466(20)
C(5) – C(6)	1.604(19)	C(5') – C(6')	1.590(16)
C(6) – C(7)	1.419(19)	C(6') – C(7')	1.443(15)
C(7) – C(8)	1.336(16)	C(7') – C(8')	1.441(14)
C(7) – C(10)	1.515(13)	C(7') – C(10')	1.520(11)
C(8) – C(9)	1.660(15)	C(8') – C(9')	1.597(14)
C(10) – O(1)	1.198(12)	C(10') – O(1')	1.174(10)
C(10) – O(2)	1.281(12)	C(10') – O(2')	1.296(10)
C(11) – C(12)	1.372(11)	C(11') – C(12')	1.332(12)
C(11) – C(16)	1.355(12)	C(11') – C(16')	1.353(13)
C(11) – O(2)	1.447(9)	C(11') – O(2')	1.441(10)
C(12) – C(13)	1.387(11)	C(12') – C(13')	1.423(12)
C(13) – C(14)	1.320(10)	C(13') – C(14')	1.333(12)
C(14) – C(15)	1.399(10)	C(14') – C(15')	1.384(12)
C(14) – O(3)	1.393(9)	C(14') – O(3')	1.412(10)
C(15) – C(16)	1.380(12)	C(15') – C(16')	1.419(13)
C(17) – C(18)	1.527(13)	C(17') – O(3')	1.447(14)
C(18) – C(19)	1.423(16)	C(17') – C(18')	1.466(17)
C(17) – O(3)	1.426(10)	C(18') – C(19')	1.230(3)
C(19) – C(20)	1.575(16)	C(19') – C(20')	1.710(3)

TABLE 7.5

Bond angles of the non-hydrogen atoms (°) with E.S.D.'s in parentheses

Molecule A		Molecule B	
C(1)–C(2)–C(3)	117.6(19)	C(1')–C(2')–C(3')	113.1(15)
C(2)–C(3)–C(4)	118.2(16)	C(2')–C(3')–C(4')	110.8(12)
C(3)–C(4)–C(5)	117.7(11)	C(3')–C(4')–C(5')	118.3(13)
C(3)–C(4)–C(9)	105.0(11)	C(3')–C(4')–C(9')	100.2(11)
C(5)–C(4)–C(9)	110.2(10)	C(5')–C(4')–C(9')	113.8(9)
C(4)–C(5)–C(6)	111.0(12)	C(4')–C(5')–C(6')	114.9(11)
C(5)–C(6)–C(7)	115.2(14)	C(5')–C(6')–C(7')	110.3(9)
C(6)–C(7)–C(8)	113.4(11)	C(6')–C(7')–C(8')	119.4(9)
C(6)–C(7)–C(10)	113.7(10)	C(6')–C(7')–C(10')	108.9(8)
C(8)–C(7)–C(10)	109.9(9)	C(8')–C(7')–C(10')	109.2(8)
C(7)–C(8)–C(9)	110.6(10)	C(7')–C(8')–C(9')	111.5(8)
C(4)–C(9)–C(8)	109.9(10)	C(4')–C(9')–C(8')	112.7(9)
C(7)–C(10)–O(1)	121.2(9)	C(7')–C(10')–O(1')	126.9(8)
C(7)–C(10)–O(2)	114.8(8)	C(7')–C(10')–O(2')	110.0(7)
O(1)–C(10)–O(2)	123.7(8)	O(1')–C(10')–O(2')	123.0(8)
C(12)–C(11)–C(16)	124.3(7)	C(12')–C(11')–C(16')	123.8(8)
C(12)–C(11)–O(2)	116.5(8)	C(12')–C(11')–O(2')	120.6(8)
C(16)–C(11)–O(2)	118.9(7)	C(16')–C(11')–O(2')	115.3(8)
C(11)–C(12)–C(13)	117.8(7)	C(11')–C(12')–C(13')	115.5(8)
C(12)–C(13)–C(14)	119.6(7)	C(12')–C(13')–C(14')	121.7(8)
C(13)–C(14)–C(15)	122.0(7)	C(13')–C(14')–C(15')	123.2(8)
C(13)–C(14)–O(3)	126.4(6)	C(13')–C(14')–O(3')	123.0(8)
C(15)–C(14)–O(3)	111.5(6)	C(15')–C(14')–O(3')	113.8(8)
C(14)–C(15)–C(16)	119.7(7)	C(14')–C(15')–C(16')	114.2(8)
C(11)–C(16)–C(15)	116.5(7)	C(11')–C(16')–C(15')	121.6(7)
C(18)–C(17)–O(3)	103.6(8)	C(18')–C(17')–O(3')	111.1(12)
C(17)–C(18)–C(19)	112.9(10)	C(17')–C(18')–C(19')	119.1(18)
C(18)–C(19)–C(20)	111.7(11)	C(18')–C(19')–C(20')	109.1(21)
C(10)–O(2)–C(11)	117.1(6)	C(10')–O(2')–C(11')	118.9(6)
C(14)–O(3)–C(17)	115.9(6)	C(14')–O(3')–C(17')	117.4(7)

TABLE 7.6

Planes associated with different fragments of molecules A and B.

Plane No.	Molecule fragment	Equation of the plane	R.M.S. displacement of atoms from plane (Å)
Molecule A			
1.	Phenyl ring (C11 to C16)	5.26(3)X+15.41(5)Y-6.38(6)Z=1.12(11)	0.01
2.	Alkoxy chain (O3 to C20)	5.36(5)X+16.37(12)Y-4.56(12)Z=4.7(3)	0.08
3.	Carboxylic group (C10,O1,2)	5.60(18)X+15.30(8)Y+5.9(3)Z=22.9(3)	0.00
4.	Cyclohexyl group (C4 to C9)	9.04(4)X+7.27(14)Y+5.70(8)Z=18.17(11)	0.23
5.	Alkyl chain (C1 to C3)	5.0(3)X+16.8(4)Y+4.50(25)Z=21.82(12)	0.00
Molecule B			
6.	Phenyl ring (C11' to C16')	6.83(3)X+9.70(7)Y+9.09(6)Z=1.16(19)	0.01
7.	Alkoxy chain (O3' to C20')	6.14(6)X+10.84(21)Y+9.46(9)Z=6.15(3)	0.15
8.	Carboxylic group (C10',O1',2')	4.91(18)X+16.75(8)Y-4.8(3)Z=2.72(14)	0.00
9.	Cyclohexyl group (C4' to C9')	7.11(4)X+12.81(9)Y+5.81(9)Z=4.82(6)	0.20
10.	Alkyl chain (C1' to C3')	3.9(3)X+17.8(3)Y-4.6(3)Z=2.55(25)	0.00

TABLE 7.7

Dihedral angles (°) between various planes

Planes	Angles	Planes	Angles	Planes	Angles	Planes	Angles	Planes	Angles
1 2	6.5	2 3	77.3	3 5	7.2	4 8	103.0	6 8	95.6
1 3	81.7	2 4	105.1	3 6	20.8	4 9	18.6	6 9	13.8
1 4	108.6	2 5	70.4	3 7	17.9	4 10	97.1	6 10	90.1
1 5	74.6	2 6	97.2	3 8	75.5	5 6	28.0	7 8	91.7
1 6	102.0	2 7	93.2	3 9	10.5	5 7	25.1	7 9	13.4
1 7	98.2	2 8	2.6	3 10	69.8	5 8	68.6	7 10	86.3
1 8	6.8	2 9	87.1	4 5	35.2	5 9	16.8	8 9	85.2
1 9	91.2	2 10	8.4	4 6	16.1	5 10	63.0	8 10	6.0
1 10	11.9	3 4	29.1	4 7	20.5	6 7	4.8	9 10	79.4

TABLE 7.8

Intermolecular Distances Shorter than 3.7Å

A(x, y, z) — A(1+x, y, -1+z)

C1 — C20 3.538 Å

A(½ + x, ½ - y, z) — A(x, -1+y, z)

C13 — O2 3.655 Å
C19 — O3 3.669 Å

A(x, y, z) — B(x, 1+y, 1+z)

O3 — C12' 3.564 Å
O1 — C17' 3.487 Å
C15 — C13' 3.591 Å

B(x, y, z) — B(-x, -y, 1-z)

O2' — C11' 3.310 Å
O2' — C16' 3.616 Å
O2' — O2' 3.105 Å

TABLE 7.9

Lengths of the molecules A, B and their associations

Molecule / Associated Molecules (with symmetry)	From atom	To atom	Length* in Å
A(x, y, z)	C1	C20	19.09
B(x, y, z)	C1'	C20'	18.85
A(x, y, z) and A(1+x, y, -1+z)	C1	C20	39.54
A(½ + x, ½ - y, z) and A(x, -1+ y, z)	C1	C20	23.08
A(x, y, z) and B(x, 1+y, 1+z)	C1	C1'	23.90
B(x, y, z) and B(-x, -y, 1-z)	C1'	C1'	21.02

* The model length of BPPCC molecule is 19.15 Å.

REFERENCES

1. N. K. Pradhan, *Ph.D. Thesis*, University of North Bengal (1998).
2. N.K. Pradhan and R. Paul, *Mol. Cryst. Liq. Cryst.*, **366**, 157 (2001).
2. P. S. White, PC version of NRCVAX (1988), University of New Brunswick, Canada.
4. W. Haase, H. Paulus and H.T.Müller, *Mol. Cryst. Liq. Cryst.*, **97**, 131(1983).
5. P. Zugenmaier, *Liq. Cryst.*, **29**, 613 (2002).
6. P. Mandal, S. Paul, K. Goubitz and H. Schenk, *Mol. Cryst. Liq. Cryst.*, **258**, 209 (1995).
6. International tables for X-ray crystallography, Vol. III, Kynoch Press, Birmingham, (1962).
8. S. Gupta, R.A. Palmer, M. Schadt and S.P. Sengupta, *Liq. Cryst.*, **28**, 1309 (2001).
9. S. Gupta, A. Nath, S. Paul, H. Schenk and K. Goubitz, *Mol. Cryst. Liq. Cryst.*, **257**, 1 (1994).
10. A. Nath, S. Gupta, P. Mandal, S. Paul and H. Schenk, *Liq. Crystals*, **20**, 765 (1996) and references therein.
11. S. Gupta, P.Mandal, S. Paul, M. de Wit, K.Goubitz and H. Schenk, *Mol. Cryst .Liq. Cryst.*, **195**, 149 (1991) and references therein.
12. W. Haase and H. Paulus, , *Mol. Cryst. Liq. Cryst.*, **100**, 111 (1983).
13. U. Baumeister, H. Hartung and M. Jaskolski, *Mol. Cryst. Liq. Cryst.*, **88**, 167 (1982) and references therein.
14. P. Mandal, S.Paul, H. Schenk and K. Goubitz, *Mol. Cryst. Liq. Cryst.*, **135**, 35 (1986).
15. U. Baumeister, H. Hartung, M. Gdaniec and M. Jaskolski, *Mol. Cryst. Liq.Cryst.*, **69**,119(1981).
16. W. B. Schweizer and J. D. Dunitz, Abst.04-1-04, 12th International Congress of Crystallog., Ottawa, (1981).
17. S. Bhattacharjee and G. A. Jeffrey, *Mol. Cryst. Liq. Cryst.*, **101**, 247 (1983).
18. P. Mandal, S.Paul, C. H. Stam and H. Schenk, *Mol. Cryst. Liq. Cryst.*, **180B**, 369 (1990).
19. P. Zugenmaier, and A. Heiske, *Liq. Crystals*, **15**, 835 (1993).
20. G. V. Vani and K. Vijayan, *Mol. Cryst. Liq. Cryst.*, **51**, 253 (1979).
21. J. Doucet, J. P. Mornon, R. Chevallier and A. Lifchitz, *Acta Cryst.*, **B33**, 1701 (1977).
22. M. Cotrait, C. Destrade and H. Gasparaux, *Acta Cryst.*, **B31**, 2704 (1975).
23. S. Gupta, K. Bhattacharyya, S.P. Sengupta, S. Paul, A. Kalman and L. Parkanyl, *Acta Cryst.*, **C55**, 403 (1999).
24. R.F. Bryan, Proc. Pre-Congress Symp. on Organic Crystal Chemistry, Poznan, Poland (1979) and references therein.
25. W. Haase and M.A. Athanassopoulou in *Liquid Crystals*, D.M.P. Mingos, Ed., Springer-Verlag, Vol. I, pp. 139-197 (1999).

26. P. Mandal and S. Paul, *Mol. Cryst. Liq. Cryst.*, **131**, 223 (1985).

27. R.F. Bryan and P.G. Forcier, *Mol. Cryst. Liq. Cryst.*, **60**, 133 (1980).

28. H. Allouchi, M. Cotrait, C. Canlet and J.P. Bayle, *Liq. Cryst.*, **28**, 1177 (2001).

29. M.A. Sridhar, N.K. Lokanath, J. Shashidhara Prasad, C.V. Yelammagad and S.K.Varshney, *Liq. Cryst.*, **28**, 45 (2001).

30. K. Hori, M. Kurosaki, H. Wu and K. Itoh, *Acta Cryst.*, **C52**, 1751 (1996).

31. P. Mandal, B. Majumdar, S. Paul, H. Schenk and K. Goubitz, *Mol. Cryst. Liq. Cryst.*, **168**, 135 (1989).

32. H. Paulus and W. Haase, *Mol. Cryst. Liq. Cryst.*, **92**(Letters), 237 (1983).

Chapter VIII

MINIMUM ENERGY CONFIGURATION OF PAIRS OF ETHYL, PENTYL AND HEPTYL MEMBERS OF 5-(trans-4-ALKYLCYCLOHEXYL)-2-(4-CYANOPHENYL) PYRIMIDINE

Part of this work has been published in *Mol. Cryst. Liq. Cryst.*, **365**, 535 (2001)

8.1 INTRODUCTION

Intermolecular interactions are extremely important to understand the mesogenic behaviour of liquid crystals. It is the anisotropy in molecular interactions that is responsible for the occurrence of the liquid crystalline phases. An atomic scale analysis of intra- and intermolecular forces acting on molecules in mesophases is extremely difficult because of the complicated averaging effects due to intra- and intermolecular motions. On the contrary, such an analysis seems quite possible in crystal structures of mesogenic compounds assuming the constituent molecules as rigid bodies and this analysis can be used as precursors of liquid crystal structures [1-9]. Based on interaction calculations classically used in conformational analysis, in this chapter attempt has been made to explore the nature of molecular interactions for ethyl, pentyl and heptyl members of a mesogenic homologous series 5-(trans-4-alkylcyclohexyl)-2-(4-cyanophenyl) pyrimidine [ECCPP, PCCPP and HCCPP respectively. in short]. The crystal structures of the compounds [10-12] were determined by co-workers by analyzing the X-ray intensity data obtained from single crystals using CAD4 diffractometer. In this laboratory several physical properties of the title compounds had also been determined by optical birefringence measurements and by X-ray scattering technique [13]. All the compounds exhibit nematic phase but HCCPP shows SmA phase as well. Thermal stability of the compounds is very large, so also the melting points as shown below. The interaction energy for a pair of molecules has been calculated for different configurations considering both van der Waals' and electrostatic interactions and the most favourable arrangement for the pair has been found by examining the minimum energy. Properties of these dimers have been compared with the previous results obtained from X-ray diffraction studies both in solid and mesomorphic phases.

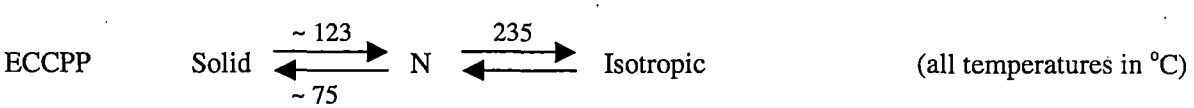

PCCPP Solid $\underset{\sim 68}{\overset{\sim 100}{\rightleftharpoons}}$ N $\overset{\sim 235}{\rightleftharpoons}$ Isotropic

HCCPP Solid $\underset{\sim 75}{\overset{\sim 82}{\rightleftharpoons}}$ Sm A $\overset{\sim 158}{\rightleftharpoons}$ N $\overset{\sim 223}{\rightleftharpoons}$ Isotropic

8.2 METHOD OF CALCULATION

The total interaction energy for a pair of molecules, whose centre of masses are separated by the distance R, is given by

$$U(R) = -\sum_{i,j} C_{ij}/r_{ij}^{6} + \sum_{i,j} A_{ij} \exp(-B_{ij} r_{ij}) + D \sum_{i,j} q_i q_j/(\varepsilon r_{ij})$$

where r_{ij} is the distance of the ith atom of the first molecule from the jth atom of the second molecule. The molecules are assumed to be rigid. A Buckingham type potential has been used for Van der Waals' interaction. The coefficients A, B and C are taken from Cotrait *et al.*[14]. Partial atomic charges are used to calculate electrostatic interactions. The constant D takes care of the unit used and the value of the dielectric permittivity is taken as 1. Partial atomic charges are calculated using MNDO method [15] in which interaction between the valence shell electrons of different atoms are considered explicitly whereas the inner shell electrons are considered as a frozen core. Interaction between electrons in different orbits of the same atom is considered to some extent. The geometry of the molecules, as obtained from crystal structure analysis[10-12] along with the atom numbering scheme are shown in Figure 8.1. For all the three compounds coordinates, both fractional and orthogonal, of the atoms along with the partial atomic charges are given in Tables 8.1 at the end of the chapter.

To facilitate the calculation of the interaction energy using the above expression a molecule-fixed orthogonal coordinate system is defined as follows. By taking the origin at the center of mass of the molecule, Z-axis is defined as the molecular long

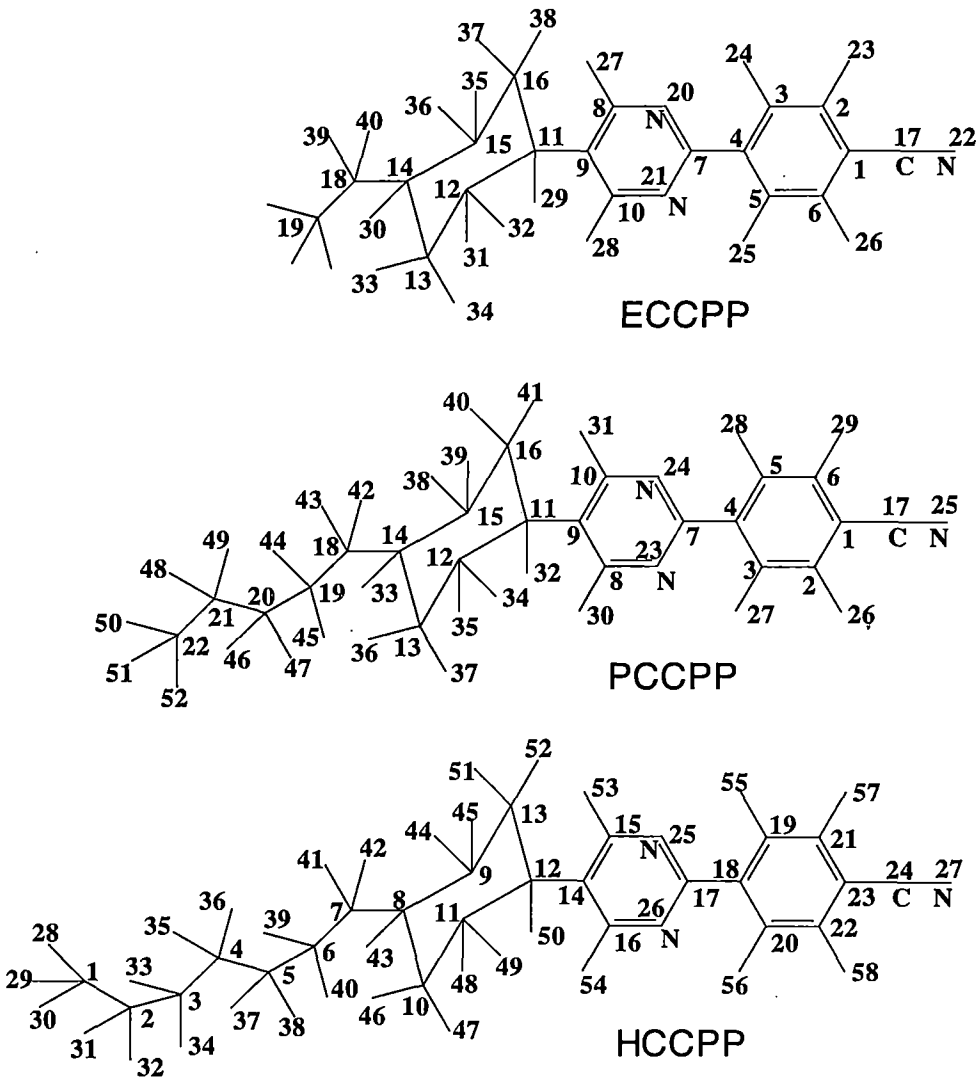

Figure 8.1 Molecular structures of ECCPP, PCCPP and HCCPP with atom numbering scheme.

axis along the least-squares fitted line through all the non-hydrogen atoms; Y-axis is chosen in such a manner so that YZ-plane is the plane of the of the molecule and X-axis is taken perpendicular to the plane of the molecule and considered as the stacking

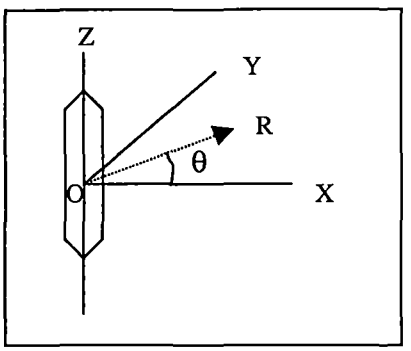

Figure 8.2 Molecule fixed coordinate system

direction. This is shown in Figure 8.2. The symbol R is used to denote the distance of center of mass of the second molecule from that of the first one in the XY-plane, θ being the angular separation of R from the X-axis. All the calculations are done on a Pentium PC, necessary codes are written in FORTRAN.

Energy minimization for a pair of molecules has been carried out by considering both the parallel (↑↑) and antiparallel (↑↓) combination of molecules. Since the molecules are flat, stacking and in-plane interaction energy has been minimized separately and then search has been made for the overall minimum energy configurations. Thus we first find the stacking energy by moving the second molecule along X-axis (so that R=X, θ=0) and for each value of X, relative molecular translation along Z-axis is considered. After finding the minimum energy position, full rotation of the second molecule along X-, Y- and Z-axis are also applied to see if there is any further reduction of stacking energy. Similarly by translating the second molecule along Y-axis (so that R=Y, θ=90°) the in-plane interaction energy is calculated as a function of Z. Rotations about the three axes are also applied subsequently to find the minimum in-plane interaction energy. A search is then made to find the overall minimum energy configuration by varying R in the whole θ range (0 to 360°) at

interval of 5°. As before possibility of translation along Z and rotation along the three axes were also explored in the above search. Resolution of the translational movement was 0.1 Å and it was 1° for the rotations.

8.3 RESULTS AND DISCUSSION

The variation of stacking energy as a function of translation along Z-axis for different stacking distances is shown in Figure 8.3 for ECCPP, Figure 8.4 for PCCPP and Figure 8.5 for HCCPP.

When two parallel (↑↑) ECCPP molecules, stacked one exactly above the other, are considered it is observed that for stacking distances below 4 Å the molecules repel each other; an attractive energy of -7.38 Kcal/mol is found at a stacking distance of 4.5 Å. Stacking energy thereafter increases with increasing distance. When translation of the second molecule relative to the first one along the molecular axis is considered in addition, it is observed that even at a stacking distance of 3.0 Å attractive interaction energy results in. Thus at R=3.0 Å and Z=12.2 Å observed value is -4.12 Kcal/mol. With increasing stacking distance the energy further decreases even at smaller Z-values. But when the stacking distance is increased beyond 3.9 Å, the interaction energy increases with or without translation along the Z-axis. The lowest stacking energy (-9.6 Kcal/mol) is achieved at a stacking distance of 3.9 Å and also translation of 3.9 Å. When interactions between different faces of the molecules were considered further reduction of energy was observed. Thus minimum stacking energy is found to be -12.55 Kcal/mol at R=3.9 Å, θ=180° and Z=-3.9 Å and R_Z=194° i.e. when the second molecule is rotated by 194° around the molecular axis.

Similarly, for antiparallel (↑↓) pair of ECCPP molecules, stacked one above the other, attractive energy of -9.71 Kcal/mol was found at a stacking distance of 4.2 Å, below which the molecules repel each other. Stacking energy varies in the same manner as in case of (↑↑) pair when translation along molecular axis is also considered. Minimum stacking energy is achieved (-11.07 Kcal/mol) in this case at R=4.2 Å and

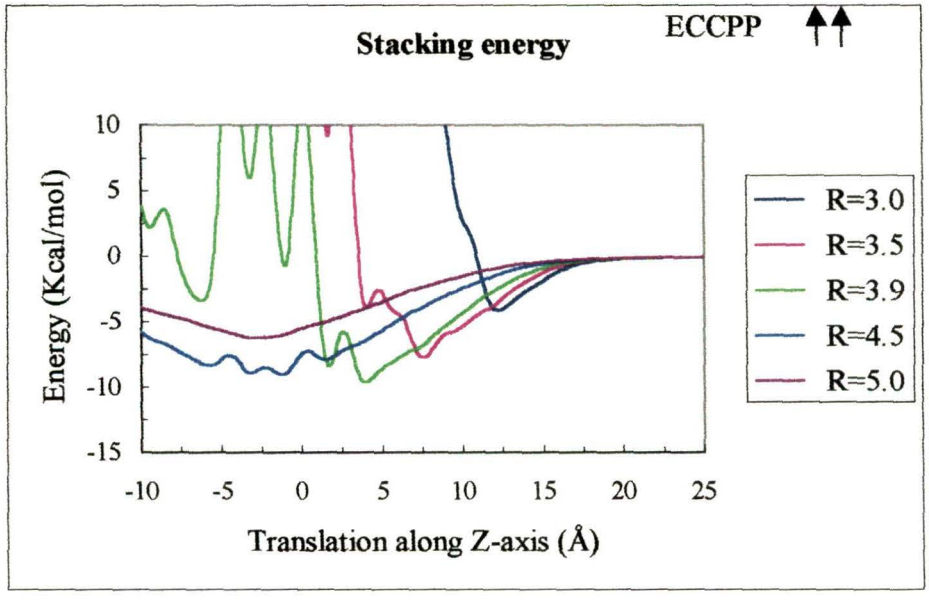

(a)

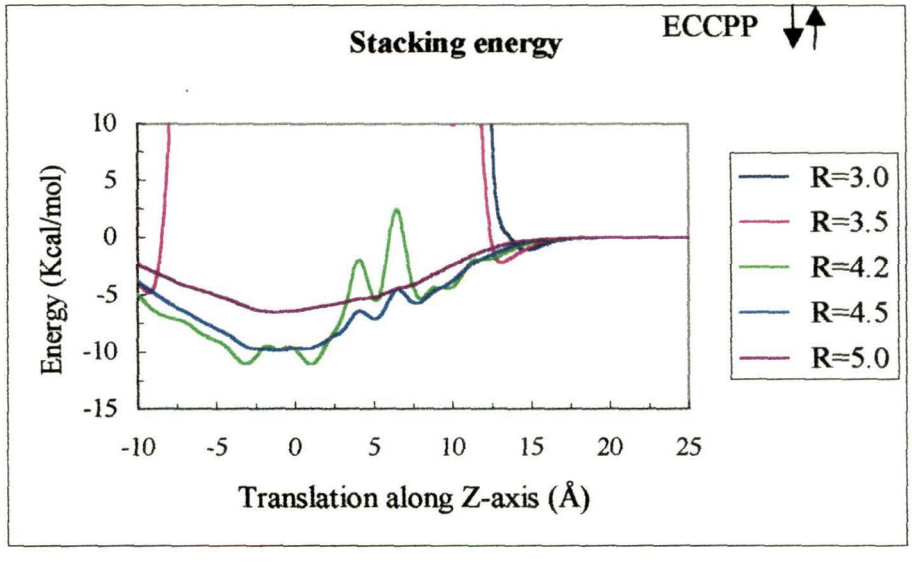

(b)

Figure 8.3 Stacking energy of ECCPP as a function of translation along Z-axis (a) for parallel (↑↑) and (b) for antiparallel (↑↓) pair of molecules.

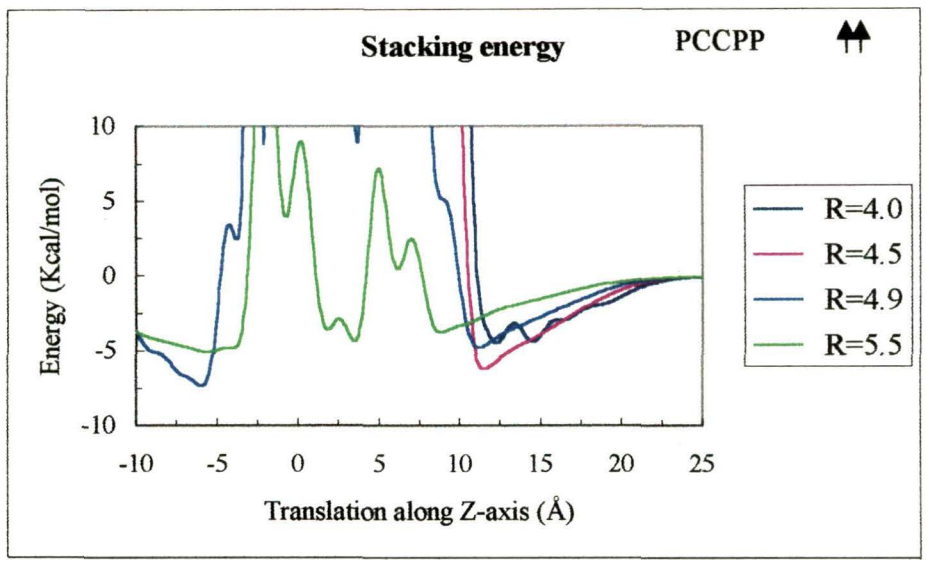

(a)

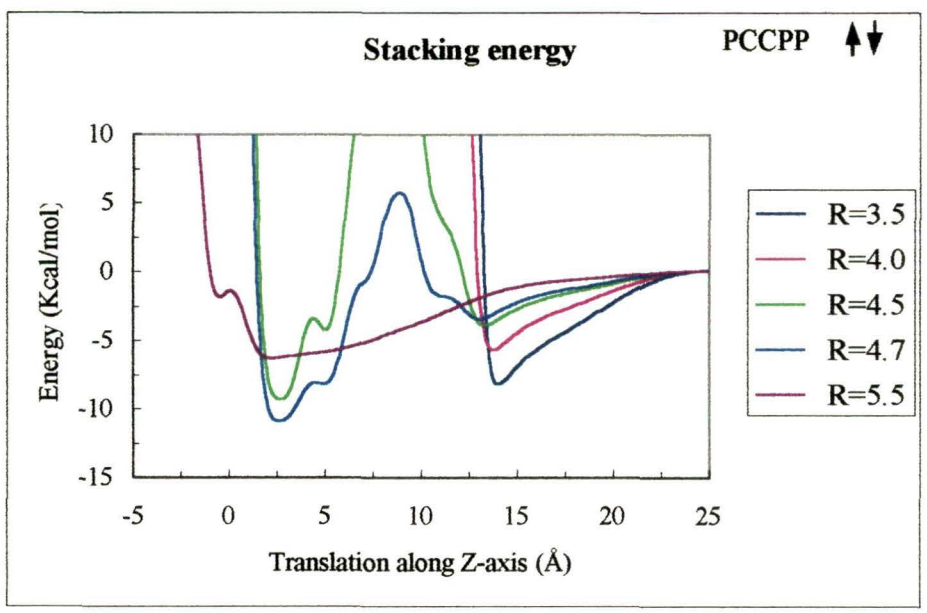

(b)

Figure 8.4 Stacking energy of PCCPP as a function of translation along Z-axis (a) for parallel (↑↑) and (b) for antiparallel (↑↓) pair of molecules.

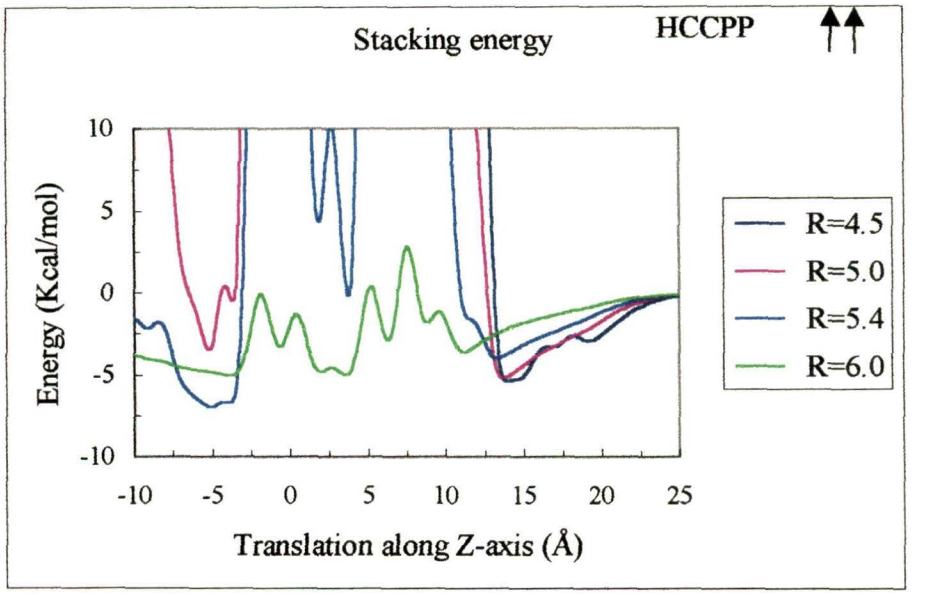

(a)

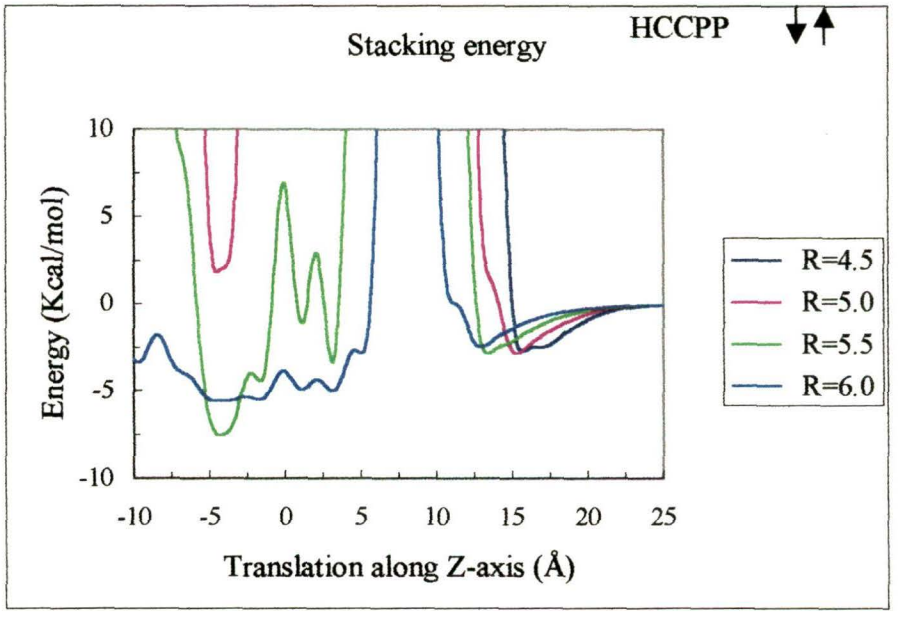

(b)

Figure 8.5 Stacking energy of HCCPP as a function of translation along Z-axis (a) for parallel (↑↑) and (b) for antiparallel (↑↓) pair of molecules.

Z=1.0 Å which further reduces to -12.89 Kcal/mol when rotations of 2° about Y and 26° about Z are applied.

In case of PCCPP and HCCPP molecules, for both the (↑↑) and (↑↓) combinations, attractive energy is observed only when the stacking distance is greater than 5.5 Å if no relative translation along the molecular axis is considered. However, for (↑↑) PCCPP molecules, at a relative translation of 12.0 Å the stacking energy becomes -4.5 Kcal/mol at R=4.0 Å. This reduces to -6.2 Kcal/mol at R=4.5 Å with at smaller translation (Z=11.5 Å). However, minimum stacking energy of -7.3 Kcal/mol is obtained at a distance 4.9 Å and at relative translation -6.0 Å. This becomes -8.88 Kcal/mol when –4° and 45° rotations are applied in addition about the X- and Z-axis. The (↑↓) pair of PCCPP shows similar type of variation of energy with relative translation along Z. The minimum stacking energy of -10.85 Kcal/mol is obtained at R=4.7 Å and Z=2.6 Å. Rotation of –15° thereafter along the molecular axis reduces the energy by 1 Kcal/mol.

In case of HCCPP molecules, for both the pairs, the variation of stacking energy with Z translation is similar to that of PCCPP molecules. For (↑↑) pair the stacking energy of -6.94 Kcal/mol is obtained at R=5.4 Å and Z=-5.1 Å. However, the minimum stacking energy is achieved at R=-5.5 Å and Z=4.0 Å which reduces to -8.65 Kcal/mol when rotation of –9° around Y-axis is applied. For (↑↓) pair, on the other hand, minimum stacking energy (-7.52 Kcal/mol) is observed at the same stacking distance but with Z=-4.3 Å. Rotation by –27° around Z-axis reduces the energy further to -9.08 Kcal/mol. The minimum energy values along with the van der Waals' and electrostatic components in different configurations are given in Table 8.2.

The in-plane interaction energy, for both the (↑↑) and (↑↓) pairs of ECCPP, is found to minimize at a lateral displacement of 5.8 Å but at relative translation of -3.3 Å for (↑↑) and -1.3 Å for the (↑↓) pairs, the energy values being -5.40 Kcal/mol and -6.01 Kcal/mol respectively. When rotations are applied these reduce respectively to -6.05 and -6.29 Kcal/mol. PCCPP molecules also found to have almost similar in-plane

interaction energy, -6.18 and -6.96 Kcal/mol for the (↑↑) and (↑↓) combinations. However; for HCCPP this interaction is found to be much stronger, energy values being -11.48 and -9.75 Kcal/mol respectively for the (↑↑) and (↑↓) combinations. The positions and orientations of the second molecule, at which the above minimum in-plane interaction energy values are observed, are given in Table 8.2.

We have also searched the overall minimum energy configurations of the pairs following a procedure as stated earlier. For the (↑↑) pair of ECCPP molecule the stacking energy minimum configuration is the configuration for overall minimum energy (-12.55 Kcal/mol). However, for the (↑↓) pair, the overall minimum energy (-13.41 Kcal/mol) is observed when the molecules are stacked at 4.06 Å along with lateral displacement of -1.09 Å and relative translation of -0.9 Å. Rotations Rx = -1, Ry = -1 and Rz =14° are also have to be applied to arrive at the above minimum. For the (↑↑) pair of PCCPP the overall minimum energy (-11.23 Kcal/mol) configuration is found at a stacking distance 4.83 Å, lateral displacement 1.29 Å along with Z=3.9 Å, Ry = -10 and Rz = -7. The (↑↓) pair, however, have slightly lower energy (-12.85 Kcal/mol) being stacked at -4.44 Å with lateral shift of 1.19 Å, Z=2.5 Å, Rx = -7, Ry = -1 and Rz = -31°. On the other hand, for the (↑↑) HCCPP pair, the overall minimum energy (-14.56 Kcal/mol) is achieved at a small stacking distance of 1.11 Å but with large lateral displacement of -4.15 Å. Relative translation along molecular axis in this case is 1.1 Å and rotations Rx = -4, Ry = -1 and Rz = -1° are applied. But for the (↑↓) combination the overall minimum energy (-11.94 Kcal/mol) is found when the second molecule is stacked at a distance -4.16Å with lateral displacement 2.4Å, Z=1.8 Å and Rz = -3°. For each compound it is observed that in all cases (stacking, in-plane and overall minimum) main contribution to the total interaction energy comes from Van der Waals' interaction, the contribution of the electrostatic interaction in no case is greater than 4%.

The most favourable arrangement of the dimers corresponding to the overall minimum interaction energy is shown in Figures 8.6 and are used to compare with the

TABLE 8.2
Interaction energy values (Kcal/mol)

Compound	Vdw	Elec	Total
ECCPP (↑↑)			
Stacking(R=3.9,θ=180,Z=-3.9,Rz=-166)	-12.67	0.12	-12.55
In-plane(R=5.8,θ=90,Z=-3.3,Rx=4,Ry=1,Rz=-1)	-5.88	-0.17	-6.05
Overall(R=3.9,θ=180,Z=-3.9,Rz=-166)	-12.67	0.12	-12.55
ECCPP (↑↓)			
Stacking(R=4.2,θ=0,Z=1,Ry=-2,Rz=26)	-12.67	-0.22	-12.89
In-plane (R=5.8,θ=90,Z=-1.3,Ry=6)	-5.96	-0.32	-6.29
Overall(R=4.2,θ=345,Z=-0.9,Rx=-1,Ry=-1,Rz=14)	-13.11	-0.30	-13.41
PCCPP (↑↑)			
Stacking (R=4.9,θ=0,Z=-6.0,Rx=-4,Rz=45)	-9.06	0.18	-8.88
In-plane (R=5.6,θ=90,Z=-5.6,Ry=-1,Rz=-27)	-6.18	0.00	-6.18
Overall (R=5.0,θ=15,Z=3.9,Ry=-10,Rz=-7)	-11.19	-0.04	-11.23
PCCPP (↑↓)			
Stacking (R=4.7,θ=0,Z=2.6,Rz=-15)	-11.53	-0.32	-11.85
In-plane (R=5.5,θ=90,Z=5.4,Ry=3)	-6.82	-0.14	-6.96
Overall (R=4.6,θ=165,Z=2.5,Rx=-7,Ry=-1,Rz=-31)	-12.54	-0.31	-12.85
HCCPP (↑↑)			
Stacking (R=5.5,θ=180,Z=4.0,Ry=-9)	-8.34	-0.31	-8.65
In-plane (R=4.7,θ=90,Z=-2.4,Rz=-7)	-11.21	-0.27	-11.48
Overall (R=4.3,θ=285,Z=1.1,Rx=-4,Ry=1,Rz=-1)	-15.24	0.68	-14.56
HCCPP (↑↓)			
Stacking (R=5.5,θ=180,Z=-4.3,Rz=-27)	-9.06	-0.02	-9.08
In-plane (R=4.8,θ=90,Z=-5.6,Rx=1,Ry=86)	-9.58	-0.17	-9.75
Overall (R=4.8,θ=150,Z=1.8,Rx=-3)	-12.02	0.08	-11.94

R, Z in Å and θ, Rx, Ry, Rz in degrees

crystallographic data and also with mesophase data obtained from X-ray scattering studies[13].

The lengths of ECCPP, PCCPP and HCCPP molecules, obtained from stereo model in most extended conformations, are respectively 17.25, 21.2 and 23.5 Å. For ECCPP molecules, we find that the (↑↑) and (↑↓) pairs have minimum energy values -12.55 and -13.41 Kcal/mol at a stacking distance of 3.9 and 4.1 Å respectively, the length of the respective dimers being 20.5 and 18.1 Å. Thus the (↑↓) pair is energetically more favourable than the (↑↑) pair though the energy difference is about 4%. In the crystal structure of ECCPP there are two molecules per asymmetric unit and association of different types between the molecules have been observed. However, bimolecular associations between two same type of molecules across the centre of

symmetry with associated pair length of 25 Å is assumed to play key role in mesophase formation since this pair length is closer, than the other possible pairs, to the apparent length of the molecule in nematic phase (23.5Å) [13]. The average intermolecular distance between the neighbouring molecules in ECCPP is found to be 4.0 Å in solid state and 5.0 Å in nematic state. We thus find that calculated stacking distance agrees well with the solid state data. The length of the dimer, however, differs considerably from its values in crystalline and nematic states. But, it is observed that when the second molecule is translated 2.5 Å further along the molecular axis from the minimum energy configuration the increase in total energy is only ~3 Kcal/mol. Length of the dimer then becomes reasonably close to the nematic phase value.

In PCCPP, the (↑↑) pair has minimum energy of -11.23 Kcal/mol with associated length of 25.31 Å and stacking distance is 4.83 Å. The respective values for the (↑↓) dimer are -12.85 Kcal/mol, 21.7 Å and 4.44 Å. Thus the (↑↓) dimer is favourable in this case also. A bimolecular association across the centre of symmetry is observed in the

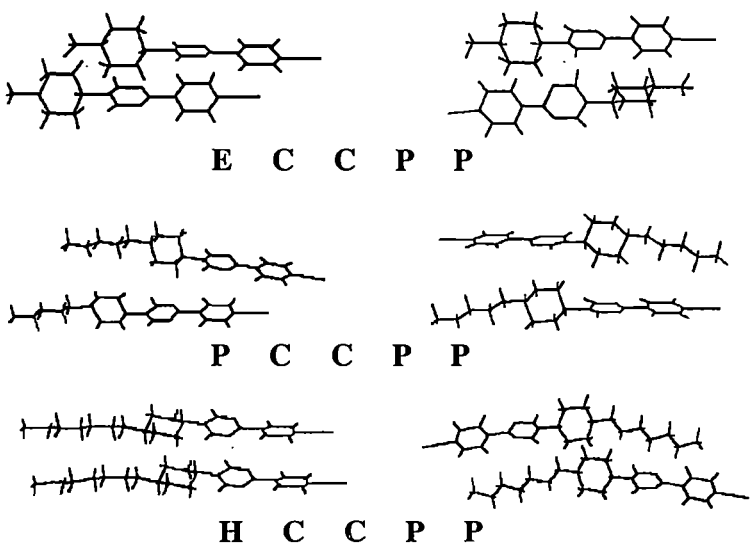

Figure 8.6 Configurations of the (↑↑) and the (↑↓) dimers at the overall minimum interaction energies.

crystalline state, the length of the pair being 27.8 Å [13]. The apparent length of the molecules in nematic phase is 25.8 Å [13]. Average intermolecular distance in crystal state is 3.8 Å and in nematic state it is about 5 Å. Thus we find that calculated stacking distance lies midway between the values in solid and nematic states. It is also observed that when the second molecule is shifted by about 2 Å along molecular axis from the minimum energy configuration the total energy increases by about 2 Kcal/mol and then the dimer length becomes closer to the associated length in nematic phase.

In HCCPP, the (↑↑) dimer has energy -14.56 Kcal/mol at a stacking distance of 1.11 Å and lateral displacement of 4.15 Å and the (↑↓) dimer possesses energy -11.94 Kcal/mol at a stacking distance of 4.16 Å with lateral displacement of 2.4 Å. The lengths of the respective dimers are 24.4 and 27.0 Å. Thus the (↑↑) dimer, in this case, has considerable lower energy than the (↑↓) dimer but it essentially stabilizes due to in-plane interaction. In the crystal structure of HCCPP bimolecular association across the centre of symmetry is found and the length of the pair is 32 Å, which becomes 33.7 Å in smectic phase and 37 Å in nematic phase [13]. The average intermolecular distances in crystal and mesogenic states are 4.6 Å and 5.0 Å respectively. Thus the calculated (↑↓) stacking distance is slightly less than the crystal state data but the difference in dimer length is quite large. However, if we increase the dimer length by reducing the overlap region by about 3 Å energy of both the dimers becomes ~9.0 Kcal/mol.

In all cases we also observe that if we make stacking distance of the dimers around 5 Å and if we further slide one molecule of the dimer along the molecular axis by 2 to 3 Å, the interaction energy at best increases by 5 Kcal/mol from the value at the overall minimum energy configurations.

We may thus conclude that the dispersion forces play the key role in stabilizing both the stacking and in-plane interactions. That the dimer energy do not change drastically when the stacking distance is increased by ~ 1 Å and molecular overlap is decreased by ~ 3 Å, indicate that the compounds are capable of retaining molecular order up to a considerable extent against thermal agitations. Thus the compounds

exhibit mesogenic behaviour instead of directly going from crystalline state to a completely random and disorganized isotropic melt. In case of HCCPP in-plane interaction energy is observed to be much stronger compared to the other two compounds. The stacking energy plays a major role in mesophase stability, the significant contribution of in-plane interaction may, however, favour the smectic phase.

It may be pointed out that to get better quantitative results one has to consider interactions between the other nearest neighbours and at least the next nearest neighbours and also statistical averages of the relevant data has to be considered. However, the present calculation shows that even rigid body approximation of the real molecules and consideration of only the dispersion and electrostatic forces can explain mesophase stability and behaviour to a considerable extent.

TABLE 8.1

Positional coordinates and partial atomic charges

Compound:ECCPP

Serial No.	Atom Name	Fractional coordinates			Orthogonal coordinates			Charge
		x	y	z	X	Y	Z	
1	C1	0.3827	-0.0562	0.3258	0.35329	5.87123	-9.96649	0.0143
2	C2	0.4072	-0.033	0.151	0.61219	7.04551	-9.26427	-0.0432
3	C3	0.4153	0.0076	0.1735	0.50669	7.06362	-7.89642	0.0058
4	C4	0.3997	0.0264	0.37	0.14691	5.91796	-7.18333	-0.0379
5	C5	0.3745	0.0026	0.5408	-0.1194	4.76584	-7.90994	-0.0004
6	C6	0.3654	-0.0379	0.521	-0.0303	4.73115	-9.27531	-0.0169
7	C7	0.4122	0.0696	0.3965	0.09559	5.92266	-5.71556	0.163
8	C8	0.4697	0.1271	0.2756	0.67543	6.90521	-3.76216	0.1167
9	C9	0.4421	0.1482	0.4519	0.11452	5.88914	-3.02055	-0.1847
10	C10	0.3964	0.1254	0.5964	-0.479	4.89664	-3.78858	0.1221
11	C11	0.466	0.1917	0.4785	0.24075	5.89795	-1.51202	-0.0074
12	C12	0.4129	0.2187	0.3459	-0.7438	6.80196	-0.86546	-0.0725
13	C13	0.4365	0.2625	0.3646	-0.6237	6.86054	0.64648	0.0359
14	C14	0.4453	0.277	0.594	-0.5764	5.50323	1.30813	-0.0494
15	C15	0.4961	0.2494	0.7276	0.37535	4.59005	0.63639	-0.0313
16	C16	0.4696	0.2057	0.7101	0.20905	4.52352	-0.87928	0.0214
17	C17	0.3755	-0.0985	0.3024	0.48268	5.85249	-11.3882	-0.0498
18	C18	0.4677	0.321	0.6024	-0.476	5.62575	2.81606	-0.0173
19	C19	0.4763	0.3402	0.8186	-0.4582	4.36767	3.62175	0.0252
20	N1	0.4557	0.0887	0.2444	0.67588	6.94728	-5.0801	-0.2517
21	N2	0.3813	0.0865	0.5726	-0.4932	4.89081	-5.12061	-0.2524
22	N3	0.3697	-0.1323	0.2812	0.58543	5.85293	-12.5262	-0.0802
23	H2	0.42	-0.048	-0.002	0.90467	7.93639	-9.82958	0.0722
24	H3	0.436	0.022	0.05	0.7543	7.88678	-7.45634	0.0691
25	H5	0.366	0.016	0.669	-0.3343	4.02323	-7.40301	0.0655
26	H6	0.35	-0.052	0.639	-0.1961	3.94473	-9.69512	0.0576
27	H8	0.511	0.141	0.163	1.24943	7.6657	-3.27495	0.0837
28	H10	0.374	0.134	0.733	-0.8852	4.07959	-3.47054	0.0758
29	H11	0.529	0.202	0.387	1.1758	6.52139	-1.06902	0.0028
30	H14	0.388	0.269	0.702	-1.4356	4.78853	0.9676	-0.0038
31	H121	0.405	0.21	0.194	-0.8129	7.70349	-1.27966	0.0314
32	H122	0.372	0.2	0.462	-1.2842	6.00176	-1.50633	0.0293
33	H131	0.499	0.268	0.29	0.33029	7.36132	0.9429	-0.0051
34	H132	0.402	0.279	0.261	-1.2568	7.55157	1.02004	0.017
35	H151	0.545	0.263	0.604	1.07096	5.41963	1.12654	0.0296
36	H152	0.496	0.259	0.875	0.31363	3.71718	1.05522	0.0334
37	H161	0.513	0.183	0.78	1.01875	4.01962	-1.45575	0.0164
38	H162	0.411	0.199	0.748	-0.6755	4.24582	-1.2305	0.0121
39	H181	0.509	0.33	0.531	0.12454	6.11343	3.172	0.0248
40	H182	0.435	0.347	0.508	-1.1354	6.2967	3.51221	-0.0111

Compound: PCCPP

Serial No.	Atom Name	Fractional coordinates			Orthogonal coordinates			Charge
		x	y	z	X	Y	Z	
1	C1	0.5925	0.2702	-0.0344	11.0725	1.91915	-0.5064	0.0164
2	C2	0.5153	0.2615	-0.0779	9.83702	1.85736	-1.1468	-0.0333
3	C3	0.4647	0.2477	-0.0269	8.68385	1.75934	-0.396	-0.0065
4	C4	0.4889	0.2442	0.0664	8.72708	1.73448	0.97751	-0.0421
5	C5	0.5667	0.2534	0.1096	9.9749	1.79982	1.61348	-0.0064
6	C6	0.6177	0.2668	0.059	11.1337	1.895	0.86857	-0.0327
7	C7	0.4341	0.231	0.121	7.48092	1.64072	1.78131	0.1591
8	C8	0.3122	0.2178	0.1262	5.21099	1.54697	1.85786	0.1191
9	C9	0.3338	0.2169	0.2195	5.20629	1.54058	3.23138	-0.192
10	C10	0.4111	0.2204	0.2581	6.46476	1.56544	3.79964	0.1213
11	C11	0.2803	0.2084	0.2776	3.96898	1.4802	4.08671	0.0054
12	C12	0.2178	0.3576	0.2528	2.92378	2.53993	3.72161	0.0052
13	C13	0.1664	0.3466	0.3155	1.70532	2.4618	4.64465	0.0032
14	C14	0.1311	0.1515	0.3155	1.0545	1.07606	4.64465	-0.0542
15	C15	0.1935	0.004	0.338	2.10779	0.02841	4.97589	0.0032
16	C16	0.244	0.0143	0.274	3.31527	0.10157	4.03371	0.0052
17	C17	0.6449	0.2834	-0.0883	12.2714	2.01291	-1.2999	-0.05
18	C18	0.0824	0.1378	0.3813	-0.1276	0.97875	5.61333	0.0047
19	C19	0.013	0.2619	0.3598	-1.3142	1.8602	5.29682	0.0013
20	C20	-0.0347	0.2347	0.4256	-2.4779	1.667	6.2655	-0.0146
21	C21	-0.1003	0.3684	0.4102	-3.6208	2.61663	6.03879	-0.0218
22	C22	-0.1487	0.3382	0.4736	-4.787	2.40213	6.97214	0.0417
23	N1	0.3605	0.2251	0.0753	6.32133	1.59882	1.10853	-0.2511
24	N2	0.46167	0.2282	0.2106	7.60226	1.62084	3.10036	-0.2513
25	N3	0.6849	0.2933	-0.133	13.2019	2.08322	-1.958	-0.0821
26	H2	0.498	0.265	-0.148	9.82081	1.88222	-2.1788	0.0685
27	H3	0.407	0.241	-0.057	7.75003	1.71175	-0.8391	0.0808
28	H5	0.583	0.248	0.179	9.9757	1.76147	2.63516	0.081
29	H6	0.673	0.274	0.092	12.0108	1.94614	1.35438	0.0653
30	H8	0.257	0.211	0.09	4.34961	1.49867	1.32494	0.0782
31	H10	0.433	0.217	0.326	6.57528	1.54129	4.79923	0.0771
32	H11	0.31	0.227	0.346	4.22115	1.61231	5.09366	0.021
33	H14	0.098	0.13	0.249	0.73144	0.92335	3.66567	0.0175
34	H121	0.187	0.344	0.184	2.65305	2.44333	2.70877	0.008
35	H122	0.244	0.483	0.258	3.38437	3.4306	3.79816	0.0067
36	H131	0.127	0.444	0.299	1.05017	3.1536	4.40175	0.0123
37	H132	0.198	0.371	0.385	1.98777	2.6351	5.6678	0.0032
38	H151	0.169	-0.118	0.336	1.66472	-0.8381	4.94645	0.0117
39	H152	0.23	0.025	0.411	2.46547	0.17757	6.05057	0.0017
40	H161	0.211	-0.009	0.208	2.99189	-0.0639	3.06209	0.0108
41	H162	0.284	-0.078	0.286	4.00092	-0.554	4.21037	0.0031
42	H181	0.065	-0.001	0.386	-0.4687	-0.0071	5.68253	0.0028
43	H182	0.117	0.166	0.447	0.22661	1.17905	6.58054	0.002
44	H191	0.029	0.397	0.363	-1.0331	2.81977	5.34393	0.0067
45	H192	-0.019	0.239	0.297	-1.633	1.69755	4.37231	0.0014
46	H201	0.001	0.247	0.496	-2.1237	1.75437	7.3019	0.0026
47	H202	-0.055	0.099	0.422	-2.8366	0.70317	6.2125	0.0061
48	H211	-0.133	0.356	0.34	-3.9205	2.52856	5.00533	0.003

PCCPP Table continued

49	H212	-0.078	0.502	0.419	-3.2477	3.56556	6.16834	-0.0084
50	H221	-0.169	0.204	0.466	-5.1284	1.44895	6.86025	-0.0117
51	H222	-0.117	0.352	0.541	-4.4936	2.50015	7.96437	-0.0022
52	H223	-0.191	0.431	0.465	-5.5297	3.06126	6.84553	0.0031

Compound: HCCPP

Serial No.	Atom Name	Fractional Coordinates			Transformed coordinates			Charge
		x	y	z	X	Y	Z	
1	C1	1.4855	0.1849	-0.2097	19.96817	3.28131	-1.9224	0.0466
2	C2	1.3837	0.1515	-0.1916	18.5892	2.68858	-1.75647	-0.0216
3	C3	1.3414	0.1899	-0.0794	17.71971	3.37004	-0.72789	-0.0063
4	C4	1.2392	0.1545	-0.0645	16.34459	2.74182	-0.5913	-0.0055
5	C5	1.1889	0.1956	0.0369	15.40135	3.4712	0.33828	0.0021
6	C6	1.0834	0.1612	0.0432	14.00756	2.86072	0.39603	-0.0106
7	C7	1.0267	0.2074	0.1319	13.01682	3.6806	1.20918	0.0115
8	C8	0.9146	0.17944	0.1271	11.56838	3.18441	1.16517	-0.0542
9	C9	0.9169	0.1018	0.1954	11.40492	1.80658	1.79131	-0.0018
10	C10	0.8578	0.2351	0.1999	10.62138	4.17218	1.83256	0.0056
11	C11	0.7469	0.2085	0.2014	9.17075	3.70012	1.84631	0.0074
12	C12	0.7523	0.1311	0.2732	9.0378	2.32655	2.50453	0.0145
13	C13	0.8061	0.0752	0.1967	9.95616	1.33453	1.80322	0.0037
14	C14	0.644	0.1052	0.2812	7.60267	1.86692	2.57787	-0.1967
15	C15	0.5729	0.062	0.176	6.97335	1.10028	1.61346	0.1215
16	C16	0.6077	0.1235	0.3991	6.79529	2.19168	3.6587	0.1196
17	C17	0.4525	0.05958	0.3051	5.03739	1.05733	2.79697	0.1593
18	C18	0.3485	0.03229	0.3196	3.63993	0.57303	2.92989	-0.0394
19	C19	0.293	-0.0253	0.2311	3.16677	-0.44898	2.11858	0.0011
20	C20	0.3058	0.0632	0.4237	2.78817	1.12157	3.88422	-0.0018
21	C21	0.198	-0.0523	0.2468	1.88329	-0.92814	2.26251	-0.0332
22	C22	0.2105	0.0363	0.4401	1.49879	0.64419	4.03456	-0.0246
23	C23	0.1567	-0.0215	0.3522	1.0461	-0.38208	3.22875	0.013
24	C24	0.0591	-0.0526	0.3705	-0.27865	-0.93346	3.39651	-0.0513
25	N1	0.4779	0.03849	0.1857	5.70687	0.68306	1.70238	-0.2506
26	N2	0.5133	0.10179	0.413	5.52473	1.80641	3.78613	-0.249
27	N3	-0.0171	-0.0785	0.3854	-1.31467	-1.39238	3.53311	-0.0816
28	H11	1.541	0.184	-0.114	20.42094	3.26534	-1.04508	-0.015
29	H12	1.515	0.16	-0.28	20.55204	2.83942	-2.56687	0.002
30	H13	1.474	0.243	-0.235	19.88984	4.31238	-2.15433	-0.0124
31	H21	1.32	0.155	-0.294	18.04847	2.75069	-2.69521	-0.0037
32	H22	1.39	0.096	-0.169	18.60735	1.70365	-1.54929	0.0062
33	H31	1.402	0.19	0.023	18.22002	3.37182	0.21085	0.0014
34	H32	1.328	0.243	-0.106	17.62029	4.31238	-0.97174	0.0027

HCCCC Table continued

35	H41	1.254	0.1	-0.035	16.45406	1.77464	-0.32086	0.0048
36	H42	1.185	0.153	-0.166	15.9252	2.7152	-1.52179	-0.0002
37	H51	1.239	0.198	0.134	15.77973	3.51379	1.22843	0.0029
38	H52	1.175	0.248	0.006	15.30759	4.40111	0.055	0.001
39	H61	1.096	0.108	0.083	14.05915	1.91661	0.76089	0.0033
40	H62	1.035	0.155	-0.061	13.67146	2.75069	-0.55921	0.0016
41	H71	1.074	0.208	0.233	13.34735	3.69125	2.136	0.0055
42	H72	1.019	0.263	0.093	13.02658	4.6673	0.85257	0.0034
43	H81	0.867	0.175	0.019	11.25377	3.10562	0.17418	0.0154
44	H91	0.968	0.106	0.302	11.76943	1.88112	2.76855	0.0024
45	H92	0.95	0.063	0.145	11.97937	1.11802	1.32927	0.0118
46	H101	0.906	0.242	0.304	10.95515	4.29463	2.78688	-0.0014
47	H102	0.856	0.285	0.158	10.71659	5.05772	1.44845	0.0108
48	H111	0.697	0.203	0.099	8.80999	3.60252	0.90757	0.0054
49	H112	0.714	0.245	0.253	8.5955	4.34787	2.31935	0.0091
50	H121	0.798	0.138	0.373	9.35115	2.449	3.41943	0.0171
51	H131	0.816	0.024	0.248	9.93997	0.42591	2.27351	0.0126
52	H132	0.76	0.071	0.093	9.64865	1.25999	0.85257	0.0071
53	H151	0.592	0.045	0.087	7.47455	0.79859	0.79756	0.0769
54	H161	0.654	0.155	0.481	7.16716	2.75069	4.40951	0.0764
55	H191	0.323	-0.046	0.157	3.76793	-0.81633	1.43928	0.0732
56	H201	0.346	0.106	0.485	3.13883	1.88112	4.44618	0.0766
57	H211	0.157	-0.093	0.183	1.52927	-1.65042	1.67763	0.0647
58	H221	0.178	0.058	0.507	0.88542	1.02929	4.64786	0.0605

REFERENCES

1. A. I. Kitaigorodski, *Molecular Crystals and Molecules,* Academic Press, New York(1973).

2. F. Laupretre and L. Monnerie, *Eur.Polym.J.,* **14**, 415(1978).

3. D. Sy and M. Ptak, *J.Physique-lett.,* **40**, L-137(1979).

4. M. Pesquer, M. Cotrait, P. Marsau and V. Volpilhoc, *J.Physique*, **41**, 1039(1980).

5. M. Cotrait, P. Marsau, M. Pesquer and V. Volpilhoc, *J.Physique*, **43**, 355(1982).

6. H. Perrin and J. Berges, *J.Physique Lett.* **43**, 531(1982).

7. K. Tokita, K. Fujimura, S. Kondo and M. Takeda, *Mol.Cryst.Liq.Cryst.Lett.*, **64**, 171(1981).

8. N. K. Sanyal, S. N. Tiwari and M. Roychoudhury, *Mol.Cryst.Liq.Cryst.* **132**, 81(1986); *J.Phys.Soc.Jpn.* **55**, 1171(1986).

9. M. R. Wilson and D. A. Dunmur, *Liq.Crystals*, **5**, 987(1989).

10. P. Mandal, B. Majumdar, S. Paul, H. Schenk and K. Goubitz, *Mol. Cryst.Liq.Cryst.* **168**, 135(1989).

11. P. Mandal, S. Paul, C. H. Stam and H. Schenk, *Mol.Cryst.Liq. Cryst.*, **180B**, 369(1990).

12. S. Gupta, P. Mandal, S. Paul, M de Wit, K. Goubitz and H.Schenk, *Mol.Cryst.Liq.Cryst.* **195**, 149(1991).

13. S. Gupta, B. Majumdar, P. Mandal, R. Paul and S. Paul, *Phase Transitions*, **40**, 73(1992).

14. P. M. Cotrait, D. Sy and M. Ptak, *Acta Cryst.* **B31**, 1869(1975).

15. M. J. S. Dewar and W. Thiel, *J.Am.Chem.Soc.* **99**, 4899(1977).

Chapter IX

SUMMARY AND CONCLUSION

Liquid crystal is currently an important field of research from the view of basic sciences as well as from application point of view. In this context studies on different physical properties of liquid crystals and understanding them in relation to their structures are important. Since mixtures are used in commercial display devices studying the properties of mixtures are also of much interest. Phase behaviour exhibited by a compound and the thermal stability of a particular phase depends upon the nature of intermolecular phases. Keeping this in view several physical properties of nine pure thermotropic liquid crystals and four binary mixtures have been studied in the thesis by employing optical microscopy, DSC, X-ray diffraction techniques as well as dielectric constants measurements. Crystal and molecular structure analysis and interaction energy calculation have also been done in few compounds. A chapter wise summary and important conclusions are given below.

In Chapter I, a general introduction to the field of liquid crystals has been given with a short review on liquid crystals, especially thermotropic liquid crystal systems. Different modifications of liquid crystals have been described briefly. Emphasis has been given on the discussions on the nematic, smectic A, smectic B and other smectic like soft crystal phases which have been studied in the present work. A brief survey of applications of liquid crystals in various fields have also been given. List of investigated compounds are also given in this chapter.

In Chapter II, Maier-Saupe mean field theory of nematic phase and McMillan's theory of smectic A phase have been discussed because some of the experimental results have been compared with the observations of these theories. Theory of X-ray diffraction from liquid crystals and methods of analysis of X-ray photographs to identify different phases and to calculate various molecular parameters have been described in detail. Maier-Meier theory of dielectric properties of liquid crystals and theoretical basis of calculation of the effective dipole molecular moment in nematic phase as well as the dipole-dipole correlation factors have also been described. Theory of crystal structure analysis by direct methods from CAD4 diffractometer data have been outlined. Details of the used experimental set up have been described.

In Chapter III, results of texture, DSC and X-ray studies on two di-Schiff's base compound, BMBT and BBBT, have been presented. The compound BMBT shows only ordinary nematic phase, whereas, BBBT forms a highly ordered smectic like tilted crystal phase and a skewed cybotactic nematic phase. Another di-Schiff's base compound BOCP, which forms only skewed cybotactic nematic phase, showed parallel imbricated mode of molecular packing in the crystalline state. However, in BBBT the molecules are arranged in tilted layers as precursor to the observed tilted smectic like crystal phase. In both the compounds supercooling effect has been observed. However, thermal range of supercooling of smectic phase, observed from DSC and X-ray measurements, is found to differ to some extent. This anomalous behaviour might be due to difference in container geometry, sample thickness and external alignment field. Two crystal phases are also observed in BBBT. The transition temperatures and the thermodynamic parameters observed by us differ slightly from those reported previously, particularly at T_{NI}. The average intermolecular distance (D) in the nematic phase is found to increase slightly with temperature in both cases. Observed D values are in the range 5.12-5.53 Å in BMBT and 5.02-5.24 Å in BBBT. In both the systems the apparent molecular length (*l*) is found to be less than the model lengths (L) of the respective molecules. This suggests that either the molecules are not in the most extended conformation or the molecules are tilted or both. If the molecules are assumed to be in most extended conformation then the tilt angle (β_t) is found to decrease by about 9° from a value of ~50° over the nematic range of BBBT. Value of β_t measured directly from X-ray photograph is found to be almost equal to the mean of the above β_t values. However, in BMBT the observed β_t is about half the above value. In BBBT the transverse correlation length in the cybotactic groups is found to be about five molecular diameters. Moreover, an abrupt change in the values of the above molecular parameters is observed at T_{SM-N} signifying a first order phase transition, ΔH and ΔS values also support this observation. Orientational order parameters, $\langle P_2 \rangle$ and $\langle P_4 \rangle$, are found to agree well with MS theory and Faber's theory in BBBT but the agreement is not so well in BMBT. In both the systems the $\langle P_2 \rangle$ values are

on the higher side of the normal range. These compounds were found to be effective in GLC phase separation. High melting point, long range of nematic phase and high $<P_2>$ values are the possible factors for their effectiveness in GLC phase separation.

In Chapter IV, X-ray studies on another two Schiff's bases 6OBPAA and 8OBPAA and their equimolar mixture have been reported. In both the compounds and the mixture N, SmA and SmB phases have been observed over a wide range of temperatures. No change in phase sequence or no appreciable change in transition temperatures is observed between the two homologues except that the temperature T_{NI} is 10°C less in 8OBPAA than in 6OBPAA and in the mixture SmB phase is enhanced by about 15°. Moreover, it is observed that replacement of the flexible butyl chain of the Schiff's base 6O.4 (or 4O.4) by a rigid azophenyl group in 6OBPAA or in 8OBPAA increases the transition temperatures and the stability of the different phases substantially, however, the SmH/SmG phase is suppressed altogether. From X-ray studies it is observed that in all cases d (layer spacing) or *l* decreases as one moves from SmB to N phase, reverse trend is observed in D. All these parameters show higher values in the higher homologue and the mixture show intermediate values. Systematic increment of D values from SmB to I phase suggests that the molecules are most efficiently packed in SmB phase and in isotropic phase the packing is least efficient. In the mixture the packing is of intermediate nature. Since *l*/L or d/L ratio is observed to be slightly higher than unity in all phases, a bimolecular association of the molecules, with almost complete overlap, are assumed to exist in the mesophases. The orientational order parameters, $<P_2>$ and $<P_4>$, calculated from X-ray data of the samples have been compared with those obtained from McMillan's theory in SmA phase and Maier-Saupe theory in N phase and found to be in good agreement. The values of the adjustable parameter α are found to increase with chain length as is expected from McMillan's theory, in the mixture α values are found to be in between the pure compounds. Moreover, the values of T_{SmA-N} calculated from McMillan's theory are found to be in excellent agreement with observed values. SmA-N transition is found to be of first order type.

In Chapter V, results of X-ray diffraction and dielectric studies on binary mixtures of a carboxylate and a cyanobiphenyl (BPPCC+2CB) in three concentrations have been presented. Dielectric behaviour of pure BPPCC has also been studied. It is observed that replacement of only 25% 2CB molecules, which exhibit virtual nematic phase, by nematogenic BPPCC molecules induces monotropic nematic phase but to get enantiotropic nematic phase 50% molecules have to be replaced (Mixtures II). Since this mixture and another with 75% BPPCC (Mixture III) are found to be nematic at ambient temperature with long range (36° and 51°), they are expected to be useful in commercial display devices. The apparent molecular length (l) and the average intermolecular distance (D) are found to increase very slowly with temperature in all mixtures. Mean value of D is found to be 5.13 Å in Mixture II and 5.19 Å in Mixture III which are more than the value 5.0 Å usually found in N phase of nCB compounds. It is also observed that the packing of the dissimilar molecules in the mixtures is less efficient than that in the pure components. The average l value of the molecules is found to be 19.6 Å in both the mixtures, considerably different from the value expected from simple additive rule. In both the pure components some sort of bimolecular association is reported to exist in the nematic phase. If the associated lengths of those pairs are taken as the effective lengths of the molecules within nematic phase, then the calculated l values in the mixtures become 20.15 Å and 19.43 Å respectively, very close to the observed value (19.6 Å). Thus bimolecular association within same type of molecules (homo dimmers) is likely to be present in the mixtures as well. The orientational order parameters, $\langle P_2 \rangle$ and $\langle P_4 \rangle$, values at different temperatures agree well with those obtained from Maier-Saupe theory. In the mixtures no significant change in order parameters is observed. Moreover, in these mixtures the molecules are found to be less ordered than the mono- and di-Schiff's base molecules described in Chapter III and IV. Since the molecules of the previous systems are longer and less rigid than the present molecules, they are expected to be less ordered as observed.

The compound BPPCC shows small but negative anisotropy, however, all the three mixtures show large positive anisotropy. 2CB molecules are expected to have

large positive dielectric anisotropy like all other members of the **nCB** series. Thus the dielectric behaviour of the mixtures is dominated by the 2CB component. Even when only 25% of the BPPCC molecules are replaced by the 2CB molecules substantial positive anisotropy is yielded. Replacement of 50% and 75% BPPCC molecules by 2CB molecules results in larger $\Delta\varepsilon$. In all the mixtures dielectric permittivity in the isotropic phase ε_{iso} is found to be larger than $\bar{\varepsilon}$ in the nematic phase, no such jump is observed in BPPCC. But effective value of the dipole moment within nematic phase of BPPCC, calculated from Maier and Meier equations, is found to be about 20% less than the free molecule value. These suggest presence of some sort of anti-parallel dipolar associations within nematic phase of the mixtures and BPPCC. In mixtures this dipolar association breaks down completely or partially in the isotropic phase resulting in the increase of effective dipole moment of the molecules and thereby increasing the permittivity. In BPPCC probably no such change in molecular associations takes place during the N-I transition. Slight change in the value of effective dipole moment at T_{NI} also suggests this. In BPPCC the values of dipole-dipole correlation factors ($g_{\parallel}$ and $g_{\perp}$) in nematic phase were also calculated using Bordewijk theory. These values suggest parallel components of the molecular dipole moments are strongly correlated in antiferroelctric fashion at low temperatures but at high temperatures this correlation is almost negligible. However, over the entire nematic range the correlation of the perpendicular component is ferroelectric type but almost negligible.

In Chapter VI, the crystal and molecular structure of the biphenyl 2CB, which exhibits virtual nematic phase, is described which was determined by direct methods from single crystal X-ray diffraction data. The crystal belongs to monoclinic system with space group $P2_1$, cell parameters being a=8.584(4), b=5.865(3), c =11.833(3) (Å) and β=92.30(3)°. Refinement led to R=0.079 with $I>2\sigma(I)$. The molecules are found to be in the most extended conformation. The phenyl rings are highly planar and the dihedral angle between them is 1.46°. Antiparallel pairs of 2_1 symmetry related molecules are arranged in layers and the layers are stacked along [001]. The thickness of these layers is equal to the length of

crystallographic *c*-axis. van der Waals' type of contact is found to exist between the 21 symmetry related molecules and length of such paired molecules is found to be 1.13 times the molecular length. However, in several nCB or nOCB compounds, where monotropic or enantiotropic mesophases are observed, dipole-dipole or dipole-induced dipole type contact is found to exist and the associated pair length is about 1.4 times the molecular length. Moreover, imbricated type of molecular packing is observed which is assumed to be necessary for the formation of nematic phase. In contrast 2CB molecules are arranged in tilted smectic type layers. Moreover, van der Waals' type of contact encompasses all the molecules within a layer. So the melting point is well above the range of thermal stability of the nematic phase. However, while cooling from isotropic melt, dipole-dipole interaction may give rise to parallel imbricated mode of packing as observed in the fifth member onwards of *n*OCB series of compounds and this in turn may sets in nematic phase.

In Chapter VII the crystal and molecular structure of BPPCC, a nematogenic compound, determined by direct methods has been presented. The crystal belongs to monoclinic type with space group $P2_1/a$, a =11.2483(22), b = 20.2968(44), c = 17.6311(14) Å, β = 100.342(11)° and two independent molecules within unit cell. Refinement converged to an R-value of 0.106. Some bond lengths and angles are found to deviate considerably from the standard values as has been reported earlier in mesogenic compounds. The molecules are in the most extended conformation and are roughly in the *a-c* plane. But unlike 2CB the molecules are packed in parallel-imbricated manner. Crystal – nematic transition may thus be of displacive type. Presence of bimolecular association due to van der Waals' interaction is found in both crystalline and nematic phases. It is inferred that as a result of van der Waals' interactions bimolecular associations exist in the crystalline state as well as in the nematic phase and play a dominant role in the mesophase stability.

In Chapter VIII, the pair intermolecular interaction energy of ECCPP, PCCPP and HCCPP, three pyrimidine mesogenic compounds, has been calculated in the crystalline state by atom-atom potential method taking into account van der Waals' and electrostatic interactions and considering the molecules as rigid bodies.

Stacking, in-plane and overall minimum energy configurations have been calculated to find the most favourable arrangements for both parallel and anti-parallel dimers. For each compound it is observed that in all cases (stacking, in-plane and overall minimum) main contribution to the total interaction energy comes from van der Waals' interaction, the contribution of the electrostatic interaction in no case is greater than 4%. Energetically most favourable configurations of the dimers have been compared with the data obtained from crystal structure analysis and X-ray scattering studies in mesophases. It is concluded that the dispersion forces play the key role in stabilizing both the stacking and in-plane interactions and the dimer energy do not change drastically when the stacking distance is increased by ~ 1 Å and molecular overlap is decreased by ~ 3 Å which indicate that the compounds are capable of retaining molecular order up to a considerable extent against thermal agitations. Thus the compounds exhibit mesogenic behaviour. In case of HCCPP in-plane interaction energy is much stronger compared to the other two compounds. The stacking energy plays a major role in mesophase stability, the significant contribution of in-plane interaction may be responsible for the formation of smectic phase in HCCPP.

APPENDIX

LIST OF PUBLICATIONS

A. Papers:

1. *Small angle X-ray scattering studies on smectic and nematic phases of a toluidine compound*, P.K.Sarkar, S. Paul and P. Mandal, *Mol. Cryst. Liq. Cryst*, **265**, pp. 249 – 255 (1995).

2. *Molecular structure and packing in the crystalline state of 4-n-ethyl-4'-cyanobiphenyl (2CB) by single crystal X-ray diffractometry*, Pranab Sarkar, Parimal Sarkar, P. Mandal and T.Manisekaran, *Mol. Cryst. Liq. Cryst.*, **325**, pp. 91 – 97 (1998).

3. *X-ray scattering studies on two nematogenic p-alkanyl 1-2-chloro- (p-alkylbenzoyloxy)-benzoates and their mixtures*, Parimal Sarkar, Pranab K. Sarkar, Sukla Paul and Pradip Mandal, *Phase Transitions*, **71**, pp.1–12 (2000).

4. *Minimum energy configuration of dimmers of ethyl pentyl and heptyl members of 5-(trans-4-alkyl cyclohexyl)-2-(4-cyanophenyl) pyrimidine*, Pranab Kumar Sarkar, Sukla Paul and Pradip Mandal, *Mol. Cryst. Liq. Cryst.*, **365**, pp. 535-542 (2001).

5. *Crystal and Molecular Structure of the Nematogenic Compound p-Butoxyphenyl trans -4- Propyl Cyclohexane Carboxylate*, Sonali Ghosh, Pranab K. Sarkar, Pradip Mandal and Sukla Paul, *Mol. Cryst. Liq. Cryst.* (communicated). This paper was accepted for presentation at the 19th ILCC, Edinburgh,2002 (Ref. No. ILCC 2002-133).

B. Abstracts:

1. *X-ray diffraction study on lithium stearate*, P. K. Sarkar, S. Paul and P. Mandal, presented at the National Seminar on Liquid Crystals, Mysore University, Mysore, India (1993).

2. *Apparent variation of intermolecular distance in nematogens with degree of ordering: An experimental verification with n-pentyl cyanobiphenyl*, G. Chowdhury, P. K. Sarkar and R. Paul, presented at the National Seminar on Liquid Crystals, Northeastern Regional Institute of Science and Technology, Itanagar, India (1994).